THE UNIVERSITY *of* EDINBURGH

New Cyclisations of Iminyl Radicals Generated by Flash Vacuum Pyrolysis

Maria Ieva

Degree of Doctor of Philosophy

School of Chemistry

University of Edinburgh

May 2012

Contents

Declaration

The scientific work described in this Thesis was carried out in the School of Chemistry at the University of Edinburgh between June 2007 and December 2010. Unless otherwise stated, it is the work of the author and has not been submitted in whole or in support of an application for another degree or qualification at this or any other University or institute of learning.

Signed:

Date: 16th May 2012

Acknowledgements

First of all I would like to acknowledge Professor Hamish McNab for his kindness, guidance and patience throughout the years of my PhD and without whom this thesis would have not been possible. His support and encouragement was thoroughly missed at the end of this journey.

A major thanks goes at EPSRC for funding without which all the research described in this thesis could have not been possible.

I would like also to say a sincere thank you to Dr. Karen Johnston who helped me with all the practical work in the lab but also who taught most of my skills with computational chemistry and NMR during my first year. I would like to say thank you to Mr. A. Taylor who ran all my mass spec samples and Mr. J. Millar and Mr. J. Bella for their help with the NMR instruments. Thanks you goes also to Dr. Patricia Richardson for her help with computational chemistry.

A big thank you goes also to Dr. Alison Hulme that helped me to finish this journey when Hamish couldn't do it anymore.

Thank you to everyone in my group for their friendship because they made my staying in Edinburgh and in the McNab group a wonderful experience. A special thank goes to Rich that kept encouraging me and had to deal with some of my chemistry too.

Thank you to all the crazy chemists that surrounded me in the chemistry department, people from all over the world that helped my personal development and made this PhD journey even more special.

'The chemists are a strange class of mortals impelled by an almost insane impulse to seek their pleasure among smoke and vapour, soot and flame, poisons and poverty; yet among all these evils I seem to live so sweetly, that I may die if I would change places with the Persian King'.

Johann Joachim Becher, 1635-1682

Acta Laboratorii Chymica Monacensis, 1669.

Thank you to the 'Italian community' too, that helped me to never forget by beautiful background and laughed with me about our silly mistakes in this everyday learning

process. Thanks especially to Armando and Irene that never let it go and never gave up on me and our friendship.

A special thanks goes to the people that had to stand this last period of misery and that had to listen to my moaning all the time (thanks people in Bay 7) and that helped me to understand that ‘a bit of misery is good!’ (*c.f.* Dr. Hamza)

Un grazie speciale va alla mia famiglia che con il loro amore ed il loro affetto mi hanno supportato e sostenuto e non hanno mai smesso di credere in me. La loro presenza mi ha aiutato a non dimenticare le vere cose importanti nella vita ed a non perdere mai di vista il vero obiettivo.

I could never say thanks enough to Tonia, a friend and a wonderful person that throughout this last year of my journey was always there for me. She was there for me when I was crying, desperate but also to share the lovely moments that helped me in the horrible thesis writing process.

Last thanks goes to Paul, my best friend, that with his support and love made me believe that everything is possible and, even when all the odds were against, he made me believe that I could do it.

I would like to dedicate this thesis to
Professor Hamish McNab,
the mentor, the gentleman, the fighter and the scientist
who dedicated his life to research until his last days.

"WHERE SHALL I START, PLEASE YOUR MAJESTY?" (S)HE ASKED.
"BEGIN AT THE BEGINNING," THE KING SAID GRAVELY,
"AND GO ON TILL YOU COME TO THE END: THEN STOP."

LEWIS CARROLL

1. Abbreviation

δ_C	chemical shift of Carbon
δ_H	chemical shift of Hydrogen
m/*z*	mass to charge ratio
T	temperature
mp	melting point
bp	boiling point
DMF	*N*,*N*-Dimethyl formamide
NMR	Nuclear Magnetic Resonance
FVP	Flash Vacuum Pyrolysis
T_f	furnace temperature
T_i	inlet temperature
P	pressure
t	time of pyrolysis
s	singlet
d	doublet
dd	doublet of doublets
t	triplet
m	multiplet
quat	quaternary carbon
J	coupling constant for protons 3 bonds apart in Hertz
mmol	millimoles
min	minute
lit	literature
LAH	Lithium Aluminium Hydride
NaH	Sodium Hydride
THF	Tetrahydrofuran
IR	Infrared Spectroscopy
bs	broad singlet
DMSO	Dimethyl Sulfoxide
DCM	Dichloromethane
h	hour

Me	Methyl
Et	Ethyl
AcOH	acetic acid
eq	equivalent
s. m.	Starting material
N/A	non available
Aq	aqueous
r.t.	room temperature

Abstract

The formation of iminyl radicals from a range of precursors, including hydrazone imines and oxime ethers, under FVP conditions is well documented in the literature.[1] Once formed, the iminyl radical can undergo cyclisation onto various aromatic ring systems including phenyl rings, thiophenes and furans to form new fused aromatics.[2] The aim of this thesis was to expand the scope of cyclisation of iminyl radical onto pyrrole-type rings and 2-azole rings, generating novel heterocyclic cores *via* pyrolysis of the corresponding oxime ether precursors (Scheme I)

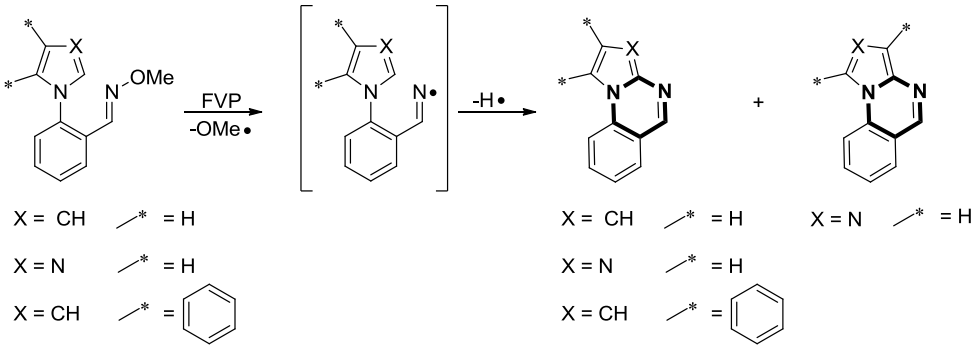

Scheme I

In addition, the cyclisation of iminyl radicals onto C-C double bonds was investigated and afforded isoquinolines shown in Scheme II, providing a new way to synthesise these heterocyclic cores.

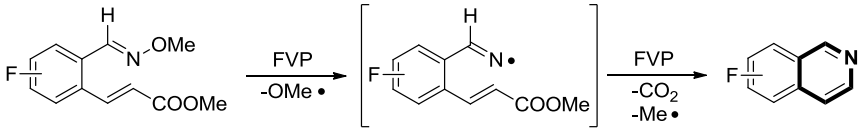

Scheme II

Mechanistic predictions were supported by DFT calculations in which the thermodynamics and kinetics of the systems were established and the products of iminyl cyclisation reactions were characterised using a range of 2D NMR experiments.

Chapter 1:

Review on general methods to form iminyl radicals and their reactivity.

1. Introduction

In the last thirty years imiyl radicals have captured the attention of organic synthetic chemists due to their high potential in organic synthesis. The iminyl radical is a radical centred on a nitrogen atom which is double-bonded to carbon as shown in Figure 1. It was confirmed by e.s.r. analysis that the unpaired electron is located in a 2*p* orbital orthogonal to the π-system of C=N[1].

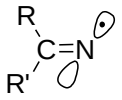

Figure 1[3]: general iminyl radical structure with unpaired electron located in a 2*p* orbital.

2. Generation

Iminyl radicals can be generated in different ways: in solution with an initiator, in solution by photolysis, in solution by microwaves, or in the gas phase.

2.1. Solution

In the next section all the different ways to generate iminyl radicals in solution are explored.

2.1.1. Solution with an initiator

Forrester and co-workers first discovered a useful method for the generation of iminyl radicals.[4] One of the first examples is shown in Scheme 1.[4(ii)]

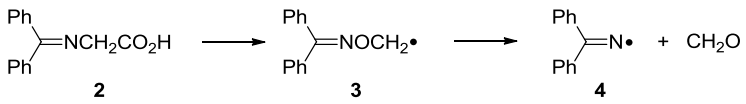

Scheme 1

The oximinoacetic acid **2** reacts with persulfate to give the oximinomethyl radical **3**. Then the loss of formaldehyde occurs resulting in the formation of the iminyl radical

4. The same group developed different routes – for example by thermal decomposition of suitable *tert*-butyl iminoxyperacetates **5** (Scheme 2).[3]

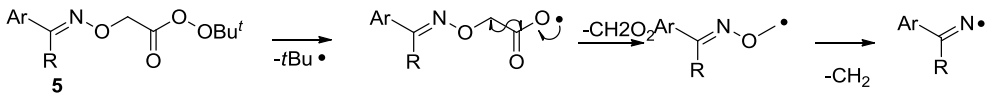

Scheme 2

The reaction is carried out in benzene and involves cleavage of a peroxide unit, followed by decarboxylation and loss of formaldehyde (*c.f.* Scheme 1).

In Scheme 3, reaction between oxime ethers **6** and a *tert*-butoxyl radical giving the iminyl radical **1** *via* abstraction of a hydrogen atom and loss of the ketone **7** is described.

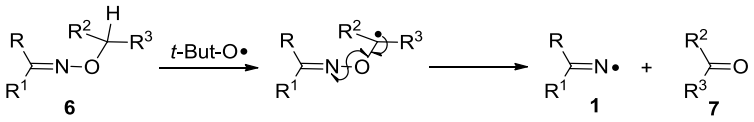

Scheme 3

The success of this reaction is due to the nature of R^2 and R^3. The order of reactivity of ethers is: diphenylmethyl > benzyl > isopropyl > methyl.

Zard and co-workers developed other methodologies in the nineties,[5] forming the iminyl radical **1** by reaction of an oxime ester **8** with tributyltin radical. One of these examples is given below. (Scheme 4)[5(vi)]

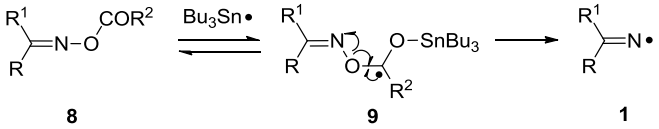

Scheme 4

This kind of reaction is limited to the use of an oxime benzoate (**8**, R^2 = Ph) since in the first step the addition of the stannyl radical to the oxygen atom is an equilibrium

and the formation of the iminyl radical **1** is favoured by the weakness of N-O bond in the intermediate **9**.

Another route developed by Zard and co-workers was the formation of iminyl radicals by the use of nickel and acetic acid in propanol (Scheme 5).[6]

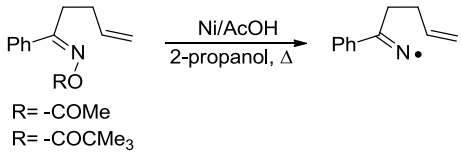

Scheme 5

In this case, the iminyl radical is formed by single electron transfer from nickel. The anion radical **10** thus formed collapses with formation of the iminyl radical **1** and a carboxylate anion (Scheme 6).

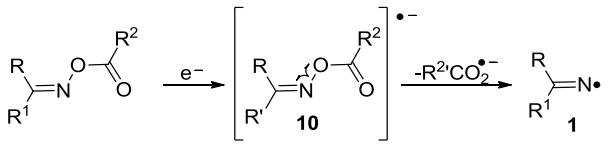

Scheme 6

A more recent methodology was developed by Bowman and co-workers where the iminyl radical is formed by reaction of a vinyl radical with a nitrile (Scheme 7).[7]

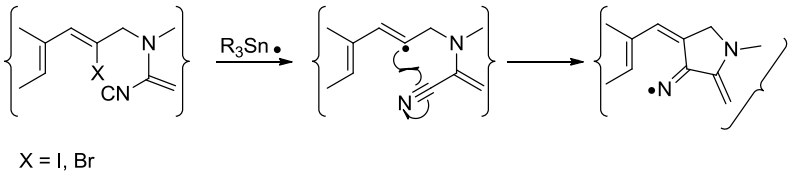

Scheme 7

2.1.2. By photolysis

One of the first examples of iminyl radical generation by photolysis was achieved by Ingold and co-workers.[8] The reaction involves hydrogen abstraction from imine **12** by a *tert*-butoxy radical **11**.

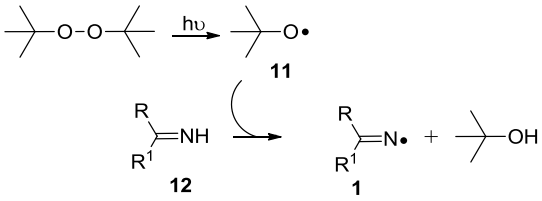

Scheme 8

In the midnineties, Zard and co-workers,[9] inspired by the work of Forrester[4] and Barton,[10] used the photolysis method in a different way (Scheme 9).

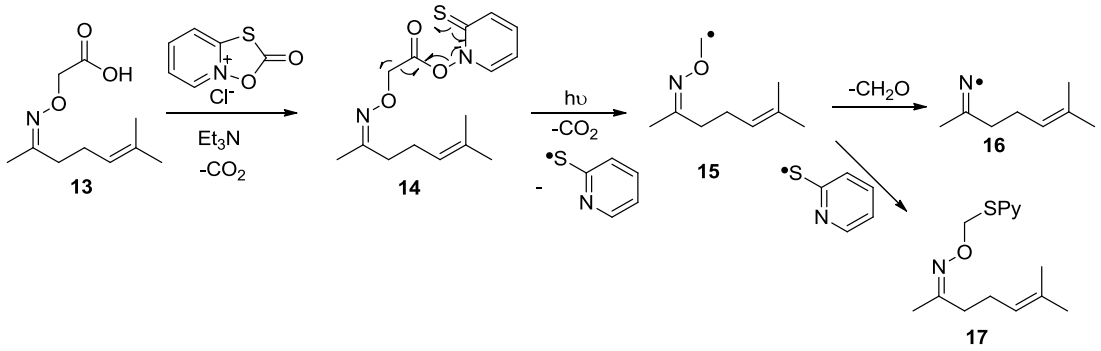

Scheme 9

The *O*-carboxymethyl oxime **13** is transformed into an ester of *N*-hydroxy-2-thiopyridone **14**. At this point, photolysis is used to induce a decarboxylation, forming the methyl radical (**15**). This undergoes further transformation to **16** or **17**, in the first case forming the iminyl radical by the loss of formaldehyde.

This kind of reaction was limited by the fact that the loss of formaldehyde was not quick enough and after the loss of CO_2 the radical gives the unwanted sulfide **17** by capture of the thiohydroxamate ester **14**.

In 2002, Tsunooka and co-workers[11] also proved that the irradiation of an *O*-acyloxime **8** directly gives iminyl radical **1** in a reasonable yield (Scheme 10).

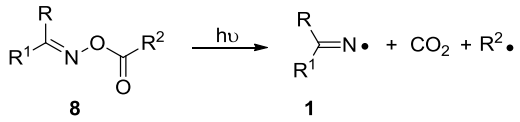

Scheme 10

Some of the acyloximes that have been photolysed are shown in Scheme 10a:

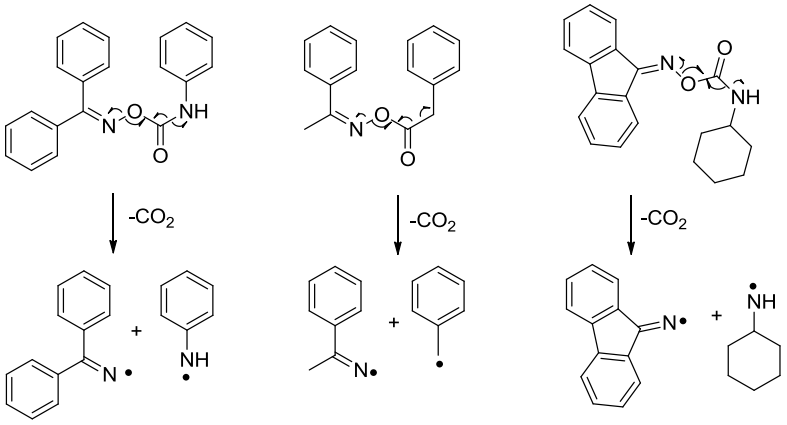

Scheme 10a

In all the three cases a stabilised iminyl radical is formed. The driving force, however, is the fact that a decarboxylation occurs giving, in the first two cases, stable radicals (anilinyl radical and benzyl radical).

Photoreactivity studies have been carried out on these species and it has been seen that there is not a substantial difference in dissociation of *O*-acyloxime when the photolysis it is conducted in a film or in benzene.[11]

2.1.3. By microwaves

Microwaves are an unusual method for generating iminyl radicals. One of the few examples found in literature is the irradiation of a solution of *O*-phenyl oxime ethers in toluene with the use (in some cases) of emimPF_6. This work was carried out by Walton and co-workers.[12]

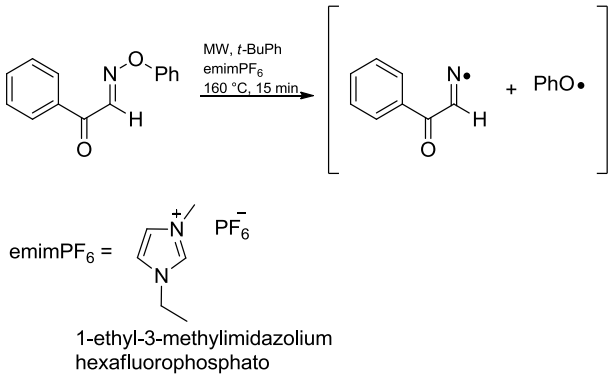

Scheme 11

Other substrates used for generating iminyl radical under microwave irradiation are illustrated in Figure 2.

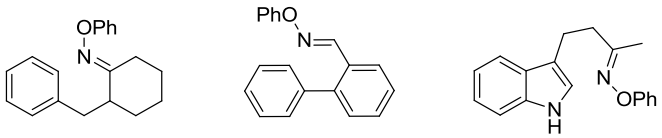

Figure 2: examples of precursors to generate an iminyl radical under microwave conditions.

In these three examples emimPF_6 was not required and the reactions were conducted using *tert*-BuOH as solvent.

The first two show a cyclisation onto a benzene ring, while the third involves a cyclisation onto the indole ring.

2.2. Gas phase

The first examples of the formation of iminyl radicals in the gas phase were obtained from camphor oxime[13] and camphor nitro imine[14] by pyrolysis under reduced pressure. More recent examples have been published by Bird and co-workers[15] using azine **18** pyrolysis as source of two iminyl radicals exploiting the weakness of the N-N bond.

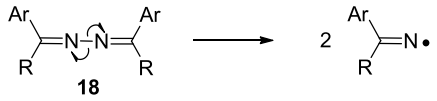

Scheme 12

This kind of source was not the most appropriate for other applications, in some cases the corresponding oxime esters were found to be more suitable.

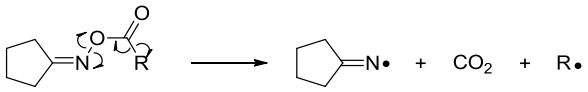

Scheme 13

However, this methodology was not found to be general. Various oximes were pyrolysed and while some of them were successful (such as **19)**, others, underwent a rearrangement (as shown with cyclic oxime ester **20** Scheme 14).

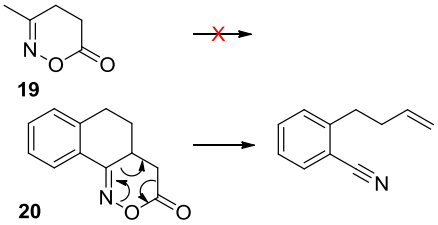

Scheme 14

At the beginning of 1980s, McNab[16] generated iminyl radicals *via* FVP (Flash Vacuum Pyrolysis) at 600 °C and 10^{-2} Torr. The starting materials were disubstituted 1,5-diazapentadienes **21**. The reaction mechanism proceeds in the same way for all the compounds with leaving groups X (Scheme 15).

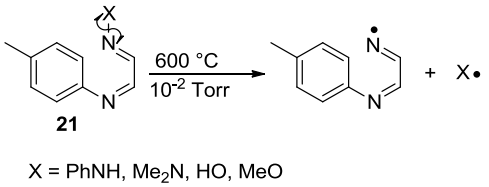

Scheme 15

In the most recent studies, it was discovered that the oxime *O*-methyl ethers were the most suitable precursors for the generation of iminyl radicals by FVP, because no side-products were obtained.[17]

3. Reactivity in the gas phase

The reactivity of iminyl radicals is different in solution phase and the gas phase. An overview of the reactivity of iminyl radicals concentrating on gas phase examples is given below. Iminyl radicals can react in different ways including β-cleavages, cyclisations and rearrangement.

3.1. β-cleavage

It has been known since the seventies that one of the major products from iminyl radicals are cyano derivatives **22** as proved by Bird and co-workers (Scheme 16).[15]

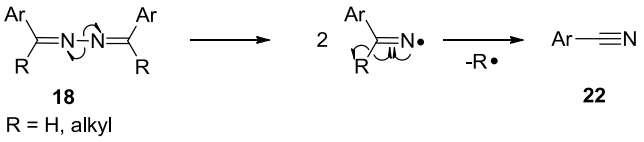

Scheme 16

It is important to distinguish the difference between the ketazines (**18**, R = alkyl) and aldazines (**18**, R = H). In the first case, aromatic ketazines give benzonitrile with a yield oft 80-100%. In the second case, the yield of nitrile is lower because the C-H bond is stronger than the corresponding C-C bond.

In the case of azines derived from cyclic ketones, β-cleavage gives more complicated results.

An example involving H-atoml transfer was reported by Crow and Khan[18] (Scheme 17)

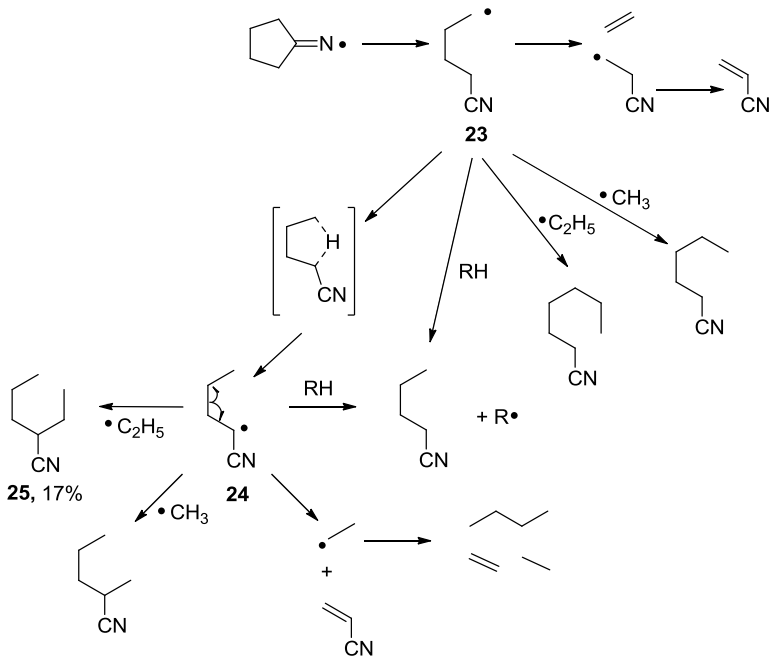

Scheme 17

The cleavage of the ring results in more rotational freedom even if there is not any thermochemical advantage. In this case, the radical **23** rearranges to a more stable α-cyano radical **24** leading to the major product 3-cyanohexane **25** in 17% yield.

As shown in Scheme 17, a large number of products were formed due to the coupling between radicals. The efficiency of the coupling was improved by using oxime esters as shown in Scheme 13, because the oxime esters produce an additional mole of the radical R˙.

Recently discovered examples of β-cleavage were reported by McNab and co-workers who investigated the properties of 1-(2-arylaminophenyl)-alkaniminyls **26 (**Scheme 18**).**[19]

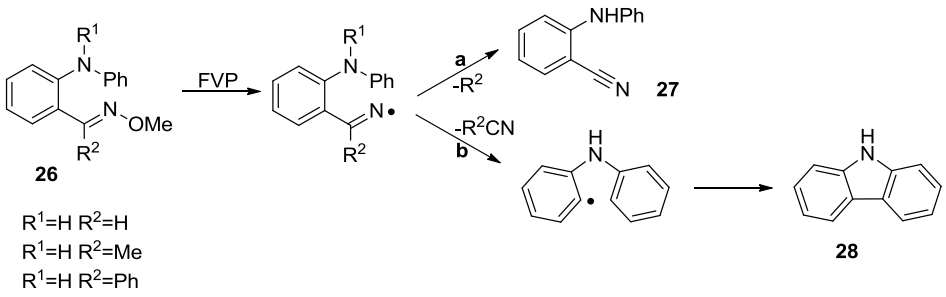

Scheme 18

The major products were the result of β-cleavage: in case **a**, it was possible to observe the cleavage of the C-R^2 bond resulting in the formation of the nitrile **27**; case **b** occured only when R^2 = Ph. Where R^2 = Me or H, β-cleavage of the C-H and C-Me bonds was favoured compared to the aryl bond C-C. In the case in which R^2 = Ph, two aryl C-C bonds that are similar in energy were both cleaved, leading to product **28** as well.

Another two products are formed when R^2 = H or Ph as shown in Scheme 19.

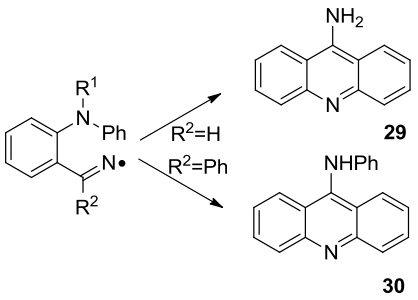

Scheme 19

It is believed that acridines **29** and **30** are formed by H radical transfer and the radical **31** which is formed is involved in the cyclisation (Scheme 20).

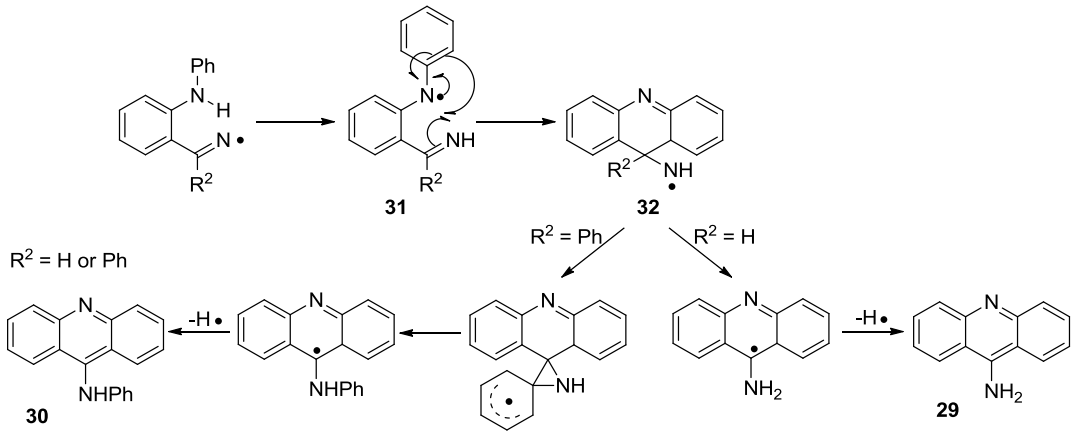

Scheme 20

The primary aminyl radical **32** can be stabilised *via* with a 1,2 hydrogen or phenyl group shift.

In the mideighties various attempts to generate 5-membered rings fused onto a benzene ring by cyclisation of iminyl radicals were carried out in the McNab research group.[20] Unfortunately, these attempts were unsuccessful. As shown in Scheme 21, pyrolysis of phenyl-2-propanone *O*-methyloxime **33** gave nitrile **35** and bisbenzyl **34** due to β-cleavage. Unexpectedly, acetonitrile and bisbenzyl were even obtained from the pyrolysis of phenylacetaldehyde *O*-methyloxime.

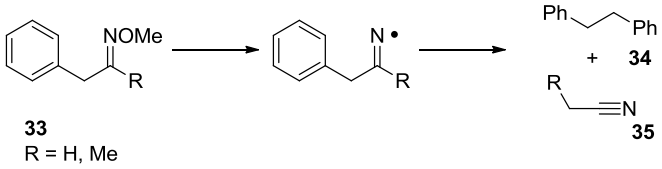

Scheme 21

3.2. Rearrangement

When iminyl radicals are generated *ortho* to a phenoxyl group as in compound **36**, they rearrange generating phenoxyl radicals **37** as shown in Scheme 22.[21]

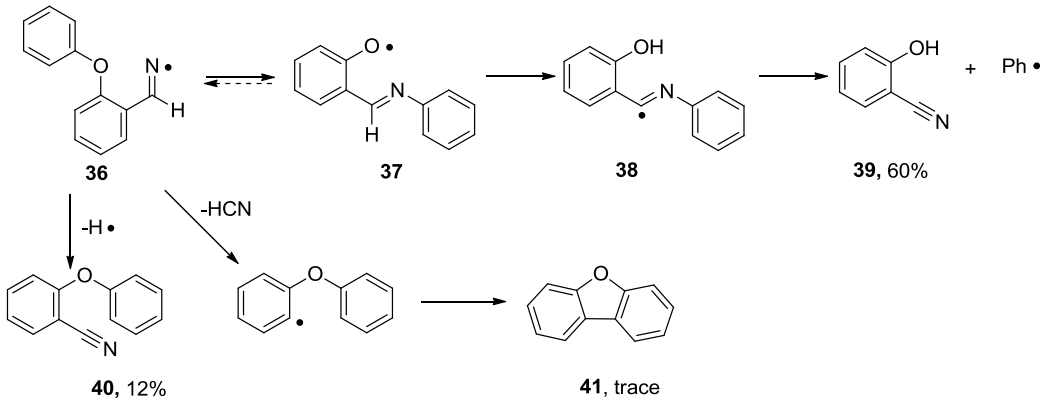

Scheme 22

2-Cyanophenol **39** is due to the rearrangement of the iminyl radical **36** to a phenoxyl radical **37** by *ipso* attack, and subsequent loss of a phenyl radical and formation of the nitrile group. It is noteworthy that in this case the β-cleavage to give **40** and **41** is not favoured due to the strength of the C-H and C-aryl bonds.

Even in the case in which the aldiminyl radical **36** is substituted for the ketimiyl radical **42**, the major products are **39** and **40** (Scheme 23).

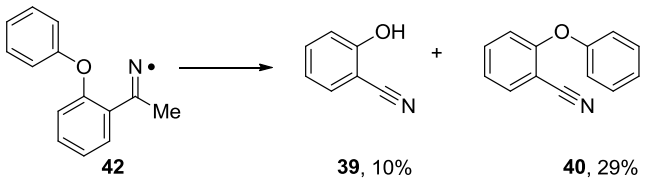

Scheme 23

In this case, the percentage of **40** produced is higher than the one reported in Scheme 22 because of the loss of a methyl radical is esier than the loss of a hydrogen radical.

When the oxygen atom in compound **42** is replaced by an NR group, there is no evidence of intramolecular rearrangement.

As often happens and as previously described, the radical species can react to give mixtures of products. An example is given by a work from McNab and co-workers where the idea was to pyrolyse the *ortho N*-alkyl substituted oxime ethers **43** (Scheme 24).[22] The major product for the all three starting materials was 2-

cyanophenol **39**, salicylaldehyde **49** and 2-alkylbenzonitrile **45** *via* common intermediate **44**. The formation of **44** arise from a homolytic cleavage of the oxime ether bond followed by rearrangement to give an imidoyl radical **48** that undergoes β-cleavage to give **39**. Alternatively, the phenoxyl radical **47** can abstract a hydrogen atom followed by hydrolysis of the imine functionality to give **49**. The presence of the cyclised product **46** was only observed for **43 (i)**.

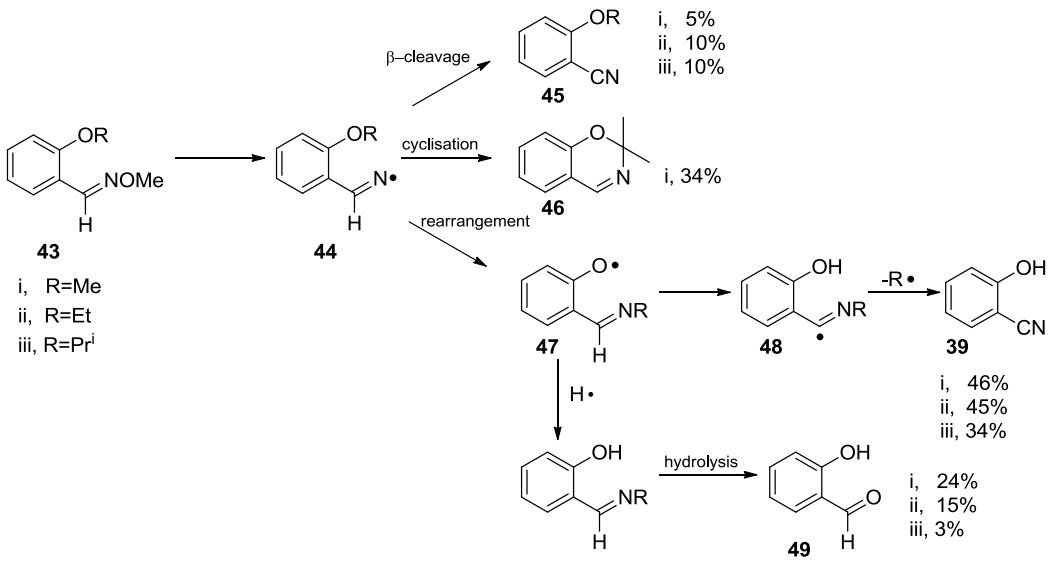

Scheme 24

Attempted cyclisation of iminyl radicals onto a thiophenyl group connected to a fused indole ring provided another significant result, in which an aldimine **51** was obtained. Unfortunately, the nitrile derivative **50** was a significant product again (Scheme 25).[23]

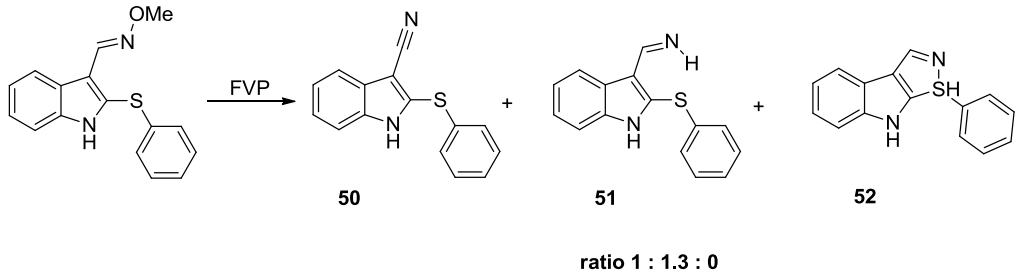

Scheme 25

In this case, the driving force for the reaction was the formation of the aldimine **51**, which is particularly stable due to the fact that there is a possible interaction between the imine proton and the sulfur. In addition, there is a significant energy barrier towards the formation of **52** due to the strain that would arise from the formation of two fused 5-membered rings.

3.3. Cyclisation

In the mideighties, the reactivity of some iminyl radicals toward aryl systems was reviewed (Scheme 26).[24]

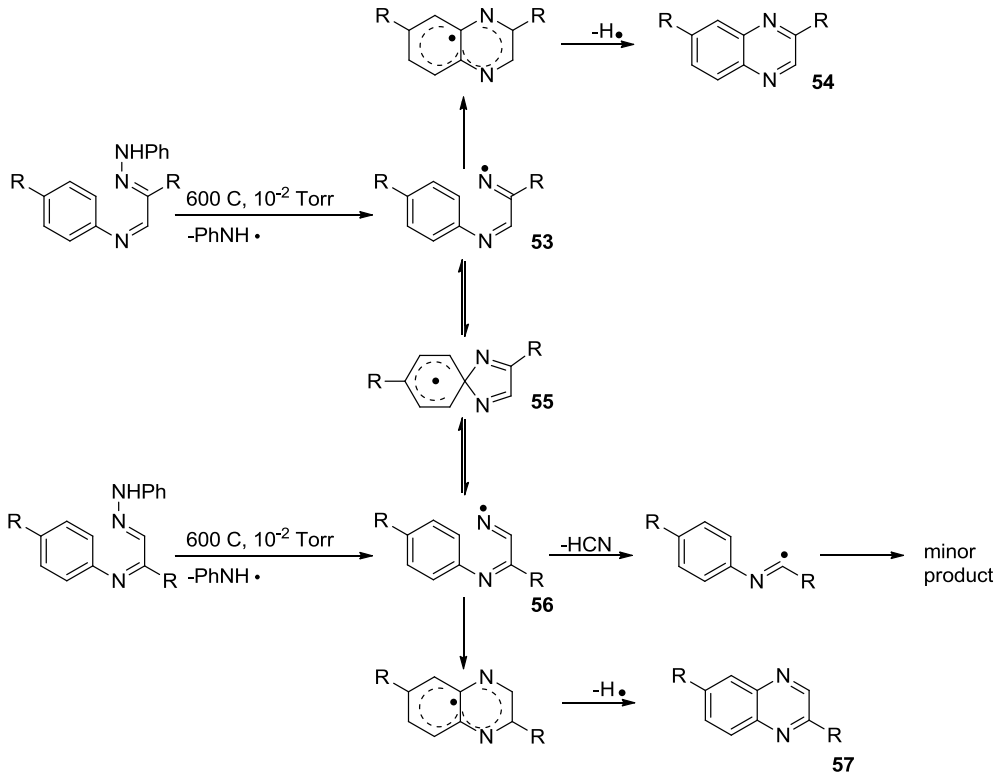

Scheme 26

The iminyl radicals can be formed by FVP of hydrazone imines (**21**, X = NHPh, *c.f.* Scheme 15) giving radical **53** which can directly cyclise to give the quinoxaline **54** or interconvert *via* spiro-radical **55** to form radical **56** which can also cyclise to give the quinazoline **57**. Assuming that the spiro intermediate has an equal probability of converting to radical **53** or **56**, the ratio of *ipso* or *ortho* attack is 3 : 5 for **53** and from the second radical **56** is 7 : 6. In addition, an *ipso* attack is favoured by an *o*-OMe substituent while straight forward cyclisation is favoured by *o*-Me and *o*-chloro substituents.

In the case where two *ortho*-methyl substituents are present on the benzene ring (Scheme 27), quinoxalines are the minor products. Instead, the major product is 7-methylindole **58**.

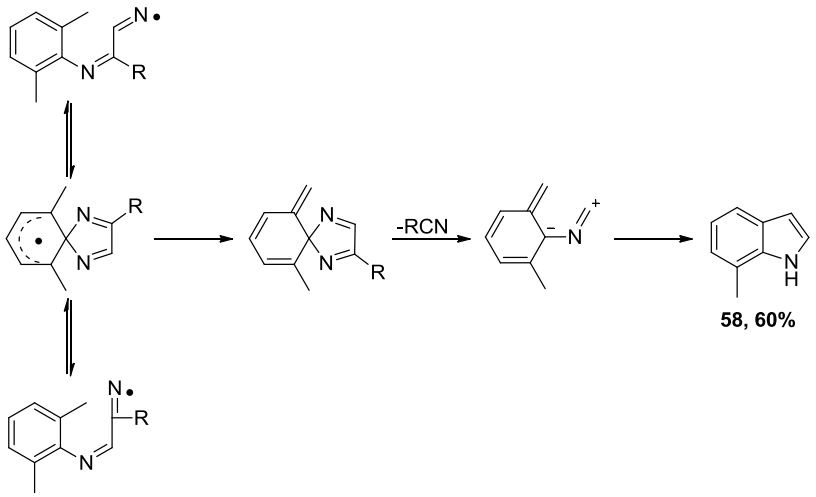

Scheme 27

Analysing the reactivity of the iminyl radicals **59** shown in Scheme 28, it is evident that the corresponding quinolines **60** were formed as the major products by direct cyclisation, without rearrangement *via* a spiro intermediate. Cinnamonitriles **61** are significant by-products of β-cleavage. It is worth noting that this is an unusual method to produce isomerically pure 7-substituted quinolines.

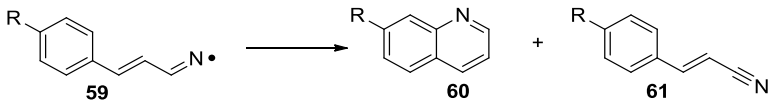

Scheme 28

Another example of cyclisation is given by the thiophenoxyl iminyl systems shown in Scheme 29. The iminyl radicals are generated by FVP of the oxime ether **62** as described and subsequent cyclisation to give benz[*d*]-isothiazoles **64**. This behaviour is different from the corresponding indole-fused systems (*c.f.* Scheme 25).

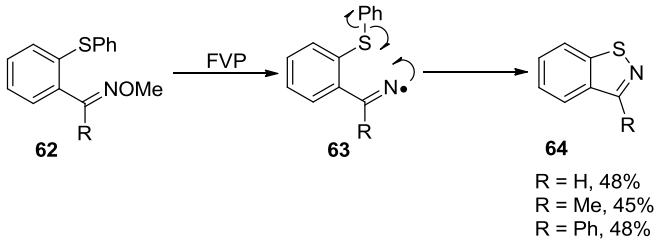

Scheme 29

Thiophenoxyl iminyl radicals **63** can also undergo β-cleavage: when R = Me both products **65** and **66** are observed; when R = H only **65** is observed due to the higher energy of the C-H bond compared to the energy of C-C bond (Scheme 30).[25]

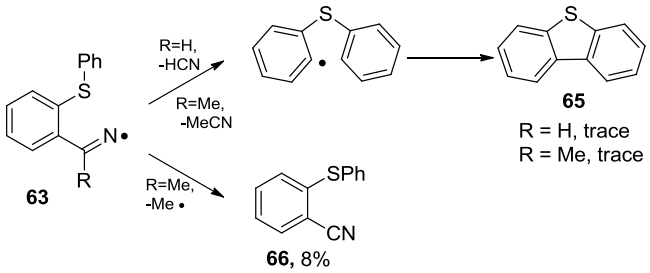

Scheme 30

The next example reports a cyclisation of iminyl radical onto a heterocyclic ring (Scheme 31).[23]

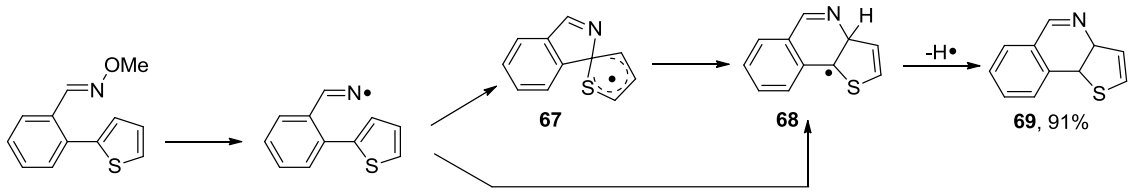

Scheme 31

The reaction proceeds with an excellent yield to give a single regioisomeric product **69** (91%). It is not clear whether the reaction proceeds *via* formation of a spiro intermediate **67** (with 100% cleavage of the N-C bond rather than the C-C bond) or whether direct cyclisation occurs giving **68**.

Another three examples were explored in the McNab group.[2] In the first example, the iminyl radical **69** is bonded to a heterocyclic ring (pyridine), while the other examples show the cyclisation of iminyl radicals **70** and **71** onto two different heterocyclic rings (furan and thiophene rings) to generate three different three-ring fused heterocyclic systems **72**, **73** and **74** (Scheme 32).

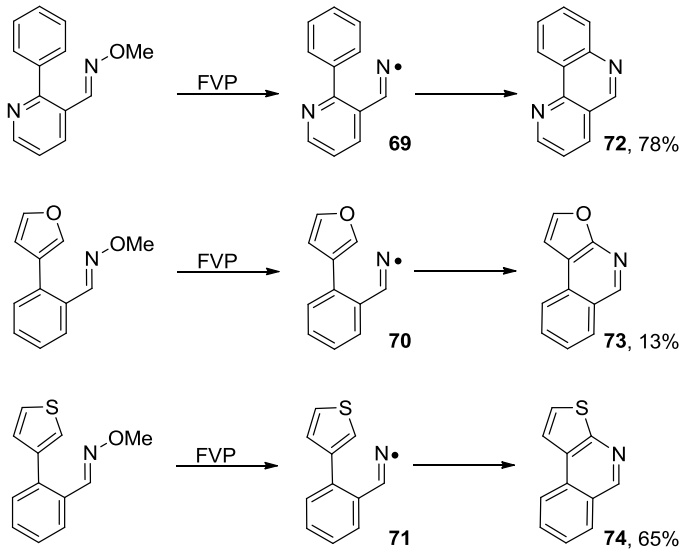

Scheme 32

In all three cases isomerically pure products, nominally obtained by direct cyclisation, were isolated. However, it is perhaps more likely that these products were obtained by initial formation of a spiro intermediate, followed by selective C-N rather than C-C migration.

In addition, all three products were obtained as single products and cyclisation onto the 4-position was not observed (Scheme 33). This is due to the fact that if the iminyl radical attacks at position 2, the resulting radical **75** is stabilised through the aromatic structure, otherwise, attacking in position 4, the resultant radical **76** is not stabilised.

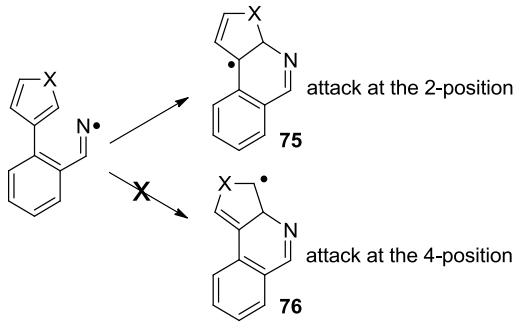

Scheme 33

The other products synthesised by McMillan by the same iminyl cyclisation procedure are reported in Figure 3.[2]

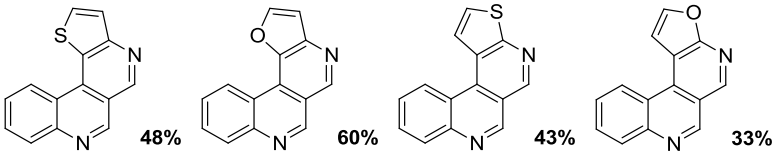

Figure 3: cyclisation products obtained *via* iminyl radical formation from corresponding oxime ethers under FVP conditions.

Chapter 2:

Rearrangement and cyclisation reactions on the 1-arylpyrrol-2-iminyl – 2-aryliminopyrrol-1-yl radical energy surface.

This work as been submitted for publication as '*Rearrangement and cyclisation reactions on the 1-arylpyrrol-2-iminyl – 2-aryliminopyrrol-1-yl radical energy surface*', Scott Borthwick, Jonathan Foot, Maria Ieva, Hamish McNab, Emma J. Rozgowska and Andrew Wright.

Manuscript **ID OB-ART-09-2010-000726** has been recommended for publication in *Organic & Biomolecular Chemistry* subject to revision in line with suggested corrections.

Acknowledgements

The following people are gratefully acknowledged for their contribution to this chapter: Prof. Hamish McNab for conceived of the overall project idea, Mr. Scott Borthwick, Mr. Jonathan Foot, Dr. Emma Rozgowska and Mr. Andrew Wright for the experimental work. The Author developed all the DFT studies described in the following chapter.

Introduction

In previous papers we have explored the cyclisation reactions of iminyl radicals, generated in the gas-phase under flash vacuum pyrolysis (FVP) conditions.[26] In some cases, *e.g.* aryliminoiminyls, these reactions are dominated by *ipso*-attack and rearrangement *via* spirodienyl radicals (Scheme 34, X = N),[27] leading to mixtures of cyclisation products. The mechanism was supported by ^{15}N-labelling experiments.[28] However, corresponding rearrangements are not observed for arylvinyliminyls[29] (Scheme 1, X = CH) so the products must be formed either by direct cyclisation or by formation of the spirodienyl intermediate followed by exclusive migration of the C=N bond.

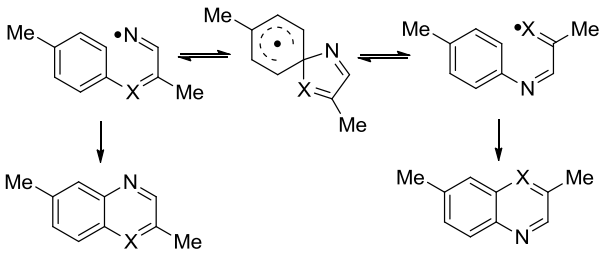

Scheme 34

The aims of the work reported here are summarised in Scheme 35. First, we hoped to generate the iminyl **77** (X = N) by the standard method involving FVP of the corresponding oxime ether. With two fused 5-membered rings, the spirodienyl intermediate **79** (X = N) is necessarily more strained than its analogue in Scheme 1 but, if rearrangement were to take place, generation of the pyrrol-1-yl radical **78** (X = N) would provide complementary entry to the energy surface. However, almost nothing is known about the synthetic organic chemistry of pyrrol-1-yl radicals except that a dimeric product is obtained when a vast excess of pyrrole is decomposed in the presence of *t*-butyl peroxide.[30] Tetra-arylpyrrol-1-yl radicals have been characterised by EPR spectroscopy;[31a] more recently, the pyrrol-1-yl radical itself has been implicated in UV photodissociation experiments[32b] and its electron affinity has been measured.[32c] Meanwhile, considerable theoretical work on the structure of the pyrrol-1-yl radical has been carried out.[32c,32]

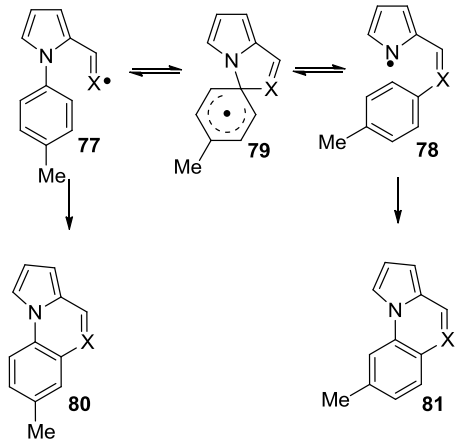

Scheme 35

In the context of the present work, inventing a general FVP precursor to pyrrol-1-yl radicals for use in synthetic and mechanistic chemistry was therefore a major target. With a precursor for **78** (X = N) in place, the strategy was extended to the case of the 2-styrylpyrrolyl **78** (X = CH), though no attempt was made to create a route to the vinyl radical (**77**, X = CH). Finally, the mechanistic details of the rearrangement processes were analysed by DFT calculations at B3LYP/cc-pVDZ level.

Results

The iminyl precursor **84** was made by the route shown in Scheme 36. Vilsmeier formylation of 1-(*p*-tolyl)pyrrole **82** gave, in our hands, a mixture of the 2- and 3-formyl isomers, from which the 2-isomer **83** was obtained by recrystallisation (70%).[33] Condensation with *O*-methylhydroxylamine hydrochloride gave the oxime ether **83** (83%) as a mixture of *E*- and *Z*-isomers which were not separated.

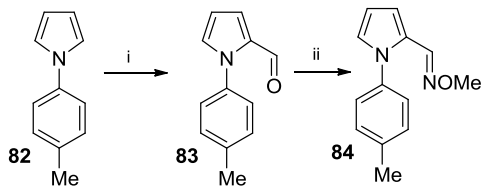

Scheme 36 ***Reagents and conditions:*** **(i) DMF/$POCl_3$, 20 °C; (ii) $MeONH_2$, EtOH, reflux.**

In order to design a precursor for the pyrrol-1-yl radicals **78**, it was essential for the molecule to have a weak N-X bond which would cleave homolytically upon pyrolysis. Often we have used benzyl or allyl groups for this purpose,[27] but it is known that *N*-benzyl- or *N*-allyl- pyrrole undergoes rearrangement by 1,5-sigmatropic shifts rather than radical cleavage.[34] However, we have also shown that hydrazones are useful generators of iminyl radicals[27,28] and so the possibility of using derivatives of *N*-(dimethylamino)pyrrole **85** was investigated. FVP of *N*-(dimethylamino)pyrrole **85** itself showed the formation of pyrrole **86**, as well as some unidentified products, which suggests that homolysis could be followed by hydrogen atom capture, a standard reaction of aminyl and phenoxyl radicals (Scheme 37).[27] The temperature profile of the **85**→**86** conversion (Fig. 4) shows that temperatures of 800-850 °C are required to complete the homolysis.

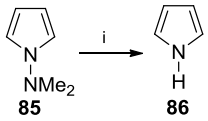

Scheme 37 Reagents and conditions: (i) FVP, 850 °C.

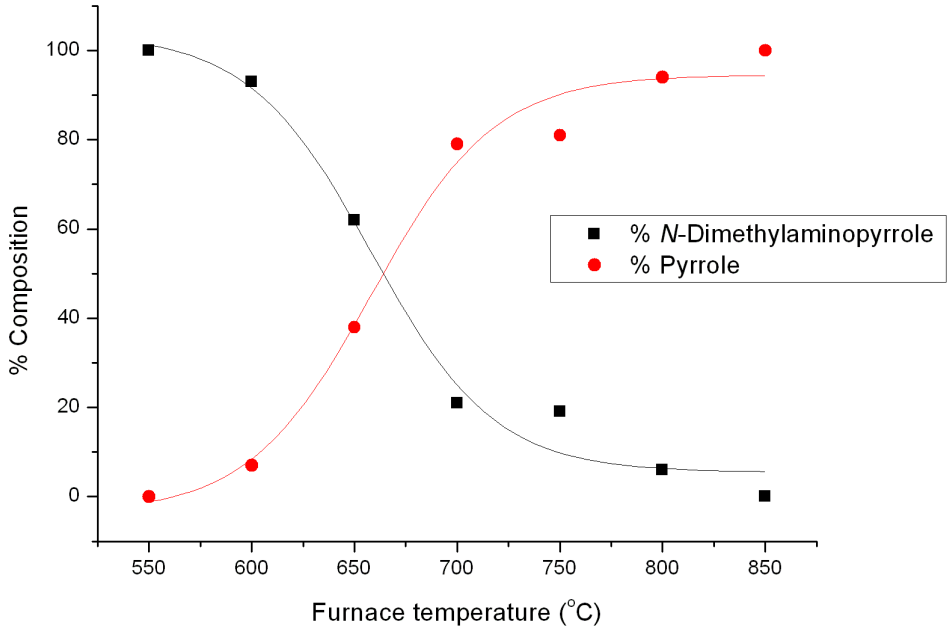

Figure 4: Temperature profile of 85→86 conversion.

With this result in hand, a precursor to **78** (X = N) was made in two steps. First, formylation of **85** was carried out by the literature method;[36] the 2-formyl isomer **87** was isolated as the major product (52%) after chromatography, though some of the 3-formyl product **90** was also obtained (12%). The imine **88** (97%) was synthesised by condensation with *p*-toluidine (Scheme 38). The precursor to **78** (X = CH) was made by Wittig reaction[35] of the aldehyde **87** with the ylide **90a** which gave the 2-styryl compound **89** (Scheme 38). The corresponding 3-styryl compound **91** was made similarly by reaction of the 3-formylpyrrole **90**.

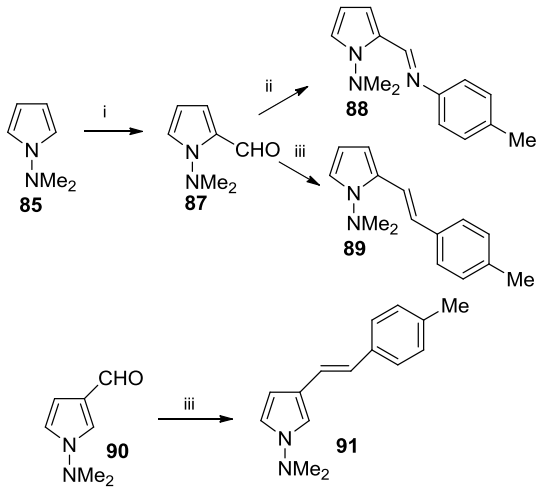

Scheme 38 Reagents and conditions: **(i) DMF/$POCl_3$, 1,2-dichloroethane, reflux; (ii) *p*-$MeC_6H_4NH_2$, EtOH, reflux; (iii) Ph_3P=CHAr 90a, toluene, reflux.**

FVP of the oxime ether **84** gave two heterocyclic products in essentially equal amounts (40% and 41% isolated yields), together with small amounts of 1-*p*-tolylpyrrole-2-carbonitrile **94** (8%) and 1-*p*-tolylpyrrole **82** (5%), all of which were separated by chromatography (Scheme 39). The heterocyclic products were identified as 7-methylpyrrolo[1,2-*a*]quinoxaline **92** and 8-methylpyrrolo[1,2-*a*]quinoxaline **93** by the NOESY data shown in Figure 5. Compound **92** is characterised by the correlation of a pyrrole proton at δ_H 7.86 (corresponding to H-1) with a doublet benzenoid proton at δ_H 7.82 (corresponding to H-9). Compound **93** is characterised by the correlation of a pyrrole proton at δ_H 7.91 (due to H-1) with a 'singlet' benzenoid proton at δ_H 7.68 (due to H-9).

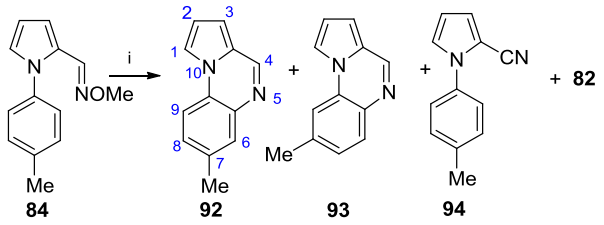

Scheme 39 Reagents and conditions: (i) FVP, 650 °C.

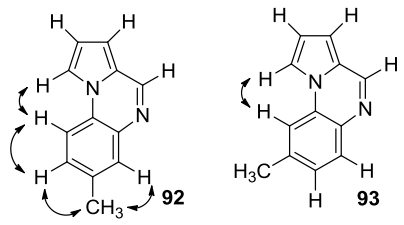

Figure 5: NOE data for 92 and 93.

The formation and unambiguous characterisation of **92** and **93** suggests that the iminyl **77** (X = N) is able to undergo *ipso*-attack to generate the spirodienyl radical **79** (X = N) (Scheme 35) which subsequently rearranges to the two regioisomeric products. However, it is unclear whether interconversion *via* the spirodienyl is complete or whether this reaction mode competes with direct cyclisation at the *ortho*-position.

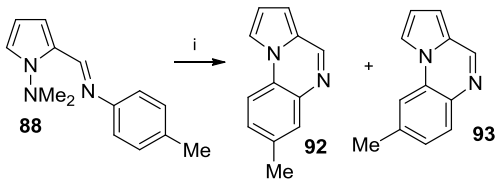

Scheme 40 Reagents and conditions: (i) FVP, 800 °C.

More information on this point was gained by FVP of the *N*-dimethylaminopyrrole **88** at 800 °C (Scheme 40) which provided the two methylpyrrolo[1,2-*a*]quinoxalines **92** (23% of the mixture) and **93** (73% of the mixture) (4% of mixture not assigned). First, this provides further evidence that the pyrrol-1-yl radical **78** (X = N) can be generated by this route and that it is capable of cyclisation reactions to provide 6-membered ring products. Second, the formation of the two heterocyclic products **92** and **93** shows that at least some cyclisation *via* the spirodienyl must take place. However, the fact that these products were obtained in unequal ratio (in contrast to

the result from FVP of **84**) is evidence that direct cyclisation must also play a part in the energy surface summarised by Scheme 35 (see Discussion section) and provides the major product from the pyrrol-1-yl.

In contrast, FVP of the styryl compound **89** at 750 °C gave only 8-methylpyrrolo[1,2-*a*]quinoline **95** (50% yield) (Scheme 41). NOESY analysis confirmed the structure by correlation of a pyrrole proton with a 'singlet' benzenoid proton (*c.f.* **93** in Fig. 5). In this case *E/Z*-isomerisation of the alkene[36] is followed by direct cyclisation at the *ortho*-position, or by spirodienyl formation followed by exclusive migration of the C-N bond. Such high regioselectivity has major advantages in the use of pyrrol-1-yl radicals as a synthetic route to unusual pyrrolo[1,2-*a*]quinolines.

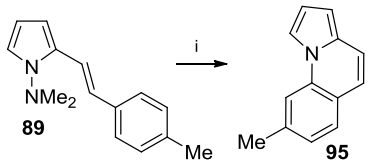

Scheme 41 Reagents and conditions: (i) FVP, 750 °C

Only low yields of products could be isolated from FVP of the 3-styryl isomer **91** at 750 °C which suggests that the 3-substituted pyrrol-1-yl radical has no clear route to products (Scheme 42). The two compounds that were isolated in greatest amounts were the known[37] deaminated pyrrole **96** (11%) (*c.f.* Scheme 37) together with some 8-methylpyrrolo[1,2-*a*]quinoline **95** (5%).

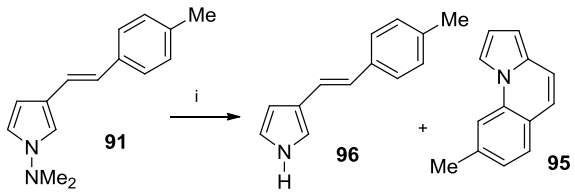

Scheme 42 Reagents and conditions: (i) FVP, 750 °C.

Discussion

To summarise the experimental results, independent generation of the iminyl **77** (X = N) and of the pyrrol-1-yl **78** (X = N) radicals results in isomeric mixtures of the cyclisation products 7-methylpyrrolo[1,2-*a*]quinoxaline **92** (*i.e.* **80**, X = N) and 8-methylpyrrolo[1,2-*a*]quinoxaline **93** (*i.e.* **81**, X = N), though in different ratios from the two precursors. In contrast, generation of the pyrrol-1-yl **78** (X = CH) provides only 8-methylpyrrolo[1,2-*a*]quinoline **95** (*i.e.* **81**, X = CH). The situation is summarised by Scheme 43, an extension of Scheme 35, in which the iminyl **77** (X = N) is potentially in equilibrium with the direct cyclisation intermediate **97** (X = N) and the spirodienyl radical **79** (X = N). Similarly, the pyrrol-1-yl **78** (X = N) can equilibrate with its direct cyclisation intermediate **98** (X = N) and with the spirodienyl **79** (X = N).

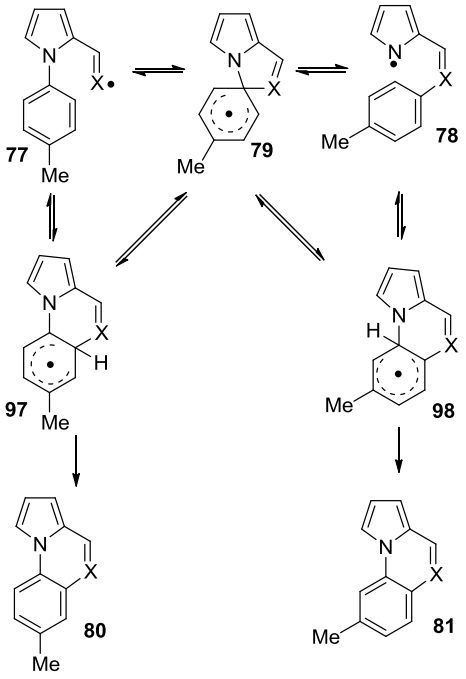

Scheme 43

The energy surface of the *N*-phenyliminyl corresponding to **77** (X = N) was modelled by DFT calculations (B3LYP/cc-pVDZ) (Fig. 6).[38] These show that the difference in barrier between the iminyl **77** (X = N) and the direct cyclisation intermediate **97** (X = N) and between the iminyl and the spirodienyl **79** (X = N) is 21.5 kJ mol^{-1} in favour

of the direct cyclisation. The corresponding difference between the pyrrol-1-yl **78** (X = N), its direct cyclisation intermediate **98** (X = N) and the spirodienyl **79** (X = N) is 26.6 kJ mol^{-1}, again in favour of the direct cyclisation. This suggests that the direct cyclisation is relatively favoured kinetically in the case of the pyrrol-1-yl, as found by experiment. Thermodynamically, the spirodienyl **79** (X = N) lies 40.6 kJ mol^{-1} above the direct cyclisation intermediate **97** [from the iminyl **77** (X = N)] and some 59.9 kJ mol^{-1} above the direct cyclisation intermediate **98** [from the pyrrol-1-yl **78** (X = N)]. Again, direct cyclisation from the pyrrol-1-yl is relatively favoured thermodynamically, though it is somewhat surprising that the spirodienyl route can compete at all, given the high relative energies of its intermediate and transition states.

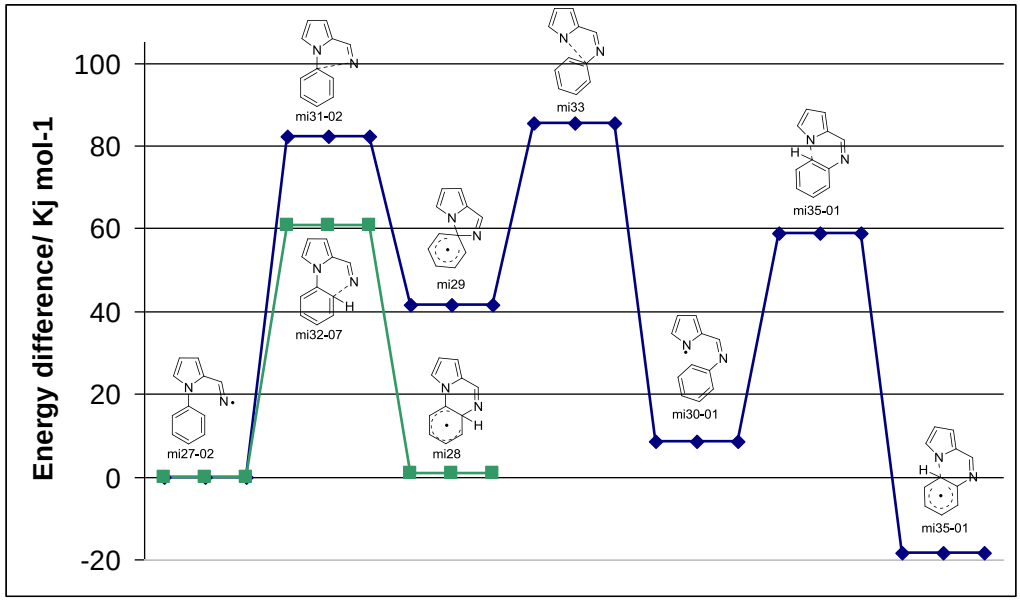

Figure 6: The iminyl 77 (X = N) – pyrrol-1-yl 79 (X = N) energy surface; codes refer to the structures given in experimental section.

By comparison, the difference in energy between the transition states relating the pyrrol-1-yl **78** (X = CH), its direct cyclisation intermediate **97** (X = CH) and the spirodienyl **79** (X = CH) is 55.6 kJ mol^{-1}, in favour of the direct cyclisation. Similarly, the energy of the spirodienyl **79** (X = CH) itself is some 72.9 kJ mol^{-1} higher than that of the direct cyclisation intermediate **97** (X = CH). The results of the calculations clearly suggest that only one isomer is formed by FVP of **88**, because

direct cyclisation of the pyrrol-1-yl takes place, rather than formation of the spirodienyl and exclusive migration of the C-N bond. Nevertheless, cleavage of the C-N bond in the spirodienyl **79** (X = CH), if formed, is indeed favoured over C-C cleavage by 31.8 kJ mol^{-1}. The very high energy of the vinyl radical **77** (X = CH) may help to explain why no precursor of such species under FVP conditions is known.

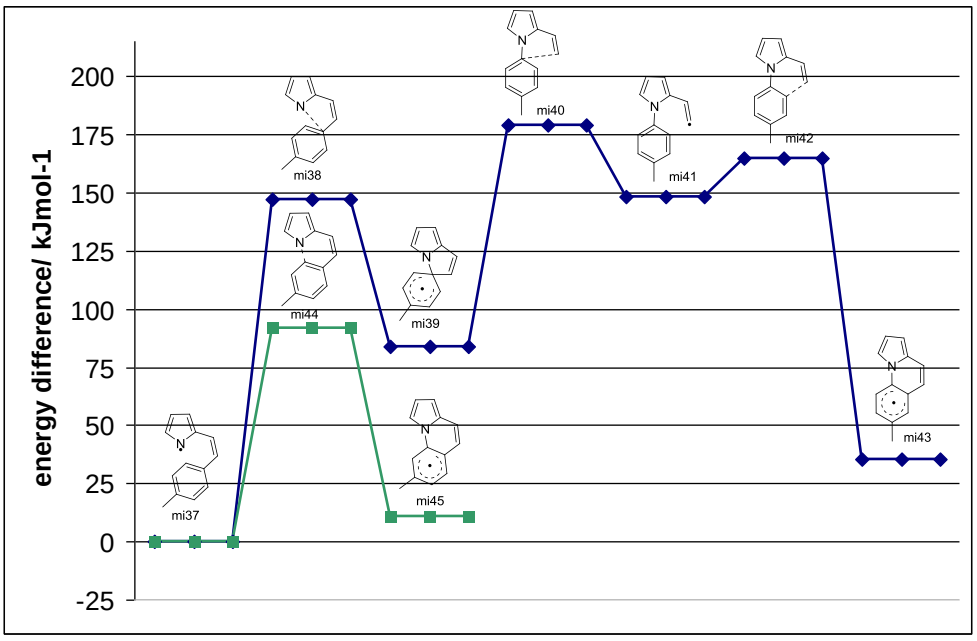

Figure 7: The vinyl 77 (X = CH) – pyrrol-1-yl 79 (X = CH) energy surface; codes refer to the structures given in the experimental section.

Finally, it is worth noting that pyrrol-1-yl radicals generated by homolysis of the N-N bond, are formed as σ- radicals[39] (*e.g.* σ **99**, Figure 7a) but intersystem crossing to the π-surface to give π-**99** (Figure 7a) is likely to be facile.[32a] Delocalisation of the π-radical might promote some reactivity at the 3-position of species such as **78**. In practice, whatever the electronic nature of the radical species involved, there is no doubt from the experimental results [including the very low yield of cyclisation product(s) by FVP of the 3-substituted precursor **91**] that the pyrrolyl radical species *behave* as σ- radicals localised on the nitrogen atom.

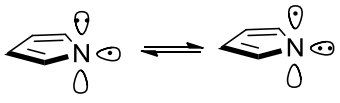

σ **99** π **99**

Figure 7a: rappresentation of equilibrium between σ- radical form and π-radical form of pyrrol-1-yl radical 99.

Conclusion

We conclude that FVP reactions of 1-aminopyrrole derivatives provide useful routes to pyrrol-1-yl radicals, whose cyclisation chemistry is explored here for the first time. Cyclisation of 2-vinylpyrrol-1-yls proceeds regiospecifically to provide an unusual route to the pyrrolo[1,2-*a*]quinoline ring system. On the other hand, cyclisation of pyrrol-1-yls containing an arylimino side chain takes place *via* spirodienyl radical formation and rearrangement, in competition with direct cyclisation. This result was confirmed by the cyclisation behaviour generation of an isomeric iminyl radical.

Chapter 3:

Generation of new fused heterocyclic rings *via* iminyl radicals cyclising onto pyrrole type and indole type rings and study of their reactivity.

1. Introduction

As was mentioned in Chapter 1, there have been several reports of heterocyclic ring formation by cyclising iminyl radicals onto aryl and heterocyclic rings. However a cyclisation of an iminyl radical onto a pyrrole ring has never been reported. Attempts have been made within the McNab group[40] to cyclise different heteroatomic radicals onto pyrrole rings some of which are shown in Scheme 44.

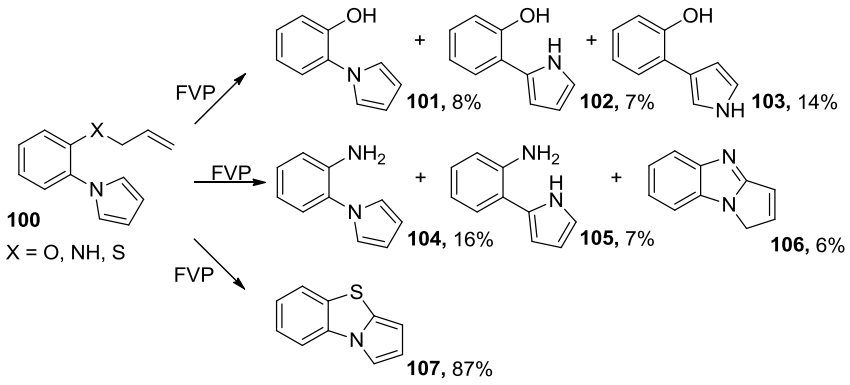

Scheme 44

Pyrolysis of *N*-[2-(allyloxy)phenyl]pyrrole (**100**, X = O) gave the three isomers (**101**, **102** and **103**) of *N*-(hydroxyphenyl)pyrrole. This is due to a [1,5]-sigmatropic shift although it not possible to assign whether it is a rearrangement of the radical generated in the gas phase **108** or a rearrangement of the *N*-(2-hydroxyphenyl)pyrrole **101** (Scheme 45).

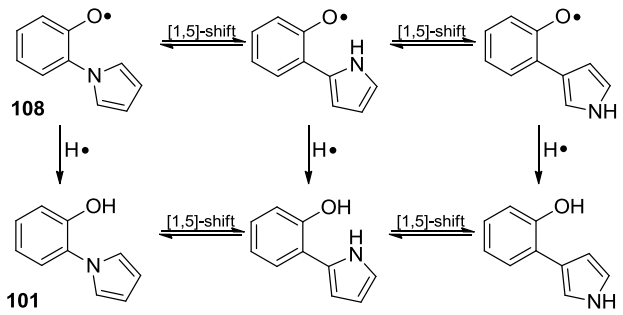

Scheme 45

Likewise, in the second example in Scheme 44 (**100**, X = NH), the formation of the first two products **104** and **105** might occur in the same way described in Scheme 45

involving a [1,5]-sigmatropic shift. The third product **106** is the cyclisation of a NH radical on a pyrrole followed by a rearrangement (Scheme 46).

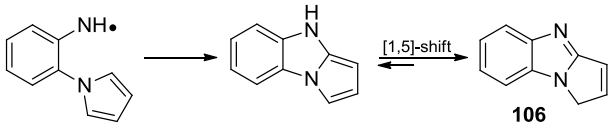

Scheme 46

It was isolated but found not to be stable to purification by chromatography. In a later project, it was possible to perform full characterisation of the cyclised product using the crude reaction mixture. In the last example in Scheme 44 cyclisation was observed upon pyrolysing *N*-[2-(allylthio)phenyl]pyrrole (**100**, X = S). The cyclised product **107** was obtained in high yield.

2. Aim of the project

The aim of this project was to form 6-membered rings (**111**) by cyclising iminyl radical **109** (starting from oxime ether **110**) onto pyrrole. If successful, it was planned to try to cyclise the iminyl radical **113** onto indole to form a 6-membered ring **114** and/or a 7-membered ring **115**. It was also hoped to extend this methodology to the carbazole system generating a 7-membered ring **116** (Scheme 47).

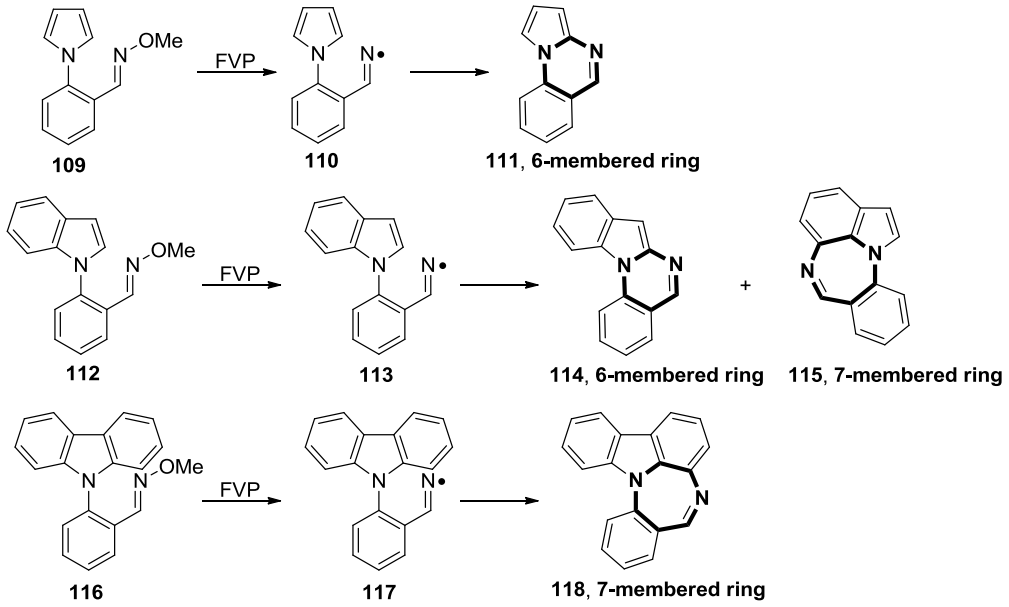

Scheme 47

3. Synthesis of the FVP precursors

The syntheses of the three oxime ethers **109**, **112** and **116** follow similar paths. The most significant difference was in the first step for each compound of the series.

3.1. 2-(Pyrrol-1-yl)benzaldehyde *O*-methyloxime

2-(Pyrrol-1-yl)benzaldehyde *O*-methyloxime **109** was inteded to be synthesised *via* the following retrosynthetic pathway (Scheme 48):

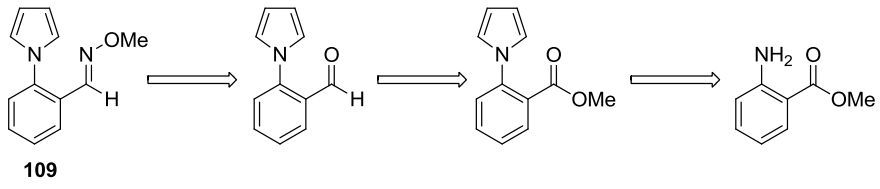

Scheme 48

The first step in the synthesis consisted of formation of the pyrrole ring by reaction of methyl anthranilate with 2,5-dimethoxytetrahydrofuran, Scheme 49. This step proceeded in the short time of 20 mins.[41] The evidence that methyl 2-(pyrrol-1-yl)benzoate **119** was generated was the appearance in the ^{1}H NMR spectrum of the typical signals (double triplet) of the pyrrole at 6.69 and 6.19 ppm.

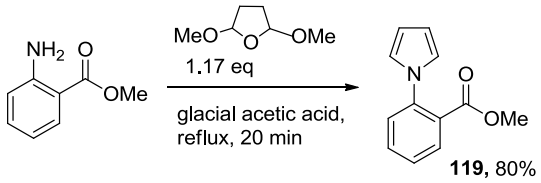

Scheme 49

The subsequent step provided the corresponding alcohol **109** by reduction of the ester functionality. To do so, a standard procedure was followed using lithium aluminium hydride in dried diethyl ether (Scheme 50).[42] In this case, the evidence of the successful reaction was the disappeance of the signal corresponding to the methyl group in the ^{1}H NMR spectrum and the appearance of the signal at 4.51 ppm integrating for two protons due to the formation of the CH_2.

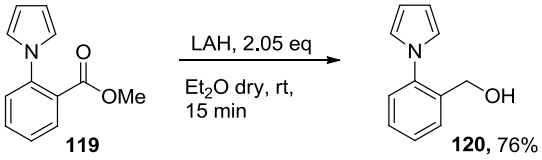

Scheme 50

2-(Pyrrol-1-yl)benzaldehyde **121** was obtained by oxidation of the corresponding alcohol **120** with MnO_2 in toluene (Scheme 51).[43] The signal at 9.92 ppm in the ^{1}H NMR spectrum is indicative of the H in the aldehyde functional group and confirmed the success of the reaction.

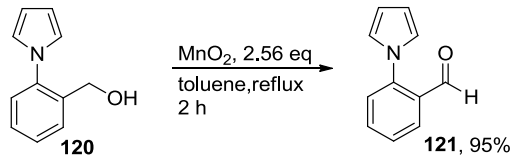

Scheme 51

The target FVP precursor **109** was obtained by reacting **121** with *O*-methyl-hydroxylamine hydrochloride in methanol. In this specific case, a pH of approximately 4 was necessary, so a few drops of AcOH were added (Scheme 52).[43] In the oxime ether formed, the aldehyde proton shifts from δ_H 9.92 ppm to 7.84 ppm and a new peak integrating as 3H at 3.97 ppm emerged due to the methoxy group.

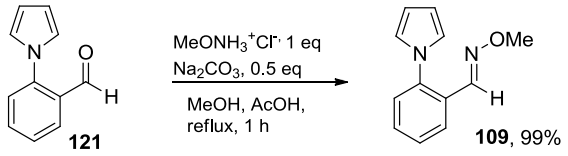

Scheme 52

3.2. 2-(Indol-1-yl)benzylaldehyde *O*-methyloxime

The synthesis of 2-(indol-1-yl)benzylaldehyde *O*-methyl-oxime **112** was planned from the following retrosynthetic path (Scheme 53).

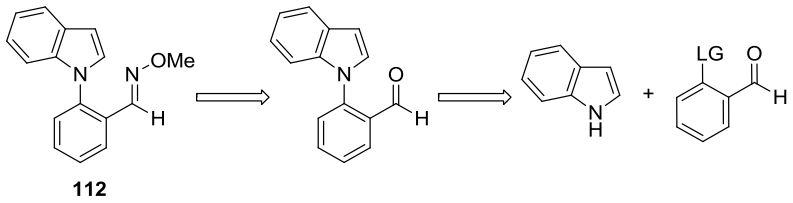

Scheme 53

The first reactions to be tried were those between indole or skatole and 2-fluorobenzaldehyde (entry 1, Table 1).

Entry	reactant	base	solvent	temperature (°C)	time (h)
1	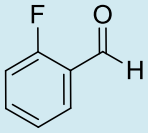	Cs_2CO_3	DMF	rt→140	16
2	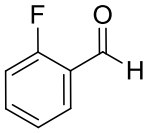	Cs_2CO_3	DMSO	rt→160	16
3	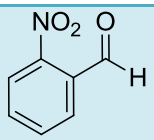	Cs_2CO_3	DMF	rt→140	16
4	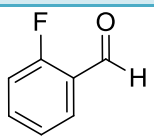	NaH	DMF (dry)	rt→140	16

Table 1: reaction conditions used for attempted SNAr described in Scheme 53.

The reason behind using skatole alongside indole was due to the possible deprotonation of the N-H proton in indole leading to a resonance form in which the negative charge would reside in the 3-position, resulting in substitution at this carbon instead of the nitrogen (Scheme 54). With the use of skatole, the only substitution that can potentially occur is at the 1-position.

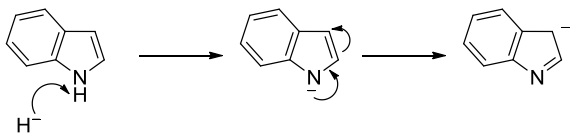

Scheme 54

These two reactions were carried out using Cs_2CO_3 in DMF ranging from room temperature to reflux (≈140 ºC). Unfortunately neither of the desired products was found after the work-up of any of these reactions. The only evidence that was found from the reaction was the disappearance of the aldehyde peak. It was not possible to identify any products. The same two reactions were repeated substituting DMF with DMSO to increase the polarity of the system (entry 2, Table 1). Several attempts were made with temperatures ranging between room temperature and 160 ºC. These

reactions were also unsuccessful and again the only evidence that can be reported is the disappearance of the aldehyde peak.

At this point it was decided to change strategy by altering the leaving group in the *ortho* to the benzaldehyde (entry 3, Table 1). Unfortunately the result here was the same: no desired products were formed and the crude ^{1}H NMR spectrum did not show the presence of an aldehyde peak. In a last attempt at this step, a different deprotonating reagent was tested (entry 4, Table 1). Indole and skatole were reacted with sodium hydride first in dry DMF. The solution showed signs of formation of an anion by formation of yellow solution from a colourless one. At this point, 2-fluorobenzaldehyde was added and the reaction heated a 140 °C for 16 h. Unfortunately, no products were observed by TLC.

It was subsequently decided to try a different approach starting from *o*-iodobenzoic acid reacting with indole. The ester **122** was formed in a second step by adding methyl iodide to the reaction mixture (Scheme 55).[44] This reaction gave 45-50 % yield, but required five days for the starting material to be consumed. The formation of the ester was evident by the appearance of the methyl peak at 3.55 ppm in the ^{1}H NMR spectrum.

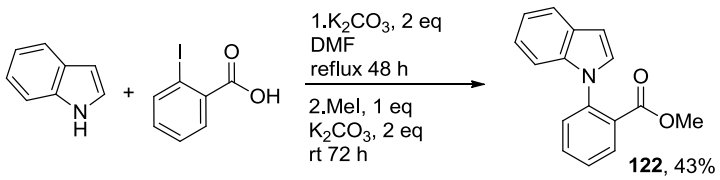

Scheme 55

The subsequent two steps were the same as those described in Schemes 50 and 51. Firstly reduction with LAH to obtain the corresponding alcohol **123** followed by an oxidation step to afford the 2-(indol-1-yl)benzaldehyde **124** in good yield (Scheme 56). As described in the case of the pyrrole system, the evidence for the formation of the alcohol **123** was given by the appearance of a peak in the ^{1}H NMR spectra integrating for two protons at 4.41 ppm and for the aldehyde **124** at 9.72 ppm for the carbonyl proton.

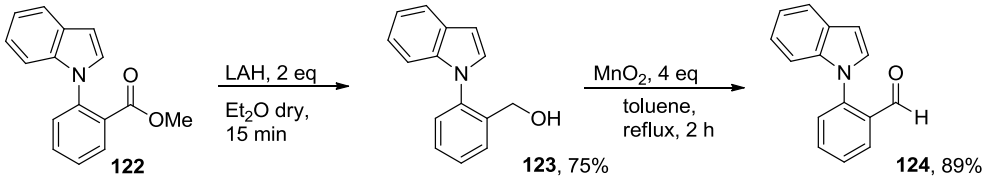

Scheme 56

2-(Indol-1-yl)benzaldehyde *O*-methyloxime **112** was then obtained using a standard procedure by reacting the aldehyde **124** with *O*-methylhydroxylamine hydrochloride in ethanol while heating under reflux (Scheme 57). Again, the appearance of the methyl peak and the ^{1}H NMR shift of the aldehyde group compared with the one of the oxime were evidence of the success of the reaction.

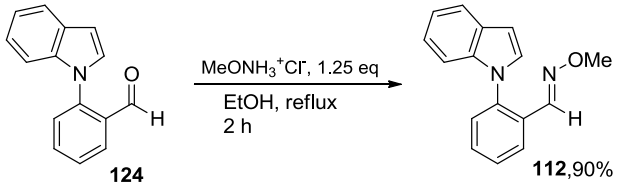

Scheme 57

3.3. 2-(Carbazol-1-yl)benzylaldehyde *O*-methyloxime

The retrosynthetic path to 2-(carbazol-1-yl)benzylaldehyde *O*-methyloxime **116** was almost identical to that used to access the indole oxime (Scheme 58).

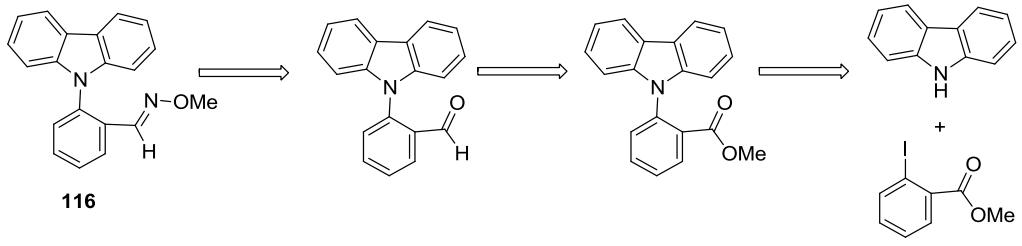

Scheme 58

The first step was the reaction described by Glaser, Blount and Mislow to obtain ester **125** (Scheme 59).[45] 9*H*-Carbazole and methyl 2-iodobenzoate were reacted in the presence of K_2CO_3 and copper powder. A minimal quantity of nitrobenzene was

used as solvent. The work-up of this reaction was particularly difficult due to the fact that the resultant crude mixture was a hard orange solid which needed to be broken up before it could be suspended in water and chloroform.

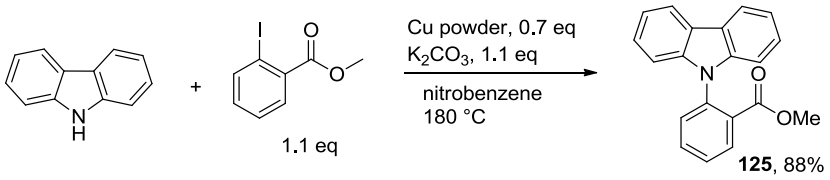

Scheme 59

It is thought that this reaction proceeds either by deprotonation of the carbazole N-H proton followed by aromatic substitution onto the methyl 2-iodobenzoate or *via* coordination of the copper to methyl 2-iodobenzoate and carbazole thus aiding coupling of the two reagents.

The steps to access the carbazole oxime **116** were the same as those previously used. The same considerations already made for pyrrole-based system and indole-based system led to the success of the reaction for the carbazole-based system.

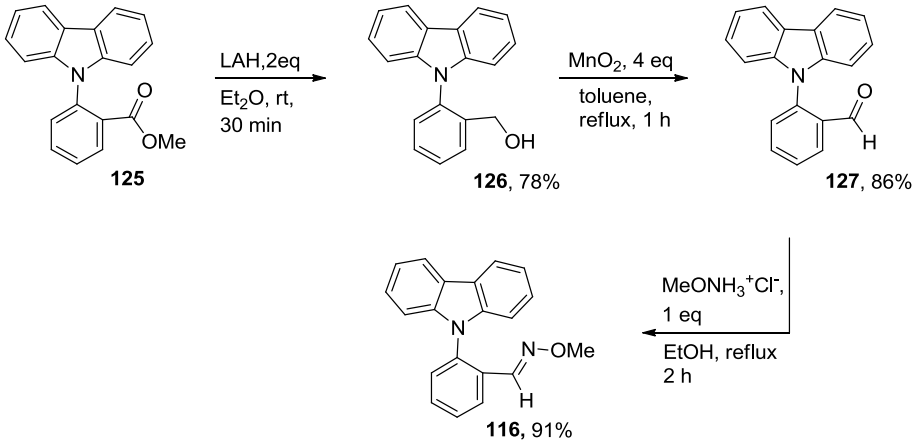

Scheme 60

4. FVP of the oxime ethers

The three oxime ethers produced **109**, **112** and **116** which were then all subjected to FVP. This involved heating the starting material into the gas phase and passing this

material through a furnace at high temperatures under reduced pressure. A reaction takes place within the furnace tube and the product is collected in a liquid nitrogen cooled trap. The optimal furnace temperature is the one at which the starting material is no longer present (or the majority of it is transformed) and the desired product does not undergo decomposition.

The first attempt of FVP is usually carried out on a small scale (≈ 30 mg) until the optimal temperature is found, at which point the pyrolysis is then performed on a larger scale. The resultant crude produced is then analysed with the appropriate techniques and purified if necessary.

4.1. FVP of 2-(pyrrol-1-yl)benzaldehyde *O*-methyloxime

Pyrolysis of oxime **109** at 700 ºC successfully generated the target cyclised material pyrrolo[1,2-*a*]quinazoline **111** along with the corresponding nitrile **128** (Scheme 61).

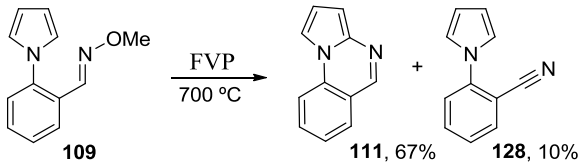

Scheme 61

The crude reaction mixture was purified by Kugelrohr distillation and it was kept at low temperature to prevent degradation. Attempts to separate the two products **111** and **128** were unsuccessful. Therefore, all the analyses were performed on the mixture.

Proof that the cyclised product was obtained was given overall by ^{1}H NMR spectroscopy. From the spectrum it was possible to notice the disappearance of methyl signal from the methoxyl substituent and the shifting of the proton in the α position to the oxime group from 7.84 to 8.48 ppm. 2D NMR spectroscopy was carried out to further confirm the structure of **111**.

The COSY spectrum of the cyclised product is shown in Figure 8. The coupling between nuclei through bonds can be seen in COSY spectrum. The COSY spectrum in Figure 8 shows the coupling between protons '**a**' (as H_3) and '**b**'(as H_2), which both couple with '**c**'(as H_1). It is also possible to see the coupling among protons '**f**',

'**e**' and '**g**' (as H_7 H_8 and H_6), and between '**e**' and '**d**' (as H_9), but the most significant of all is the coupling between '**h**' and '**d**'(as H_5 and H_9).

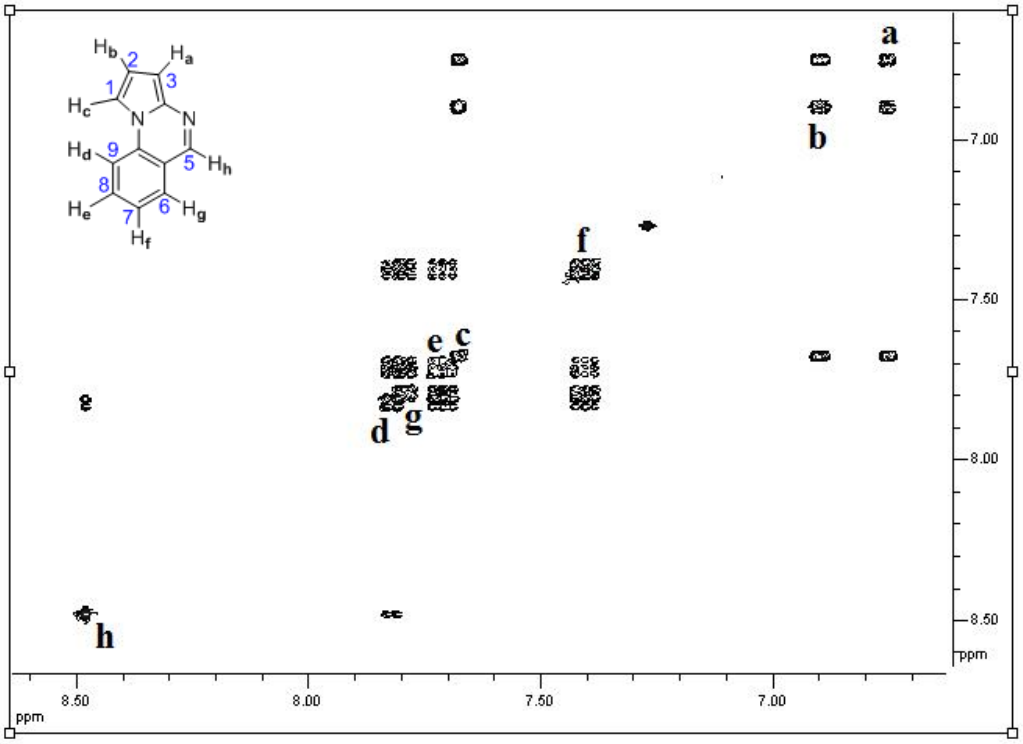

Figure 8: COSY spectrum of compound 111.

There are two possible locations for '**h**' in the molecule as can be seen in Figure 9. Compound A shows a possible zig-zag 5-bond coupling and compound B places '**d**' close to '**h**' in bond distance.

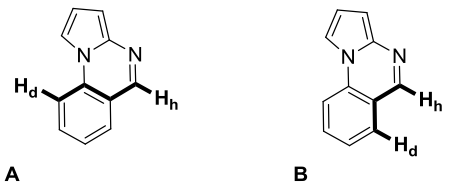

Figure 9: two possible H-H interactions in the COSY spectrum of compound 111.

In order to assign the position of proton '**d**', a ^{1}H NOESY analysis was performed (Figure 10). In this spectrum interaction between protons close in space can be seen. Looking at this spectrum, it can be noticed that proton '**b**' interacts with '**c**' and '**a**', '**f**' interacts with '**e**' and '**g**' (confirming the data from the COSY spectrum) and,

most importantly, '**g**' interacts with '**h**'. This last interaction allows unequivocal assignment of the proton nearest '**h**' in space.

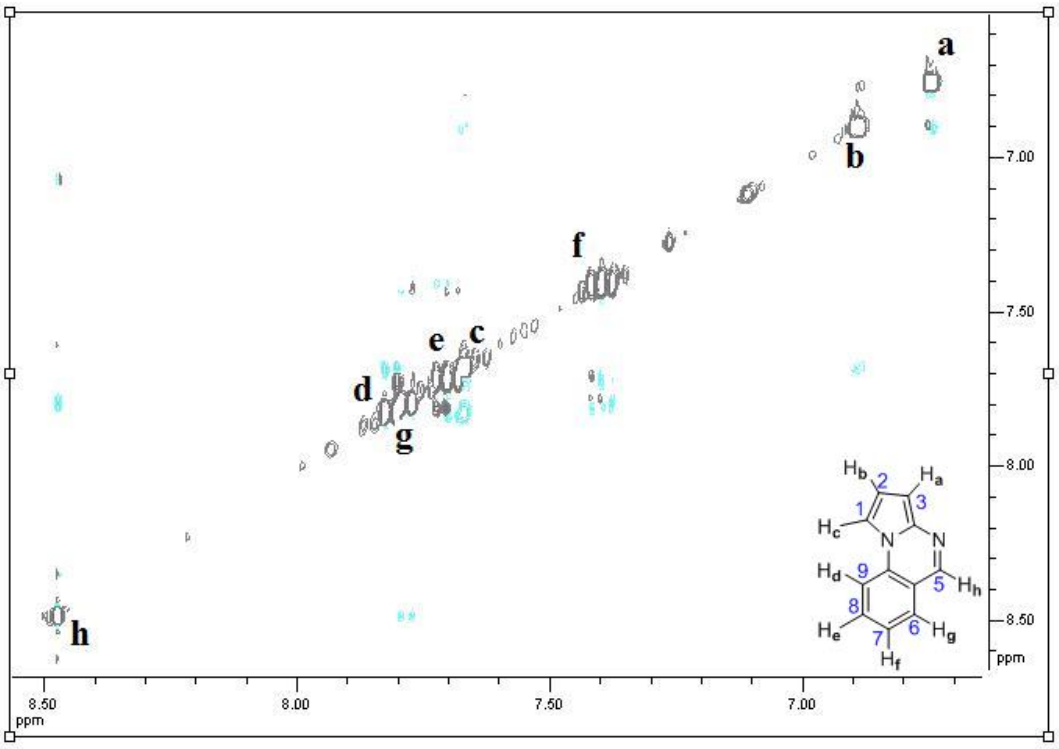

Figure 10: NOESY spectrum of compound 111.

The proposed mechanism for the cyclisation involves:

1. formation of nitrogen-centred radical **110** as a consequence of the cleavage of the weak N-O bond in the oxime group;
2. attack of the N-radical onto the pyrrole ring placing the radical in the 5-membered ring **129**;
3. loss of a H-radical with a restoration of the aromaticity.

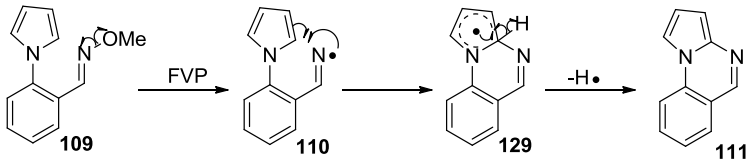

Scheme 62

The cyclised product **111** is a 3-ring system unknown in the literature as a parent compound. This compound has been mentioned by an Italian group,[46] but the paper contains a different isomer.

An example of a substituted pyrrolo[1,2-*a*]quinazoline is reported by Fryer *et al.*[47] Substituted pyrrolo[1,2-*a*]quinazolines were obtained according to the route shown in Scheme 63.

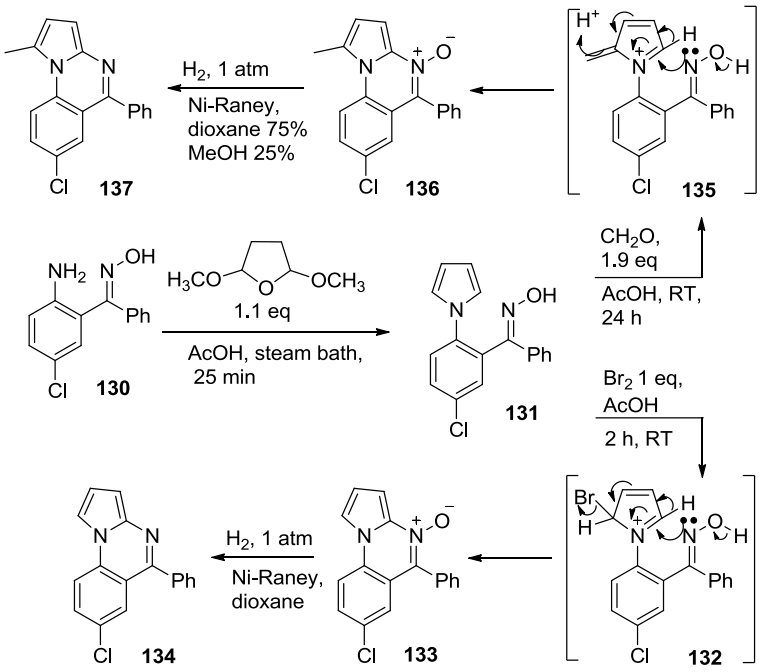

Scheme 63

o-Amino-5-chlorobenzophenone oxime **130** was reacted with dimethoxytetrahydrofuran to obtain the pyrrole moiety **131**. At this point, to achieve compound **134**, bromine in glacial acetic acid was added and species **133** was isolated. It was thought that mechanistically, the reaction proceeded *via* formation of intermediate **132** that then cyclised with simultaneous elimination of bromide to give **133**. The *N*-oxide species was then reduced with hydrogen and Raney-Nickel. Similarly, 1-methyl-pyrrolo[1,2-*a*]quinazoline **137** was obtained by reacting oxime **131** with formaldehyde (37% solution) in acetic acid, forming the *N*-oxide **137**. Again the reaction was thought to go *via* formation of positive charged intermediate **135**. The *N*-oxide was then reduced to the desired species **137**.

Because of the lack of information on these kinds of systems, it will be very interesting to study some properties of the parent member of this heterocyclic system.

As was well documented in the introduction, the formation of the second compound is due to the breaking of the N-O bond to form the iminyl radical and subsequent *β*-cleavage of the C-H bond (Scheme 64).

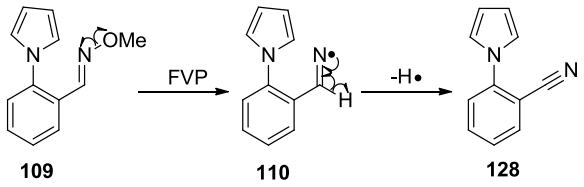

Scheme 64

Identification of nitrile **128** was confirmed subsequently by work carried out in the McNab group.[48] The desired compound was obtained by the different route shown in Scheme 65.

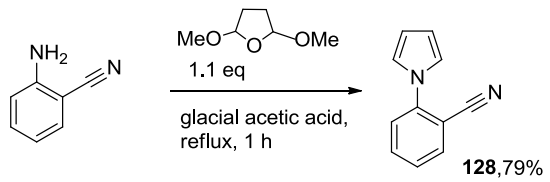

Scheme 65

The additional proof reinforced the theory of β-cleavage as an alternative mechanism to the cyclisation.

4.2. FVP of 2-(indol-1-yl)benzaldehyde *O*-methyloxime

Pyrolysis of compound **112** was carried out at 650 ºC and also yielded cyclised material indolo[1,2-*a*]quinazoline **114**, this validating this method of generating these 6-membered fused ring systems. One of the side products was assigned to be 2-indol-1-yl-benzonitrile **138**, another product was identified as aldehyde **124** and finally cyclised product **139** was identified. It is important to note that no traces of the 7-membered ring **115** were detected (Scheme 66).

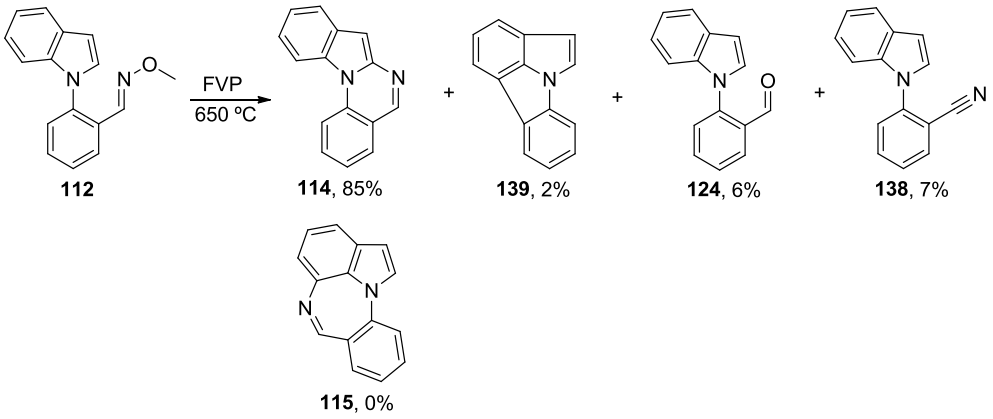

Scheme 66

The crude mixture collected in the 'U'-tube was an orange oil. The column-purified product was analysed by ^{1}H NMR. This analysis confirmed that the indolo[1,2-*a*]quinazoline **114** was obtained as the major product (85%). Proof that the cyclised product was obtained was given by ^{1}H NMR spectroscopy. From the spectrum it is possible to see the disappearance of methyl signal from the methyl oxime ether at δ 3.99 ppm proving that the starting material was consumed. 2D NMR spectroscopy was performed to fully characterise the compound. The COSY spectrum (Figure 11) shows the couplings among proton '**f**' (as H_{11}) with '**g-i**' (as $H_{10\text{-}8}$) and '**h**' (as H_9) and the coupling between proton '**b**' (as H_4) with '**c**' (as H_3) and '**d**' (as H_2) and weakly with '**e**' (as H_1). Proton '**e**' also couples with '**d**', '**c**' and '**a**' (zig-zag interaction). The final important coupling for the identification of the protons in the phenyl ring is the one between '**g-i**' with '**h'**. The last coupling to be reported is the one between '**l**' (as H_7) and '**f**'.

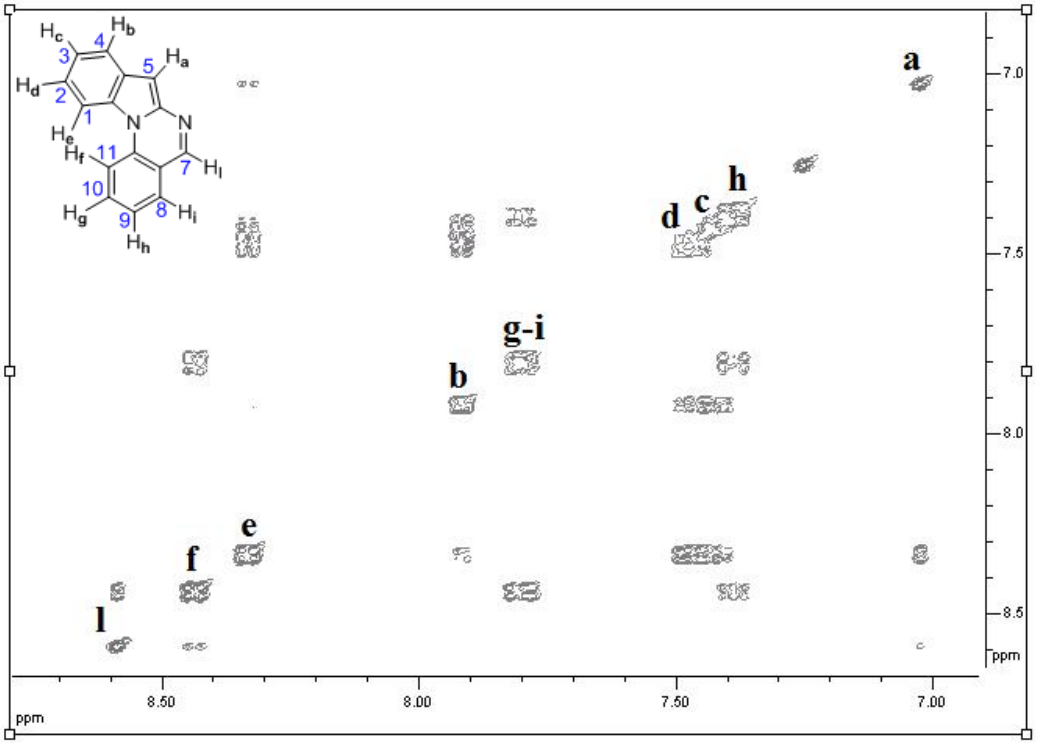

Figure 11: COSY spectrum of compound 114.

Also in this case there are two possible locations for the proton '**f**' as can be seen in Figure 12.

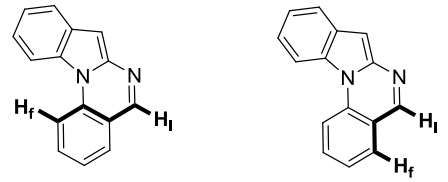

Figure 12: two possible H-H interactions in the COSY spectrum of compound 114.

NOESY analysis was performed to avoid any doubt. In the ^{1}H NOESY spectrum (Figure 13) it can be seen that proton '**l**' interacts with '**i**' which is important to identify the position of '**f**'. Proton '**f**' interacts strongly with '**e**' and also with '**g**'. These interactions make it possible to assign the resonances to the correct protons and to confirm the structure of the heterocycle. The NOESY spectrum also shows an interaction between '**i**' and '**h**' as well and '**c**' and '**b**'. Finally, proton '**a**' (as H_5) can help to identify the adjacent proton which must therefore be proton '**b**' judging by the weak, but visible interaction.

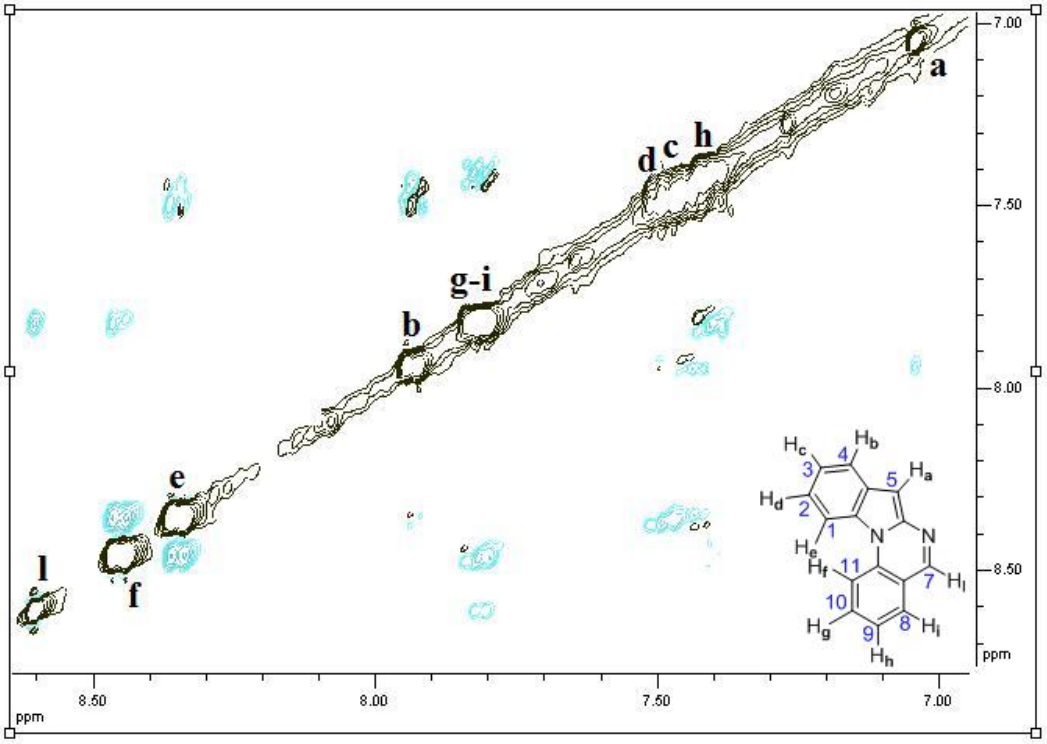

Figure 13: NOESY spectrum of compound 114.

The mechanism for the cyclisation is the same as proposed in the case of pyrrolo[1,2-*a*]quinazoline (Scheme 67).

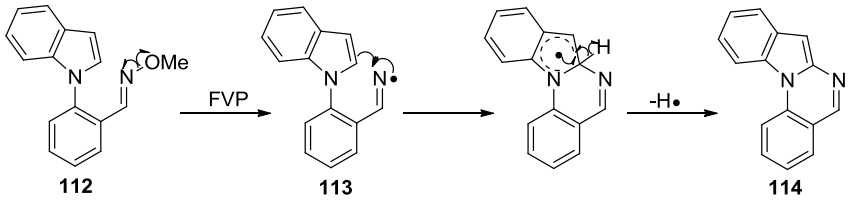

Scheme 67

The cyclised product **114** is a four-fused ring system which was previously unknown in the literature. Recently, however, Vidal e al.[49] reported a method to synthesise substituted indolo[1,2-*a*]quinazolines such as **141** (i and ii). They proved that these kind of systems can be synthesised by [3 + 2] intramolecular addition of an azido moiety with the C=C of a ketenimine **140** functionality present in the substrate (Scheme 68).

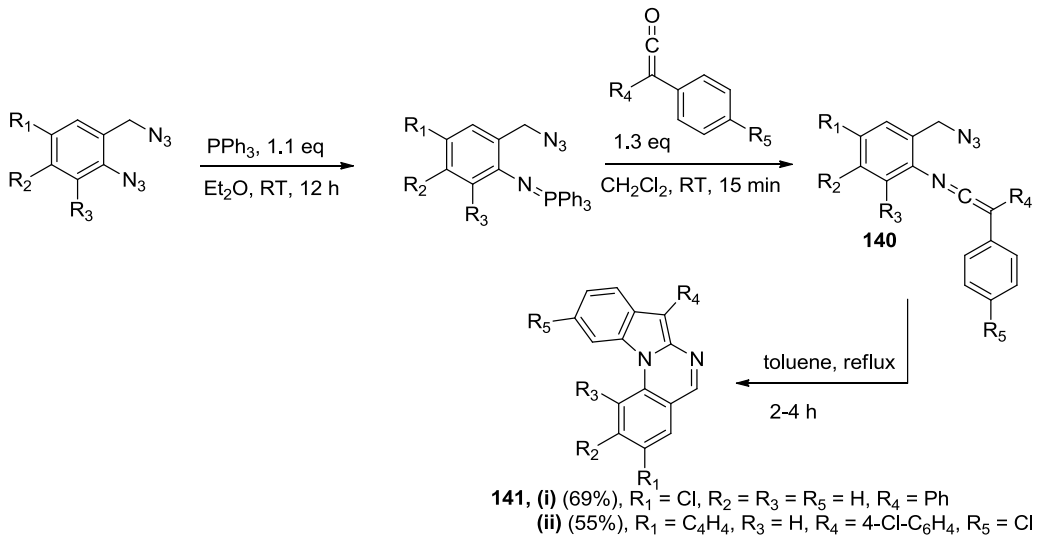

Scheme 68

The examples with best yields are reported in Scheme 68. The reaction is thought to proceed *via* formation of a di-radical **143** after loss of N_2 from product of the [3 + 2] cycloaddition **142**. The di-radical can then rearrange to give **144** that can then cyclise to give intermediate **145**. The final product **141** is obtained after loss of H_2, (Scheme 69).

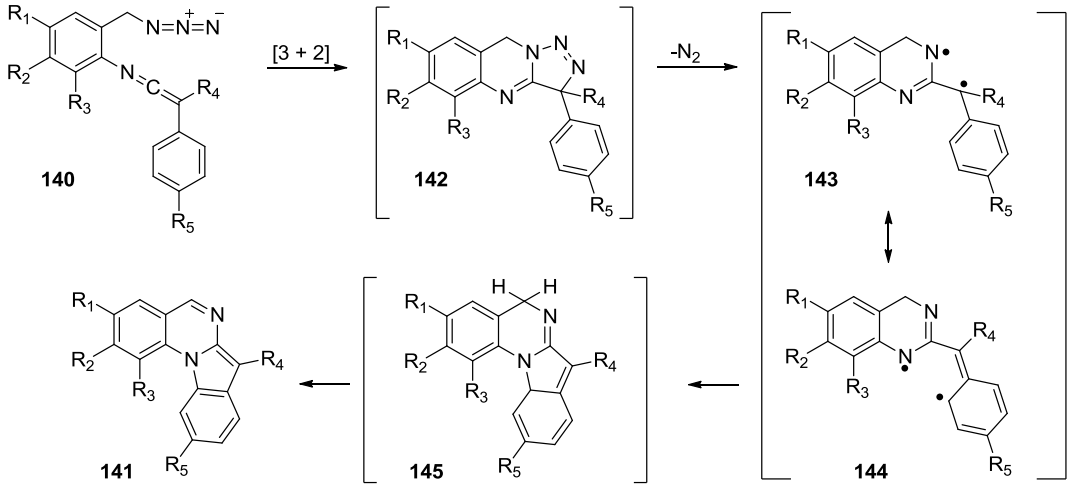

Scheme 69

Of course, a limit to this methodology is given by the availability of the ketenimines and azido substrates. Because nothing is known about the parent compound, some of the properties of interest will be studied.

The crude pyrolysed product also included three side products. The first was assigned as cyclised product **139**. The ^{1}H spectrum was compared with spectrum reported in the literature.[50]

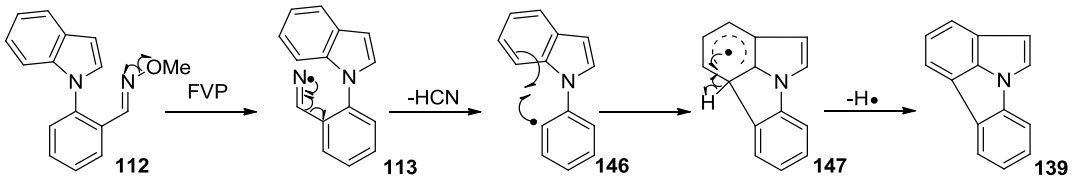

Scheme 70

The proposed mechanism for the cyclisation involves:

1. formation of nitrogen-centred radical as a consequence of the cleavage of the weak N-O bond in the oxime group **113**;
2. β-cleavage of C-C bond with loss of HCN and formation of phenyl radical **146**;
3. attack of the phenyl radical onto the indole core forming a new 5-membered ring and placing the radical inside the phenyl ring (**147**);
4. loss of a H-radical with a restoration of aromacity to give **139**.

The third compound isolated from the mixture was aldehyde **124**. It was possible to identify this compound by comparing the ^{1}H NMR spectrum with the one obtained previously. The mechanism by which this compound was formed under FVP conditions is not clear at this point.

The last product isolated from the crude mixture was 2-indol-1-yl-benzonitrile **138**. The nitrile derivative is again formed by β-cleavage of the C-H bond (*c.f.* Scheme 64). This compound is known in the literature and its ^{1}H NMR spectrum was compared with the original spectrum confirming the structure assigment.[51]

4.3. FVP of 2-(carbazol-1-yl)benzaldehyde *O*-methyloxime

Pyrolysis of **116** was performed at 700 °C and did not afford any of the desired 7-membered cyclised material **117**, but the corresponding 2-carbazol-9-yl-benzonitrile **148** was obtained instead in 55% yield (Scheme 71).

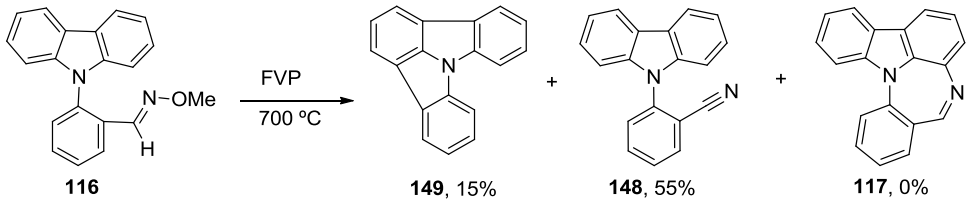

116 **149**, 15% **148**, 55% **117**, 0%

Scheme 71

Nevertheless, nitrile **148** is unknown in the literature and was therefore fully characterised by ^{1}H NMR and ^{13}C NMR. The main proof that this compound was obtained was provided by IR spectroscopy in which a typical signal for nitrile at 2359 cm^{-1} was observed.

This outcome of the pyrolysis is probably due to the fact that formation of a 7-membered ring is far less favoured than formation of a 5-membered ring. As is known in the literature, rearrangement often occurs to a 6-membered ring.[52]

The formation of the nitrile **148** follows the same mechanisms previously reported (*c.f.* Schemes 62 and 65) and is shown in Scheme 72.

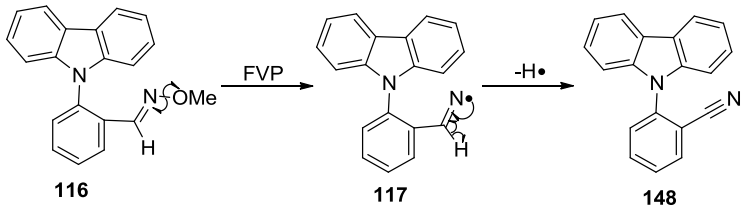

116 **117** **148**

Scheme 72

Another product from the pyrolysis was isolated (15%) and identified as cyclised product **149**, which had already been synthesised *via* a different route in the McNab group.[53] Again, this cyclised product can be obtained *via* the mechanism described in Scheme 70.

5. Density Functional Theory (DFT) calculations

DFT calculations are a tool of computational chemistry that can be used in organic chemistry to confirm experimental results or to predict the course of a reaction.
DFT calculations have been used in this work to gain an understanding of why products were obtained in certain ratios. Calculations make it possible to draw an energy profile which can help in understanding kinetically and thermodynamically controlled reaction pathways.

5.1. Pyrrole based iminyl system

As described previously, FVP of 2-(pyrrol-1-yl)benzaldehyde *O*-methyloxime formed two products, **111** and **128**, in 67% and 10% yield respectively. The corresponding calculated reaction profile is shown in Figure 14.

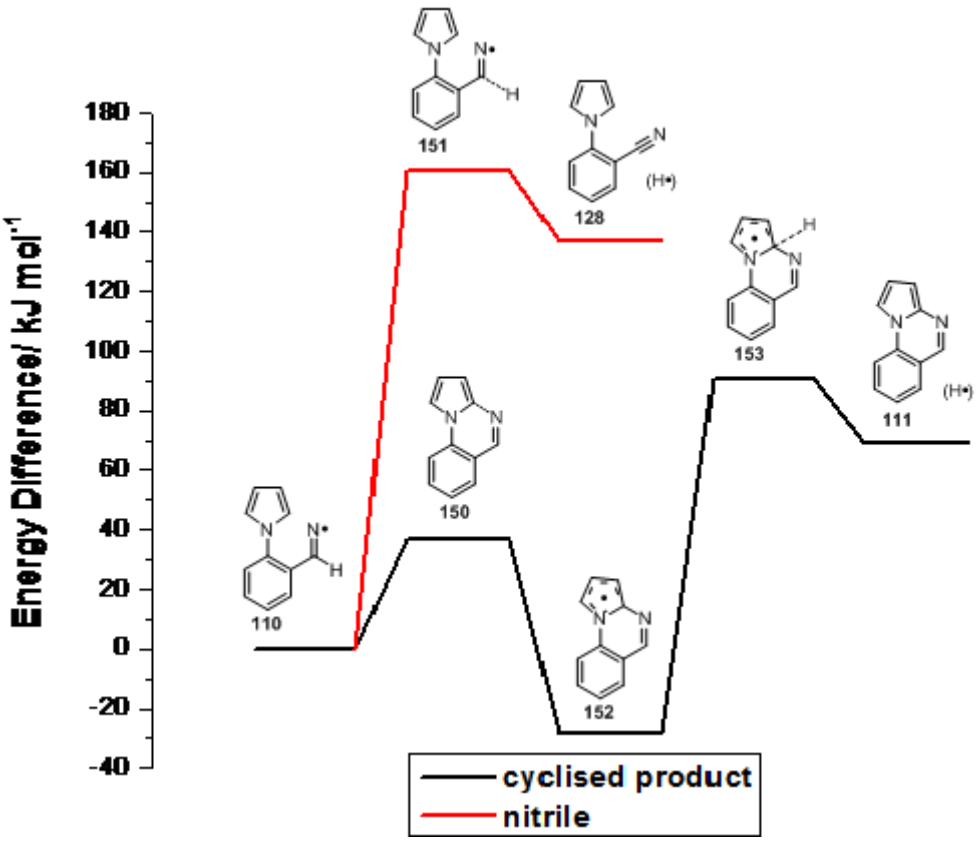

Figure 14: calculated energy profile of compound 111 and 128.

The first point to note is that the energy barrier to attack of the iminyl radical onto the pyrrole ring leading to TS **150** is lower than the barrier that leads to loss of the H radical leading to formation of the nitrile **128**. Having attacked the pyrrole ring *via* TS **150**, intermediate **152** is formed which is much more stable than the starting iminyl radical. Finally, cyclised intermediate **152** must lose H· to form product **111.** The barrier for loss of this H· to achieve **153** is ≈40 kJ/mol lower than the corresponding barrier to loss of H· to yield the nitrile. This is another reason for preferred formation of **111**. The major product (seen experimentally) is favoured thermodynamically and kinetically.

It is important to note that the energy levels of the nitrile and cylised products are quite high. That is due to the fact that it is not possible to compare the energy of molecules with different numbers of atoms, so it is necessary to include the energy of H· to both of these final products. This is not an accurate approximation because the H radical is probably not a free radical, but may be trapped by the surface of the furnace tube of the FVP apparatus. This explains why the energies of the two final products are both calculated to be higher than that of the starting material.

5.2. DFT calculations on the indole system

FVP of 2-(indole-1-yl)benzaldehyde *O*-methyloxime generated two main products **114** and **138**, **114** being the major species. DFT calculations have been performed to prove that the major product is favoured thermodynamically and kinetically. In the case of the indole system, the formation of a 7-membered ring leading to **115** was possible although none of this material was observed experimentally. To prove that this was the less favoured possible product, the calculations on this pathway have been included in the energy profile (Figure 15).

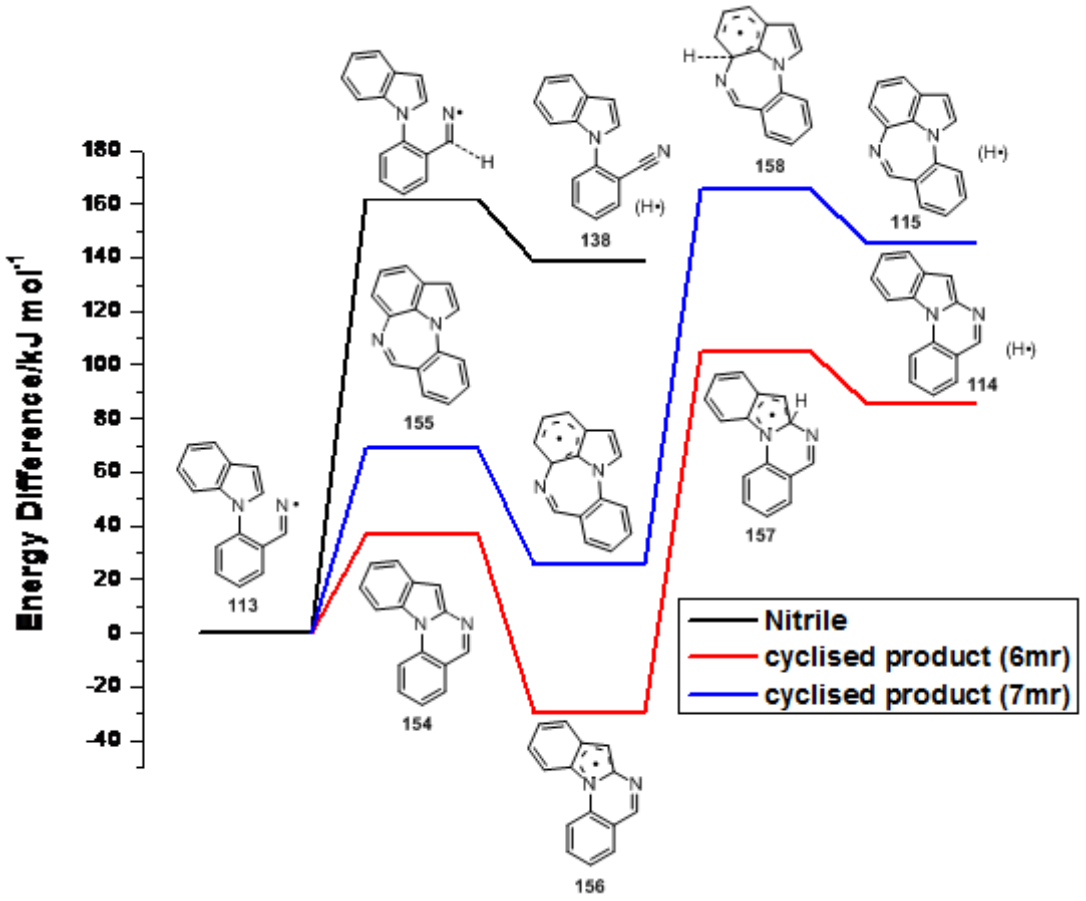

Figure 15[54]: calculated energy profile of compound 114, 115 and 138.

In the graph it can be seen that the highest energy barrier is that of loss of H· to yield the nitrile. This does not explain why the nitrile **138** is observed experimentally when the 7-membered cyclised product **115** is not. It therefore has to be taken into account the fact that the nitrile product **138** is lower in energy than the 7-membered ring **115**. It is important to notice that the major product (6-membered ring) has the lowest energy barrier among the three. Comparing the 6-membered ring profile and the 7-membered ring profile it is clear that the energy required to reach the first transition state (the attack of iminyl radical to the 1-position to give **154** or in the 7-position to give **155** of the indole ring) is about 33 kJ/mol lower in the case of the 6-membered ring. It is important to note that the first intermediate **156** for the formation of the 6-membered ring is lower in energy than the starting material. The energy barriers to achieve the final products are quite similar (140 kJ/mol for the 7-membered ring to

give TS **158** and 135 kJ/mol for the 6-membered ring to give TS **157**) but the final 6-membered ring **114** has energy about 60 kJ/mol lower than the 7-membered ring **115**.

6. Reactivity

In the previous paragraphs, two interesting compounds were reported. They are the two new cyclised products pyrrolo[1,2-*a*]quinazoline **111** and indolo[1,2-*a*]quinazoline **114**. We were interested in examining the properties of these new heteroaromatic systems and chose to test their reactivity with electrophiles in classic electrophilic aromatic substitution.

6.1. Reactivity of pyrrolo[1,2-*a*]quinazoline with trifluoro acetic acid

Trifluoroacetic acid (TFA) was selected as a source of H^+ as it is cheap, commercially available and also available in deuterated form. An initial test with TFA demonstrated that compound **111** did not undergo decomposition. Consequently the behaviour of compound **111** was examined when using a large excess of d-TFA to dissolve it, monitoring by ^{1}H NMR. Exchange in one or more protons of the molecule with deuterium from the d-TFA was expected, *via* electrophilic aromatic substitution. By ^{1}H NMR spectroscopy we observed that deuterium exchanged with protons in the molecule depending on the reactivity of the position.

The most reactive position was found to be $H_{\mathbf{c}}$ (as H_1) (Figure 16). The exchange with deuterium was immediate. After the time to prepare the NMR sample the percentage of the H_C was already at an equilibrium value of 20%. The next position that reacts with deuterium is at H_a (as H_3). In Table 2 the disappearance of the H_a with time is reported.

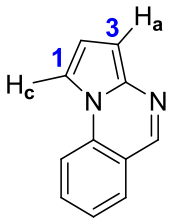

Figure 16: indication of likely reaction position for an electrophilic aromatic substitution in substrate 111.

Minutes	Percentage of H_A	Minutes	Percentage of H_A
0	83	**34**	45
1	76	**38**	44
5	72	**43**	43
8	69	**52**	37
10	67	**61**	34
11	65	**67**	31
13	64	**73**	28
14	63	**80**	27
16	61	**85**	26
18	61	**89**	25
24	54	**95**	23
31	50		

Table 2: time *vs* percentage of H_a exchanged with deuterium in compound 111.

These data are explained by the curve reported in Figure 17. It can be noticed that the half-life is about 29 min.

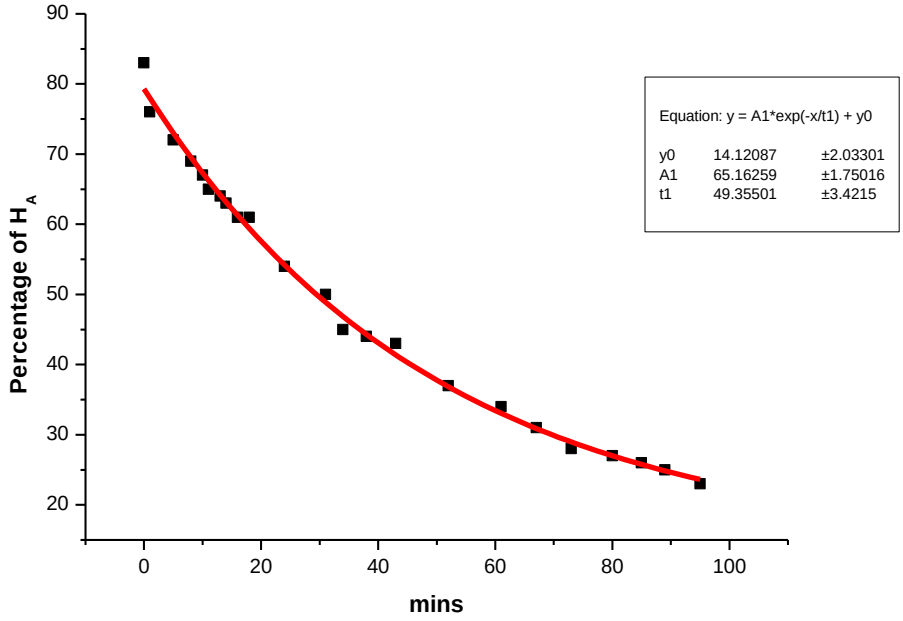

Figure 17: half-time curve of deuterium exchange related to 3-position of compound 111.

It is proposed that the 1-position is more reactive towards electrophiles than the 3-position because the carbocationic intermediate is more stable. When deuterium attacks the 1-position, the resultant cation has two resonance forms before breaking the aromaticity of the phenyl ring while the cation resulting from the attack from deuterium in the 3-position has only one resonance form before breaking the aromaticity of the phenyl ring (Scheme 73).

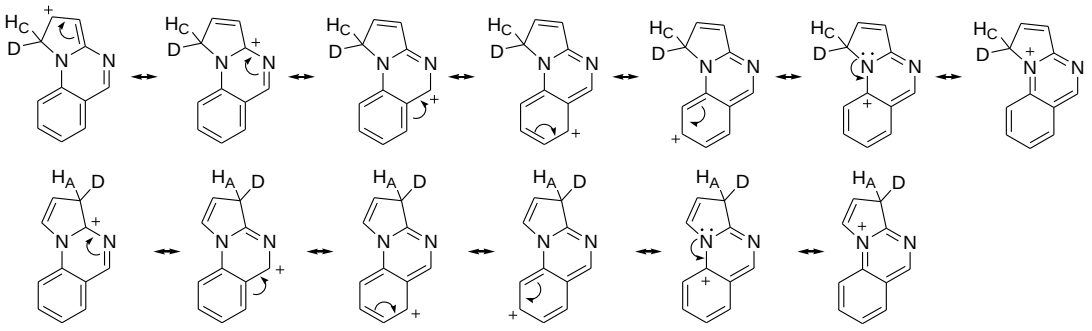

Scheme 73

6.2. Reactitvity of pyrrolo[1,2-*a*]quinazoline with 4-methyl-benzenediazonium tetrafluoroborate

Another electrophile tested with newly formed pyrrolo[1,2-*a*]quinazoline **111** in an electrophilic aromatic substitution reaction was 4-methyl-benzenediazonium tetrafluoroborate **159**. This substrate was selected as it is a strong electrophile that had the potential to react with multiple positions of the pyrrole ring. Experimentally, the reaction afforded a single product selectively **160** which was isolated in 80% yield (Scheme 74).

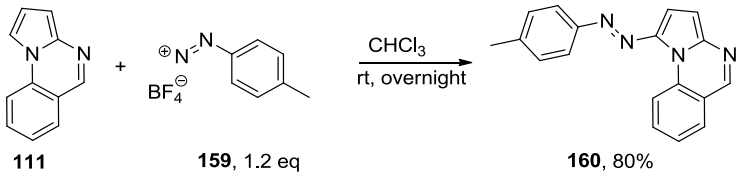

Scheme 74

The fact that just one, mono-substituted product was obtained can lead us to conclude that the 4-methyl-benzenediazo group may be sufficiently bulky to disfavour or prevent double addition to the pyrrole ring, and/or that the strongly withdrawing diazo group may deactivate the ring towards further addition.

Taking into account results obtained with reaction with d-TFA, it was expected that cyclised product would react with diazonium salt in position 1 of the pyrrole ring. The regioselectivity obtained experimentally was confirmed based on the ^{1}H NMR spectrum of the isolated product. It has been reported in the literature[55] that the value of the one-bond carbon–proton coupling constant ($^{1}J_{CH}$) for the C-H next the N-atom (position 2) is higher than the coupling constant for C-Hs in position 3 and 4 of the pyrrole ring (Figure 18).

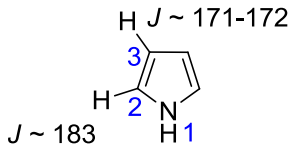

Figure 18: C-H coupling constant values for pyrroles.

This led to the thought that measuring the $^{1}J_{CH}$ coupling constants of the C-H bonds of the product would give information about the position in which the reaction had occurred.

It was important to assign protons '**l**' and '**m**' (Figure 19) to be able to assign the corresponding carbons by 2D HSQC. To do so, a 2D NOESY NMR spectrum was measured. It was possible to assign protons '**h**' and '**g**' that appear as a doublet at δ 7.34 ppm that interacts with singlet corresponding to methyl group at δ 2.44 ppm (Figure 19).

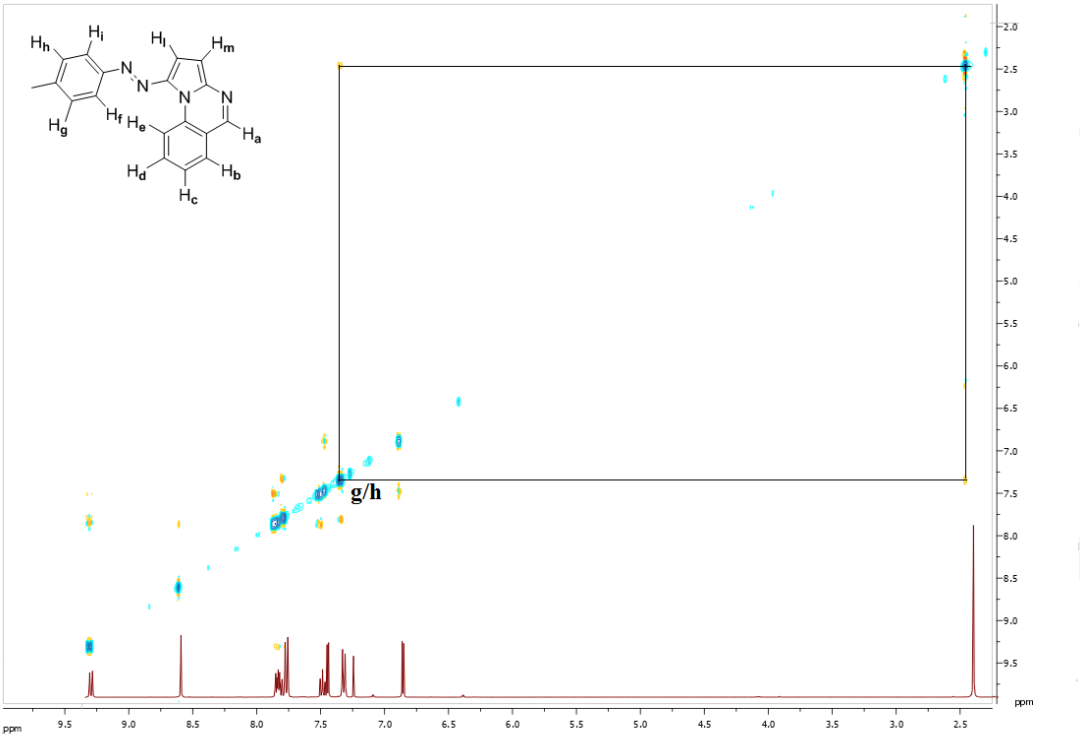

Figure 19: NOESY spectrum of compound 160.

From protons '**g**' and '**h**' it was possible to assign protons '**i**' and '**f**' at δ 7.78 ppm based on cross peaks that were evident in the expanded spectrum shown in Figure 20.

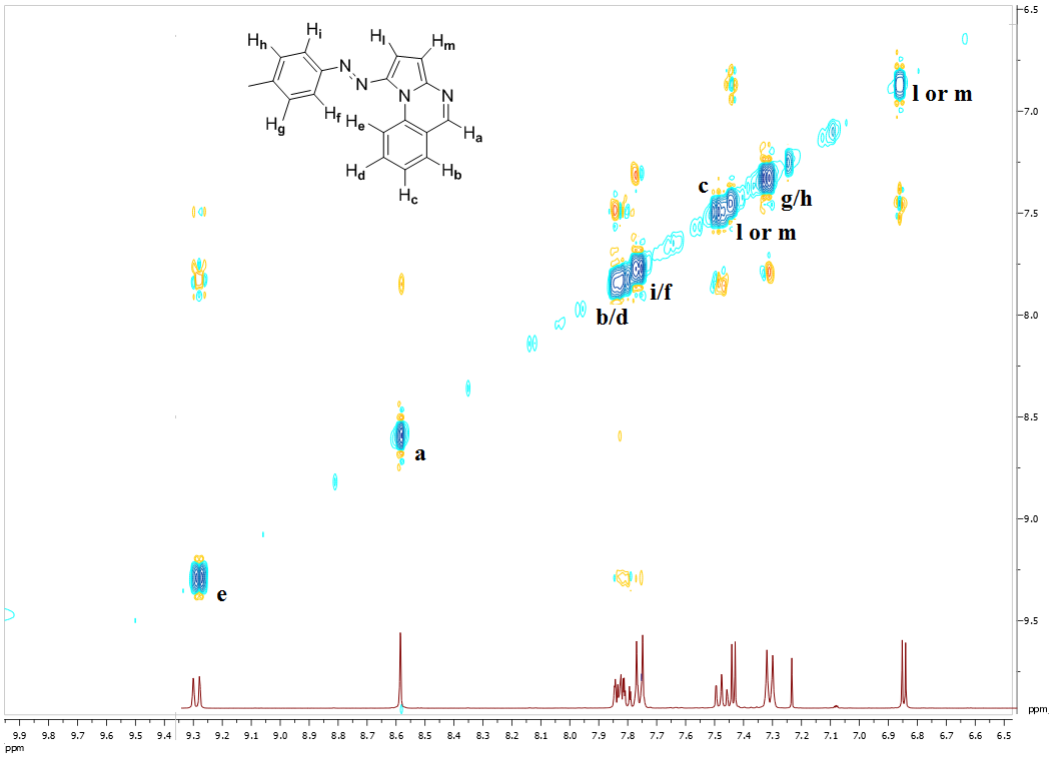

Figure 20: NOESY spectrum of compound 160.

It was also possible to assign proton '**a**' as the deshielded singlet at δ 8.59 ppm as it would not be expected to couple strongly with any other hydrogen nuclei. Looking closely at the NOESY spectrum, proton '**a**' does show a weak interaction with a proton which resonates at 7.83 ppm and which was consequently possible to attribute to proton '**b**'. The second doublet of the fused phenyl ring can then be identified as the deshielded doublet at δ 9.29 ppm that interacts with triplet at δ 7.84 identified as '**d**'. Therefore the signal at δ 7.50 ppm which correlates with both '**b**' and '**d**' can be assigned as proton '**c**'. Finally, the two remaining doublets can be as attributed to protons '**l**' or '**m**' of the pyrrole ring, although it is not possible to differentiate them unequivocally. Using 2D HSQC NMR it was then possible to assign the ^{13}C resonances resulting from the tertiary carbon atoms of the pyrrole system as having chemical shifts of δ 104.6 ppm and 106.3 ppm (Figure 21).

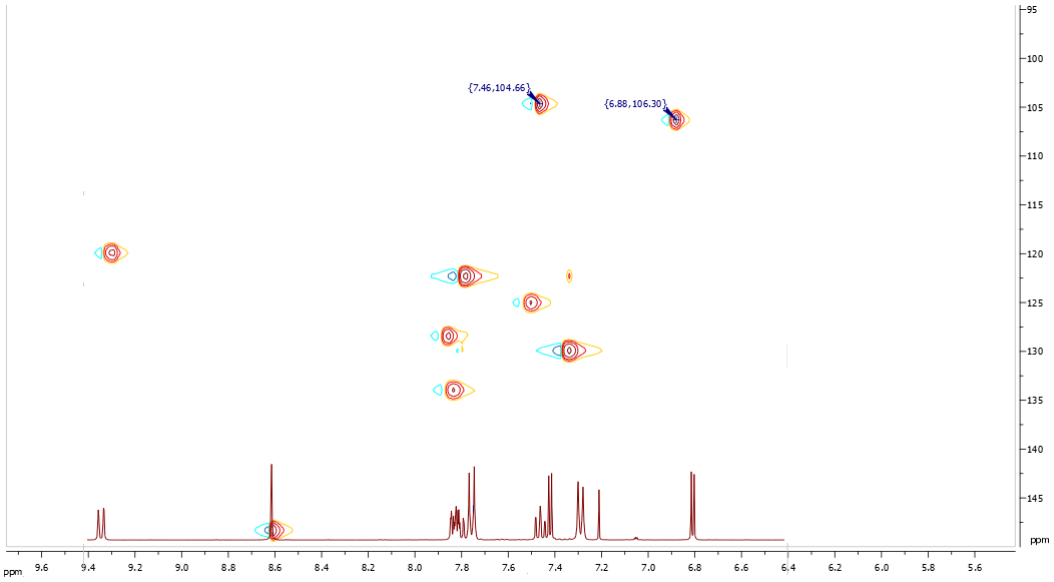

Figure 21: HSQC spectrum of compound 160.

At this point, a C-H coupled ^{13}C experiment was run to assess the $^{1}J_{CH}$ coupling constants. For comparison, Figure 25 shows the ^{13}C spectra of compound **160** acquired with (Figure 22, **a**) and without (Figure 22, **b**) proton decoupling.

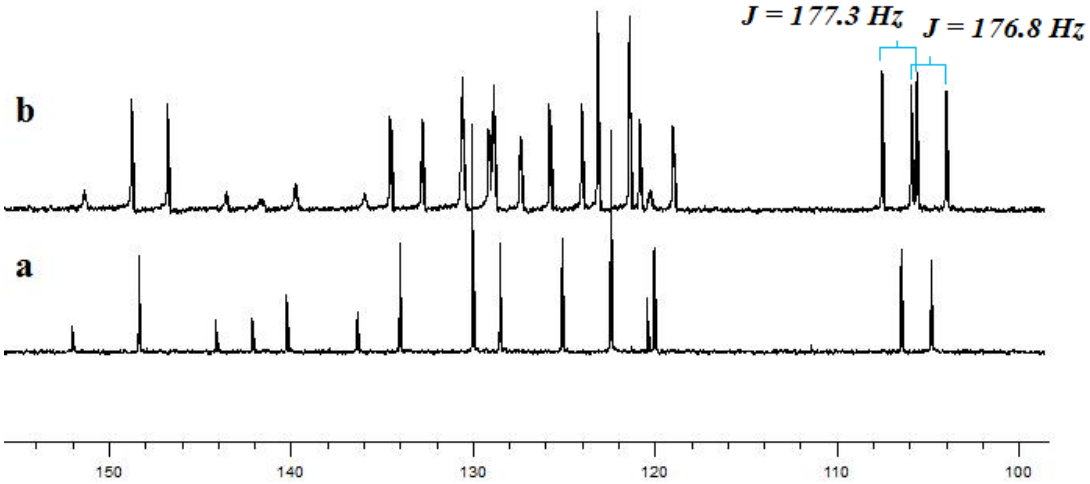

Figure 22: ^{13}C spectrum of compound 160 with C-H coupling (b) and without C-H coupling (a).

The measured coupling constants for the pyrrole-type system were $^{1}J_{CH}$ = 177.3 Hz and 176.8 Hz. Firstly, both these values are similar to the typical one-bond proton–carbon coupling constants found in the 3- and 4-position of pyrrole systems as stated in Figure 18. Secondly, (and more importantly) the values are similar to one another

which is an indication that they are related to electronically similar C-Hs in positions 3 and 4. These observations are consistent with the S_EAr reaction of 4-methyl-benzene tetrafluoroborate having occurred at position 2.

6.3. Reactitvity of pyrrolo[1,2-*a*]quinazoline with oxalyl chloride

The next electrophile to be reacted with pyrrolo[1,2-*a*]quinazoline **111** was oxalyl chloride (Scheme 75).

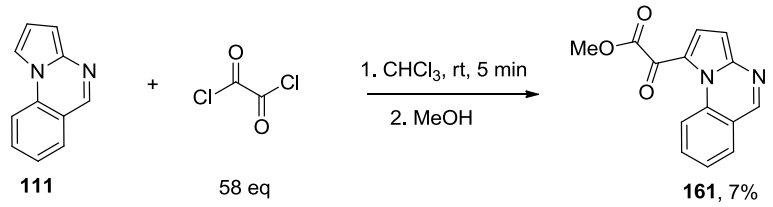

Scheme 75

One product was isolated and fully characterised which could be identified as compound **161** resulting from electrophilic aromatic substitution at position 1 followed by esterification with methanol (Scheme 75). This reaction afforded just 7% of isolated product **161** (this is probably due to use of large excess of oxalyl chloride and to its high reactivity – it probably caused decomposition of the starting material **111**). This reaction introduces a functional handle onto the heterocyclic core for potential future transformations. ^{1}H NMR showed the appearance of a singlet at δ 4.03 ppm, the typical chemical shift for methoxy groups. In analogy with compound **161**, disappearance of the three signals associated with the pyrrole ring in **111** and the appearance of two new doublets was observed. In structure **160** the two doublets were recorded at δ 7.46 and 6.87 ppm (J = 4.7 Hz) while for compound **161** they were reported at 7.87 and 6.87 ppm (J = 4.8 Hz). An additional proof was given by ^{13}C in which the presence of two quaternary carbons at δ 173.1 and 165.2 ppm was noted.

6.4. FVP of pyrrolo[1,2-*a*]quinazoline at 950 °C

Performing FVP at high temperatures on cyclised systems can lead to ring contraction and rearrangement to more constrained and higher energy molecules.[56]

FVP at 950 °C of dibenz[*b*,*f*]azepine compound **162** generates pyrrolo[3,2,1-*jk*]carbazole **139**, a much more strained system compared to the initial dibenz[*b*,*f*]azepine (Scheme 76).

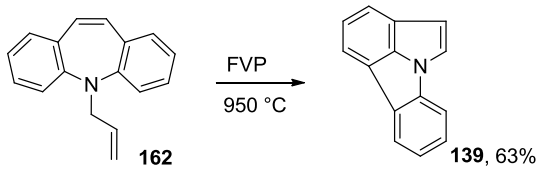

Scheme 76

The mechanism proposed in this case was initial formation of *N*-centred radical **163** (Scheme 77) which may then undergo *trans*-annular attack on the double bond of the azepine ring, forming a 4-membered transition state **164**. This can then evolve with formation of a phenyl radical and with consequent re-establishment of aromaticity in the form of an indole ring **146**. Finally, cyclisation of the phenyl radical into the adjacent indole system forms a new 5-membered ring **139** with loss of a hydrogen radical (Scheme 77).

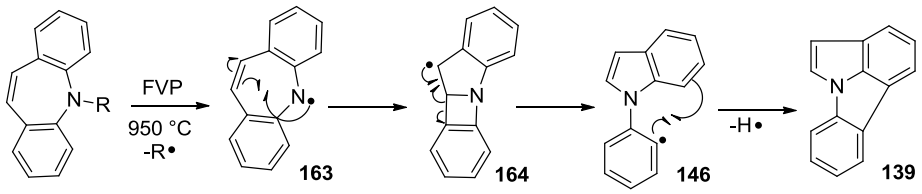

Scheme 77

It was envisioned that in the case pyrrolo[1,2-*a*]quinazoline **111** and indolo[1,2-*a*]quinazoline **114** it would also be possible to obtain rearrangement after formation of *N*-centred radicals **165** and **166** at these high temperature (Figure 23).

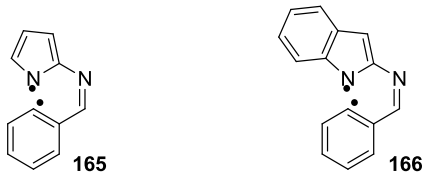

Figure 23: possible breaking point at 950 °C under FVP conditions for compounds 111 and 114.

FVP of pyrrolo[1,2-*a*]quinazoline **111** was performed at 950 °C (with silica wool in the furnace tube to increase the contact time of the molecules in the furnace) and pleasingly, afforded two main products **167** and **168** as shown in Scheme 78.

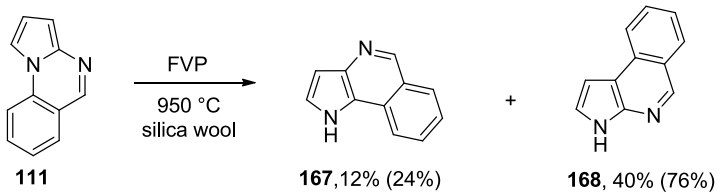

Scheme 78

The yields quoted in parentheses are NMR yields. In a work carried out by Dupas et al,[57] product **167** was synthesised by a different route, as shown in Scheme 79.

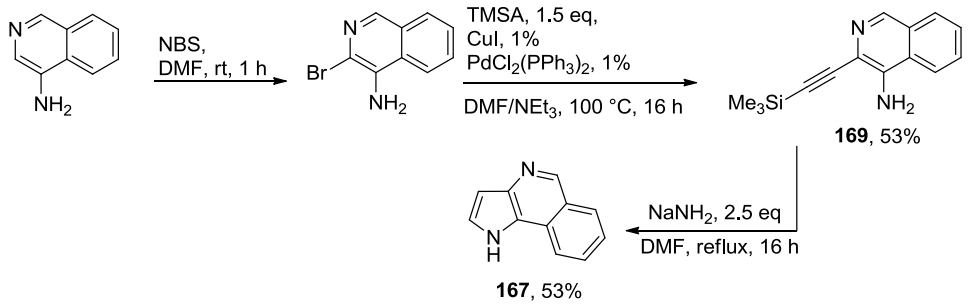

Scheme 79

4-Aminoisoquinoline was brominated with NBS in position 3. Sonogashira reaction allowed the installation of the trimethylsilylacetylene functionality in 3- position of the isoquinoline ring giving cyclisation precursor **169**. The cyclisation was obtained with sodium azide in DMF. Interest was shown for this compound for its potential capability to act as a good receptor for carboxylic acids and amines.

The appearance of a broad singlet at a δ 9.27 ppm was observed by ^{1}H NMR. This is related to the N-H proton and is broadened as a result of concentration dependent dimerisation/aggregation of compound **167**. This would explain why, although chemical shifts of all the other protons signals are compatible with ones reported in the literature, a $\Delta\delta = 0.47$ ppm for N-H is observed (δ 9.70 ppm reported).

Compound **168** is also known from work carried out by Maes et al..[58] It was synthesised according to route shown in Scheme 80.

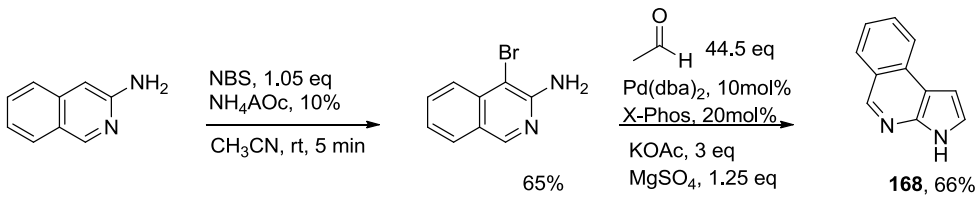

Scheme 80

Product **168** was obtained *via* Pd-catalysed annulations of 3-amino-4-bromoisoquinoline with acetylaldehyde. The aldehyde reagent has to be used in large access due to trimerisation. Compound **168** has been assessed for antimalarial activity, especially against protozoa *Plasmodium Falciparum*, which causes the most serious infections. 3*H*-Pyrrolo[2,3-*c*]isoquinoline amine is part of the families of pyrrolo isoquinolines that, among others, have been tested *in vitro* and *in vivo* by Pieters et al.[59] Despite showing moderate cytotoxic activity, similar to other compounds of the series, there is a lack of selectivity. Nevertheless, interest in these compounds stays high due to possible structural modifications which might improve their properties. It is thought that the activity of the compound is due to the presence of adjacent N-atoms capable of inserting within and interacting with the DNA of the protozoa.

^{1}H NMR analysis of compound **168** was reported by Maes in d_6-DMSO and the chemical shifts of the compound isolated in this work were very similar in $CDCl_3$, confirming the identity of compound **168** (Table 3).

^{1}H NMR 168 in $CDCl_3$ (ppm)	^{1}H NMR 168 in d_6-DMSO (ppm)
10.28 (br s)	11.96 (br s)
8.93	8.90
8.20	8.26
8.05	8.12
7.74	7.75
7.50	7.50
7.46-7.33	7.46
7.01	7.03

Table 3: comparison of chemical shift of peaks in ^{1}H NMR for 168 in both $CDCl_3$ and d_6-DMSO

It is worth noting that the only difference lies in the chemical shift of the broad peak associated with proton N-H that appears to be at lower field when NMR is run in d_6-DMSO. This is associated with the fact that d_6-DMSO is much more polar and can participate in hydrogen bonding with the N-H.

The proposed mechanism for the formation of compound **168** may follow two different pathways (Scheme 81 and 82):

1. cleavage of the *N*-phenyl bond with formation of a di-radical **165**;
2. attack of the phenyl radical onto the 3-position of the pyrrole ring forming a new 6-membered ring **170**;
3. two consecutive [1,5]-sigmatropic shifts of the hydrogen with restoration of the aromaticity to give **168**.

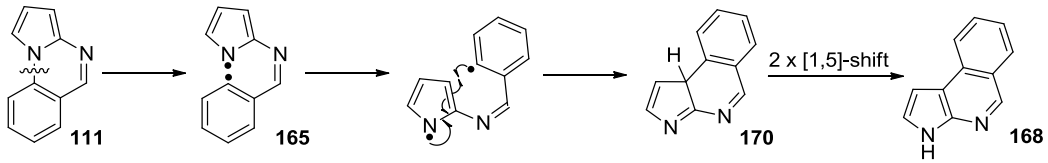

Scheme 81

Alternatively:

1. cleavage of the *N*-phenyl bond with formation of a di-radical species **165**;

2. attack of the phenyl radical onto the 2-position of pyrrole ring forming a new 5-membered, *spiro*-intermediate **171**;
3. rearrangement of the system with 'migration' of the C-C bond into 3-position of the pyrrole ring **170**;
4. two consecutive [1,5]-sigmatropic shifts of the hydrogen with restoration of aromaticity to give **168**.

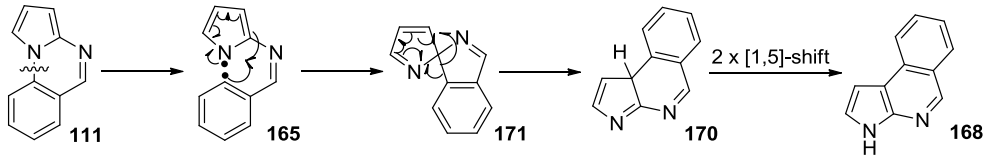

Scheme 82

The proposed mechanism for the formation of compound **167** may undergo the following pathway (Scheme 83):

1. cleavage of the *N*-phenyl bond with formation of a di-radical species **165**;
2. attack of the phenyl radical onto the 2-position of pyrrole ring forming a new 5-membered, *spiro*-intermediate **171**;
3. rearrangement of the system with 'migration' of the C-N bond into 3-position of the pyrrole ring forming **172**;
4. two consecutive [1,5]-sigmatropic shift of the hydrogen with a restoration of aromaticity to give **167**.

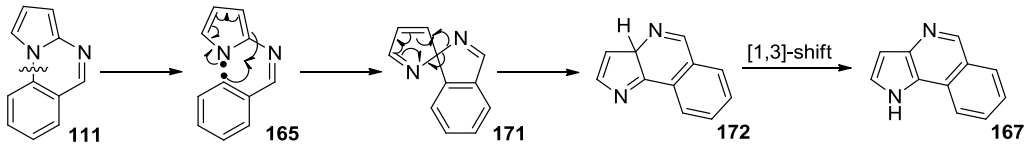

Scheme 83

The fact that compound **168** could be obtain by two different pathways may explain why this regioisomer is obtained in higher ratio. In fact, if the only possible pathway was the generation of the *spiro*-intermediate **171**, the breakage of C-N and formation of intermediate **171** should be favoured due to the lower strength of the C-N bond compared with the C-C bond. This, consequently, should result in a higher ratio in favour of compound **167** in contrast with what was observed experimentally. In

addition, the formation of **167** confirms the formation of a *spiro*-intermediate because the product could not be obtained otherwise.

6.5. FVP of indolo[1,2-*a*]quinazoline at 950 °C

Following the previously described results, FVP at 950 °C of indolo[1,2-*a*]quinazoline **114** was performed and successfully afforded the two desired products 11*H*-indolo[2,3-*c*]isoquinoline **173** and 7*H*-indolo[3,2-*c*]isoquinoline **174** along with nitrile **175** and recovered starting material.

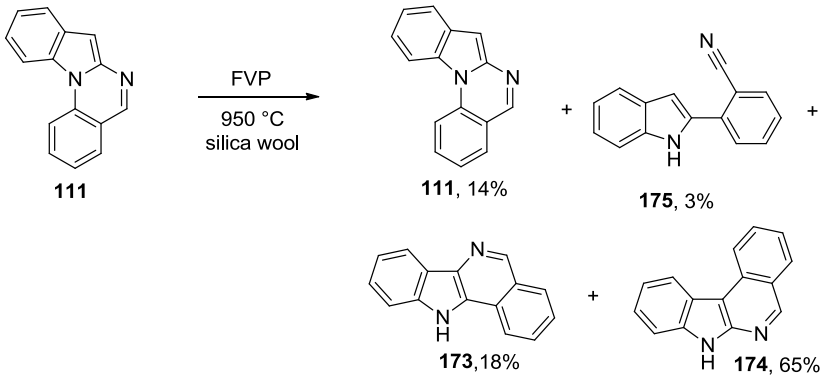

Scheme 84

Both products **173** and **174** have been previously reported by Maes et al.[60] It was observed that population from Central and Western Africa used the root of the plant *Cryptolepis sanguinolenta* to treat fevers, including those caused by malaria. Three main alkaloids (**176**, **177** and **178**) were extracted from this plant (Figure 24).

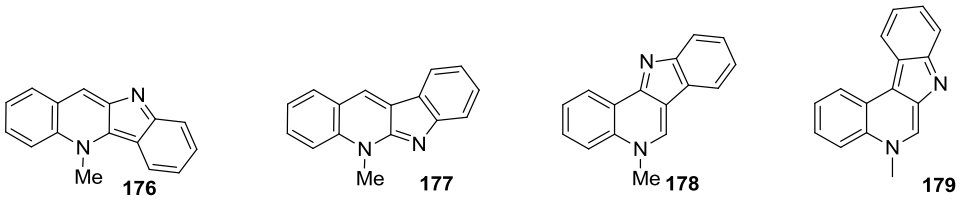

Figure 24: natural and synthetic alkaloids for potential cure of malarial fever.

Compound **179** was then synthesised for comparison. It was found that these isomeric indoloisoquinolines had some antiplasmodial activity with isomer **176** being the most active but also the most cytotoxic. On the other hand, isomer **179** was found to be the less active but more selective.

It was then decided to synthesise the corresponding de-methylated isoquinoline equivalents of **177** and **178**, compounds **173** and **174**, to compare their activities. Compound **173** was synthesised *via* a selective Buchwald–Hartwig reaction of 4-bromoisoquinoline with 2-bromoaniline followed by Pd-catalysed intramolecular direct arylation. The best results were obtained under microwave heating (Scheme 85).

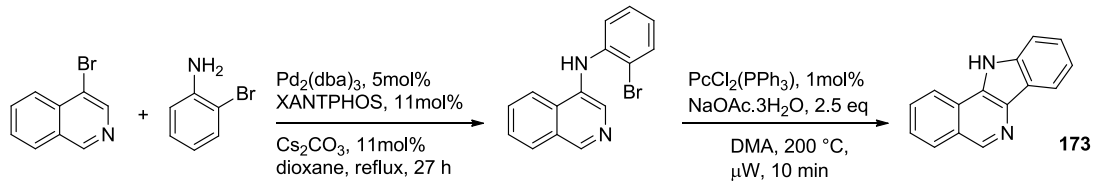

Scheme 85

After several attempts, compound **174** was synthesised *via* two key reactions steps: Stille–Kelly reaction to give protected amine **180** and intramolecular insertion of nitrine (**181**) in the 3-position of the isoquinoline ring to give the desired product (Scheme 86).

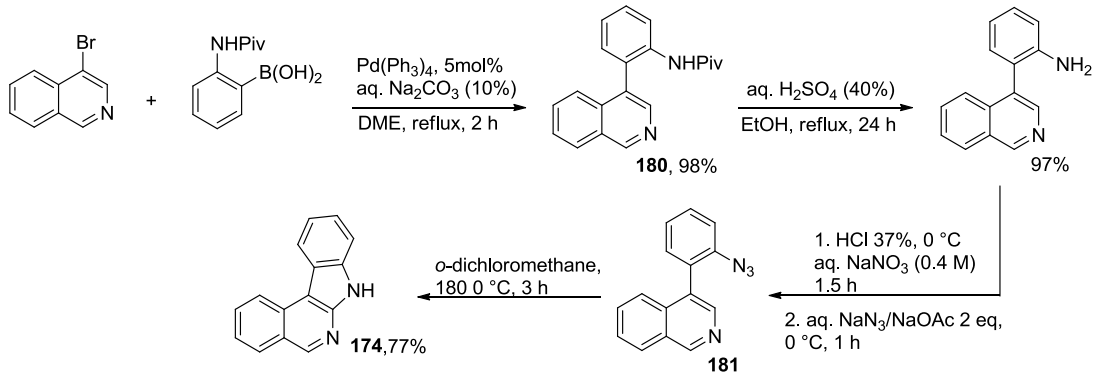

Scheme 86

Compared to the lead compound **179,** it was found that the indoloisoquinolines **173** and **174** possess antiplasmodial activity, but with relatively high cytotoxicity.

In the end, the synthetic pathway to **173** proposed in this work is longer than the one illustrated Maes' previous work. However for compound **174**, the pathway proposed in this work is simpler than the previously published route. It is important to note that it is possible to obtain both compounds by the same synthetic pathway. The formation of the two products was confirmed by ^{1}H NMR techniques. The

appearance of the broad singlet at δ 12.33 ppm for **173** and 12.24 ppm for **174** was observed. The chemical shifts of the protons are all comparable with those reported in the literature. The mechanism proposed for formation of the two indoloisoquinolines **173** and **174** is similar to that proposed for compound **167** and **168** (*c.f.* Schemes 81, 82 and 83). The mechanistic proposal is in agreement with the observed product distribution – the major product is the product in which 'migration' of C-C bond is observed. Again this is probably due to yield contributions from the direct cyclisation pathway (*c.f.* Scheme 81).

A third product was obtained from the reaction mixture. As only ^{1}H and ^{13}C were obtained, the assignment could not be confirmed unequivocally. Nevertheless, in the ^{1}H NMR it is possible to observe the presence of a broad singlet at δ 8.50 ppm and 9 aromatic signals as well as 6 quaternary signals in the ^{13}C NMR.

A proposed mechanism for the formation of this product is illustrated in scheme 87.

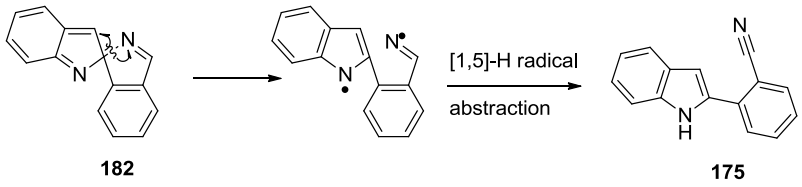

182 **175**

Scheme 87

Once *spiro*-intermediate **182** is formed, C-N bond cleavage can occur followed by [1,5]-H radical abstraction by *N*-indole from α-position to iminyl radical.

7. Conclusion

In this chapter, a methodology to obtain pyrrolo[1,2-*a*]quinazolines and indolo[1,2-*a*]quinazolines *via* FVP of the corresponding synthesised oxime ethers was presented. It was clear from the experimental results that:

- it was possible to obtain oxime ethers **109**, **112** and **116** in good overall yields *via* a simple route;
- FVP at appropriate temperatures of the aforementioned oxime ethers **109** and **112** successfully afforded the previously unknown pyrrolo[1,2-*a*]quinazoline **111** and indolo[1,2-*a*]quinazoline **114** in good yields. This proved our initial hypothesis to be correct. The corresponding nitriles **128** and **138** were obtained as main side products alongside the cyclised products. In the case of the carbazole analogue, only nitrile **148** was obtained proving that formation of 7-membered rings *via* this route is challenging;
- DFT calculations were used to understand the ratio of the cyclised products to nitriles in the case of pyrrolo[1,2-*a*]quinazoline and indolo[1,2-*a*]quinazoline. Formation of cyclised products **111** and **114** was found to be kinetically and thermodynamically favoured;
- the reactivity of pyrrolo[1,2-*a*]quinazoline **111** towards strong electrophiles (such as deuterium and di-azo salts) was studied. The system was found to be most reactive at position 1 followed by position 3;
- the rearrangement of systems **111** and **114** was also examined, performing pyrolysis at 950 °C successfully afforded systems **167** and **168** from pyrrolo[1,2-*a*]quinazoline and systems **173** and **174** from indolo[1,2-*a*]quinazoline.

Chapter 4:

Generation of new fused heterocyclic rings *via* iminyl radicals cyclising onto 2-azoles type rings and study of their reactivity.

1. Introduction

In the previous chapter the synthesis of pyrrolo[1,2-α]quinazoline **111** and indolo[1,2-α]quinazoline **114** *via* FVP was discussed. This work led us to consider the possibility of extending the scope of this FVP-induced iminyl radical cyclisation to substrates in which cyclisation occurs onto 2-azole type rings and hindered pyrrolo-type systems in positions 2 and 5.

1.1. Cyclisation of iminyl radicals onto 2-zoles type systems.

A series of 2-azol-1-yl-benzaldehyde *O*-methyloximes were synthesised within the McNab group [61,49] which, based on previous work, it was believed would produce the heterocycles shown in Figure 25 after FVP.

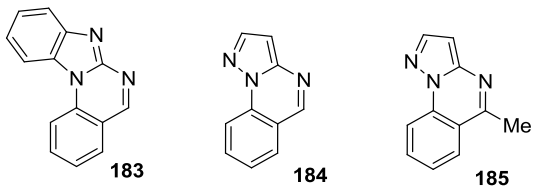

Figure 25: novel aromatic fused rings previously synthesised *via* iminyl radical generated by FVP.

Synthesis of the oxime ether precursors was achieved as shown in Scheme 88.

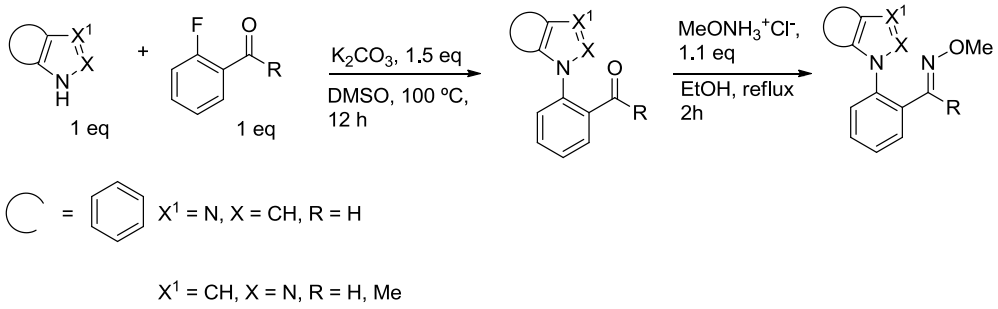

Scheme 88

A nucleophilic aromatic substitution reaction of a 2-azole with 2-fluorobenzaldehyde or 2′-fluoroacetophenone was chosen as the first step of the sequence. The reaction proceeded satisfactorily with the three substrate combinations investigated and the desired products could be isolated in yields between 50-60%. The second step of the synthesis was the now familiar condensation reaction between the carbonyl

compound and *O*-methylhydroxylamine hydrochloride in ethanol under reflux to obtain the FVP precursors **186**, **189** and **192**. Yields recorded for the condensation were above 80% for all substrates. Pyrolysis of the three oxime ether intermediates was performed using the standard FVP apparatus with a furnace temperature of 700 °C.

While for compounds **186** and **189** (Scheme 89) cyclisation could only feasibly occur at one point of the heteroaryl ring, compound **192** had two possible cyclisation points: position 2 on the imidazole ring (generating a 6-membered ring) or position 7 on the phenyl-fused ring generating a 7-membered ring. As was observed previously for related indole-type systems (*c.f.* Scheme 66), only the 6-membered cyclised product was formed along with a nitrile side product resulting from β-cleavage of the iminyl radical.

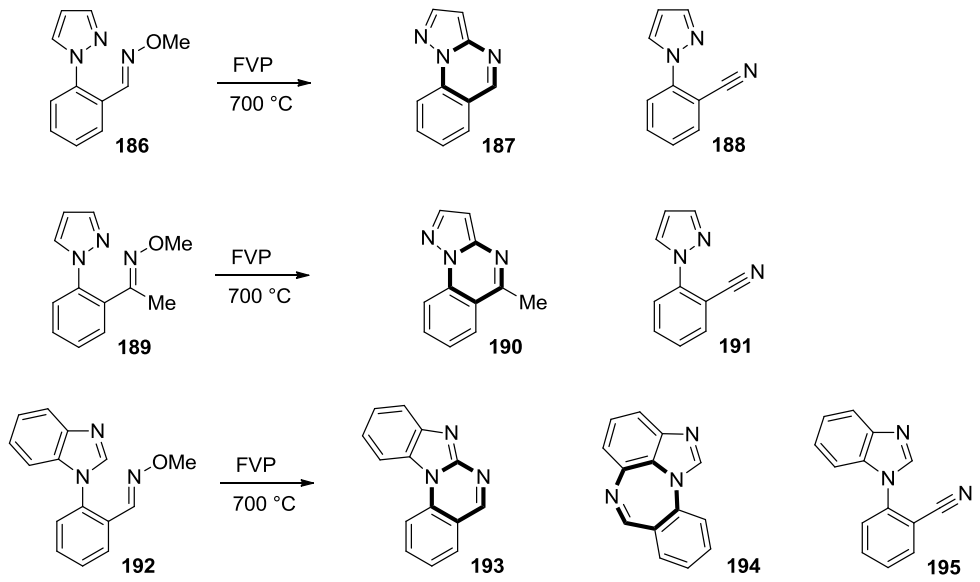

Scheme 89

The electronic effects of adding *N*-atoms at positions 2 or 3 was then investigated. It was thought that introducing an electron-withdrawing group would make the 2-azole ring less prone to donating electrons during the cyclisation with the iminyl radical. This would facilitate β-cleavage and therefore higher yields of corresponding nitrile products **188**, **191** and **195** would be expected. Results from the FVP reactions are shown in Table 4.

entry	oxime ether	cyclised product (NMR%)	nitrile (NMR%)	other product (NMR%)
1[62]	**186**	**187**, 74 (N/A)	**188**, 26(N/A)	0
2[62]	**192**	**193**, 70 (43)	**193**, 20	**imine,** 10
3[49]	**189**	**190**, 52 (43)	**191**, 48	0
4	**109**	**111**, 92 (63)	**128**, 8	0

Table 4: Yields obtained by FVP of 2-azole systems 187, 193, 190 and pyrrolo[1,2-*a*]quinazoline 111. Yields in brackets are the isolated yields.

Entry 4 in Table 4 corresponds to the pyrolysis of 2-(pyrrol-1-yl)benzaldehyde *O*-methyloxime **109** and is listed to provide comparison with the other results. It is clear from the distribution of products that, as predicted, 'adding' an additional nitrogen into the 5-membered heterocyclic ring (entry 1-3, Table 4) results in an increase in the yield of nitrile products with concomitant decrease in the yield of cyclised products. It can be concluded that the original hypothesis formulated on frontier orbitals was correct. The yield of the nitrile in the crude NMR of the pyrolysed product increased further when a methyl group was introduced in the α-position to the C-N double bond. This can be explained by the fact that cleavage of the C-C bond requires less energy (346 kJ mol^{-1}) than cleavage of the C-H bond (411 kJ mol^{-1}). In addition to this, nitrile formation from the pyrolysis of substrate **189** is particularly facile as adding a methyl group in α to the *N*-radical increases the energy of the SOMO so making the iminyl radical a nucleophilic radical. This discourages even more the reaction with electron rich system like the 2-azole reported. The product distribution is shifted accordingly – formation of the cyclised and nitrile products was observed in an approximately 1:1 ratio.

1.2. Cyclisation of iminyl radicals onto substituted pyrrole-type rings.

Systems like the one shown in Figure 26 were previously studied in the McNab group.[49]

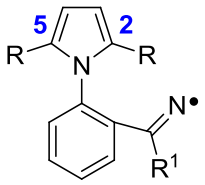

Figure 26: indication of possible cyclising sites for the iminyl radical.

Substituents were introduced in the expected cyclisation points positions 2 and 5 to study their effect on the cyclisation process and to extend the scope of the synthetic method. Also, following the results from entry 3 in Table 4, it seemed likely that introducing an alkyl substituent α to the iminyl radical would disfavour formation of a cyclised product upon FVP. The systems that were investigated are shown in Scheme 90.

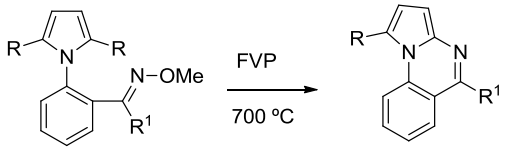

196 (i), R = H, R^1 = Me
(ii), R = H, R^1 = Ph
(iii), R = Me, R^1 = Me

197 (i), R = H, R^1 = Me
(ii), R = H, R^1 = Ph
(iii), R = Me, R^1 = Me

Scheme 90

The oxime ethers were obtained using a similar protocol to that which had been successfully used previously (as described in chapter 3) and were then pyrolysed at an optimised temperature which was determined for each of the substrates individually. Results of the cyclisation reactions are reported in Table 5.

entry	R	R^1	Cyclised product, (NMR %)	Nitrile, (NMR%)	byproduct, (NMR%)
1	H	H	92 (63)	8	0
2[49]	Me	Me	93 (78)	7	0
3[49]	H	Me	92 (67)	8	0
4[49]	H	Ph	87 (76)	0	13 (imine)

Table 5: entry 1 refers to product 111 described in the previous chapter; yields in brackets refer to isolated yields.

The results showed that introducing a substituent in the cyclisation position does not affect the yield of the cyclised product (results compared with R = H described exhaustively in the previous chapter). Moreover, substrates bearing a substituent α to the C-N double bond undergo cyclisation in comparable yields to the parent compound. Compound **197 (ii)** was obtained in lower yield and this can be explained considering that the iminyl radical generated by FVP is probably stabilised by the phenyl ring. As a result, it is more likely to abstract an *H*-radical from the environment that it has been generated in.

2. Aims of the project

With the above results in hand, several targets were set for further investigation which will be discussed in this chapter. As described in the previous section, it was known that iminyl radicals generated under FVP conditions can give rise to fused heterocyclic products by intermolecular attack on various 2-azole ring systems (*c.f.* Figure 28). Of immediate interest was the synthesis and FVP of compound **198** (Scheme 91).

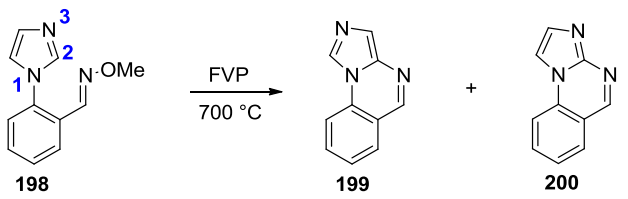

Scheme 91

This could potentially lead to two different products **199** and **200**. As seen in Chapter 4, Section 1.2, employing substrates with more nitrogen rich heterocycles led to a decrease in the amount of cyclised product obtained. It was of interest, then, to see if additional *N*-atom in position 3 would result in different ratio of the two products. Moreover, an additional aim was to take the 2-azole pyrolysis products – **199** and **200** if successfully obtained, **197 (iii)**, **187** and **190** which had previously been synthesised in the group – and resubmit them to FVP conditions at a higher temperature of 950 °C. It was hoped that this would facilitate the study of subbstituent effects on a rearrangement process which is known to occur at higher temperature (*c.f.* Chapter 3, sections 6.4. and 6.5.). It was shown, in fact, that pyrolysing products **111** and **114** at a furnace temperature of 950 °C resulted in the formation of new heterocyclic systems (Scheme 92).

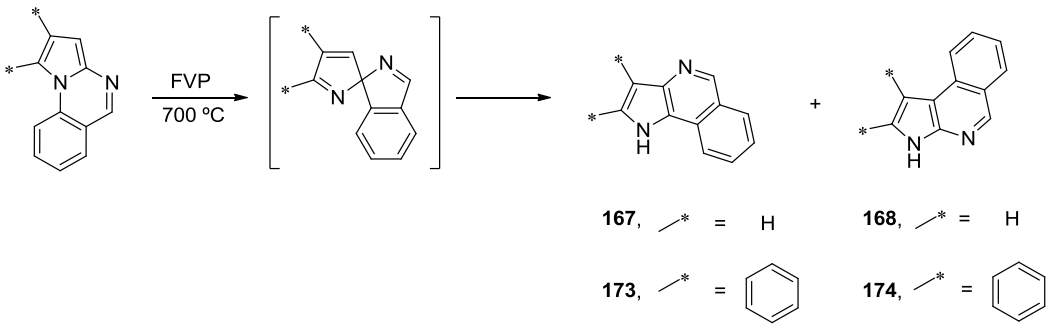

Scheme 92

This suggested that performing the reaction in the same fashion on the aforementioned compounds could result in a series of 3-fused heterocyclic compounds that are unknown in the literature (Scheme 93).

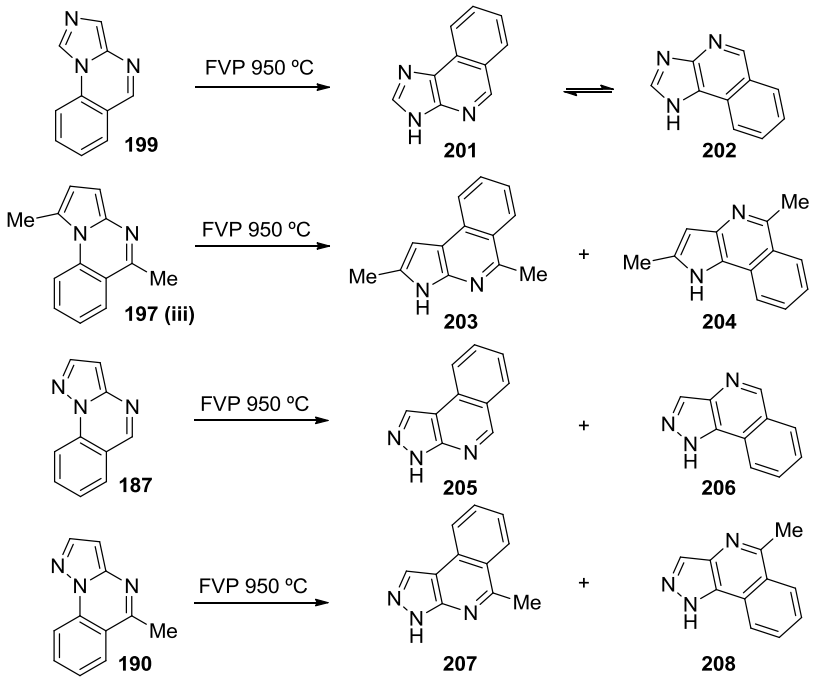

Scheme 93

Compounds **201**/**202**, **205**, **206**, **207** and **208** are of particular interest (it is worth noticing that although compounds **201** and **202** are numbered separately, they are tautomers). As described in paper published in 2009 by D. Leigh and H. McNab,[62] compounds with multipoint hydrogen bonding motifs are of great interest due to their importance in biological recognition processes and because they can be used to synthesise sophisticated materials or polymers. Fused heterocyclic ring systems are particularly sought after for these purposes as they can contain contiguous H-donors or H-acceptors in a planar or semi-planar structure that contribute to a very strong overall bonding interaction. As explained in this work, by increasing the consecutive number of donor-acceptor centres, the binding constant increases exponentially (Figure 27).

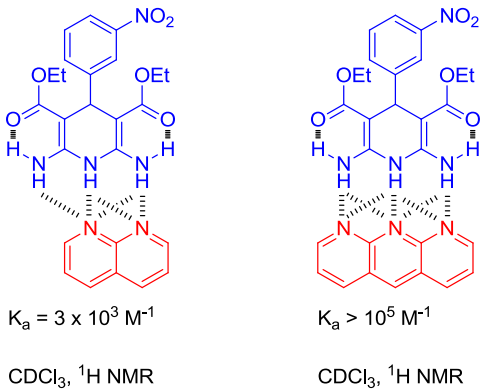

Figure 27: examples of H-donors - H-acceptors interactions in which by increasing the number of H-donor and H-acceptors sites the value of the K_a is increased.

Compounds shown in Figure 28 will provide both donor and acceptor centres in the same structure allowing potential further investigations into the relationship between the nature of the heterocyclic framework and the binding strength in hydrogen bonded dimers.

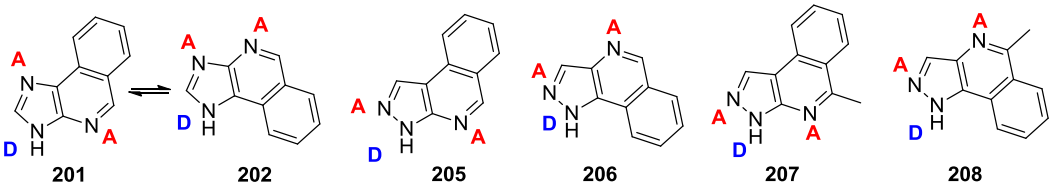

Figure 28: potential compounds with multiple H-donor and H-acceptor sites generated by FVP.

3. Synthesis and pyrolysis of {1-[2-(2,5-dimethyl-1*H*-pyrrol-1-yl)phenyl]ethylidene}(methoxy)amine

Synthesis of **{**1-[2-(2,5-dimethyl-1*H*-pyrrol-1-yl)phenyl]ethylidene}(methoxy)amine **197 (iii)** was previously achieved in the McNab group and has already been described in the introduction. The compound was resynthesised by the same optimised pathway for investigations into its isomerism induced by pyrolysis at 950 °C (Scheme 94).

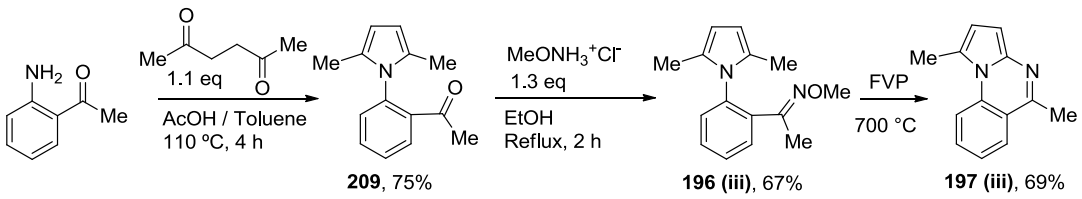

Scheme 94

Aldehyde **209** was obtained in good yield. Evidence that the isolated product was the proposed structure was given by the appearance of a typical signal associated with the pyrrole ring (at 5.96 ppm appearing as a broad singlet) and from the two methyl signals. The new ketone was then reacted with *O*-methylhydroxylamine hydrochloride in ethanol in the same manner as described before and the oxime ether product **196 (iii)** was isolated in reasonable yield. It was possible to see the appearance of a singlet integrating for 3H by ^{1}H NMR corresponding to the methoxy group at 3.94 ppm. Finally, the oxime ether was pyrolysed at 700 °C to afford the desired tricyclic product **197 (iii)**. ^{1}H NMR showed disappearance of both the methoxy signal and the singlet at 1.97 ppm (6 H) corresponding to the two methyl groups on the pyrrole and the appearance of two singlets at 2.87 ppm and 2.73 ppm that correspond to the methyl groups in position 1 and 5.

4. FVP pyrolysis of 1,5-dimethylpyrrolo[1,2-*a*]quinazoline at 950 °C

Pyrolysis at 950 °C (using silica wool inside the furnace tube as explained in chapter 3) was performed on the cyclised product **196 (iii)** in an attempt to obtain isomeric compounds **203** and **204** after rearrangement (Scheme 95).

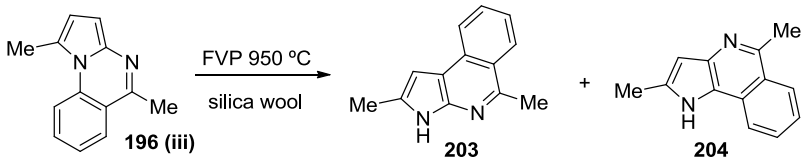

Scheme 95

^{1}H NMR of the crude mixture obtained from pyrolysis was recorded and was found to be complex. An attempt to separate the various products of the reaction mixture was made but this proved to be difficult despite applying different techniques such dry flash chromatography and Kugelrohr distillation. A few fractions of the distillate

product that seemed to contain relevant material were combined and a ^{1}H NMR spectrum was recorded (Figure 29).

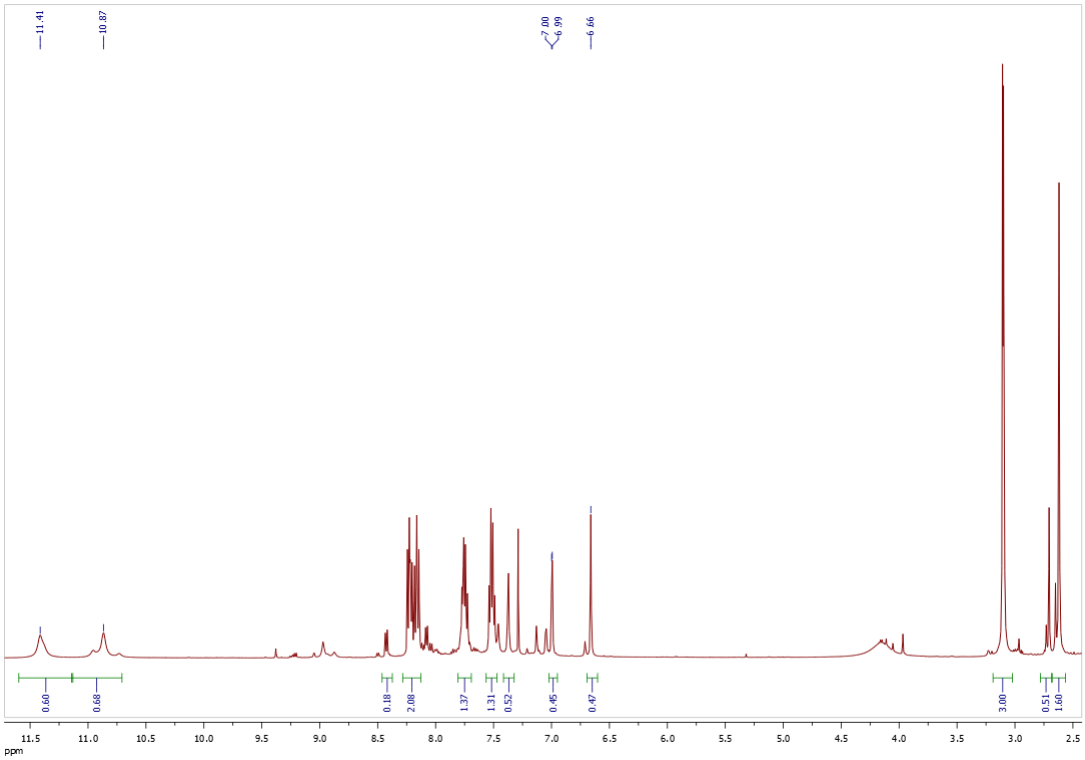

Figure 29: ^{1}H NMR of FVP mixture of compound 196 (iii).

The two protons related to the N-H in structures **203** and **204** were possibly observed in the NMR spectrum of the mixture. A 2D-TOCSY NMR was then taken to relate signals within the same spin systems and hence identify the different structures in the mixture (Figure 30).

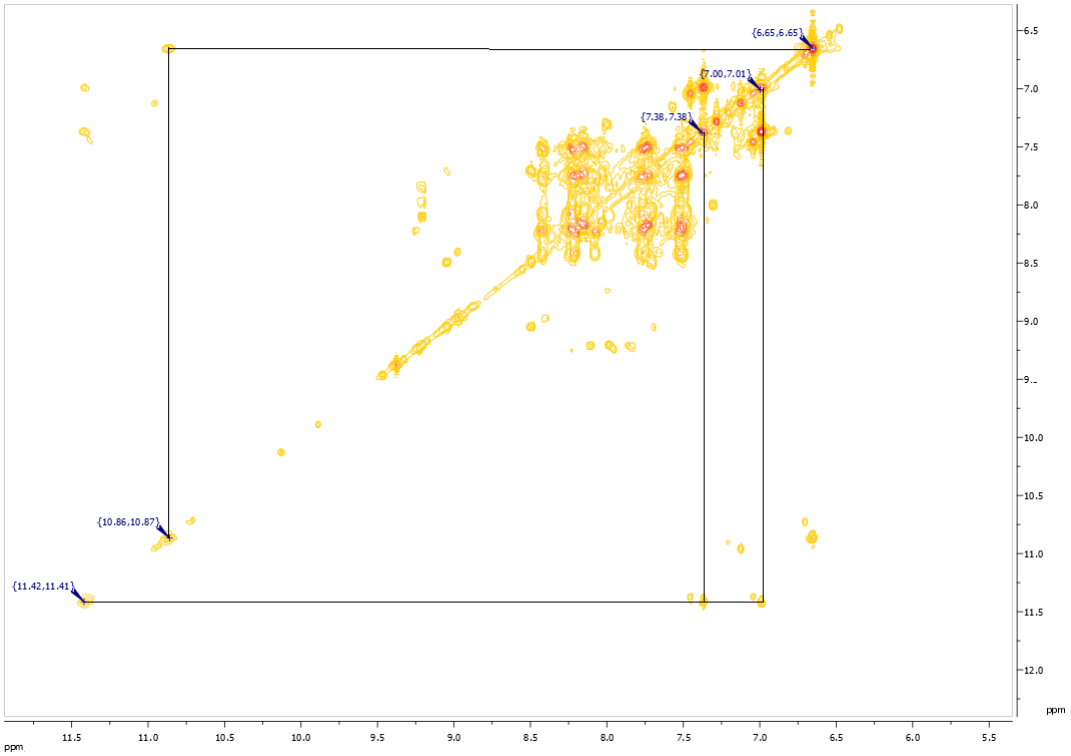

Figure 30: 2D TOCSY NMR of FVP mixture of compound 196 (iii).

As shown in Figure 30, it the protons at 11.42 ppm and 10.86 ppm are coupled with one signal in the aromatic region. All the other aromatic signals seemed not to be related to these two protons. This led to the conclusion that the desired products were not formed during the reaction; therefore it was decided to abandon this part of the project. The complexity of the result could be due to the loss of the methyl in position 2 of the pyrrolo-type system at such high temperatures that could lead to a new radical. This new radical could then undergo various transformations.

5. Synthesis and FVP of 2-pyrazol-1-yl-benzaldehyde *O*-methyloxime

Synthesis of pyrazolo[1,5-*a*]quinazoline was previously performed successfully in the McNab group.[62] As no material remained for use in the investigation of its pyrolysis at 950 °C, it was resynthesised according to the procedures already optimised in the group (Scheme 96).

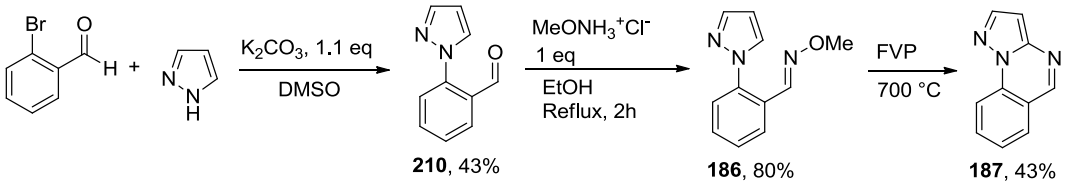

Scheme 96

The first step of the sequence was a nucleophilic substitution reaction of pyrazole with 2′-bromobenzaldehyde that proceeded in 43% isolated yield. Subsequent condensation of aldehyde **210** with *O*-methylhydroxylamine hydrochloride in ethanol gave the oxime ether pyrolysis precursor in 80%. Appearance of a singlet at 3.99 ppm that was indicative of the methoxy group was observed by ^{1}H NMR. Finally, product **186** was pyrolysed at 700 °C to afford pyrazolo[1,5-*a*]quinazoline in 43% isolated yield. ^{1}H NMR (disappearance of the methoxy resonance and of one aromatic proton resonances related to the pyrazole ring was observed) and mass spectrometry were consistent with formation of the desired tricyclic product and matched spectra obtained previously.

6. FVP pyrolysis of pyrazolo[1,5-*a*]quinazoline at 950 °C

Pyrolysis of pyrazolo[1,5-*a*]quinazoline at 950 °C was performed and one compound was isolated as the major species. It was discovered not to be either of the predicted rearrangement products (Scheme 97).

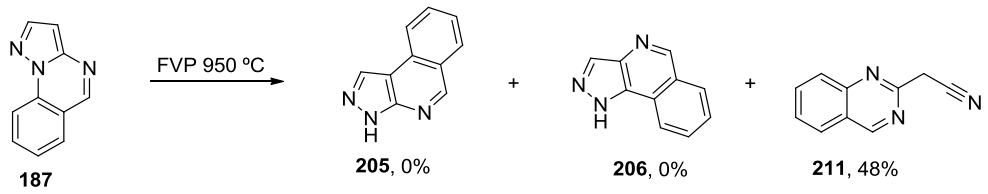

Scheme 97

At first, difficulty was encountered in the elucidation of the structure of **211** using the usual NMR techniques. Therefore crystals of the solid material were grown from hexane and an X-ray diffraction structure of the material was obtained – a pictorial representation is shown in Figure 31.

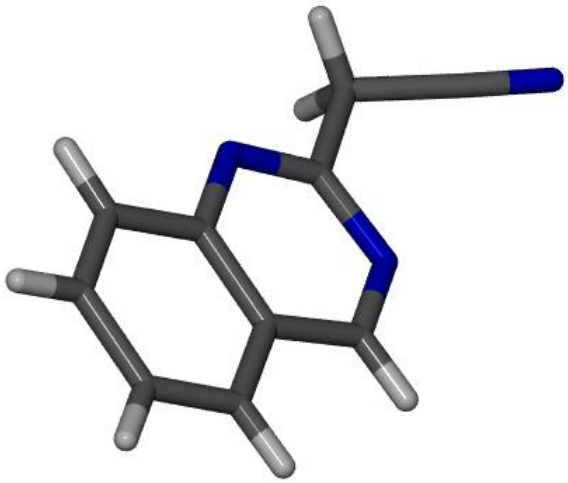

Figure 31: pictorial rappresentation of crystal structure of compound 211.

It was clear from the X-ray diffraction data that the major product obtained in 48% yield was the nitrile **211** which appeared to be a result of pyrazole ring opening. Having obtained the crystal structure, detailed NMR analysis was not necessary for structure confirmation; however, for completion and comparison with similar structures presented later in this chapter, the 2D ^{1}H NMR COSY spectrum is reported below (Figure 32).

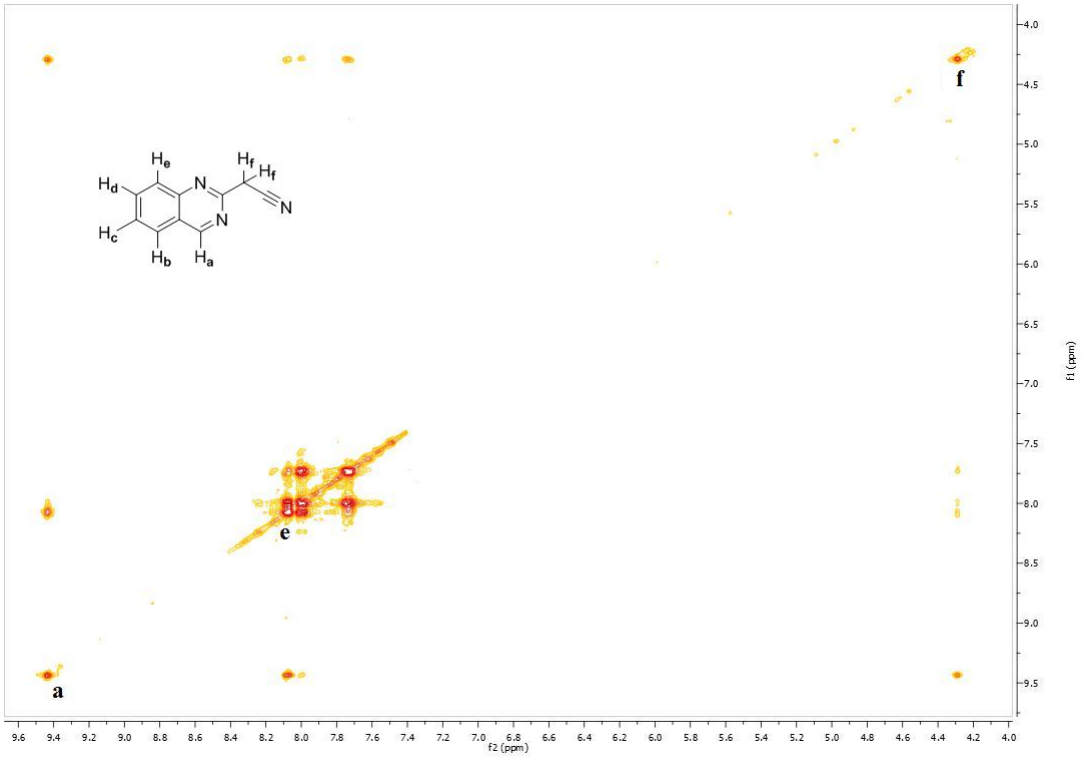

Figure 32: 2D COSY spectrum of compound 211.

It is interesting to see not only the typical **W** interaction between '**a**' (singlet, most deshielded proton in the molecule) and '**e**' (assigned in analogy with structure **111**, *c.f.* Chapter 3, Section 4.1.) but also that the spin of proton '**a**' interacts with the methylene ('**f**') protons in a **W** fashion as well (Figure 33).

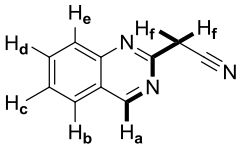

Figure 33: H-H interaction in the COSY spectrum of compound 211.

Correlation between the methylene protons '**f**' and the other aromatic protons is also evident although the couplings are weak.

The proposed mechanism for the formation of the product involves (Scheme 98):

1. homolytic cleavage of the weakest bond (*N–N*) in the pyrazole ring;
2. formation of a fully aromatic 6-membered ring by rearrangement of the di-radical with subsequent formation of the more stable iminyl radical;
3. 1,2 *H*-radical shift with formation of the nitrile moiety.

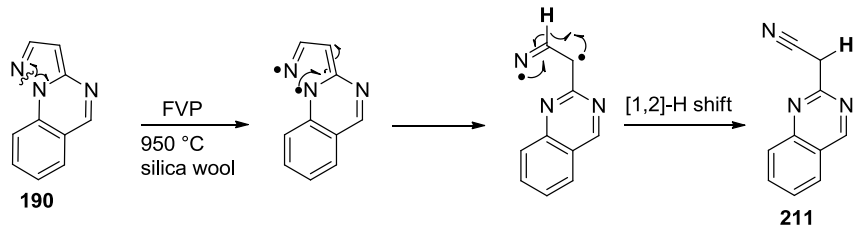

Scheme 98

Although product **211** has been reported in two patents, neither synthesis nor spectroscopic data could be found. Structures of this kind are of interest for use in the formation of polymers[63] and also have some herbicidal properties.[64]

7. FVP pyrolysis of 5-methylpyrazolo[1,5-a]quinazoline at 950 °C

5-Methylpyrazolo[1,5-*a*]quinazoline was previously synthesised in the group[49] and some material was available, so repetition of its synthesis was not necessary. In accordance with results described in previous paragraphs, pyrolysis of 5-methylpyrazolo[1,5-*a*]quinazoline did not yield either of the envisaged rearrangement products **207** and **208** but the corresponding (4-methylquinazolin-2-yl)-acetonitrile **212** instead (Scheme 99).

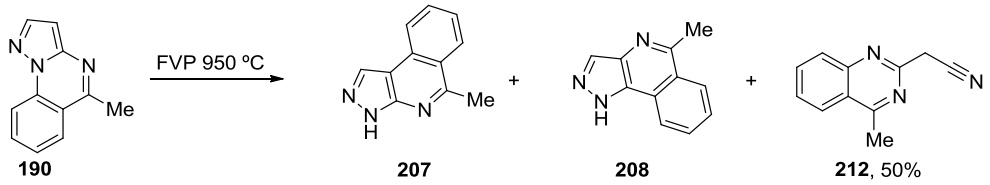

Scheme 99

Proof that product was obtained was given by comparison of ^{1}H NMR of compound **211** and compound **212**. In addition to four aromatic proton resonances, a methyl group at δ 2.97 ppm was observed instead of the downfield singlet (‘**a**’ in **211**). Critically, the presence of a singlet resonance at δ 4.20 ppm integrating for two protons could be ascribed to the methylene vicinal to the newly formed nitrile, similar to that observed in the spectrum of quinazolin-2-yl-acetonitrile **211** (at δ 4.30 ppm). The mechanism of the transformation is proposed to be the same as discussed above (*c.f.* Scheme 98). Unlike quinazolin-2-yl-acetonitrile **211**, (4-methyl-quinazolin-2-yl)-acetonitrile **212** is a previously unreported compound.

8. Synthesis of {[2-(1*H*-imidazol-1-yl)phenyl]methylidene}(methoxy) amine

The synthesis of the desired oxime ether was planned as follows (Scheme 100):

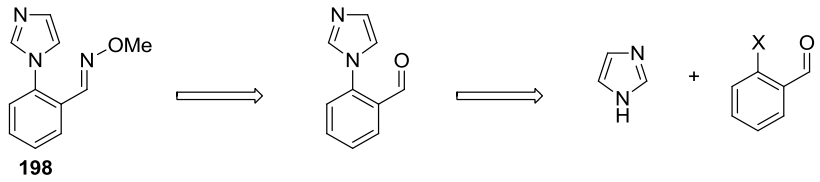

Scheme 100

Preparation of 2-(1*H*-imidazol-1-yl)benzaldehyde **213** had already been attempted in the McNab[62] group following optimised reaction procedure to give compound **210** (Scheme 101).

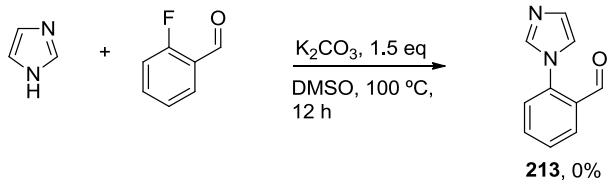

Scheme 101

Unfortunately this reaction did not yield the desired product and no by-products could be isolated and characterised. Conditions which mimicked the synthesis of compound **125** (*c.f.* Chapter 3, Scheme 59) were then trialled.

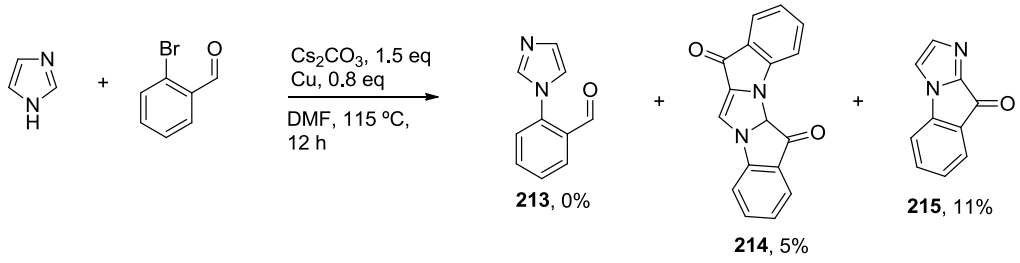

Scheme 102

As shown in Scheme 102, the desired product was not obtained; instead it was possible to isolate two by-products in poor yields by dry flash chromatography. The identity of product **215** was corroborated by comparison with characterisation data

found in the literature and the structure of **214** was tentatively assigned as shown in Scheme **102** based on NMR data.

Detection of 9*H*-imidazo[1,2-*a*]indol-9-one **215** in the reaction mixture could be explained by reaction of the desired product (formed in the nucleophilic substitution reaction between imidazole and 2′-bromobenzaldehyde) by formal C-H activation of the most acidic imidazole proton and insertion into the aldehyde C-H (Scheme 103).

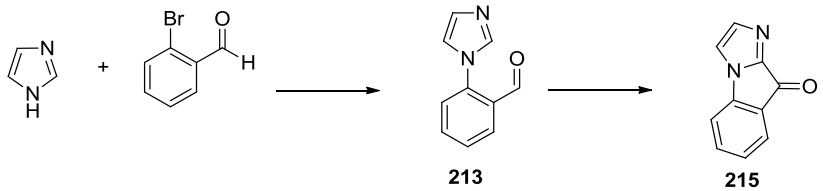

Scheme 103

In work published in 1991, Rosevear and Wilshire reported the reactions between some azoles with *o*-fluoro-acetophenone, -benzaldehyde and -benzophenone in dimethyl sulfoxide solution in the presence of anhydrous potassium carbonate. In the cases of *o*-fluoro-acetophenone and -benzophenone, carbinol products were isolated in addition to the expected substitution products, whereas a cyclic ketone by-product was found when *o*-fluoro-benzaldehyde was utilised.[65] It is therefore unsurprising in retrospect that product **215** was found under our reaction conditions, as in the example from Rosevear and Wilshire shown in Scheme 104.

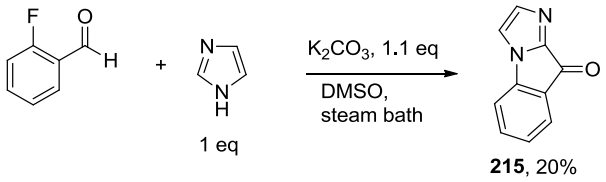

Scheme 104

This reaction yielded solely product **215**. Although there are differences in the conditions used in the paper and in the work presented in this thesis, it is clear that once the aromatic substitution of the imidazole has occurred on the 2-fluorobenzaldehyde, the oxidative cyclisation follows immediately without possibility of isolation of the corresponding aldehyde. This is possible in the presence of a base and very polar solvent at high temperatures.

Previously reported ^{1}H NMR spectrum was recorded in the C_6D_6 whereas for this work it was recorded $CDCl_3$. Taking into account this difference, it is still possible to compare the coupling constant between protons in the imidazole ring (J = 1.0 Hz in C_6D_6, J = 0.9 Hz in $CDCl_3$). This similarity with the reported data and the multiplicity of the observed proton resonances allowed us to rule out formation of the regioisomer shown in Figure 34.

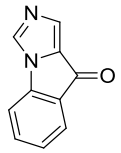

Figure 34: regioisomer of compound 215 not observed in reaction described in Scheme 104.

The proposal for the structure of the second product suggested in Scheme 102 was made based on the supposition that compound **215**, once formed, can go on to react with an additional molecule of 2′-bromobenzaldehyde as shown in Scheme 105.

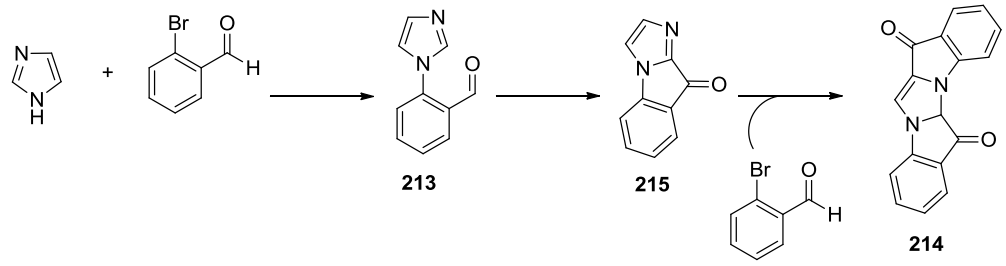

Scheme 105

The *N*-atom in position 3 of the imidazole ring is presumably involved in a nucleophilic aromatic substitution step which may be followed by cyclisation onto position 2 of the imidazole ring.

The proposed structural assignment was in agreement with the experimental data obtained. A mass to charge ratio of *m/z* = 274 was observed by mass spectrometry, consistent with the singly charged molecular ion of **214**, and NMR indicated the correct number of non-equivalent protons (10 H) in the aromatic region of the spectrum as shown in Figure 35.

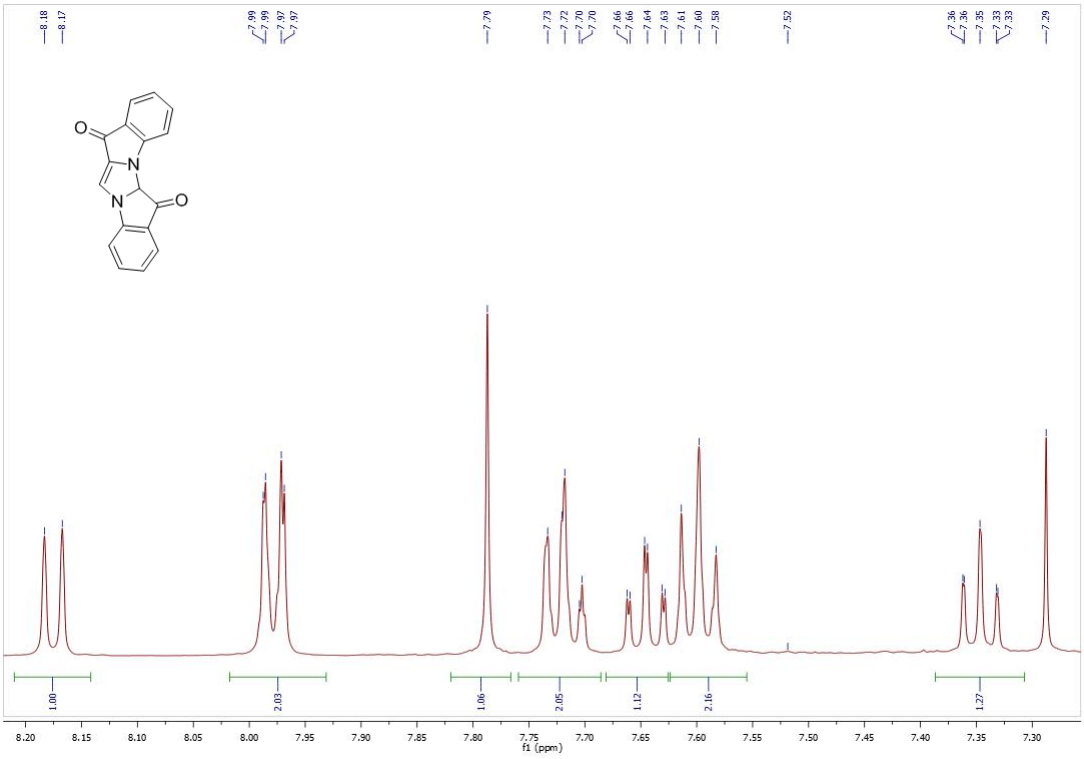

Figure 35: ^{1}H NMR spectrum of compound 214.

Also, from the ^{13}C spectrum and carbon DEPT 135 and 90 it is possible to observe the presence of two carbonyls (δ 184.7, 178.4 ppm) and 5 more quaternary carbons. Despite applying more sophisticated techniques such as COSY, HSQC and HMBC, due to the complicated nature of the spectra, no additional useful information was gained. As the assignment of these structures goes beyond the scope of this thesis, no more work was carried out towards this goal, although this interesting discovery could provide ideas for further investigations.

Other attempts were made to synthesise compound **213** using conditions reported in Table 6 according to scheme 106.

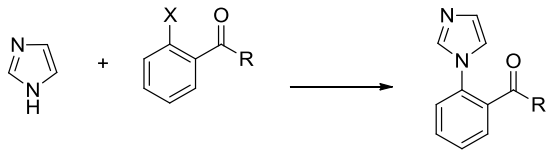

Scheme 106

entry	aryl halide	base	solvent	catalyst	product %	Temp (°C)	time (h)
1	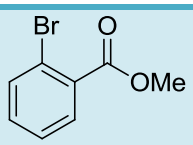	K_2CO_3	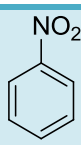	Cu	0	115	24
2	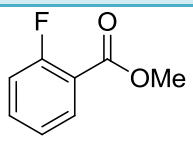	Cs_2CO_3	DMF	-	0	110	48
3[66]	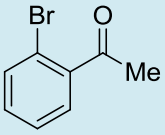	K_2CO_3	$Si(OEt)_4$	CuI (5mol%)	0	200	40 min (MW)

Table 6: reaction conditions used for attemped SNAr reaction described in Scheme 106

The conditions described in entry 1 Table 6 were derived from conditions used to obtain the precursor ester of carbazole derivative **125** (*c.f.* Chapter 3, Scheme 59). Substituting the aldehyde group with an ester to avoid the oxidative cyclisation on the imidazole ring was attempted, but unfortunately the reaction with this substrate was unsuccessful.

The conditions reported in entry 2 Table 6 are similar to those utilised for the synthesis of the other 2-azole aldehyde analogue **210** as described in Schemes 96 (Section 5). The difference in this case was the use of an ester, to avoid the unwanted side reaction described above. Unfortunately, these conditions also failed to yield the desired aldehyde **213**.

A final attempt to successfully achieve the desired coupling was performed under conditions inspired by a report by Zhang and coworkers (entry 3, Table 6).[66] They achieved excellent results by reacting 1*H*-imidazole with 4-haloanisole (Cl, Br, I) under microwave conditions in the presence of CuI (5 %). Tetraethyl orthosilicate was the solvent of choice as it was convenient to work up and able to stand high temperature. Unfortunately, with our substrate only decomposition products were observed in the crude NMR analysis.

As the nucleophilic aromatic substitution reaction in the presence of the aldehyde appeared to be problematic, it was decided to look for literature precedence of an alternative disconnection or protection strategy. S. Hecht and co-workers[67] described a way to avoid any side reactions between imidazole and 2′-bromobenzaldehyde by protecting the aldehyde, performing the nucleophilic aromatic substitution and then deprotecting the aldehyde functionality (Scheme 107).

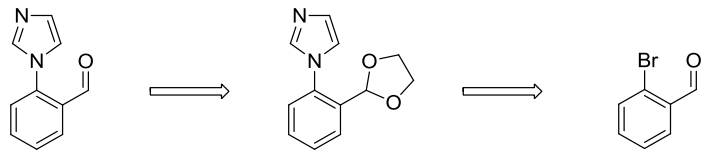

Scheme 107

Acetal protection of the aldehyde by reaction between 2′-bromobenzaldehyde with ethane-1,2-diol and *p*-toluenesulfonic acid in toluene was unproblematic and proceeded in a good yield affording compound **216** (Scheme 108).

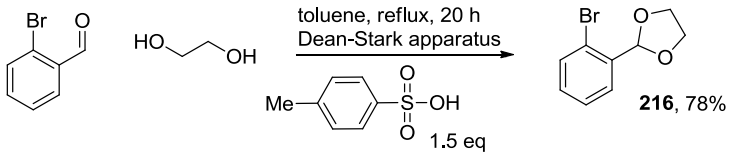

Scheme 108

Proof that product **216** was obtained were given by the disappearance of the aldehyde peak and appearance of the aliphatic protons related to the 1,3-oxolane ring at 5.55 ppm (1H, acetal proton), 4.20-4.16 ppm and 4.08-4.04 ppm (2×2H, 1,3-oxolane methylene signals) in the ^{1}H NMR spectrum. The protected substrate was then subjected to nucleophilic aromatic substitution reaction conditions with imidazole (Scheme 109).

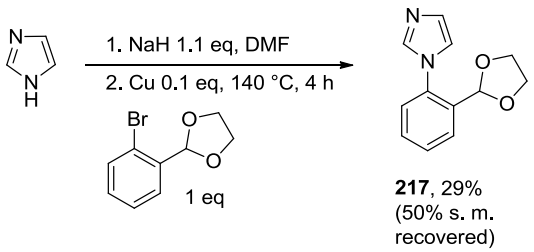

Scheme 109

Satisfyingly, the acetal-protected substrate gave the desired product although the isolated yield was low, partly due to low conversion (50 % of the starting material was recovered unreacted). NMR and mass spectroscopy analyses of the isolated product were consistent with the structure of **217**. No attempt was made to optimise the reaction conditions as a sufficient amount of **217** was isolated to allow continuation of the synthesis. However extending the reaction time and increasing the amount of copper catalyst may drive the reaction to completion and increase the yield. Deprotection was achieved by simply stirring product **217** in HCl_{aq} (1 N) for 2 h at room temperature affording product **213** in good yield (Scheme 110) after purification.

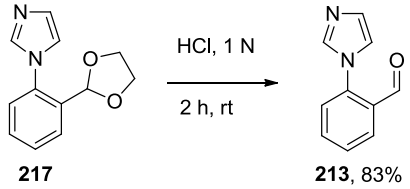

Scheme 110

Appearance of an aldehyde peak in the ^1H NMR spectrum was observed at 9.76 ppm in place of the aliphatic signals related to the oxolane ring.

The final stage of the preparation of the FVP precursor was oxime ether formation by treating aldehyde **213** with *O*-methylhydroxylamine hydrochloride (Scheme 111).

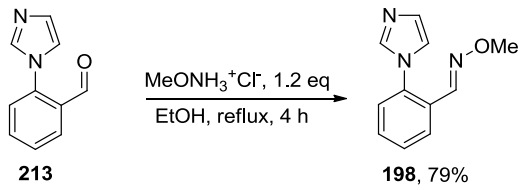

Scheme 111

The singlet related to aldehyde peak at 9.76 ppm had shifted to 7.78 ppm in the ^{1}H NMR spectrum and a new singlet at 3.95 ppm appeared (methoxy group) indicative of oxime ether formation.

9. FVP of {[2-(1*H*-imidazol-1-yl)phenyl]methylidene}(methoxy)amine

Pyrolysis of oxime ether **198** yielded two regioisomeric products – imidazo[1,5-*a*]quinazoline **199** (21%) and imidazo[1,2-*a*]quinazoline **200** (60%). Pyrolysis was performed at 700 °C and products were separated by dry flash chromatography affording the materials as yellow and orange solids respectively. No other products were isolated by chromatography (Scheme 112).

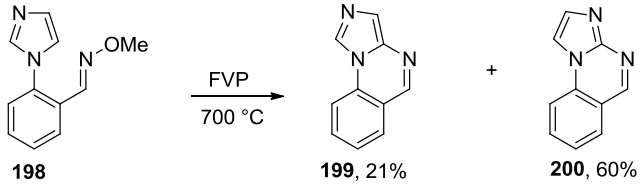

Scheme 112

Compound **200** has been reported previously by Rodway et al[68] in a patent published in 1975 in which they describe its anti-inflammatory properties, whereas heterocycle **199** is unknown in the literature. The only analytical data reported for **200** is a melting point, so both compounds were characterised by NMR and mass spectroscopy (described in subsequent paragraphs and listed in the experimental section).

9.1. Analysis of imidazo[1,5-*a*]quinazoline 199

The methoxy resonance from the FVP precursor is absent in the ^{1}H NMR of product **199** as would be expected after formation of the iminyl radical and subsequent

cyclisation. The NMR presents three singlets associated with proton '**a**', '**b**' (as H_1 and H_3) and '**c**' (as H_5) (Figure 36) at 8.54, 8.51 and 7.69 ppm.

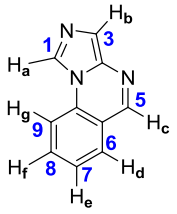

Figure 36: enumeration of compound 199.

It was not possible to unequivocally assign the individual resonances based on the simple proton NMR spectrum alone, so to aid the assignment 2D-COSY NMR was taken (Figure 37).

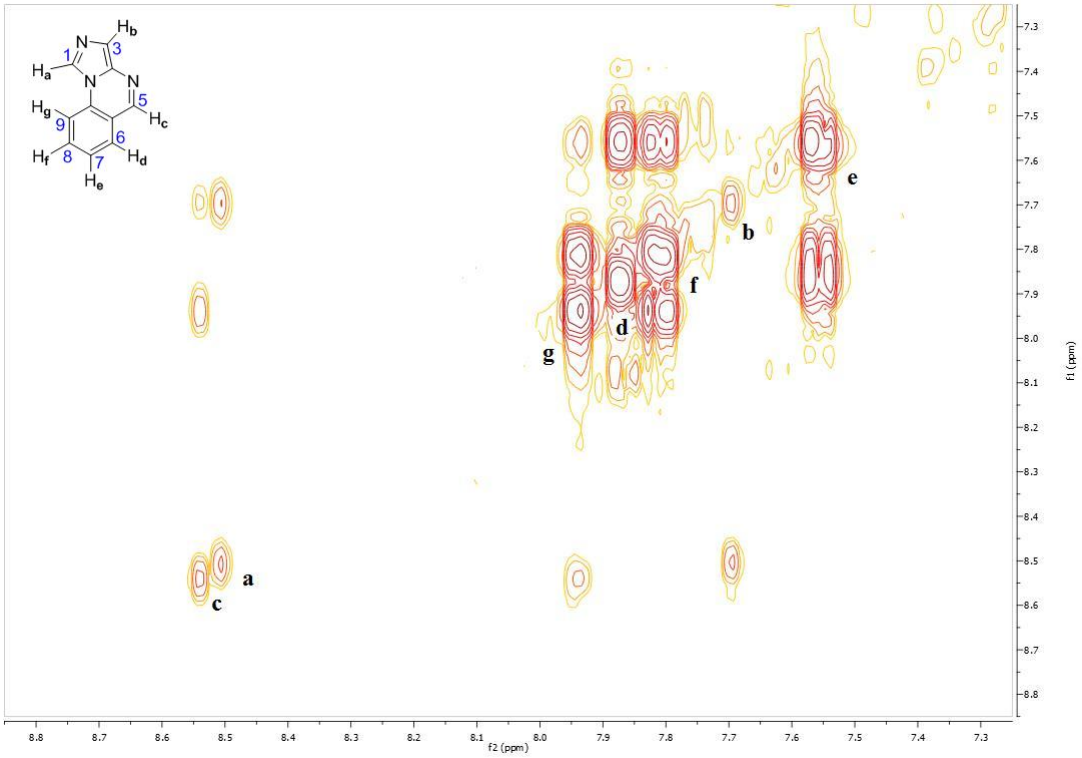

Figure 37: COSY spectrum of compound 199.

Singlets '**a**' and '**b**' correlate with one another weakly, probably interacting with each other in a **W**-fashion across the imidazole ring. The singlet at 8.54 ppm is therefore associated with proton '**c**' of the pyrimidine ring which correlates with doublet '**g**' (as H_9) in analogy with compound **111** in Chapter 3 (Figure 38).

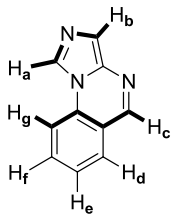

Figure 38: possible H-H interactions in the COSY spectrum of compound 199.

To differentiate between protons '**a**' and '**b**' of the imidazole ring, **a** 2D-NOESY NMR spectrum was taken in an attempt to find a through-space interaction with a proton of the aryl ring (Figure 39).

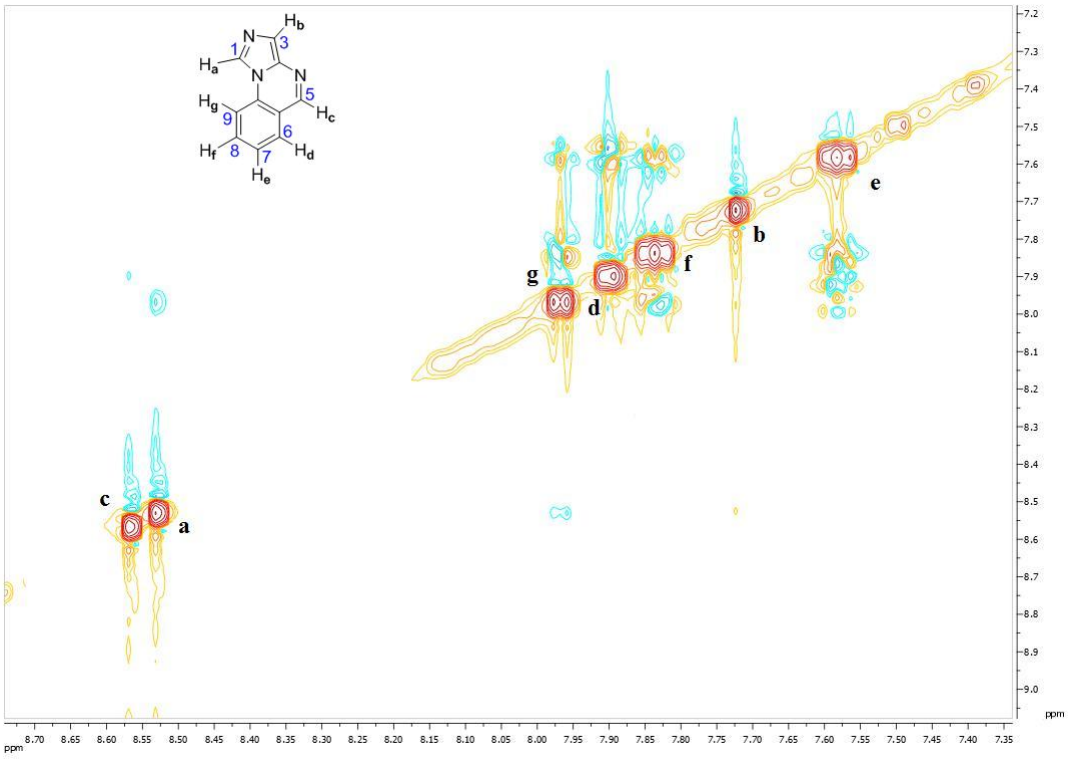

Figure 39: NOESY spectrum of compound 199.

It is clear from the above spectrum that proton '**a**' and proton '**g**' have a weak interaction with each other – consistent with the assignment drawn in Figure 41. With the identity of proton '**g**' confirmed, it was also possible to assign the remaining protons which were part of the same spin system ('**d**', '**e**', and '**f**' as H_6, H_7 and H_8) based on their multiplicity and correlations in the COSY spectrum (Figure 40).

9.2. Analysis of imidazo[1,2-*a*]quinazoline 200

Compound **200** was also identified by NMR spectroscopy. From the ^{1}H NMR the appearance of two doublets at 7.75 and 7.93 ppm[69] with small coupling costant (J = 1.5) was observed. These appear to be the two doublets related to imidazole ring protons '**a**' and '**b**' as H_1 and H_2). Also, a shift of the singlet corresponding to the proton α to the oxime ether was observed from 7.78 ppm in the starting material to 8.93 ppm in the product as it became part of the pyrimidine ring system (proton '**c**' as H_5, Figure 40).

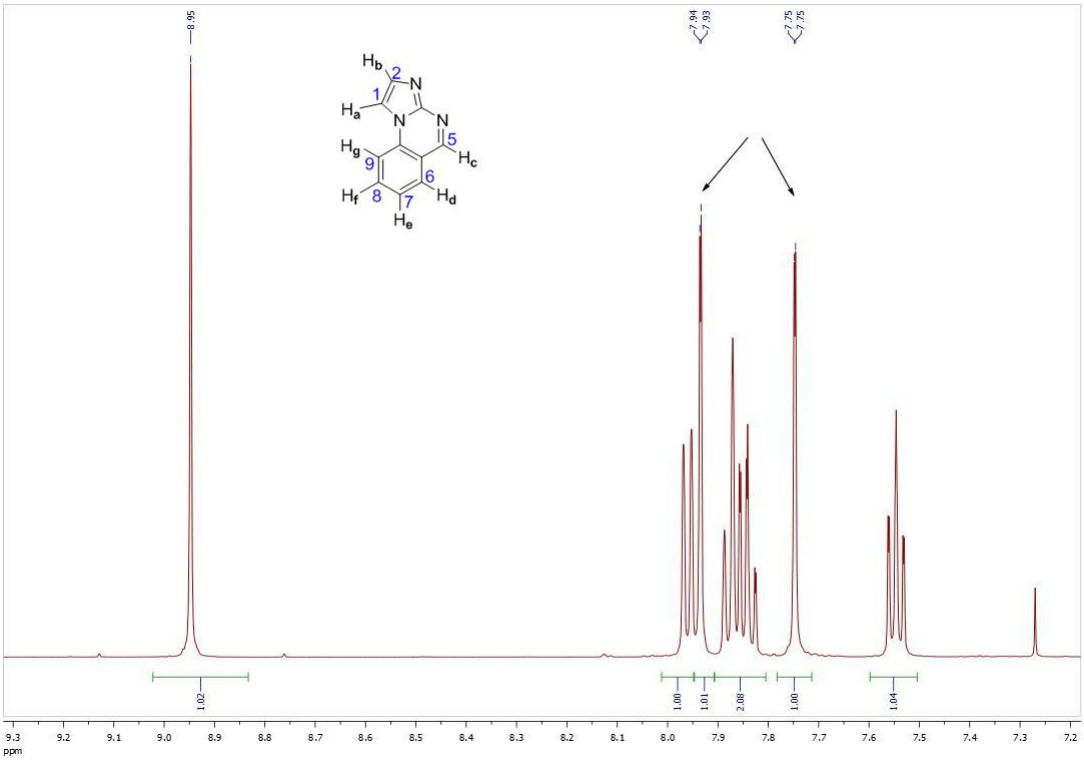

Figure 40: ^{1}H NMR spectrum of compound 200.

The assignment of the remaining proton resonances in the structure was achieved with the assistance of a 2D-COSY spectrum. Thanks to the '**W**'-type interaction between protons across the aromatic skeleton, the resonance due to proton '**g**' (as H_9) was assigned (Figure 41).

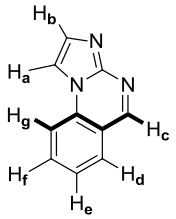

Figure 41: possible H-H interaction in the COSY spectrum of compound 200.

The cross peak due to the correlation between protons '**c**' and '**g**' is evident in Figure 42. The signal at 7.88 ppm could consequently be attributed to proton '**d**' (as H_6) on account of its splitting pattern – it was the only other nucleus expected to appear as a doublet.

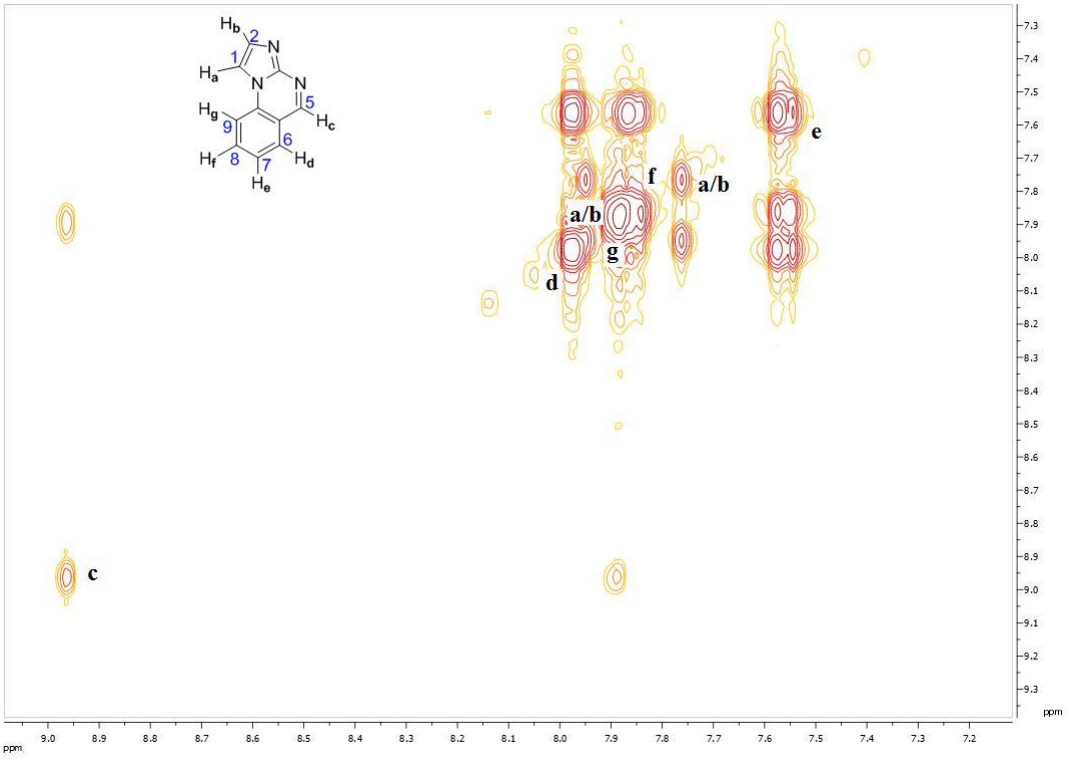

Figure 42: COSY spectrum of compound 200.

Following on from this, proton '**d**' is coupled to '**e**' (as H_7) – a triplet at 7.55 ppm – leaving proton '**f**' which gives rise to a triplet that overlap with the peaks from proton '**g**'. In an attempt to differentiate between protons '**a**' and '**b**', a 2D-NOESY experiment was performed. Unfortunately, no NOE interactions were observed between proton '**g**' and either of the imidazole resonances. Further experiments would be required in order to make an unequivocal assignment. On the basis of their

chemical shifts, the peak at 7.95 ppm was tentatively attributed to proton '**a**' as we would expect this position to be the most deshielded.

The proposed mechanism for the cyclisation involves (Scheme 113):

1. formation of a *N*-centred radical as a consequence of the cleavage of the weakest bond in the oxime group;
2. attack of the iminyl radical onto the imidazole ring at position 5 (for **199**) or position 2 (for **200**) generating a 6-membered ring ;
3. loss of an *H*-radical with restoration of aromaticity.

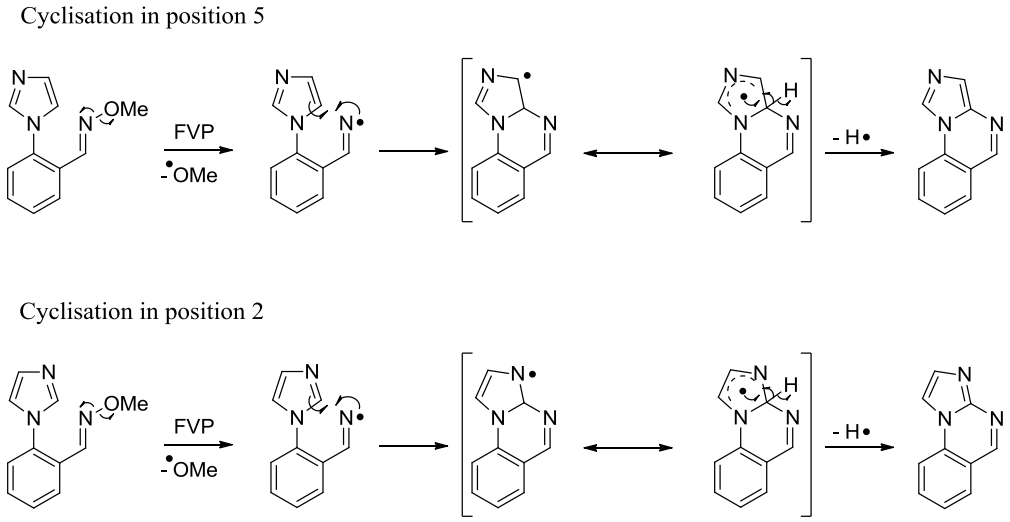

Scheme 113

With this mechanistic proposal in mind, it is possible to rationalise the product distribution that was obtained. The initial cyclisation at position 5 results in an intermediate with a carbon-centred radical resonance form, whereas during the cyclisation at position 2, the analogous resonance form bears a nitrogen-centred radical. Formation of the nitrogen-centred radical would be expected to be more energetically favourable, and indeed, this intermediate would lead to the product being formed in higher yield. In work published by T. Körtvélyesi and L. Seres[70], the calculated absolute energy of addition of a methyl radical to the carbon of C=N bond compared with the carbon of a C=C bonds was found to be lower, leading to the conclusion that less energy is required to break a π bond between C=N than C=C.

10. DFT calculations for iminyl radical cyclisation on the imidazole ring

To confirm our rationalisation as to why product **200** is achieved in higher yield (60%) than product **199** (21%), the energy profile of the system was modelled using DFT calculations (Figure 43).

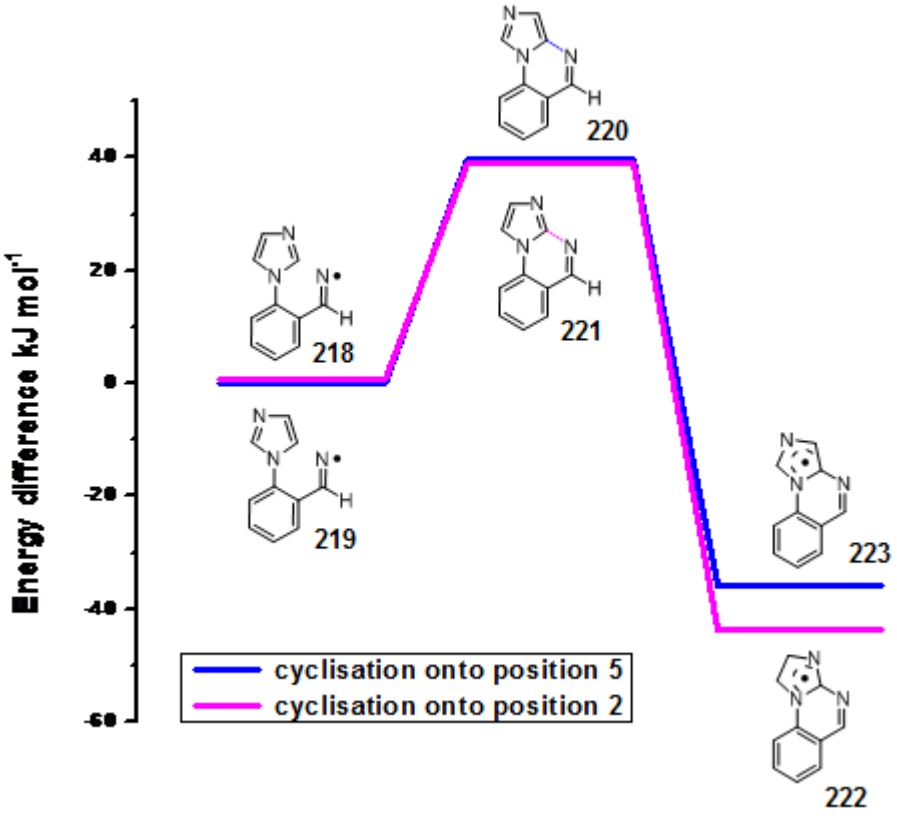

Figure 43: calculated energy profile of compound 222 and 223.

From the energy profile, it is evident that although the energy of the initial iminyl radicals **218** and **219** and transition states **220** and **221** are essentially equal, there is a ΔE = 10 kJ mol^{-1} between the two intermediates **222** and **223**. This supports our theory that the product distribution is a result of the stability of the intermediates. As the energy barriers to formation of these intermediates are equal, it is possible to say that this reaction is governed thermodynamically rather than kinetically.

11. FVP of imidazo[1,5-*a*]quinazoline at 950 °C

As discussed in the introduction, one of the aims of this project was to perform pyrolysis at 950 °C on the cyclised product **199**. It was hoped this could lead to two novel rearrangement products containing three fused rings.

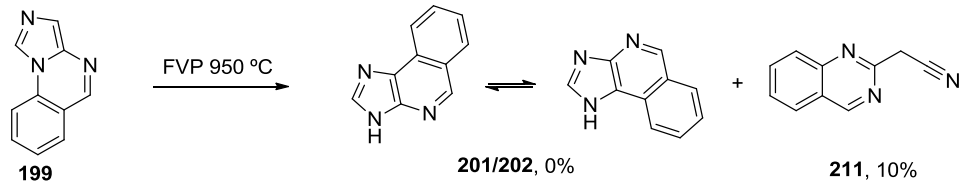

Scheme 114

Cyclised compound **199** was found to be particularly non-volatile and so a high temperature was required in the Kugelrohr oven in order to introduce it in to the gas phase. After pyrolysis, an NMR of the crude was taken and in contrast with examples discussed in Chapter 3, the resulting spectrum was complex. In addition to this, no sign of a typical peak corresponding to *N-H* around δ 9-12 ppm was observed. This led to the conclusion that the harsh conditions required to vapourise the starting material led to decomposition. Purification of the crude mixture resulted in the isolation of just one product – nitrile **211** in poor yield. An explanation of this result could be given by looking at the nature of the structure **211**. As shown in Scheme 115, alternative breaking points at such high temperature are available.

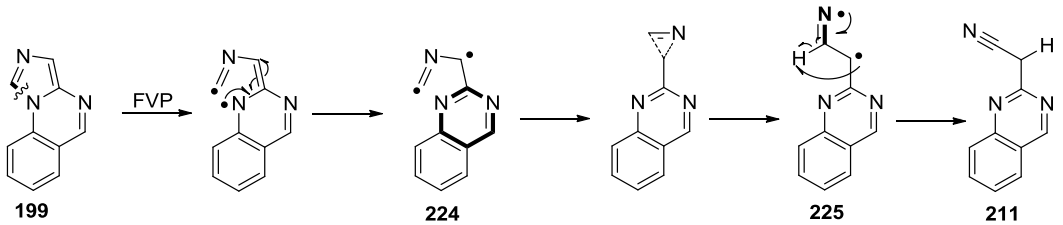

Scheme 115

Breakage of the bond highlighted in the scheme can be induced by the subsequent formation of a fully aromatic 6-membered ring (structure **224**). This di-radical could then rearrange to give a more stable *N*-centred radical **225** that could undergo β-cleavage and 1-2 *H*-radical shift to obtain the final nitrile **211**.

12. Conclusion

Systems with substituted oxime ethers and 2-azoles in place of pyrrole were investigated in this chapter.

1. a successful synthetic route to synthesise {[2-(1*H*-imidazol-1-yl) phenyl]methylidene}-(methoxy)amine **198** was found and consequent pyrolysis led to formation of imidazo[1,5-*a*]quinazoline **199** and imidazo[1,2-*a*]quinazoline **200** in a 1 : 3 ratio;
2. DFT calculations were performed to explain these results and indicated that imidazo[1,2-*a*]quinazoline **200** is formed as the major product *via* a more thermodynamically stable intermediate;
3. FVP at 950 °C of 1,5-dimethylpyrrolo[1,2-*a*]quinazoline **197 (iii)** was performed but did not produce any tricyclic rearrangement products. This is probably due to presence of a methyl group that can easily be cleaved under these conditions leading to more complicated radical systems;
4. FVP at 950 °C of the three available 2-azole systems (**199**, **187** and **190**) was performed showing unexpected results. The three systems yielded 2-substituted quinazoline systems (**211** and **212**). Although these were not the desired products, it was found that these products are of potential commercial use and have been previously patented. Also, from a mechanistic point of view it was demonstrated that the presence of an extra *N*-atom in the pyrrole ring generates more breaking points. This, in turn, generates di-radical systems that rearrange to a more stable iminyl radical.

Chapter 5:

Generation of novel substituted isoquinolines *via* iminyl radicals cyclising onto C-C double bond.

1. Introduction

The synthesis of isoquinolines has been a topic of continuing interest for chemists over many decades. The main reason behind this is that the isoquinoline backbone features in a number of classes of medicinally active alkaloids which can act as enzyme inhibitors and display antispasmodic, antimicrobial, antitumor, antifungal, anti-inflammatory, cholagogue, hepatoprotective, antiviral, amoebicidal, and anti-oxidant properties. Notable isoquinoline derivatives include the well-known painkillers morphine and codeine. Isoquinoline natural products are typically found in the *Papaveraceae*, *Berberidaceae* and *Ranunculaceae* families and are derived from the amino acids phenylalanine or tyrosine. A key precursor of their biosynthesis is 3,4-dihydroxytyramine (dopamine) linked to an aldehyde or ketone.[71]

The structure of the parent isoquinoline is shown in Figure 44.

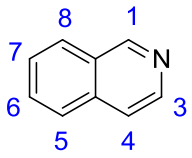

Figure 44: isoquinoline structure and its numbering.

There are few methods to synthesise isoquinoline cores. The classical methods are well-known reactions such as Bischler-Napieralski, Pictet-Spengler followed by Pictet-Gams and Pomeranz-Fritsch reactions.

One of the first reactions to be discovered for the synthesis of isoquinolines was Bischler-Napieralski reaction[72]. It involves the use of acetyl or benzoyl *β*-arylethylamine or some substance which, during the synthesis, will give rise to such an analogous amide as an intermediate. The use of phosphorus pentoxide and heating at high temperature in a solvent such as toluene is also essential. 1-Alkyl- or 1-aryl-3,4-dihydroisoquinolines are produced in this reaction, usually in moderate yields. An example is shown in Scheme 116.

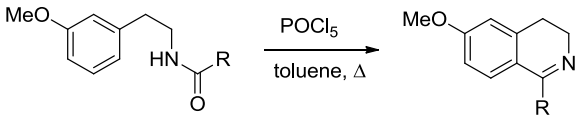

Scheme 116

The presence of an electron-withdrawing methoxy group in the *para* position to the nucleophilic site on the aromatic ring has been shown to be essential in the mechanism of the reaction.

Two variations were introduced by Pictet and Spengler,[73] and after by Pictet and Gams,[74] affording isoquinoline derivatives in drastically improved yields.

The Pictet-Spengler reaction is an acid-catalysed intramolecular cyclisation of the intermediate imine of a 2-arylethylamine, usually formed by condensation with a carbonyl compound precursor, to give 1,2,3,4-tetrahydroisoquinoline and tetrahydro-β-carboline (indole-type alkaloids) derivatives. The use of a strong acid is necessary in both reactions.[75]

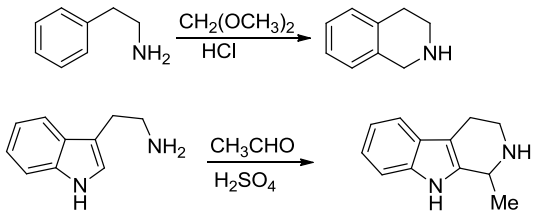

Scheme 117

Subsequent oxidation of the tetrahydroisoquinoline and tetrahydro-β-carboline products of these reactions is necessary afford the fully aromatic isoquinoline derivatives

As Cox and Cook documented[76], it is also possible to obtain a cyclisation in non-acidic aprotic media. However, the presence of an electron-withdrawing group is necessary in the α-position of the amine in order to increase the electrophilicity of the imine intermediate (Scheme 118).

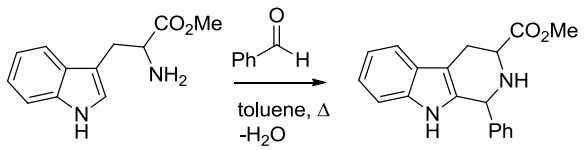

Scheme 118

In work carried out by Wu and Wang[77] it was shown that the transformation from β-arylethylamides **226** to isoquinolines can be performed in one pot and in the absence of an electron-withdrawing group in the α-position of the amine but with the presence of an electron-donating group substituent on the aryl ring. The key reagent used for this transformation is Hendrickson's reagent which is generated *in situ* from 1.5 equivalents of triflic anhydride and 3.0 equivalents of triphenylphosphine oxide. This powerful tool is used to activate the amide forming an imidate, facilitating the intermolecular cyclisation. The oxidation of the dihydroisoquinoline **227** is then carried out by adding an oxidising reagent such as MnO_2 to the reaction mixture. A downside of this reaction is the poor atom economy of it due to the generation of $OPPh_3$ and triflic acid as side products (Scheme 119).

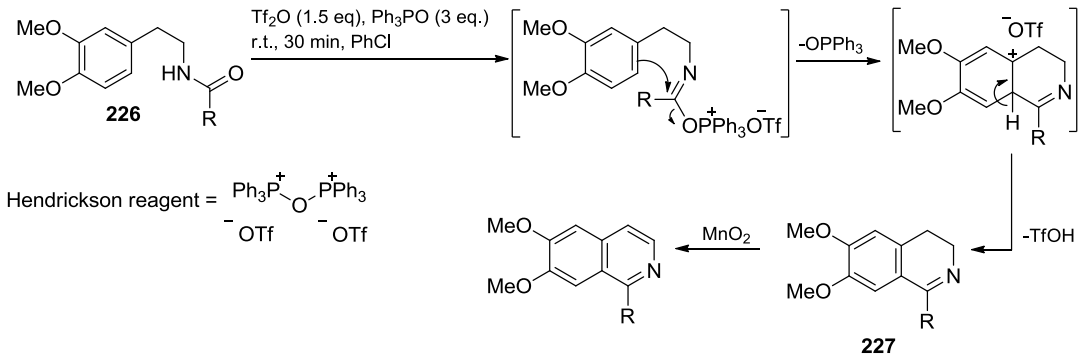

Scheme 119

The last of the classical methods is the Pomeranz-Fritsch reaction.[78] The original reaction includes the use of aromatic aldehydes and an amino acetal (Scheme 120).

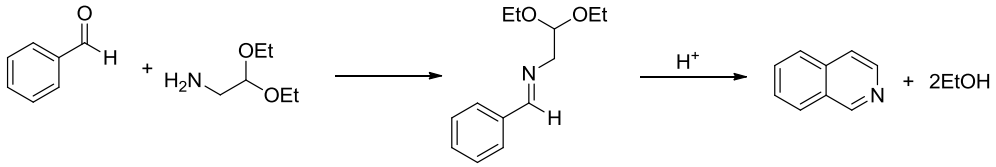

Scheme 120

An example is reported in Scheme 121 where it can be seen that the cyclisation is encouraged by the presence of two methoxy groups on the benzene ring: one used as an electron-withdrawing group *para* to the cyclising site and the other used as an electron-donating group *meta* to the aldimine functionality. The use of an acid in the reaction mixture is also necessary.[79]

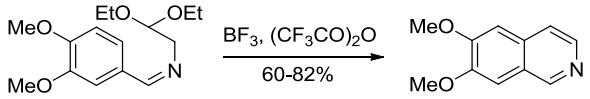

Scheme 121

A modification by Schlittler and Müller uses benzyl amines and glyoxal semiacetal (Scheme 122).[80]

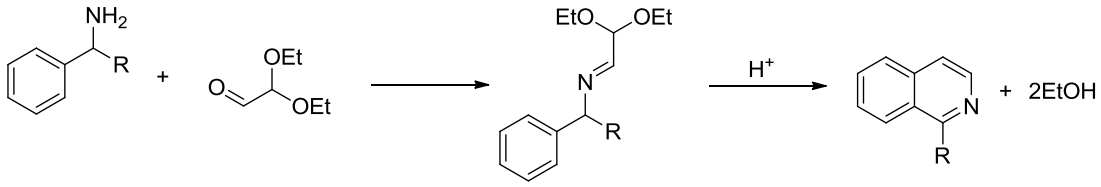

Scheme 122

A more elaborate example is reported in Scheme 123. The example shows that more than one condensation reaction can be performed to give fused heterocycles which contain isoquinoline motifs.[81]

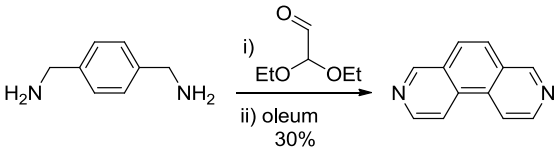

Scheme 123

Having understood the basics of the synthesis of isoquinolines, a survey of the literature reveals that there are a vast amount of examples that provide a variety of alternatives to classic methods or simply variations of the latter ones.

A good example of modification of the classic Bischler-Napieralski and Pictet-Spengler is given by Awuah and Capretta[82] who investigated the use of microwave heating. Classic conditions of this reaction usually lead to poor to moderate yields of the final products. Awuah and Capretta investigated various solvents, reaction times and temperatures in the microwave to find out that using toluene, eight equivalents of TFA at 140 °C for 30 min resulted in the desired dihydroisoqionolines in yields of >98%.

In recent years one of the most frequently exploited routes to access these kind of heterocycles is an intermolecular method that uses a cross coupling/cyclisation sequence. The most interesting advantage in this methodology is the use of milder reaction conditions that allow the tolerance of various functional groups. The main methodologies using cross coupling are reported in Scheme 124.[83]

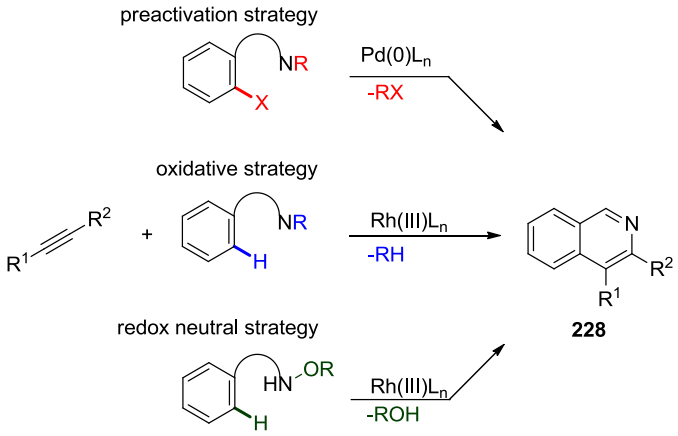

Scheme 124

Larock and co-workers pioneered the palladium-catalysed annulation of alkynes using a preactivation strategy, reporting several examples throughout the years. In a

paper published in 1998[84] they reported a method using *tert*-butylimines **229** along with 2 equivalents of an alkyne in the presence of 5 mol % $Pd(OAc)_2$, 10 mol % PPh_3, and 1 eq. of Na_2CO_3 with DMF as the solvent at 100 °C (Scheme 125).

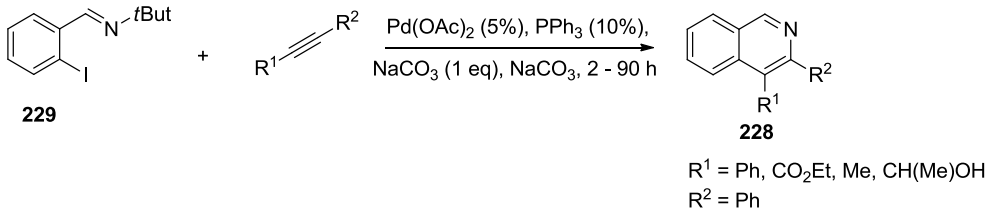

Scheme 125

In the examples reported, it is noticeable that only one of the possible regioisomers **228** was obtained, in which the aryl substituent is always in the 4-position (when $R^1 \neq$ Ph). It is also worth mentioning that all the attempts to form isoquinolines from dialkyl-substituted alkynes *via* this route were unsuccessful. Larock and co-workers[85] later discovered a procedure to perform the annulation with terminal alkynes under a different set of conditions. Sonogashira coupling between iodide **229** and the alkyne was observed prior to annulation to give the desired heterocyclic product. Therefore, the synthesis of isoquinolines was performed in two steps using optimised conditions for each reaction as shown in Scheme 126.

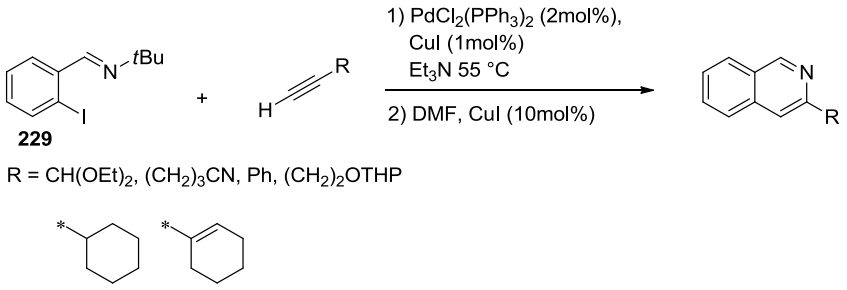

Scheme 126

Between step 1 and step 2, the solution was filtered and solvent (in this case Et_3N) evaporated before simply adding DMF and additional CuI. The yields obtained with this method ranged from good to excellent (80-90%). The limitation of this route is the availability of pre-activated imine.

This issue has been elegantly solved by the use of a rhodium catalyst system developed by N. Guimond and K. Fagnou among others.[86] A copious amount of work has been done employing conditions shown in Scheme 127.

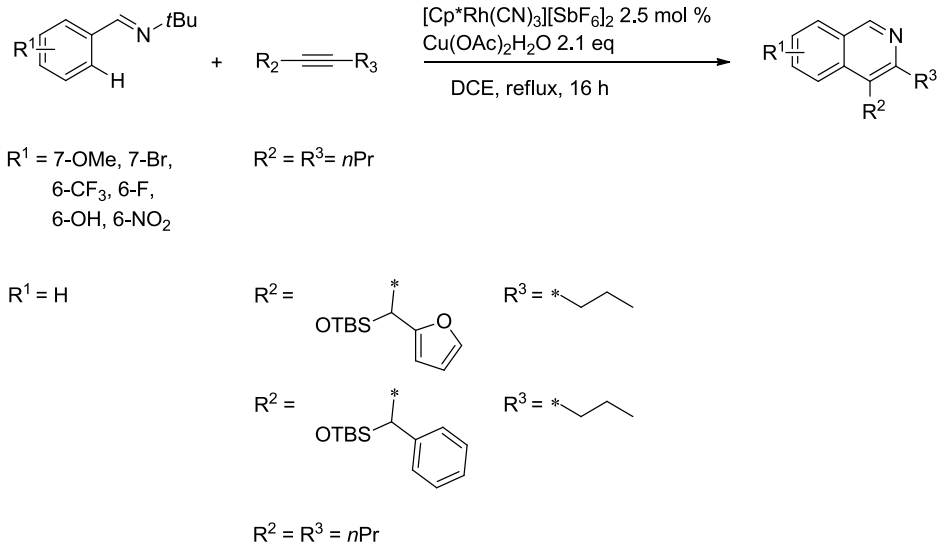

Scheme 127

The key step of this system is activation of the sp^2 C-H bond in the position *ortho* to the imine directing group. The Rh catalyst also mediates both the formation of a C-C bond and the formation of a C-N bond. The presence of $Cu(OAc)_2$ in the reaction mixture regenerates the catalyst by oxidation of Rh(I) to Rh(III).

As is shown in Scheme 127, when $R_2 \neq R_3$, one regioisomer is formed selectively with the bulkier group situated in the 4-position – probably due to the nature of the catalyst and the coordination process. The selectivity is impressive however, this is also a limitation, as isoquinolines with more steric bulk in the 3-position than in the 4-position cannot be obtained. Furthermore, a stochiometric amount of the oxidant is needed to regenerate the catalyst.

Chiba and co-workers[87] have recently developed a new Rh-catalysed system that utilises a redox-neutral strategy. The characteristics of the system and some examples are reported in Scheme 128.

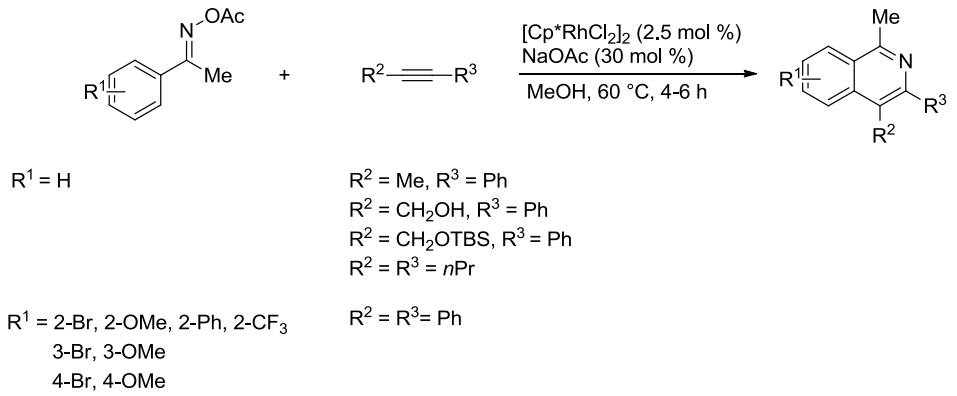

Scheme 128

The main feature is the absence of an oxisiding additive which is not required since the Rh(III) catalytic species is regenerated by intermediate **230** during the catalytic cycle (Scheme 129).

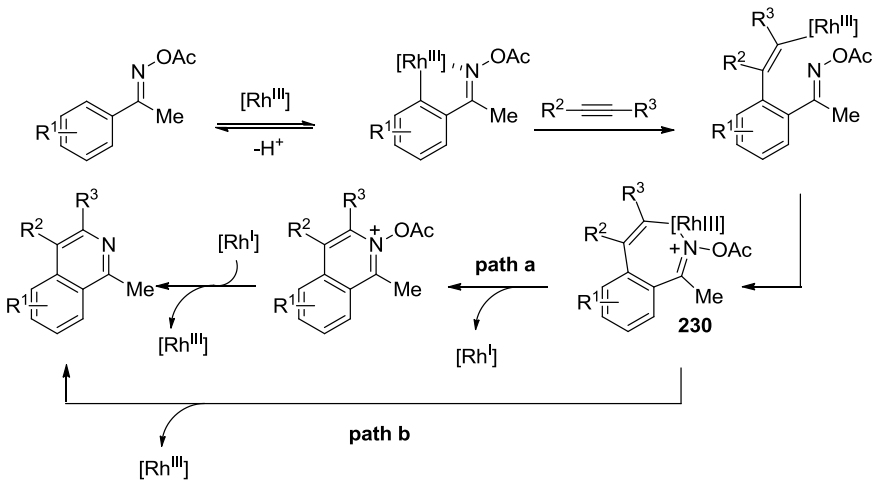

Scheme 129

The authors also demonstrated that a number of functional groups could be incorporated at the isoquinoline 1-position *via* the use of differently substituted oxime ester substrates. These analogues were generally obtained with good to excellent yields, however a drop in yield was observed when trying to introduce bulky groups in *α* to the nitrogen. This can be explained by the conformational isomerism of the oxime ester starting material, since for the reaction to occur the acetyl group should be oriented away from the aryl ring (*anti*) whereas the introduction of bulky α group favours the *syn* conformer (Figure 45).

Figure 45: two possible conformational isomers of precursor of intermediate 230.

Inspiring work was carried out by Rodriguez et al.[88] in which intermolecular addition-intramolecular cyclisation was attempted in one pot by irradiation of benzophenone *O*-acetyloxime **231** and tolane or dimethyl acetylenedicarboxylate to obtain the corresponding isoquinolines **232** and **233** in good yields. In the acyloxime motif, the N-O bond is the weakest and undergoes homolytic cleavage forming an iminyl radical when irradiated with light (Scheme 130).

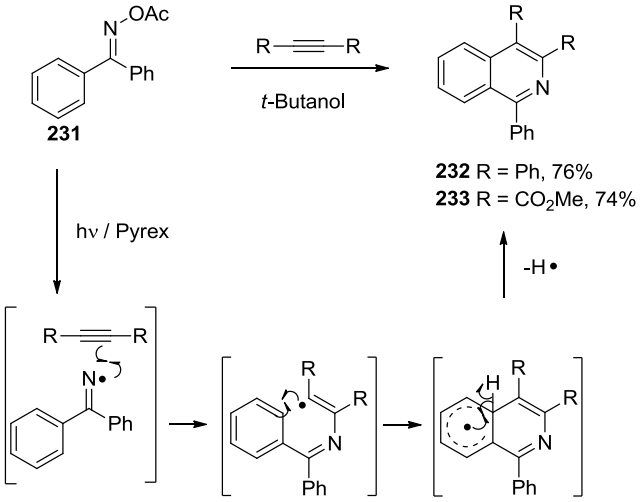

Scheme 130

When cyclisation by irradiation was attempted with 2-ethynylbenzaldehyde *O*-acetyloxime **234**, a reasonable result was obtained (**238**, 64%) in contrast with 2-vinylbenzaldehyde *O*-acetyloximes **235**, **236** and **237** that gave the corresponding isoquinolines **239**, **240** and **241** in mediocre yields (Scheme 131).

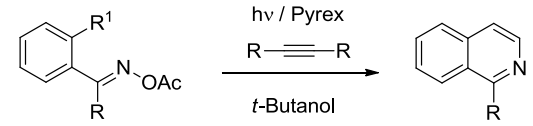

234, R = H, R^1 = CHC-

235, R = H, R^1 = CH_2CH-
236, R = Me, R^1 = CH_2CH-
237, R = Ph, R^1 = CH_2CH-

238, 64%

239, R = H, 38%
240, R = Me, 26%
241, R = Ph, 37%

Scheme 131

Nevertheless this work suggested that it might be possible to obtain isoquinolines *via* iminyl radicals, generated by FVP, cyclising into double bonds.

While there are plenty of examples in the literature of iminyl radicals undergoing intramolecular cyclisation onto aromatic and heteroaromatic systems, there is less precedent for cyclisation onto alkene systems in the gas phase. The final example of note involves the cyclisation of aryloxyls onto adjacent alkene systems.[89] In such systems it was found that carboxylic esters were particularly efficient leaving groups (Scheme 132). This is an example of pyrolytic homolytic substitution in which the ester is the leaving group – presumably as CO_2 and a methyl radical although there is no evidence of the latter fragmentation. This ester group behaved as the leaving group even in the presence of competitive α-alkyl substituents known to be leaving groups themselves under FVP conditions[90].

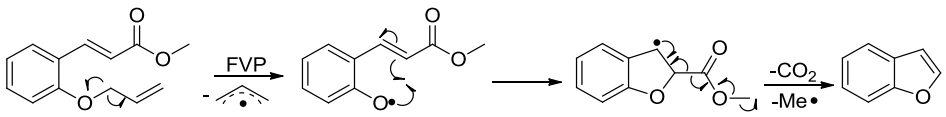

Scheme 132

Another example was given by the work carried out in the McNab research group[91] in which, under FVP conditions, methyl 3-[2-(*t*-butyl)phenyl]propenoate **242** gave benzothiophene among the products according to the same mechanism shown in Scheme 133.

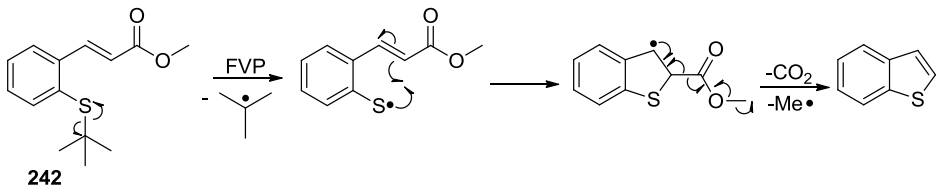

242

Scheme 133

Consequently, it was proposed that nitrogen radicals of an iminyl radical formed by FVP may also undergo a similar transformation.

2. Aim of the project

The aim of this project was to obtain a 6–membered aromatic ring by cyclising an iminyl radical (generated *in situ* from an oxime ether) onto a C-C double bond adjacent to a methyl ester, first eliminating Me· and then CO_2. This transformation would lead to the formation of isoquinoline (Scheme 134).

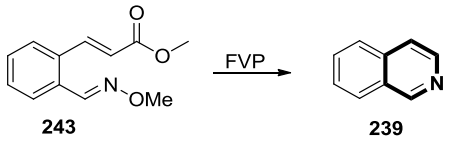

243 239

Scheme 134

If this methodology proved to be succesfull, then the versatility of this method could be extended inserting substituents onto the isoquinoline core (Figure 46).

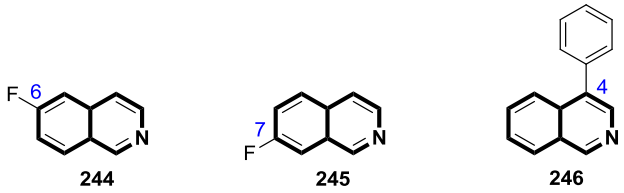

244 245 246

Figure 46: target substituted isoquinolines to be generated by FVP.

The two fluoro-substituted isoquinolines were chosen because the aldehyde precursors in their synthesis were available in-house and also because the isoquinoline products could potentially be of use in medicinal chemistry. To investigate the scope of the method further, attempts to include a substituent on the newly formed ring were also made (**246**).

3. Synthesis of 3-[2-(methixyimino-methyl)-phenyl]-acrylic acid methyl ester and related compounds

The syntheses of the four oxime ethers (Figure 47) substrates were designed to follow similar paths. The only significant difference was in the first step for one of the three compounds successfully synthesised.

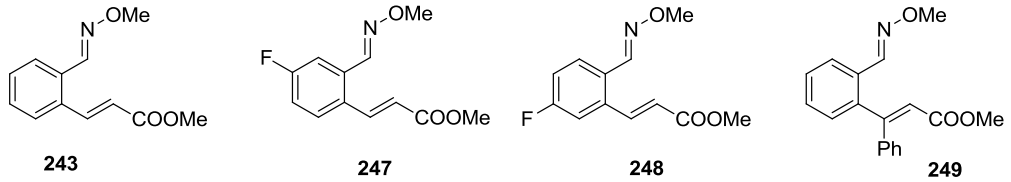

Figure 47: precursors of substituted isoquinolines to be generated by FVP.

3.1. Synthesis of 3-{2-[(methoxyimino)methyl]phenyl}prop-2-enoate

The synthesis of 3-{2-[(methoxyimino)methyl]phenyl}prop-2-enoate **243** was designed to include just two steps using low cost starting materials that are easily available. The simple retrosynthetic pathway is illustrated below (Scheme 135).

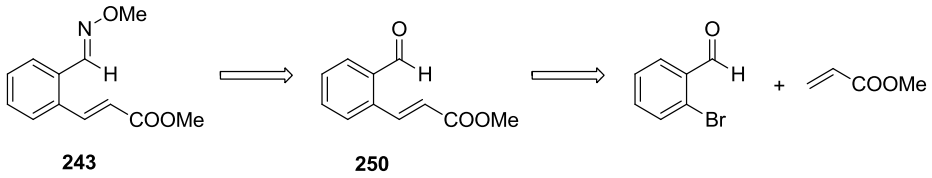

Scheme 135

The first step of the synthesis consists of a Heck cross-coupling reaction between 2-bromobenzaldehyde and methyl acrylate using a Pd catalyst as shown in Scheme 136.[92]

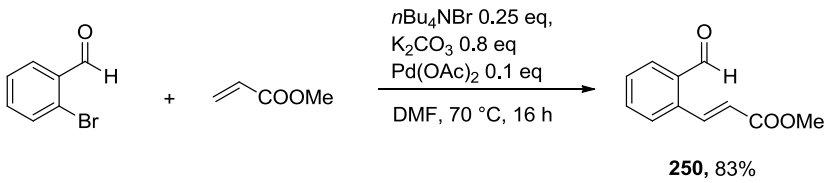

Scheme 136

The spectroscopic data obtained for this compound match the ones reported in the literature and it was obtained in improved yield compared to that previously reported (83% vs. 69%).

Conversion of the aldehyde to an oxime ether was performed in similar fashion to that described in chapter 3. 3-(2-Formylphenyl)prop-2-enoate **250** was heated at reflux in ethanol with *O*-methylhydroxylamine hydrochloride for 4 h. The product was obtained in moderate yield (27%) due to the fact that ethanol was used as solvent. *Trans*-esterification was observed to give {2-[(methoxyimino)methyl]-phenyl}but-3-enoate] **251** (30%) (if the reaction was repeated, methanol would have been used). The two products were successfully separated by dry flash chromatography. Although the yield for compound **243** was low, it afforded enough material to be carried through the synthesis to the final isoquinoline (Scheme 137).

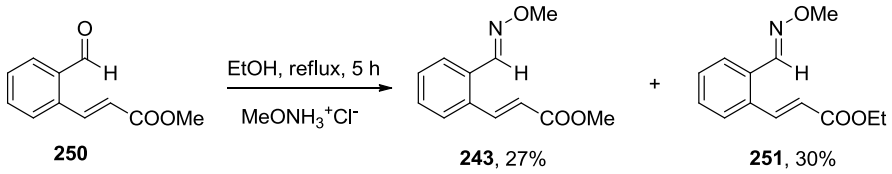

Scheme 137

The formation of the oxime ether **243** was confirmed by the presence of a peak in the NMR spectrum at 3.90 ppm integrating for 3H, which corresponded to the methoxy group. The resonance due to the aldehyde proton of the starting material was also observed to shift from 10.27 ppm to 8.30 ppm in the oxime ether product. In the case of compound **251**, a signal which integrated for 3H corresponding to the methoxy group was observed at 4.00 ppm and the aldehyde peak shifted slightly less to 8.40 ppm. In addition, the appearance of a quartet integrating for 2H at 4.26 ppm and of a

triplet integrating 3H at 1.33 ppm were observed, the typical signals associated with an ethyl ester group.

The mass spectra of these oxime ethers showed the expected fragmentation pathway that acrylates commonly undergo under mass spectrometric conditions[90] (Scheme 138).

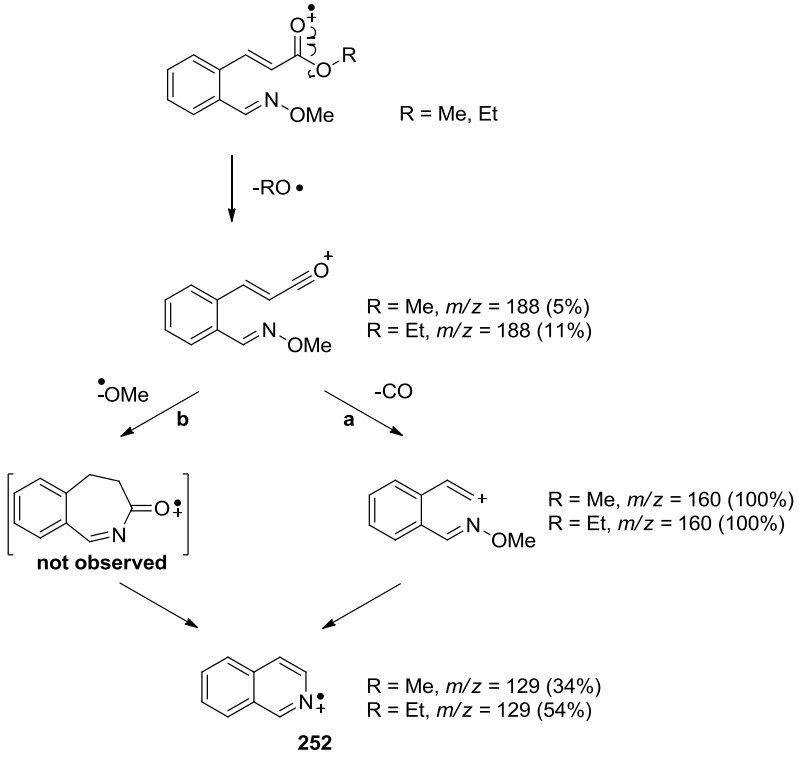

Scheme 138

In this case only fragmentation pathway **a** was observed, but if an *O*-allyl group is installed in place of C=NOR moiety, both of the pathways (**a** or **b**) are observed (Scheme 139). [90]

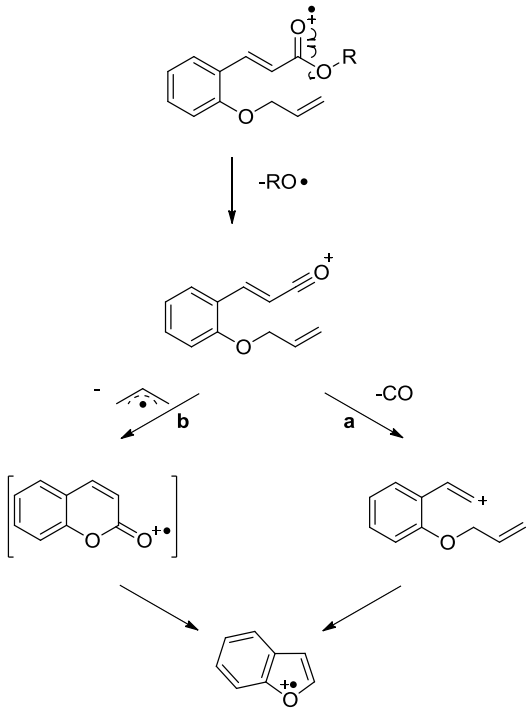

Scheme 139[90]

Ionisation of the carbonyl group is followed by standard α-cleavage of the alkoxy group that results in the first peak (R = Me, M -31, 5%; R = Et, M -45, 11%) (Scheme 138). The intensity of this peak was found to be very low under the ionisation conditions studied. Loss of CO follows (M = 160, 100% both R = Me, Et) with subsequent cyclisation to give the radical cation **252** (M = 129, R = Me, 34%; R = Et, 54%). It is important to mention that mass spectrometric breakdown peaks are obtained *via* the lowest ionisation potentials whereas the pyrolysis products are obtained *via* homolytic thermal breakdown of the weakest bond in the molecule. Consequently, it is not possible to predict the pyrolytic behaviour of a molecule based on its mass spectrometric cleavage pattern.

3.2. Synthesis of 3-{4-fluoro-2-[(methoxyimino)methyl]phenyl}prop-2-enoate and 3-{5-fluoro-2-[(methoxyimino)methyl]phenyl}prop-2-enoate

The synthesis of 3-{4-fluoro-2-[(methoxyimino)methyl]phenyl}prop-2-enoate **247** and 3-{5-fluoro-2-[(methoxyimino)methyl]phenyl}prop-2-enoate **248** was achieved in a similar fashion to the one shown above for oxime ether **243** (Scheme 140).

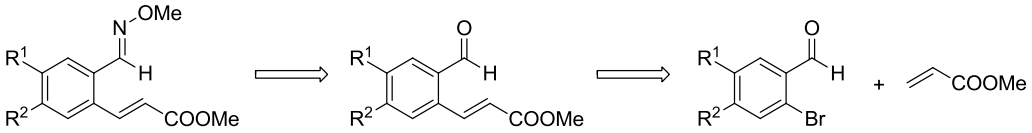

247, R^1 = F, R^2 = H
248, R^1 = H, R^2 = F

Scheme 140

As seen previously, the first step consisted of a Heck cross-coupling reaction between the substituted benzaldehyde and methyl acrylate. A synthetic procedure for the preparation of compound **247** had already been described in the literature so these conditions were utilised with both fluorinated aldehydes as shown in Scheme 141.

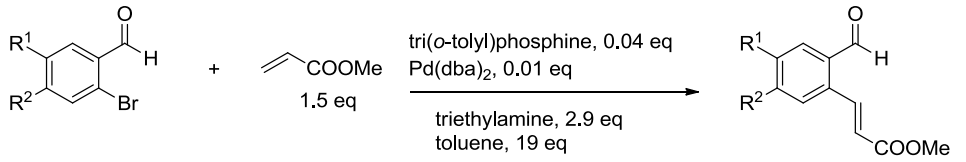

253, 71%, R^1 = F, R^2 = H
254, 33%, R^1 = H, R^2 = F

Scheme 141

Product **253** was obtained in reasonable yield (71%) and the spectroscopic data were consistent with those reported in the literature. In contrast, the yield of product **254** was considerably lower – probably due to fluorine atom in the *meta* position relative to the bromine atom deactivating the coupling.[93] Although the yield was modest, the reaction afforded enough material to be carried forward in the synthesis.

The structure of compound **254** was confirmed with NMR spectroscopy where the appearance of two doublets which displayed a large coupling constant was observed, corresponding to the protons of the *E*-alkene (J = 15.9 Hz, Figure 48. The chemical shifts of the alkene protons H_a and H_b were comparable with H_{2a} and H_{2b} (Table 7).

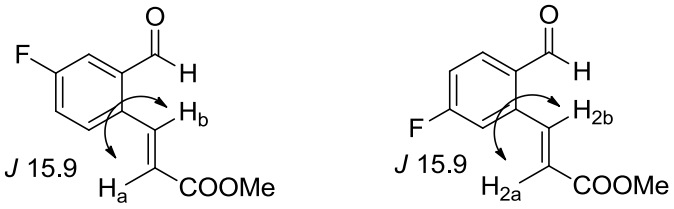

253 **254**

Figure 48: coupling constants of *E*-alkene protons of compounds 253 and 254.

	δ (ppm)	Δ (H_{2a}-H_a)
H_a	8.43	0.06
H_b	6.35	
		Δ (H_{2b}-H_b)
H_{2a}	8.49	0.02
H_{2b}	6.37	

Table 7: comparison between Δppm of *E*-alkene protons of structures 253 and 254.

As seen previously, the second step of the synthesis for both the fluorine-substituted FVP precursors was the reaction with *O*-hydroxylamine hydrochloride to transform the aldehydes into their corresponding oxime ethers. Due to the fact that trans-esterification was observed in the case of 3-(2-formylphenyl)prop-2-enoate, this time methanol was used as the reaction solvent instead of ethanol. Product **247** and **248** were obtained in high yields (Scheme 142).

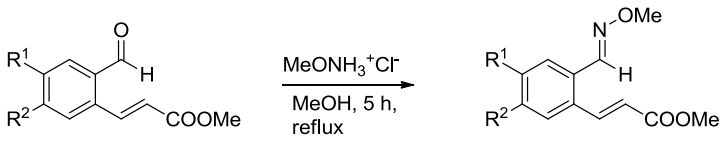

253, 70%, R^1 = F, R^2 = H
254, 82%, R^1 = H, R^2 = F

247, 70%, R^1 = F, R^2 = H
248, 82%, R^1 = H, R^2 = F

Scheme 142

Evidence that the two products were successfully obtained was again provided by NMR spectroscopy. The appearance of methoxy signals integrating for 3H at 4.03 ppm for **247** and at 3.99 ppm for **248** was observed and the aldehyde proton

resonance shifted from 10.29 ppm to 8.40 ppm for **247** and from 10.22 ppm to 8.34 ppm for **248** as a result of the transformation of the carbonyl into the oxime ether.

3.3. Attempted synthesis of 3(2-formylphenyl)prop-3phenyl-2enoate

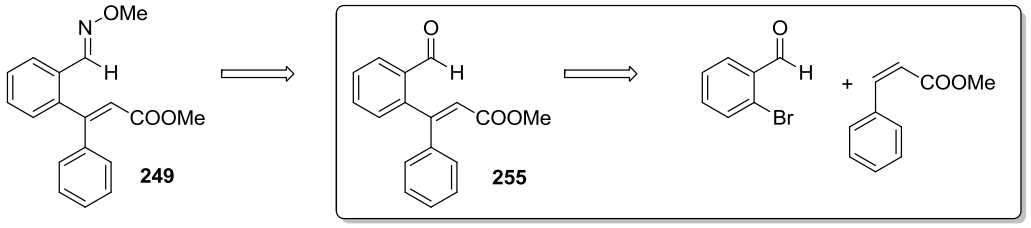

Scheme 143

Retrosynthetic analysis indicates that 3-(2-formylphenyl)prop-3-phenyl-2enoate **255** is a key intermediate in the synthesis of the title compound therefore various attempts to synthesise compound **255** *via* Heck cross coupling were made but it proved to be a challenging task. Using the conditions employed to synthesise 3-(2-formyl phenyl)prop-2-enoate, after 16 h at 120 °C, only 10% of a species which may have been product was observed (Table 8, entry a).

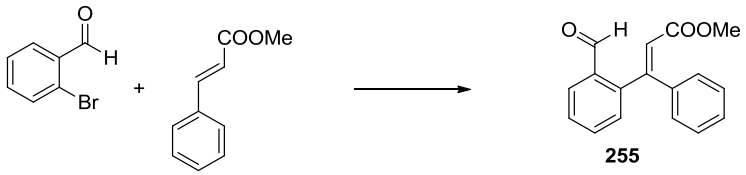

Scheme 144

entry	catalyst	ligand or additive	base	solvent	temp.(°C)	time
a	$Pd(OAc)_2$ 0.1 eq	*n*-Bu_4NBr 0.3 eq	K_2CO_3 1.1 eq	DMF	120	16 h
b	$Pd_2(dba)_3$ 0.02 eq	P(*o*-tolyl)$_3$ 0.04 eq	Et_3N 2.5 eq	toluene	120	4 days
c	$Pd_2(dba)_3$ 0.01 eq	P(*t*-Bu)$_3$ 0.02 eq	Cy_2NMe 1.1 eq	dioxane	75	16 h
d	$Pd(OAc)_2$ 0.04 eq	Et_4NCl 1 eq	Cy_2NMe 1.5 eq	Me_2NCOCH_3	100	3 days

Table 8: reaction conditions for attempeted Heck-type reactions to obtain substrate 255.

Attempts to isolate an authentic sample of the product by column chromatography and Kugelrohr distillation were unsuccessful.

The method used to obtain fluorine substituted analogues was then applied in the synthesis of compound **255** (Table 8, entry b). Despite allowing the reaction to stir at 120 °C for four days, no sign of product was detected by TLC analysis. Further investigations were carried out to explore new conditions to achieve the desired product. A paper published in 2001 by Littke and Fu[94] illustrated that aryl bromides undergo Heck cross coupling with a variety of different olefins (with different electronic properties) utilising the set of conditions illustrated in Table 8, entry c. One of the examples that caught our attention is illustrated in Scheme 145.

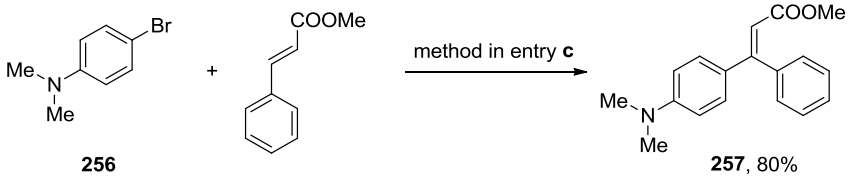

Scheme 145

Despite aryl halide **256** being moderately activated and the steric hindrance of the alkene, product **257** was obtained in good yield. Reaction with bromobenzaldehyde was initially carried out at room temperature as described in the paper, but no

product was detected even after increasing the temperature to 75 °C. This is probably due to the increased steric hindrance in the position *ortho* to the bromine of 2-bromobenzaldehyde making the oxidative addition of the aryl halide to the palladium (0) more difficult.

A solution to this problem seemed possible by following the work of Gürtler and Buchwald. They showed that it is possible to overcome some problems due to steric hindrance and successfully couple aryl halides bearing *ortho* substituents by utilising the method in entry d Table 8. A couple of examples are highlight in Table 9.

entry	arene	olefin	product
1	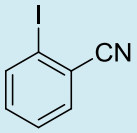	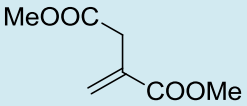	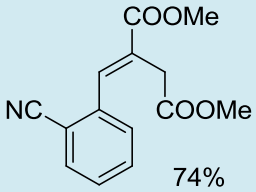 74%
2	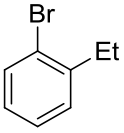	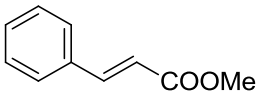	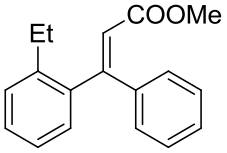 75%

Table 9: successful literature example of Heck-type reaction to afford hindered olefins.

In the example in Table 9 entry 1, they demonstrated that an aryl halide with a deactivating and sterically challenging *ortho* cyano group was compatible with this transformation even though the more active aryl iodide coupling partner was used instead of a bromide. The reaction conditions were also slightly different from the ones listed in the Table 8, entry d – the reaction mixture was stirred at 100 °C for 16 hours with 2 mol% $Pd(OAc)_2$. Table 9 entry 2 in the table better mimics the reagents chosen for our reaction (the only difference is in the group *ortho* to the bromine), and as the reaction was reported to proceed with a high yield, the reported conditions were applied to substrate Scheme 144 (Table 8, entry d). Unfortunately, under these conditions none of the desired trisubstituted olefin product **255** was formed.

To find and to optimise conditions for the Heck coupling of this substrate was beyond the scope of this thesis and so no further attempts were made to prepare compound **255**.

4. FVP of of 3-[2-(methixyimino-methyl)-phenyl]-acrylic acid methyl ester and related compounds to generate isoquinolines

The three oxime ethers produced (**243**, **247** and **248**) were subject to FVP in a manner similar to that described in chapter 3.

4.1. FVP of 3-{2-[(methoxyimino)methyl]phenyl}prop-2-enoate

Pleasingly, pyrolysis of the oxime ether **243** successfully generated isoquinoline (Scheme 146). We found that carrying out the pyrolysis at 650 °C was optimal, resulting in complete conversion of the starting material.

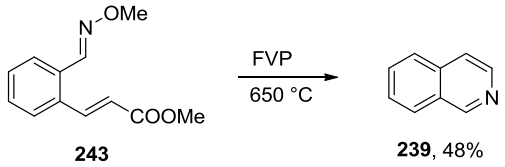

243 **239**, 48%

Scheme 146

After purification by Kugelrohr distillation the pure product was isolated in 48% yield. The moderate isolated yield is a reflection of difficulties experienced with product purification (the relatively low boiling point of isoquinoline led to some product being lost during distillation) despite the fact that the pyrolysis appeared to have proceeded reasonably cleanly. Assignment of the product as the desired isoquinoline was confirmed by NMR spectrometry and boiling point analysis, both of which were consistent with literature data. The proposed mechanism is similar to that described previously in Schemes 132 and 133.

The proposed mechanism for the cyclisation (Scheme 147) involves:

1. formation of a *N*-centred radical **258** as a consequence of the cleveage of the weakest bond in the oxime group at elevated temperature;

2. attack of the iminyl radical on the double bond generating a 6-membered ring **259**;
3. loss of a methyl radical and CO_2 with formation of an aromatic ring

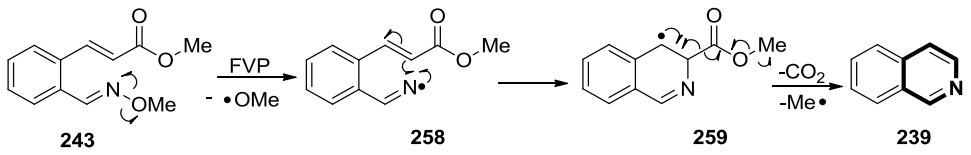

243 **258** **259** **239**

Scheme 147

Although formation of a nitrile by β-cleavage of a *H*-radical from the iminyl radical intermediate **258** is possible, isoquinoline was the sole product detected.

4.2. FVP of 3-{5-fluoro-2-[(methoxyimino)methyl]phenyl}prop-2-enoate

Pyrolysis of oxime ether **248** successfully yielded 6-fluoroisoquinoline. The optimal furnace temperature was found to be 700 °C and the product was purified by dry flash chromatography affording the desired product **245** as a colourless solid in high yield (75%).

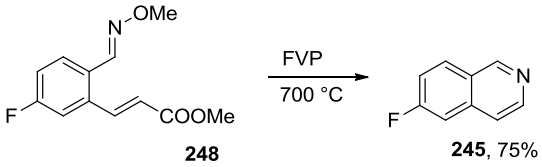

248 **245**, 75%

Scheme 148

6-Fluoroisoquinoline is commercially available and, although some characterisation data are reported, ^{13}C NMR data were not reported and the individual resonances were not assigned for ^{1}H NMR.

The structure of the cyclised product **245** was evident by proton NMR spectroscopy and in general agreement with the published data (although spectra were recorded in different solvents so a direct comparison could not be made). As was expected, the two doublets relating to the alkene at 8.05 and 6.32 ppm (J = 15.8 Hz) were no longer present in the spectrum of the product, they were replaced by two doublets at

higher chemical shift associated with the newly formed aromatic ring – 8.55 and 7.64 ppm (J = 5.8 Hz).

1D ^{1}H-NMR spectroscopy helped to unambiguously assign proton '**a**' (as H_1) due to the fact that it appears to be a singlet quite deshielded at 9.25 ppm (adjacent to the ring nitrogen).[95] Also, it is possible to assign two doublets as protons '**f**' (as H_3) and proton '**e**' (as H_4) from the newly formed ring. Proton '**f**' attached to the isoquinoline core at the 3-position, is probably the most deshielded of the two. [96]

To further confirm the structure of the cyclised product 2D NMR was carried out. From the COSY spectrum (Figure 49) it is possible to see the strong correlation between proton '**f**' and proton '**e**' and also between proton '**c**' (as H_7) with both protons '**b**' and '**d**' (as protons H_8 and H_5).

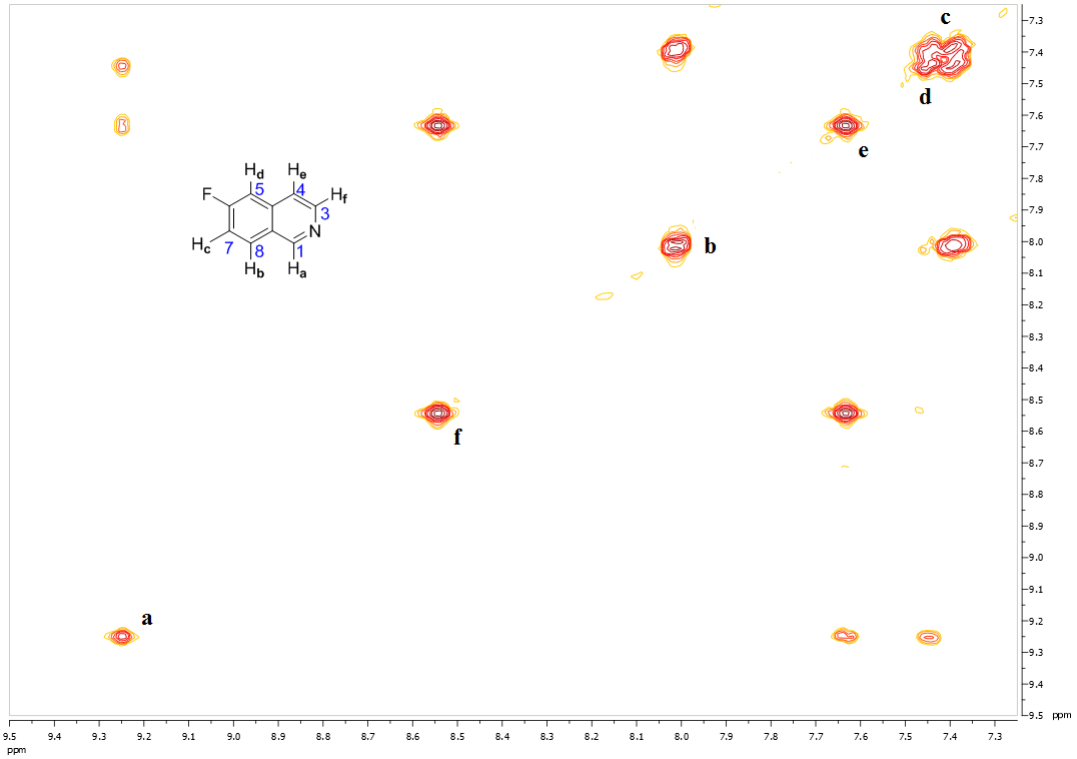

Figure 49: COSY spectrum of compound 245.

There is a noticeable correlation of proton '**a**' with both protons '**e**' and '**d**' which is attributed the **W**-type interaction between protons across aromatic systems at 5-bonds distance and the type of interaction shown in Figure 50 on the right.

Figure 50: possible H-H interactions in the COSY spectrum of compound 245.

To further confirm the structure of the molecule and to unambiguously assign the position of protons '**b**' and '**d**' and '**e**' and '**f**' a NOESY spectrum was obtained (Figure 51).

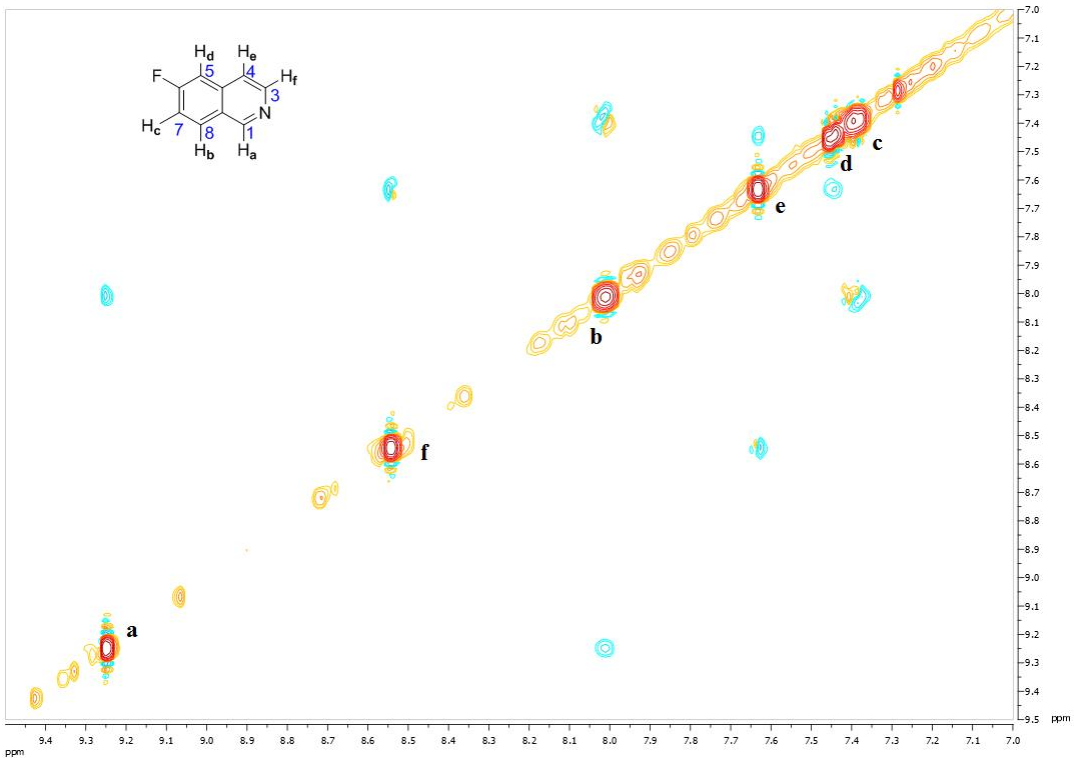

Figure 51: NOESY spectrum of compound 245.

As expected, the spectrum shows NOE interactions between protons '**e**' and '**f**', and protons '**b**' and '**c**'. No interactions are observed between '**c**' and '**d**' which suggests the latter resonance is due to the proton in the 5-position. Most importantly, there is a clear NOE interaction between protons '**a**' and '**b**' that helps to position the latter in the ring. There is also an observable interaction between '**e**' and '**d**' that unequivocally assigns proton '**e**' and '**f**' .

4.3. FVP of 3-{4-fluoro-2-[(methoxyimino)methyl]phenyl}prop-2-enoate

Pyrolysis of oxime ether **247** successfully yielded 7-fluoroisoquinoline **244**. The optimal furnace temperature for pyrolysis was found to be 700 °C and the product was purified by dry flash chromatography affording 7-fluoro-isoquinoline **244** as a colourless solid in high yield (79%).

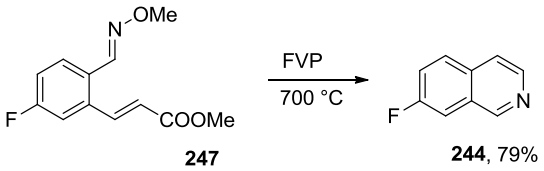

247 **244**, 79%

Scheme 149

Once again, NMR spectroscopic evidence could be used to unambiguously assign the structure of the product obtained by pyrolysis. Similarly to 6-fluoroisoquinoline, 7-fluoroisoquinoline is commercially available in small quantities from some specialist suppliers, but there is just one reference in the literature from 1964 that reports the synthesis and characterisation of the compound.[96] By analogy to the previously studied pyrolysis to produce the parent isoquinoline, the product showed loss of the methyl resonances from the oxime ether and methyl ester groups of the starting material **244**. The olefin resonances were also absent in the product, instead two doublets were observed at 8.51 and 7.64 ppm (J = 5.7 Hz), corroborating the formation of a new aromatic ring system.

As for 6-fluoroisoquinoline, using 1D ^{1}H-NMR spectrum it was possible to unambiguously assign proton '**a**'(as H_1) – it appears as a singlet at the highest chemical shift of all the observed proton resonances due to the deshielding effect of the adjacent C=N double bond. It was also possible to assign the doublets at 8.51 ppm and 7.64 ppm as proton '**f**' and proton '**e**' (as protons H_3 and H_4) from the newly formed ring in analogy with the 6-fluoroisoquinoline. The assignment was made presuming that proton '**f**' would appear at higher chemical shift, again due the deshielding effect of the *N*-atom.[96]

To further confirm the structure of the cyclised product, 2D NMR was carried out. From the COSY spectrum (Figure 52) it is possible to see the strong interaction

between proton '**f**' and proton '**e**' and also between proton '**c**' (as H_6) with both protons '**b**' and '**d**' (as protons H_8 and H_5).

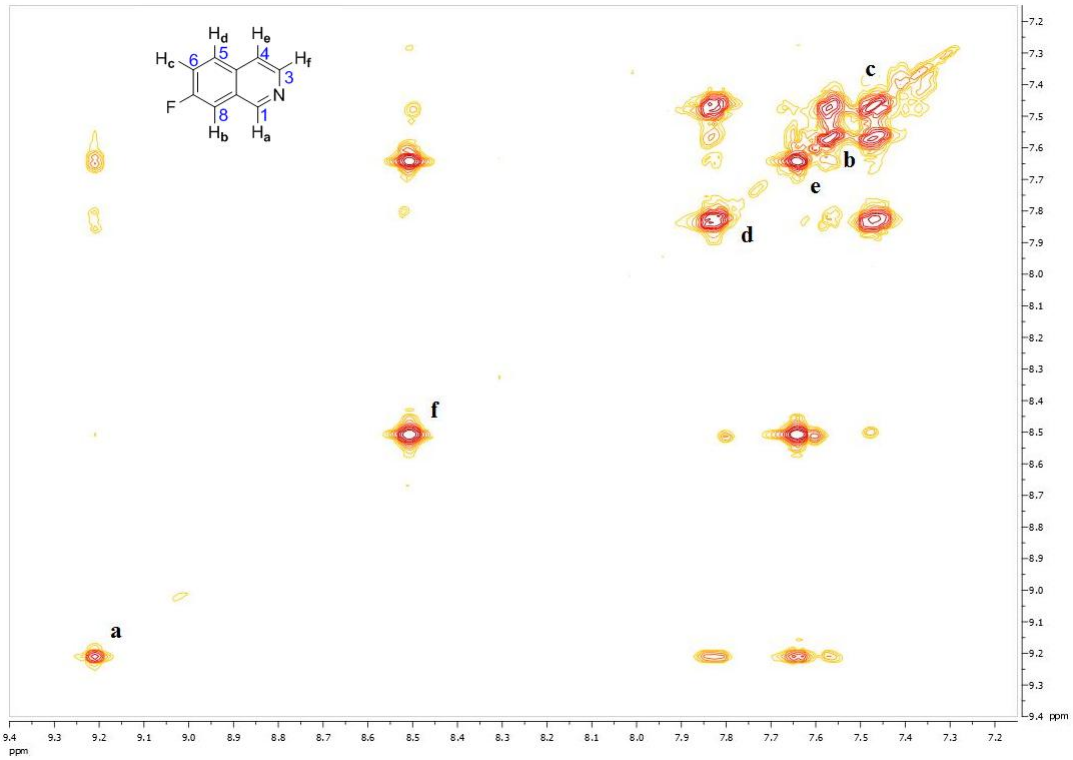

Figure 52: COSY spectrum of compound 244.

Interestingly, a long-range spin coupling interaction between proton '**a**' and protons '**d**' and '**e**' was also evident (Figure 53).

Figure 53: possible H-H interactions in the COSY spectrum of compound 244.

The structure on the left of Figure 53 shows the '**W**' shaped interaction responsible for coupling between protons '**a**' and '**d**'. W-shaped couplings of this kind are typical ^4J and ^5J distant interactions, which are often seen in flat aromatic systems. More unusual is the interaction shown in the structure on the right of Figure 53. This is a distant ^5J interaction which is not very well documented in the literature.

To finally assign the position of '**b**' and '**d**' unequivocally, a NOESY spectrum was obtained (Figure 54).

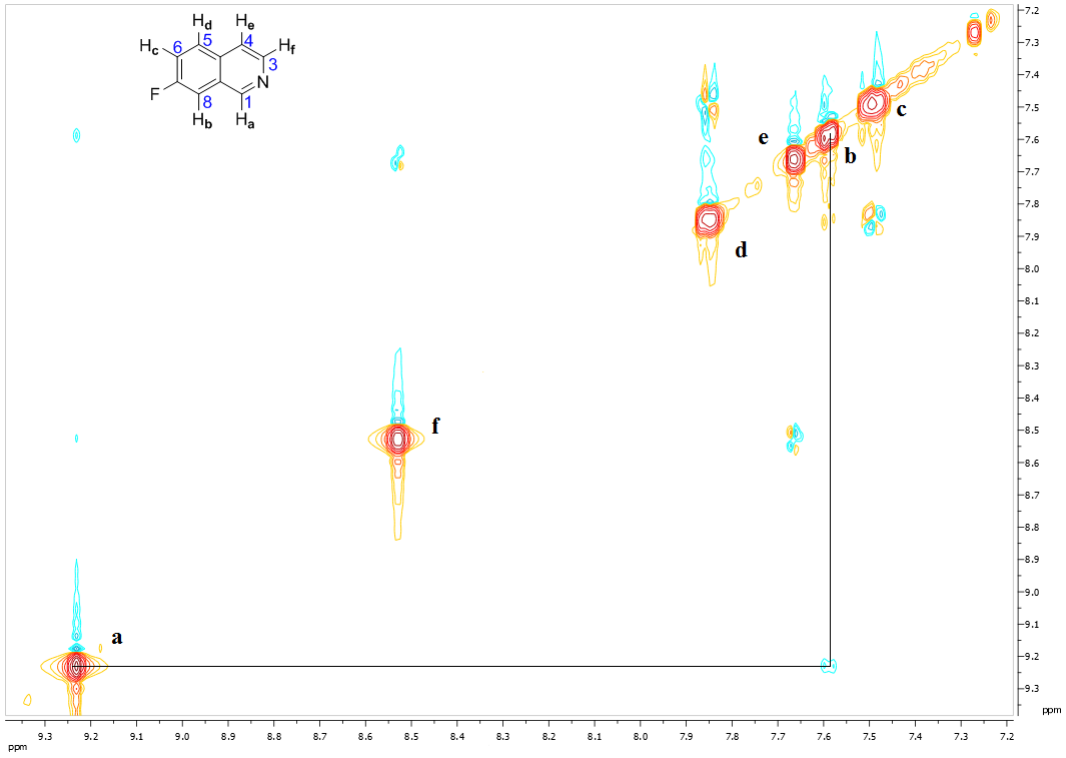

Figure 54: NOESY spectrum of compound 244.

From the spectrum it is possible to clearly see the interactions between the *peri* protons '**a**' and '**b**' (assigning the latter position), and between protons '**e**' and '**f**' and '**c**' and '**d**' (again helping to identify their relative positions). Unfortunately, due to poorer resolution of the spectrum, in this case it is not possible to see interaction between protons '**e**' and '**d**'.

The mechanism proposed for the formation of the 7-fluoroisoquinoline and 6-fluoroisoquinoline is identical to that described previously (*c.f.* Scheme 147, Section 4.1).

5. Further work carried in the McNab group to extend the scope of this project.

This paragraph briefly summarises the latest results obtained in the McNab group[97] on this subject. These results are reported to demonstrate the extended scope of the methodology applied and described in this chapter so far.

First to be synthesised was 1-methylisoquinoline as shown in Scheme 150.

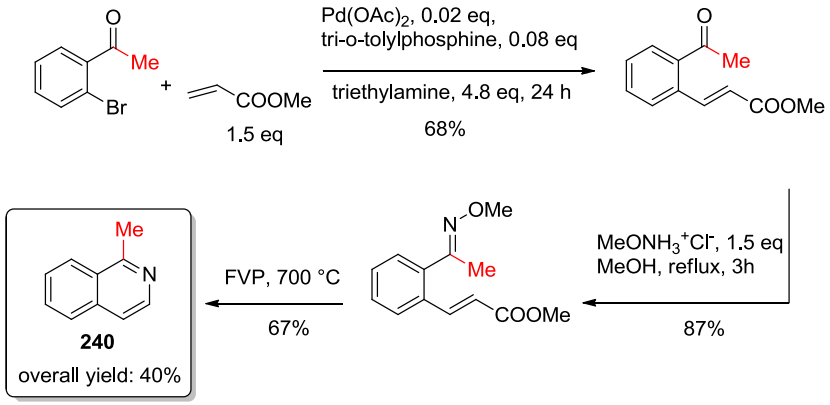

Scheme 150[97]

Although isoquinoline **240** is known in the literature, pyrolysis of the oxime ether substrate shown in Scheme 150 demonstrated that it is possible to introduce a substituent α to the nitrogen without altering the efficiency of this methodology. The yields of the pyrolysis step and of the overall synthetic sequence were comparable to those observed previously.[97]

Following this successful result, attempts to synthesise isoquinoline with substituents in position 3 were made.[97] As shown in Scheme 151, Heck reaction conditions were identified to obtain the desired aldehyde **260**, but there was still room for optimisation. The poor yield of the first step is due to the more hindered nature of the alkene and to the donating nature of the methyl α to the carbonyl. The oxime ether-forming step was also successful but it proceeded in a relatively poor yield. This low yield is probably due to the reaction being conducted in refluxing MeOH rather than in EtOH to avoid partial trans-esterification and therefore refluxing at lower temperature. Enhancement of the yield may be possible if the reaction would be carried out over a longer reaction time, heated to higher temperature in a pressurised

vessel, or heated with the use of microwave irradiation. It is worth mentioning that FVP of the equivalent ethyl ester is indeed possible and methyl acrylate was only chosen due to in-house availability.

FVP of the oxime ether thus obtained was performed and surprisingly a mixture of two regioisomeric products in an approximately 1:1 ratio was observed. It was possible to separate the two products by dry flash chromatography and the combined yield of the pyrolysis was 96%.

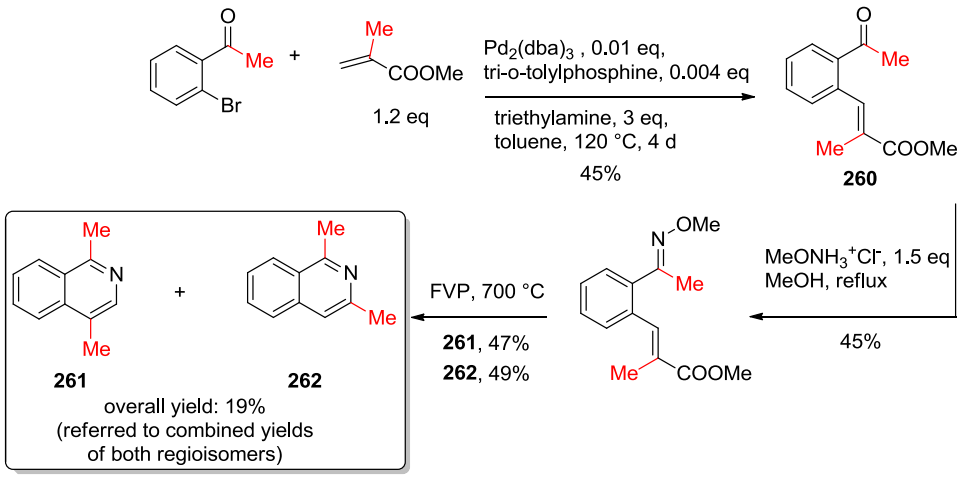

Scheme 151[97]

The expected isoquinoline product **262**, can be formed by the mechanism discussed in detail in previous paragraphs. An explanation of the presence of the regioisomeric product **261** warrants consideration of a different mechanism. As shown in Scheme 152, after the formation of the iminyl radical **263**, a 5-membered ring with the radical positioned α to the carboxylic group may be formed **264**. The ring could then open to form an alkene with the radical delocalised on the benzene ring **265**. This benzene-centred radical may then cyclise onto the α-position of the ester moiety **266**. Loss of a methyl radical and CO_2 installs the aromatic character of the fused isoquinolinic ring **261**.

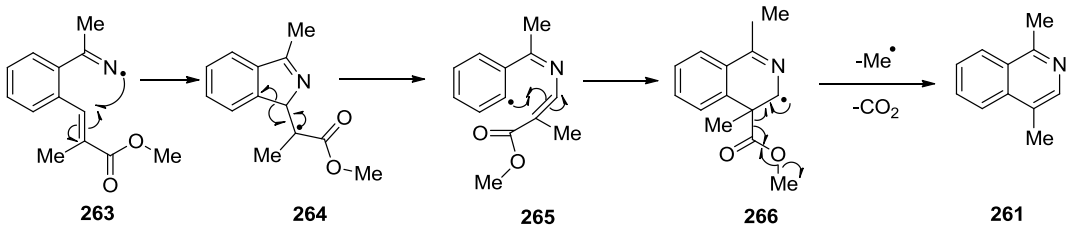

Scheme 152

Attempts to synthesise isoquinoline with a methyl group in the 4-position were also made using a synthetic pathway similar to the one described above.[97]

To overcome the problems experienced in optimising the conditions of the Heck reaction, the synthesis of aldehyde **267** (Scheme 153) was approached in a different manner.

The Wittig reaction between (carbethoxyethylidene)triphenylphosphorane and phthaldialdehyde afforded the desired olefin product **267** in 95% yield. The remaining oxime ether forming step of the synthetic sequence was unproblematic. Notably, the use of an ethyl ester substrate allowed the reaction to be conducted in refluxing ethanol without the danger of transesterification and gave the pyrolysis precursor in high yield. Finally, FVP of the oxime ether was performed affording a mixture of two isomeric products in a good overall yield. The mixture of isomers can be attributed to the two competing mechanistic pathways discussed above. Unfortunately, in this case it was not possible to separate the two products by dry flash chromatography.[97]

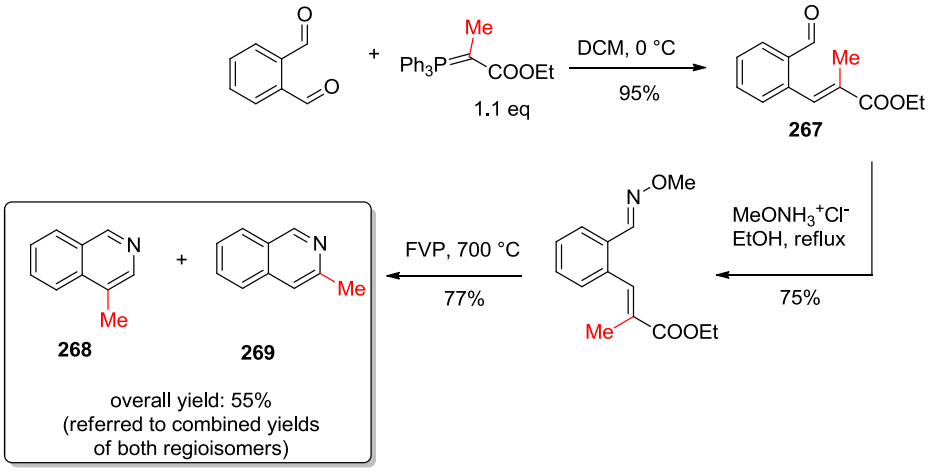

Scheme 153[97]

It can be concluded from this brief study of the substrate scope that this method for the synthesis of isoquinolines appears to be general and tolerates substituents at a number of different positions. A mixture a products was obtained in the cases in which a substituent was present α to the carboxylic group. This discovery led to the elaboration of a new mechanistic pathway that could be an interesting object for further investigations.

6. Conclusions

In this chapter a new route for the synthesis of isoquinolines was investigated. After reviewing the classical methods to obtain this class of compounds it was clear that room for improvement was present.

It has been illustrated that substituted isoquinolines such as **239**, **244** and **245** can be obtained in three steps with moderate to good overall yields. One disadvantage of this methodology lies in the poor reliability of the first step in the normal synthetic sequence. Heck reaction conditions needed to optimised for each substrate used and this impeded the synthesis of some substrates. A step towards the solution of this problem has been made by finding a valid alternative to the Heck reaction by utilising a Wittig reaction to obtain the first product of the three-step sequence.[98]
The advantages of this synthetic path rather than the conventional methods are as follows:

1. it is possible to start from cheap and commercially available starting materials;
2. various substituent groups are tolerated under these reaction conditions (such as methyl and fluorine) in different positions on the already existing aromatic ring and on the newly formed one;
3. the inconvenience of having harsh reaction conditions such as strong acid (for example in the Bischler-Napieralski, Pictet-Spengler and Pictet-Gams and Pomeranz-Fritsch reactions) is overcome;
4. the problem of requiring an oxidasing agent to oxidise the newly formed ring as employed in the work of Larock and co-workers', is avoided;
5. the final step of this synthesis has all the advantages that are characteristic of the FVP technique such as the absence of solvent and the short reaction time.

In the later work carried out in the McNab group, the synthesis of isoquinolines **261** + **262** and **268** + **269** raised the opportunity to discover a new mechanistic path for the cyclisation of iminyl radicals onto a double bond adjacent to an aromatic ring. This could potentially be an interesting subject for future developments.

Chapter 6:

Experimental.

1. Instrumental and General Techniques

1.1. Nuclear Magnetic Resonance Spectroscopy

^{1}H NMR spectroscopy was performed on a Varian Gemini 200 spectrometer operated by the author, Bruker AC250 spectrometer operated by the author, Bruker WH360 spectrometer operated by Dr K. Johnston and the author, Bruker Avance NMR spectrometers (500 MHz, with DCH cryoprobe optimised for $^{13}C/^{1}H$; 400 MHz, with BBFO+ broad band probe covering a range of nuclei including ^{19}F; 400 MHz, with BBI broad band inverse detection probe) with sample changers operated by Mr J. Bella.

^{13}C NMR spectroscopy was performed on a Bruker WH360 (90 MHz) operated by Dr K. Johnston and the author, Bruker AC250 (63 MHz) operated by the author and Bruker Avance NMR spectrometers (500 MHz, with DCH cryoprobe optimised for $^{13}C/^{1}H$; 100 MHz, with BBFO+ broad band probe covering range of nuclei including ^{19}F; 100 MHz, with BBI broad band inverse detection probe) with sample changers operated by Mr J. Bella:

Samples were analysed as solutions in [^{2}H] chloroform, unless otherwise stated. Chemical shifts (δ_H and δ_C) are quoted in ppm relative to tetramethylsilane and all coupling constants are given in Hertz (Hz).

1.2. Melting Points

All melting points were determined using Gallenkamp Capillary Tube Melting Point apparatus and are uncorrected.

1.3. Boiling Points

All boiling points were determined using Kugelrohr apparatus with a standard Hg thermometer.

1.4. Chromatography

Thin Layered Chromatography experiments were performed on MERCK TLC aluminium sheets coated with Silica gel 60 F_{254}.

1.5. Mass Spectroscopy

All mass spectroscopy data were obtained using electron impact ionisation on a Thermo Mat 900 XP instrument operated by Mr A. Taylor.

1.6. Elemental Analysis

All CHN elemental analyses were performed by the University of St. Andrews chemistry department.

1.7. Crystal structure data

The crystal structure reported was obtained with SuperNova, Dual, Cu at zero, Atlas.

1.8. Solvents

All solvents used in the experimental section were of laboratory grade and were used as supplied. Dried solvents were sodium dried.

1.9. Flash vacuum pyrolysis (FVP)

The apparatus used for flash vacuum pyrolysis is illustrated in Figure 55. It is based on the design by Dr. W. D. Crow of the Australian National University.

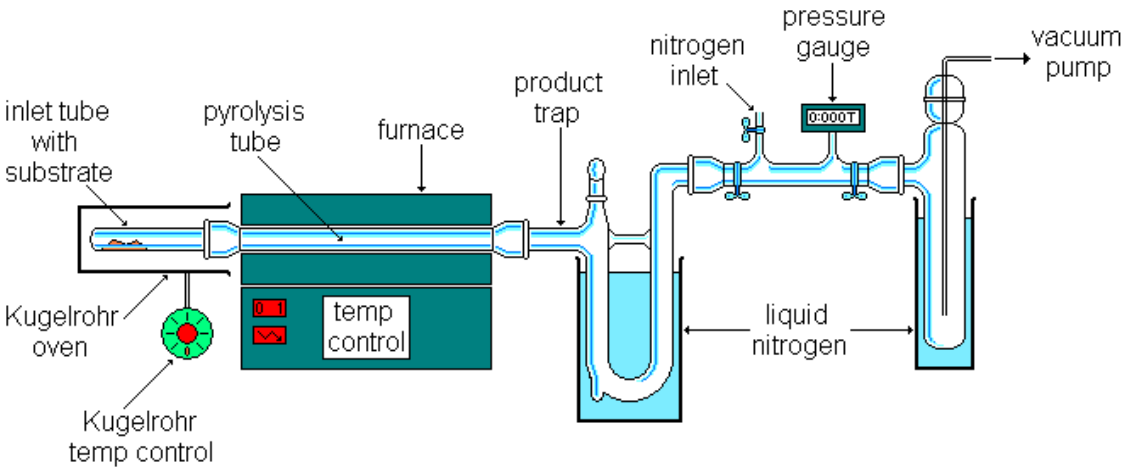

Figure 55: Flash vacuum pyrolysis apparatus

The system is evacuated by use of an Edwards Model ED100 high capacity oil pump to maintain the pressure in the region of 0.030 Torr. A glass Büchi oven is used to heat the inlet tube in which the substrate is placed until it enters the gas phase. The

gaseous substrate passes through a silica tube (30 x 2.5 cm) heated by a Carbolite electronically controlled laboratory tube furnace (model number MTF 12/38/250). The estimated contact time in the hot zone is of the order of ten milliseconds and the gaseous phase of the substrate under vacuum ensures that intramolecular reactions are strongly favoured. The products are captured at the exit of the furnace in a U-shaped trap cooled in liquid nitrogen. Upon completion of the reaction the pump is isolated and the trap allowed warming to room temperature under a dry nitrogen atmosphere.

"Small scale" pyrolyses are those involving 20-50 mg of substrate. The entire pyrolysate is dissolved in a suitable solvent (usually $CDCl_3$) for examination by NMR spectroscopy of the crude reaction products. "Large scale" pyrolyses are those involving 0.1 g or more of substrate.

Standard pyrolysis parameters used throughout in this section are reported as furnace temperature (T_f), inlet temperature (T_i), pressure (P) and time of pyrolysis (t).

2. Compounds synthesised

2.1. Methyl 2-(pyrrol-1-yl)benzoate 119

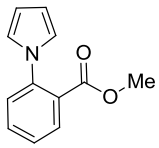

A solution of methyl anthranilate (4.54 g, 30 mmol) and 2,5-dimethoxytetrahydrofuran (4.62 g, 35 mmol) in glacial acetic acid (50 cm^3) was stirred under reflux for 20 min. After the solution had turned black, it was left to cool to room temperature and the majority of the acetic acid removed under reduced pressure. Water was added, the product extracted with diethyl ether (2 × 100 cm^3) and the extracts combined and dried over $MgSO_4$. After removing the volatiles, the residual brown oil was purified by Kugelrohr distillation to give methyl 2-(pyrrol-1-yl)benzoate as a yellow oil (4.78 g, 80%) bp 64-65 ˚C (0.5 Torr) [lit.,[98] 85-90 °C (0.5 Torr)]. δ_H (250 MHz, $CDCl_3$): 7.70-7.65 (1H, m), 7.47-7.39 (1H, m), 7.31-7.23 (2H, m), 6.69 (2H, t, *J* 2.2 Hz), 6.19 (2H, t, *J* 2.2 Hz) and 3.59 (3H, s). δ_C (63 MHz, $CDCl_3$): 167.3 (quat), 140.1 (quat), 132.1 (CH), 130.3 (CH), 127.7 (quat), 126.8 (CH), 126.5 (CH), 121.7 (2 CH), 109.5 (2 CH) and 52.2 (CH_3). Spectra are in agreement with literature values.[99]

2.2. 2-(Pyrrol-1-yl)benzylalcohol 120

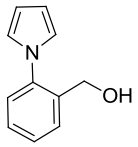

To a stirred suspension of LAH (1.82 g, 48 mmol) in dry diethyl ether (35 cm^3) under a nitrogen atmosphere, a solution of methyl 2-(pyrrol-1-yl)benzoate (4.72 g, 23.5 mmol) in dry diethyl ether (15 cm^3) was added dropwise. After 30 min, the unreacted LAH was cautiously quenched with wet diethyl ether (~5 cm^3) and water (~ 2 cm^3) until the solution became colourless with a white solid in suspension. The solution was filtered through a pad of celite and dried over $MgSO_4$. After filtration the solvent was removed under reduced pressure to give a yellow oil. The product was purified by Kugelrohr distillation to give 2-(pyrrol-1-yl)phenylmethanol as a colourless oil (3.08 g, 76%) bp 75-76 ˚C (0.5 Torr) [lit.[100] 120 °C (0.2 Torr)]. Values are different probably due to presence of small impurities. δ_H (250 MHz, $CDCl_3$): 7.57-7.50 (1H, m), 7.41-7.37 (2H, m), 7.31-7.25 (1H, m), 6.84 (2H, t, *J* 2.1), 6.32 (2H, t, *J* 2.1), 4.51 (2H, d, *J* 5.6) and 2.09 (1H, t, *J*

5.6). δ_C (63 MHz, $CDCl_3$): 139.5 (quat), 135.9 (quat), 129.0 (CH), 128.3 (CH), 127.6 (CH), 126.3 (CH), 122.3 (2 CH), 109.1 (2 CH) and 61.0 (CH_2). Spectra in agreement with literature values.[43]

2.3.2-(Pyrrol-1-yl)benzaldehyde 121

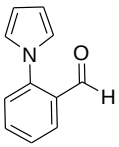

A solution of 2-(pyrrol-1-yl)benzylalcohol (3.04 g, 17.6 mmol) in toluene (15 cm^3) was slowly added to a suspension of activated MnO_2 (3.89 g, 45 mmol) in toluene (35 cm^3) then heated to reflux for 1 h. After filtration, the solvent was removed under reduced pressure. The residual yellow oil was purified by Kugelrohr distillation to give 2-(pyrrol-1-yl)benzaldehyde **52** as a light yellow oil (2.87 g, 95%) bp 69-70 ˚C (0.5 Torr) [lit.[101] 70-72 °C (0.05 Torr)]. δ_H (250 MHz, $CDCl_3$): 9.83 (1H, d, *J* 0.8), 8.01 (1H, ddd, *J* 7.8, 1.6, 0.4), 7.68 (1H, m), 7.54-7.48 (1H, m), 7.45 (1H, ddd, *J* 7.9, 1.2, 0.4), 6.94 (2H, m) and 6.41 (2H, m). δ_C (63 MHz, $CDCl_3$): 189.8 (CH), 143.7 (quat), 134.5 (CH), 130.6 (quat), 128.1 (CH), 127.4 (CH), 126.3 (CH), 123.6 (2 CH) and 110.4 (2 CH). Spectra in agreement with literature values.[43]

2.4. 2-(Pyrrol-1-yl)benzaldehyde *O*-methyloxime 109

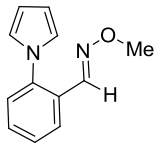

2-(Pyrrol-1-yl)benzaldehyde (2.83 g, 16.5 mmol), *O*-methylhydroxylamine hydrochloride (1.38 g, 16.5 mmol) and Na_2CO_3 (0.85 g, 8 mmol) were dissolved in MeOH (10 cm^3) and water (30 cm^3). AcOH (2 cm^3) was added to the mixture with stirring to adjust the pH to ~ 4. The solution was heated at reflux for 1 h. After cooling, the majority of MeOH was removed by evaporation at reduced pressure and more water was added (100 cm^3). The product was extracted with $CHCl_3$ (2 × 100 cm^3). The organic layers were separated, washed with water (1 × 100 cm^3) then dried over $MgSO_4$. The solvent was evaporated and the residue was distilled by Kugelrohr to give a colourless oil (2.80 g, 99%) bp 46-48 ºC (1.5 Torr); δ_H (250 MHz, $CDCl_3$): 8.00-7.94 (1H, m), 7.84 (1H, s), 7.52-7.27 (3H, m), 6.82 (2H, m), 6.34 (2H, m) and 3.97 (3H, s); δ_C (250 MHz, $CDCl_3$): 145.0 (CH), 140.1 (quat), 130.1 (CH), 127.8 (quat), 127.5 (CH), 126.5 (2 CH), 122.8 (2 CH),

109.6 (2 CH) and 62.0 (CH_3); *m/z* 200 (M^+, 9%), 168 (52), 154 (100), 127 (39), 77 (38) and 51 (43); (Found: $[M]^+$ 200.0943. $C_{12}H_{12}N_2O$ requires *M* 200.0944).

FVP of 2-(Pyrrol-1-yl)benzaldehyde *O*-methyl-oxime

FVP of compound **109** (0.090 g, T_f 700˚ C, T_i 64 °C, *P* 5.5 × 10^{-2} Torr, *t* 15 min) gave a yellow oil that condensed on the first part of the U-trap. Purification of the pyrolysate by dry flash chromatography [hexane : ethyl acetate (4 : 1)] yielded two major products identified as 2-pyrrol-1-yl-benzonitrile **128** as a colourless solid (0.009 g, 10%) and pyrrolo[1,2-*a*]quinazoline **111** as a yellow oil (0.060 g, 67%).

2.5. 2-pyrrol-1-yl-benzonitrile 128

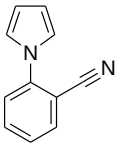

Mp 49-50 ºC (lit.,[102] 48-50 ºC); δ_H $CDCl_3$ 7.55-7.70 (2H, m), 7.25-7.40 (m, 2H), 7.05 (2H, t, *J* 2.2), and 6.33 (2H, t, *J* 2.2). [49]

2.6. Pyrrolo[1,2-*a*]quinazoline 111

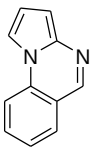

Bp 100-102 ºC (2 Torr); δ_H (360 MHz, $CDCl_3$) 8.48 (1H, s), 7.82 (1H, d, *J* 8.3 Hz), 7.79 (1H, dd, *J* 7.6, 1.3), 7.72 (1H, dd, *J* 7.6, 1.3), 7.68 (1H, dd, *J* 3.9, 1.5), 7.41 (1H, m), 6.90 (1H, dd, *J* 3.9, 1.5) and 6.75 (1H, dd, *J* 3.9, 1.5); δ_C (90 MHz, $CDCl_3$): 145.6 (CH), 138.4 (quat), 134.7 (quat), 132.2 (CH), 128.5 (CH), 123.9 (CH), 118.2 (quat), 113.6 (CH), 113.5 (CH), 108.9 (CH) and 102.5 (CH); *m/z* 168 ($[M]^+$, 100%), 140 (74), 114 (48), 84 (39), 63 (38), 50 (41) and 39 (68); (Found: $[M]^+$ 168.0684. $C_{11}H_8N_2$ requires *M* 168.0682).

2.7. Methyl 2-(indol-1-yl)benzoate 122

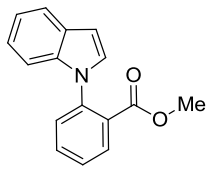

A suspension of indole (4.10 g, 35 mmol), *o*-iodobenzoic acid (8.43 g, 34 mmol) and anhydrous potassium carbonate (9.67 g, 70 mmol) in dimethylformamide (70 cm^3) was heated under reflux, with stirring, for 48 h to give 2-(indol-1-yl)benzoic acid. The product was not isolated but treated with methyl iodide (4.97 g, 35 mmol) and anhydrous potassium carbonate (9.67 g, 70 mmol) and the reaction left to stir at room

temperature for 72 h. Upon completion of the reaction, water was added (100 cm^3) and the product was extracted into ether (3 × 40 cm^3), washed with water (3 × 50 cm^3) and dried over anhydrous $MgSO_4$. Purification was achieved by distilling the crude product using a Kugelrohr oven under reduced pressure to give 2-(indol-1-yl)benzoic acid methyl ester as an orange oil **122** (3.02 g, 43%) bp 108-110 °C (1 Torr) [lit.[103] 108–110 ◦C (0.4 Torr)]. δ_H (250 MHz, $CDCl_3$): 8.09 (1H , dd, *J* 8.0, 1.9), 7.76 (2H, m), 7.59 (2H, m), 7.28 (4H, m) 6.79 (1H, d, *J* 3.3) and 3.55 (s, 3H). δ_C (63 MHz, $CDCl_3$): 166.6 (quat), 138.5 (quat), 137.1 (quat), 132.6 (CH), 131.1 (CH), 128.8 (quat), 128.7 (CH), 128.5 (quat) 128.3 (CH), 127.4 (CH), 122.1 (CH), 120.8 (CH), 120.0 (CH), 109.6 (CH), 103.1 (CH) and 52.1 (CH_3). Spectra in agreement with literature values.[45]

2.8. 2-(Indol-1-yl)benzylalcohol 123

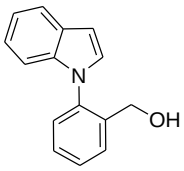

To a stirred suspension of LAH (0.76 g, 20 mmol) in dry diethyl ether (45 cm^3) under a nitrogen atmosphere, a solution of methyl 2-(indol-1-yl)benzoate (2.51 g, 10 mmol) in dry diethyl ether (15 cm^3) was added drop wise. After 30 min, the unreacted LAH was cautiously quenched with wet diethyl ether (~5 cm^3) and water (~ 5 cm^3) until the solution became colourless with a white solid in suspension. The mixture was then poured into a solution of potassium/sodium tartrate (10%), stirred, filtered through a pad of celite and dried over $MgSO_4$. After filtration the solvent was removed under reduced pressure to give a yellow oil. The product was purified by Kugelrohr distillation to give 2-(indol-1-yl)phenylmethanol as a yellow oil (1.67 g, 75%) bp 110-112 ˚C (0.5 Torr); δ_H (250 MHz, $CDCl_3$): 7.76-7.64 (2H, m), 7.48 (2H, qd, *J* 7.3, Hz), 7.39-7.34 (1H, m), 7.31-7.11 (3H, m), 7.11-7.03 (1H, m), 6.69 (1H, dd, *J* 3.2, 0.8), 4.41 (2H, s) 1.64 (1H, s). δ_C (63 MHz, $CDCl_3$): 138.1 (quat), 137.2 (quat), 137.0 (quat), 128.94 (CH), 128.89 (CH), 128.51 (CH), 128.48 (CH), 128.2 (quat), 128.1 (CH), 122.2 (CH), 120.9 (CH), 120.0 (CH), 110.1 (CH), 102.8 (CH) and 60.9 (CH_2); *m/z* 223 ($[M]^+$, 100%), 204 (45), 194 (56), 180 (60), 167 (36), 118 (13) and 77 (14); (Found: M^+ 223.0993. $C_{15}H_{13}NO$ requires *M* 223.0993).

2.9. 2-(Indol-1-yl)benzaldehyde 124

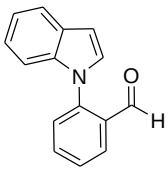

A solution 2-(indol-1-yl)benzylalcoholl (1.63 g, 7.3 mmol) in toluene (15 cm^3) was slowly added to a suspension of activated MnO_2 (6.94 g, 30 mmol) in toluene (40 cm^3) then heated to reflux for 2 h. After filtration, the solvent was removed under reduced pressure. The residual yellow oil was purified by Kugelrohr distillation to give 2-(indol-1-yl)benzaldehyde **124** as a yellow oil (1.43 g, 89%) bp 100-102 ˚C (1 Torr); δ_H (250 MHz, $CDCl_3$): 9.72 (1H, d, *J* 0.8), 8.16 (1H, dd, *J* 7.8, 1.5), 7.82-7.73 (2H, m), 7.67-7.62 (1H, m), 7.55 (1H, dd, *J* 7.8, 1.5), 7.34 (1H, d, *J* 3.2), 7.28-7.23 (3H, m) and 6.82 (1H, d, *J* 3.2); δ_C (63 MHz, $CDCl_3$): 189.6 (CH), 141.9 (quat), 138.2 (quat), 134.9 (CH), 131.9 (quat), 129.6 (CH), 128.6 (quat), 128.4 (CH), 128.1 (CH), 128.0 (CH), 121.1 (CH), 120.7 (CH), 120.67 (CH), 109.9 (CH) and 104.3 (CH); *m/z* 221 ($[M]^+$, 44%), 220 (58), 165 (50), 89 (47), 63 (62), 51 (78) and 28 (100); (Found: $[M]^+$ 221.0833. $C_{15}H_{11}NO$ requires *M* 221.0835). Spectra in agreement with literature values.[104]

2.10. 2-(Indol-1-yl)benzaldehyde *O*-methyl-oxime 112

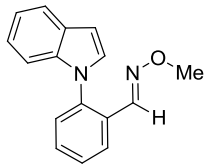

2-(Indol-1-yl)benzaldehyde **(**1.39 g, 6.3 mmol) and *O*-ethylhydroxyl-amine hydrochloride (0.66 g, 7.9 mmol) were dissolved in EtOH (50 cm^3). The solution was heated at reflux for 2 h. After cooling, the majority of EtOH was removed under reduced pressure and water was added (100 cm^3). The product was extracted with $CHCl_3$ (2 × 100 cm^3). The organic layers were separated, washed with water (100 cm^3) then dried over $MgSO_4$. The solvent was evaporated and the residue (a black, sticky oil) was distilled by Kugelrohr to give a light yellow oil that crystallised overnight to give a light yellow solid (1.42 g, 90%); bp 81-83 ºC (0.7 Torr) mp 60-62 ˚C. δ_H (250 MHz, $CDCl_3$): 8.18 (1H, m), 7.78 (1H, m), 7.77 (1H, m), 7.57 (2H, m), 7.45 (1H, m), 7.22 (4H, m), 6.79 (1H, dd, *J* 3.2, 0.7) and 3.99 (3H, s); δ_C (63 MHz, $CDCl_3$): 144.5 (CH), 137.9 (quat), 137.4 (quat), 130.3 (CH), 129.3 (quat), 129.0 (CH), 128.2 (quat), 128.0 (CH), 126.4 (CH), 122.3 (CH), 120.7 (CH), 120.6 (CH),

120.1 (CH), 110.1 (CH), 103.3 (CH) and 61.8 (CH_3); *m/z* 250 ($[M]^+$, 24%), 219 (100), 204 (7), 191 (11), 109 (5), and 95 (4); (Found C, 76.31; H, 5.41; N, 11.00%. $C_{16}H_{14}N_2O \cdot 0.1H_2O$ requires C, 76.25; H, 5.55; N, 11.10).

FVP of 2-(Indol-1-yl)benzaldehyde *O*-methyl-oxime

FVP of compound **112** (0.305 g, T_f 650˚ C, T_i 40 °C, P 1.6 × 10^{-2} Torr, t 40 min) gave an orange oil that condensed on the first part of the U-trap. Purification of the pyrolysate by dry flash chromatography on silica with [ethyl acetate : hexane (10 : 90)] as eluent yielded two major products identified as pyrrolo[3,2,1-*jk*]carbazole **139** as a colourless solid (0.005 g, 2%), 2-(indol-1-yl)benzaldehyde **124** as a yellow oil (0.015 g, 6%), 2-indol-1-yl-benzonitrile **138** as a colourless solid (0.019 g, 7%) and desired product indolo[1,2-*a*]quinazoline **114** as an orange solid (0.227 g, 85%).

2.11. Pyrrolo[3,2,1-*jk*]carbazole 139

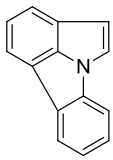

Mp 88-90 °C; δ_H (500 MHz, $CDCl_3$): 8.07 (1H, d *J* 7.7), 7.89 (1H, d, *J* 7.7), 7.78 (1H, d, *J* 7.5), 7.73 (1H, d, *J* 3.0), 7.68 (1H, d, *J* 8.0), 7.50 (1H, t, *J* 7.3), 7.47 (1H, td, *J* 8.0, 1.2), 7.32 (1H, td, *J* 7.6, 0.8), 6.85 (1H, d, 3.0); δ_C (125 MHz, $CDCl_3$): 141.2 (quat), 139.8 (quat), 131.3 (quat), 127 (CH), 123.8 (CH), 123.5 (CH), 122.8 (CH), 122.5 (CH), 122 (quat), 121.4 (CH), 119.3 (quat), 117.7 (CH), 111.8 (CH) and 109.8 (CH). Spectra were in agreement with the literature.[51]

2.12. 2-Indol-1-yl-benzonitrile 138

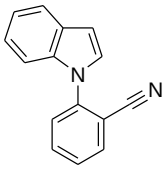

Mp 97-99 ˚C; δ_H (500 MHz, $CDCl_3$): 7.84 (1H, dd, *J* 7.8 1.4), 7.73 (1H, dt, *J* 7.9, 1.5), 7.69 (1H, m), 7.61 (1H, d, *J* 8.05), 7.48 (1H, dt, *J* 7.7, 1.0), 7.40 (1H, d, *J* 3.3), 7.33 (1H, d *J* 8.2), 7.22 (2H, m) and 6.76 (1H, d, *J* 3.32); δ_C (125 MHz, $CDCl_3$): 142.3 (quat), 136.6 (quat), 134.9 (CH), 134.2 (CH), 129.7 (quat), 128.5 (CH), 127.73 (CH), 127.71 (CH), 123.2 (CH), 121.7 (CH), 121.5 (CH), 116.8 (quat), 110.6 (CH), 110.2 (quat) and 115.4 (CH). Spectra are in agreement with literature values.[52]

2.13. Indolo[1,2-*a*]quinazoline 114

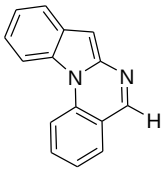

Bp 112-114 °C; δ_H (360 MHz, $CDCl_3$): 8.61 (1H, s), 8.45 (1H, dd, *J* 8.9, 0.7), 8.35 (1H, d, *J* 8.4), 7.93 (1H, dd, *J* 7.0, 0.9), 7.82 (2H, m), 7.45 (3H, m) and 7.04 (1H, s); δ_C (90 MHz, $CDCl_3$): 151.2 (CH), 142.4 (quat), 138.0 (quat), 133.3 (CH), 130.0 (quat), 129.3 (quat), 129.1 (CH), 123.0 (CH), 122.6 (CH), 122.1 (CH), 121.6 (CH), 118.6 (quat), 114.5 (CH), 114.0 (CH) and 97.0 (CH); *m/z* 218 ($[M]^+$, 50%), 116 (12) 102 (75), 89 (75), 63 (100) and 50 (75); (Found: $[M]^+$ 218.0838. $C_{15}H_{10}N_2$ requires *M* 218.0838).

2.14. Methyl 2-(indol-1-yl)benzoate 125

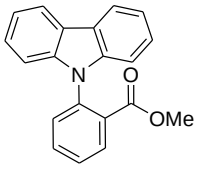

A mixture of carbazole (3.68 g, 22 mmol), methyl 2-iodobenzoate (8.65 g, 33 mmol), copper powder (1 g), potassium carbonate (4.55 g, 33 mmol) and nitrobenzene (2 cm^3) were heated at 175 ˚C for 48 h. After cooling, the resultant mixture was a red solid. A mixture of [water: CH_3Cl (1 : 1)] (100 cm^3) was added to the solid and the two layers separated. The aqueous layer was then extracted with CH_3Cl (2 × 30 cm^3) and the organic layers combined and dried over $MgSO_4$. The solvent was removed under reduced pressure and the residue oil was purified by flash dry chromatography on silica using [hexane : ethyl acetate (85 : 15)] as eluent. The resulting product was a colourless crystalline solid (5.30 g, 88%); mp 149-151 ºC (lit[105] 150-151 ºC); δ_H (360 MHz, $CDCl_3$): 8.20-8.10 (3H, m), 7.78 (1H, m), 7.61 (2H, m), 7.40 (2H, ddd, *J* 8.3, 7.2, 1.3), 7.29 (2H, ddd, *J* 8.3, 7.2, 1.3), 7.15 (2H, td, *J* 8.2, 0.8) 3.21 (3H, s); δ_C (90 MHz, $CDCl_3$): 166.3 (quat), 141.5 (2 quat), 136.8 (quat), 133.2 (CH), 131.9 (CH), 129.99 (CH), 129.96 (quat), 128.2 (CH), 125.8 (2 CH), 123.2 (2 quat), 120.1 (2 CH), 119.7 (2 CH), 109.2 (2 CH) and 52.0 (CH_3). Spectra are in agreement with literature values.[46]

2.15. 2-(Carbazol-1-yl)benzylalcohol 126

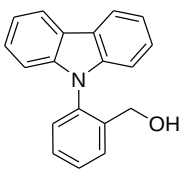

To a stirred suspension of LAH (0.38 g, 10 mmol) in dry THF (18 cm^3) under a nitrogen atmosphere, a solution of methyl 2-(carbazol-

1-yl)benzoate (1.50 g, 5 mmol) in dry THF (18 cm^3) was added drop-wise. After 30 min, the unreacted LAH was cautiously quenched with wet diethyl ether (~5 cm^3) and water (~ 5 cm^3) until the solution became colourless with a white solid in suspension. The mixture was then poured into a solution of potassium/sodium tartrate (10% in water), stirred, filtered through a pad of celite and dried over $MgSO_4$. After filtration the solvent was removed under reduced pressure. The product was purified by Kugelrohr distillation to give 2-(carbazol-1-yl)phenylmethanol as a light yellow oil (1.06 g, 78%); bp 110-112 ˚C (1.5 Torr); δ_H (250 MHz, $CDCl_3$): 8.17 (2H, ddd, *J* 7.6, 1.4, 0.7), 7.79 (1H, m), 7.60 (1H, dt, *J* 7.5, 1.6), 7.52 (1H, dt, 7.5, 1.8 Hz), 7.39 (3H, m), 7.31 (1H, dd, *J* 7.2, 1.2 Hz), 7.28 (1H, dd, 7.2, 1.1 Hz), 7.06 (1H, dd, 1.1, 0.7 Hz), 7.03 (1H, m), 4.33 (2H, m) and 1.62 (1H, m); δ_C (63 MHz, $CDCl_3$): 141.3 (quat), 139.9 (quat), 134.5 (quat), 129.3 (CH), 129.1 (CH), 128.9 (2 CH), 127.5 (quat), 126.0 (2 CH), 122.9 (2 quat), 120.3 (2 CH), 119.7 (2 CH), 109.4 (2 CH) and 60.8 (CH_2); *m/z* 273 ($[M]^+$, 100%), 244 (21), 196 (21), 179 (16), 167 (15), 83 (24) and 49 (22); (Found: $[M]^+$ 273.1145. $C_{19}H_{15}NO$ requires *M* 273.1148).

2.16. 2-(Carbazol-1-yl)benzaldehyde 127

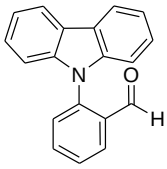

A solution of 2-(carbazol-1-yl)phenylmethanol (1.01 g, 3.7 mmol) in toluene (10 cm^3) was slowly added to a suspension of activated MnO_2 (1.29 g, 14.8 mmol) in toluene (20 cm^3) then heated to reflux for 1 h. After filtration, the solvent was removed under reduced pressure. The residual yellow oil was purified by Kugelrohr distillation to give 2-(carbazolol-1-yl)benzaldehyde **127** as an orange oil (0.88 g, 86%); δ_H (250 MHz, $CDCl_3$) 9.62 (1 H, d, *J* 0.8 Hz), 8.24 (1H, ddd, *J* 7. 8, 1.7, 0.4 Hz), 8.19 (2H, ddd, *J* 7.6, 1.4, 0.7 Hz), 7.86 (1H, ddd, *J* 7.9, 7.5, 1.7 Hz), 7.69 (1H, m), 7.56 (1H, ddd, *J* 7.9, 1.2, 0.4 Hz), 7.44 (1H, d, *J* 1.3 Hz), 7.41 (1H, d, *J* 1.5 Hz), 7.38 (1H, d, *J* 1.3 Hz), 7.35 (1H, d, *J* 1.1 Hz), 7.19 (2H, m). δ_C (63 MHz, $CDCl_3$): 189.5 (CH), 142.2 (quat), 140.2 (quat), 135.5 (CH), 133.3 (quat), 129.3 (CH), 128.8 (2 quat), 128.7 (2 CH), 126.4 (2 CH), 123.3 (quat), 120.5 (2 CH), 120.4 (2 CH) and 109.4 (2 CH); *m/z* 271 ($[M]^+$, 100%), 243 (78), 210 (10),

180 (11), 135 (10) and 120 (17); (Found: $[M]^+$ 271.0985. $C_{19}H_{13}NO$ requires *M* 271.0992).

2.17. 2-(Carbazol-1-yl)benzaldehyde *O*-methyloxime 116

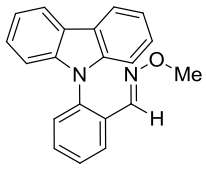

2-(Carbazol-1-yl)benzaldehyde (0.88 g, 3.2 mmol) and *O*-methylhydroxylamine hydrochloride (0.27 g, 3.2 mmol) were dissolved in EtOH (30 cm^3) and the solution was heated at reflux for 2 h. After cooling, the majority of the EtOH was removed under reduced pressure and water was added (50 cm^3). The product was extracted with $CHCl_3$ (2 × 50 cm^3). The organic layers were separated, washed with water (100 cm^3) then dried over $MgSO_4$. The solvent was evaporated and the residue did not require additional purification (0.87 g, 91%); mp 165-167 ºC; δ_H (250 MHz, $CDCl_3$): 8.21 (1H, m), 8.16 (2H, ddd, *J* 7.6, 1.4, 0.7 Hz), 7.58 (3H, m), 7.40 (3H, m), 7.33 (1H, d, *J* 1.2 Hz), 7.30 (1H, dd, *J* 1.1, 0.4 Hz), 7.11 (1H, dd, *J* 1.1, 0.7 Hz, 1H), 7.07 (1H, m) and 3.85 (3H, s); δ_C (63 MHz, $CDCl_3$): 144.6 (CH), 141.7 (2 quat), 136.1 (quat), 131.0 (CH), 129.4 (CH), 128.8 (CH), 126.9 (CH), 126.1 (2 CH), 126.0 (quat), 123.1 (2 quat), 120.2 (2 CH), 120.0 (2 CH), 109.7 (2 CH) and 61.9 (CH_3); *m/z* 300 ($[M]^+$, 100%), 269 (86), 254 (19), 241 (59), 161 (20), 133 (19), 120 (3), 84 (6) and 57 (10); (Found C, 79.72; H, 5.06; N, 9.34. $C_{20}H_{16}N_2O$ requires C, 79.98; H, 5.37; N, 9.33).

FVP of 2-(Carbazol-1-yl)benzaldehyde *O*-methyloxime

FVP of compound **116** (0.200 g, T_f 700˚ C, T_i 60 °C, *P* 2.3 × 10^{-2} Torr, *t* 20 min) gave a light yellow oil that condensed in the U-trap. Purification of the pyrolysate by dry flash chromatography on silica with [ethyl acetate : hexane (5 : 95 up to 30 : 70)] as elect afforded two main products: indolo [3,2,1-*jk*]carbazole **149** as a colourless solid (0.030 g, 15%) and 2-carbazol-9-yl-benzonitrile **148** as a light yellow solid (0.110 g, 55%).

2.18. Indolo [3,2,1-*jk*]carbazole 149

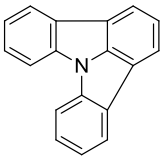

Mp 133-135 °C; δ_H (360 MHz, $CDCl_3$): 8.13 (2H, ddd, *J* 7.8, 0.9, 0.6 Hz), 8.03 (2H, d, *J* 7.4 Hz) 7.88 (2H, m), 7.56 (3H, m) and 7.35 (2H, dt, *J* 7.7, 1.0 Hz); δ_C (90 MHz, $CDCl_3$): 143.60 (quat), 138.55 (2 quat), 129.89 (2 quat), 126.53 (2 CH), 122.98 (2 CH), 122.67 (CH), 121.52 (2 CH), 119.23 (2 CH), 118.31 (2 quat) and 112 (2 CH). Spectra are in agreement with literature values.[54]

2.19. 2-Carbazol-9-yl-benzonitrile 148

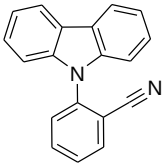

Mp 170-171 ºC; IR (nujol, cm^{-1}): 2359 (CN) and 2341; δ_H (360 MHz, $CDCl_3$): 8.15 (2H, m), 7.94 (1H, dd, *J* 8.1, 1.5), 7.81 (1H, m), 7.61 (2H, m), 7.43 (2H, ddd, *J* 8.3, 7.2, 1.1), 7.33 (2H, dt, *J* 7.6, 1.1), 7.22 (1H, m) and 7.19 (1H, m); δ_C (90 MHz, $CDCl_3$): 140.6 (2 quat), 140.5 (quat), 134.4 (CH), 134.2 (CH), 129.5 (CH), 129.4 (CH), 126.1 (2 CH), 123.8 (2 quat), 120.7 (2 CH), 120.4 (2 CH), 115.9 (quat), 112.7 (quat) and 109.6 (2 CH); *m/z* 268 ($[M]^+$, 100%), 241 (85), 161 (9), 133 (12), 120 (14), 107 (4) and 57 (4).

2.20. Pyrrolo[1,2-a]quinazolin-1-yl-*p*-tolyl-diazene 160

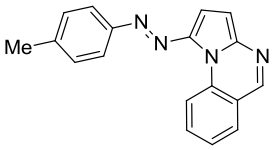

A solution of pyrrolo[1,2-*a*]quinazoline **111** (0.010 g, 0.5 mmol) and tetrafluoroboroate-4-methyl-benzenediazonium salt was made up in chloroform and stirred overnight at room temperature. The solvent was removed and the crude product was purified by dry flash chromatography on silica using [hexane : ethyl acetate (65 : 35)] as eluent affording a red solid (0.014 g, 80%); mp 155-157 ºC; δ_H (400 MHz, $CDCl_3$): 9.29 (1H, dd, *J* 8.6, 0.7), 8.59 (1H, s), 7.84 (2H, m), 7.78 (2H, m), 7.49 (1H, m), 7.46 (1 H, d, *J* 4.7), 7.33 (2H, d, *J* 8.1), 6.87 (1H, d, *J* 4.7) and 2.44 (3H, s); δ_C (100 MHz, $CDCl_3$): 151.7 (quat), 148.1 (CH), 143.8 (quat), 141.9 (quat), 140.0 (quat), 136.1 (quat), 133.8 (CH), 129.8 (2 CH), 128.3 (CH), 124.9 (CH), 122.2 (2 CH), 120.1 (quat), 119.8 (CH), 106.2 (CH), 104.6 (CH) and 21.4 (CH_3); *m/z* 286 (M^+, 100%), 257 (23), 167 (18), 105 (10), 91 (12), 78 (12) and 63 (12); (Found: $[M]^+$ 286.12157. $C_{18}H_{14}N_4$ requires *M* 286.12130).

2.21. Oxo-pyrrolo[1,2-a]quinazolin-1-yl-acetic acid methyl ester 161

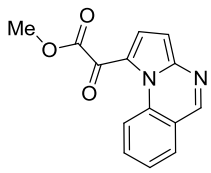

A solution of pyrrolo[1,2-*a*]quinazoline **111** (32 mg, 0.2 mmol) in $CHCl_3$ (1 cm^3) was cooled in an ice bath. At the same time a solution of oxalyl chloride (2 cm^3 in 1 cm^3 of $CHCl_3$) was also cooled down in an ice bath. The oxalyl chloride solution was added to the pyrrolo[1,2-*a*]quinazoline solution drop wise over a period of 10 min. The resulting solution was stirred at room temperature for 5 min. After this time, the volatiles were evaporated and methanol (5 cm^3) was added to the resulted oil. The solution was stirred for further 5 min, before removing residual methanol under reduced pressure. The resulting mixture was purified by column chromatography on silica gel using [hexane : ethyl acetate (60 : 40)] as eluent to give a colourless oil (0.041 g, 80%) bp 147-149 °C at 5 Torr; δ_H (500 MHz, $CDCl_3$): 8.90 (2H, m), 7.93 (1H, dd, *J* 7.8, 1.5), 7.87 (1H, d, *J* 4.8), 7.86 (1H, ddd, *J* 8.9, 7.1, 1.5), 7.60 (1H, ddd, 7.8, 7.2, 0.9), 6.87 (1H, d, *J* 4.8) and 4.02 (3H, s); δ_C (125 MHz, $CDCl_3$): 173.1 (quat), 165.2 (quat), 154.3 (CH), 147.9 (quat), 136.5 (quat), 133.6 (CH), 132.1 (CH), 129 (CH), 126.5 (CH), 123.5 (quat), 120.6 (CH), 120.3 (quat), 106.8 (CH) and 53.4 (CH_3); *m/z* 254 ($[M]^+$, 7%), 195 (100), 167 (5) and 140 (5); (Found: $[M]^+$ 254.0691. $C_{14}H_{10}O_3N_2$ requires *M* 254.0697).

FVP of pyrrolo[1,2-*a*]quinazoline 111

FVP of compound **111** was performed (0.04 g, T_f 950˚ C, T_i 85→97 °C, *P* (1.9→5.5) × 10^{-2} Torr, *t* 30 min) using silica wool in the inner part of the furnace tube. Two major products were obtained which were separated by dry flash chromatography using [hexane : ethyl acetate (80 : 20)→(60 : 40)] as eluent to give 1*H*-pyrrolo[3,2-*c*]isoquinoline amine **167** as a colourless solid (0.006 g, 12 %) and 3*H*-pyrrolo[2,3-*c*]isoquinoline amine **168** as a colourless solid (0.016 g, 40 %).

2.22. 1*H*-pyrrolo[3,2-c]isoquinoline amine 167

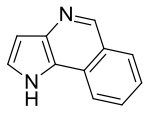

Mp 143-145 °C; δ_H (360 MHz, $CDCl_3$) 9.27 (1H, bs), 9.05 (1H, s), 8.07 (1H, d, *J* 8.2), 8.02 (1H, dd, *J* 8.3, 0.8), 7.72 (1H, ddd, *J* 7.0, 5.2, 1.2),

7.52 (1H, ddd, *J* 8.1, 7.0, 1.1), 7.42-7.39 (1H, m) and 6.94 (1H, dd, *J* 3.2, 2.1). Spectrum is in agreement with literature values.[58]

2.23. 3*H*-pyrrolo[2,3-*c*]isoquinoline amine 168

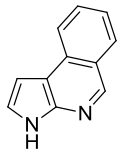

Mp 142-144 °C; δ_H (360 MHz, $CDCl_3$): 10.28 (1H, bs), 8.93 (1H, s), 8.20 (1H, dd, *J* 8.3, 1.0), 8.05 (1H, d, *J* 8.2), 7.74 (1H, ddd, *J* 8.2, 6.9, 1.3), 7.50 (1H, ddd, *J* 8.1, 6.9, 1.1), 7.46 – 7.33 (1H, m), 7.01 (1H, dd, *J* 3.4, 2.1); δ_C (90 MHz, $CDCl_3$): 146.4 (CH), 143.6 (quat), 131.3 (quat), 129.9 (CH), 128.6 (CH), 124.7 (quat), 123.8 (CH), 122.4 (CH), 122.0 (CH), 113.4 (quat), 100.1 (CH); *m/z* 168 (M^+, 100%), 140 (11) and 114 (5); (Found: $[M]^+$ 168.0691 $C_{11}H_8N_2$ requires *M* 168.0693). Spectra are in agreement with literature values.[59]

FVP of indolo[1,2-*a*]quinazoline 114

FVP of compound **114** was performed (0.094 g, T_f 975 °C, T_i 41→143 °C, *P* (3.8→8.5) × 10^{-2} Torr, *t* 40 min) using silica wool in the inner part of the furnace tube. Two major products were obtained which were separated by dry flash chromatography using [hexane : ethyl acetate (90 : 10)] as eluent to give indolo[1,2-*a*]quinazoline **114** (0.013 g, 14%), 2-(1*H*-indol-3-yl)benzonitrile **175** as a colourless solid (0.003 g, 3%), 7*H*-indolo[2,3-*c*]isoquinoline **174** as a colourless solid (0.062 g, 65%) and 11*H*-indolo[3,2-*c*]isoquinoline **173** as a yellow solid (0.017 g, 18%).

2.24. 2-(1*H*-indol-3-yl)benzonitrile 175

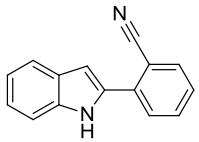

δ_H (500 MHz, $CDCl_3$): 8.50 (1H, bs), 7.83 (1H, d, *J* 7.7), 7.81 (1H, dd, *J* 7.8, 1.1), 7.80 (1H, d, *J* 7.8), 7.74 (1H, d, *J* 2.7), 7.69 (1H, td, *J* 7.7, 1.4), 7.51 (1H, d, *J* 8.2), 7.40 (1H, td, *J* 7.7, 1.1), 7.35-7.30 (1H, m) and 7.27-7.22 (1H, m); δ_C (125 MHz, $CDCl_3$): 138.8 (quat), 136.1 (quat), 133.9 (CH), 132.6 (CH), 129.8 (CH), 126.1 (CH), 125.7 (quat), 124.3 (CH), 122.8

(CH), 120.7 (CH), 119.4 (quat), 119.1 (CH), 113.8 (quat), 111.5 (CH) and 110.8 (quat).

2.25. 7*H*-Indolo[2,3-*c*]isoquinoline 174

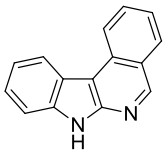

Mp 259-260 °C[106]; δ_H (400 MHz, DMSO): 12.24 (s, 1H), 9.22 (s, 1H), 8.74 (1H, d, *J* 7.7), 8.58 (1H, d, *J* 8.0), 8.28 (1H, d, *J* 8.0), 7.94 (1H, ddd, *J* 8.3, 6.9, 1.3), 7.66 (1H, d, *J* 8.1), 7.60 (1H, ddd, *J* 8.0, 6.9, 1.0), 7.54-7.47 (1H, m), 7.37 (1H, dd, *J* 8.0, 1.0); δ_C (100 MHz, DMSO): 151 (CH), 148.9 (quat), 137.7 (quat), 132.3 (quat), 131.7 (CH), 129.9 (CH), 125.3 (CH), 124.6 (quat), 124 (CH), 122.8 (CH), 122.6 (CH), 121.6 (quat), 120.5 (CH), 112.2 (CH) and 105.5 (quat). Spectra are in agreement with literature. [61]

2.26. 11*H*-Indolo[3,2-*c*]isoquinoline 173

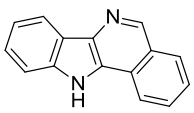

Mp > 300 °C. δ_H (500 MHz, DMSO): 12.33 (1H, bs), 9.13 (1H, s), 8.52 (1H, dd, *J* 8.2, 0.9), 8.28 (1H, d, *J* 8.2), 8.25 (1H, d, *J* 7.8), 7.91 (1H, ddd, *J* 8.2, 6.9, 1.2), 7.71 (1H, ddd, *J* 8.2, 7.0, 1.1), 7.70 (1H, dd, *J* 8.1, 0.9), 7.50 (1H, ddd, *J* 8.2, 7.1, 1.2) and 7.32 (1H, ddd, *J* 7.8, 7.1, 0.9); δ_C (125 MHz, DMSO): 145.8 (CH), 138.5 (quat), 133.5 (quat), 129.8 (CH), 128.5 (CH), 127.2 (quat), 126.4 (CH), 126.1 (quat), 125.4 (quat), 123.4 (quat), 122.6 (CH), 121.5 (CH), 119.7 (CH), 119.2 (CH) and 111.8 (CH).

2.27. 1-[2-(2,5-dimethyl-1*H*-pyrrol-1-yl)phenyl]ethan-1-one 209

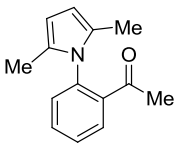

A solution of 1-(2-aminophenyl)ethan-1-one (2.02 g, 15 mmol), hexane-2,5-dione (1.94 g, 17 mmol) and AcOH (12 cm^3) was heated at reflux in toluene (20 cm^3) overnight using Dean-Stark apparatus to remove water evolved during the course of the reaction. After cooling the mixture, toluene and AcOH were evaporated and water was added (40 cm^3). The aqueous mixture was extracted with DCM (2×40 cm^3). The organic fractions were combined and dried over $MgSO_4$. The solvent was evaporated and the crude was purified by dry flash chromatography using [hexane : ethyl acetate (90 : 10)] as eluent to give a yellow oil (2.40 g, 75%); 67 °C at 2 Torr; δ_H (500 MHz, $CDCl_3$): 7.80 (1H, dd, *J* 7.8,

1.6), 7.62 (1H, td, *J* 7.6, 1.6), 7.52 (1H, td, *J* 7.6, 1.2), 7.27 (1H, dd, *J* 7.8, 1.0), 5.96 (s, 2H), 1.99 (s, 6H), 1.81 (s, 3H); δ_C ($CDCl_3$), 13.17 ($2CH_3$), 28.35 (CH_3), 107.31 (2CH), 128.92 (2CH), 129.16 (2quat), 130.04 (CH), 132.71 (CH), 137.54 (quat), 139.33 (quat), and 201.22 (quat); *m/z* 213 (M^+, 100%), 198 (33), 170 (14), and 154 (9); (Found: M^+ 213.1150. $C_{14}H_{15}NO$ requires *M* 213.1148).

2.28. {1-[2-(2,5-dimethyl-1H-pyrrol-1-yl)phenyl]ethylidene}(methoxy)amine 196 (iii)

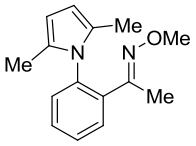

A solution of **209** (2.40 g, 11.3 mmol) and *O*-methylhydroxylamine hydrochloride (1.25 g, 15 mmol) in EtOH (15 cm^3) was heated at reflux for 3 h. After cooling, the majority of EtOH was removed under reduced pressure and water was added (50 cm^3). The aqueous solution was extracted with DCM (2×50 cm^3), the organic fractions were combined and dried over $MgSO_4$. The crude product was purified by dry flash chromatography using [hexane : ethyl acetate (90 : 10)] as eluent to give a yellow oil (1.83 g, 67%) bp 69-71 °C at 2 Torr; δ_H (500 MHz, $CDCl_3$) 7.57 (1H, dd, *J* 7.5, 1.8), 7.44 (2H, dqd, *J* 14.8, 7.4, 1.6), 7.21 (1H, dd, *J* 7.6, 1.5), 5.88 (s, 2H), 3.94 (3H, s), 1.97 (s, 6H), 1.50 (3H, s); δ_C ($CDCl_3$), 15.56 (CH_3), 64.53 (CH_3), 108.86 ($2CH_3$), 131.03 (CH), 131.67 (CH), 132.18 (CH), 132.30 (CH), 139.53 (quat), 139.67 (quat), and 158.61 (quat); *m/z* 242 (M^+, 5%), 211 (100), 195 (20), and 182 (5); (Found: M^+ 242.14174. $C_{14}H_{15}NO$ requires *M* 242.14136).

2.29. 1,5-dimethylpyrrolo[1,2-a]quinazoline 197(iii)

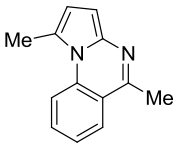

FVP of compound **196 (iii)** (0.503 g, T_f 700 ˚C, T_i 20→62 °C, P 6 × 10^{-2} Torr, t 85 min) gave a yellow solid that condensed on the first part of the U-trap. Purification of the pyrolysate by high vacuum distillation gave a yellow solid as a main product (0.28 g, 69 %) bp 135-136 °C at 1 Torr. δ_H (400 MHz, $CDCl_3$) 8.17 (1H, d, *J* 8.5 Hz), 7.85 (1H, dd, *J* 8.0, 1.5), 7.60 (1H, ddd, *J* 8.7, 7.2, 1.5), 7.37-7.31 (m, 1H), 6.56 (2H, q, *J* 4.1), 2.87 (3H, s) and 2.73 (3H, s). δ_C ($CDCl_3$), 21.15 (CH_3), 24.90 (CH_3), 103.00 (CH), 116.84 (CH),

118.14 (CH), 122.17 (2 quat), 125.90 (quat), 125.95 (CH), 129.44 (CH), 134.09 (CH), and 152.39 (quat); *m/z* 196 (M^+, 79%) and 195 (100); (Found M^+ 196.0995. $C_{13}H_{12}N_2$ requires *M* 196.0995).

Attempted synthesis of 2-(1*H*-imidazol-1-yl)benzaldehyde 213

A solution of imidazole (0.34 g, 5 mmol), 2-bromobenzaldehyde (1.31 g, 7.05 mmol), Cu powder (0.25 g, 3.93 mmol) and Cs_2CO_3 (1.30 g, 4.00 mmol) in DMF (10 cm^3) was stirred at 115 °C for 48 h. After cooling, water was added (70 ml) and the organics were extracted with $CHCl_3$ (3×70 cm^3). The organic fractions were combined and dried over $MgSO_4$. The mixture was filtered through a pad of celite to eliminate Cu residues and solvent was evaporated under reduced pressure. Dry flash chromatography was used to separate the components of the crude reaction mixture using [hexane : ethyl acetate (80 : 20) → (60 : 40)] as eluent to give dioxo-2,12-diazapentacyclo[10.7.0.$0^{2,10}$.$0^{3,8}$.$0^{13,18}$]nonadeca-3(8),4,6,10,13,15,17-heptaen-16-yl **214** as a yellow solid (0.072 g, 5%) and 9*H*-imidazo[1,2-*a*]indol-9-one **215** as an orange solid (0.093 g, 11%).

2.30. Dioxo-2,12-diazapentacyclo[10.7.0.$0^{2,10}$.$0^{3,8}$.$0^{13,18}$]nonadeca-3(8),4,6,10,13,15,17-heptaen-16-yl 214

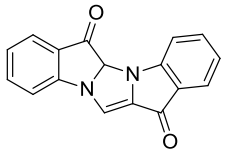

Mp 196-198 °C; δ_H (400 MHz, $CDCl_3$): 8.17 (1H, d, *J* 8.0), 7.98 (2H, dd, *J* 8.3, 1.2), 7.79 (1H, s), 7.76 – 7.68 (2H, m), 7.68 – 7.57 (3H, m) and 7.34 (1H, td, *J* 7.7, 0.7); δ_C (100 MHz, $CDCl_3$): 184.7 (quat), 178.4 (quat), 148.3 (quat), 145.2 (CH), 142.5 (quat), 137.4 (quat), 137 (CH), 133.7 (CH), 130.3 (quat), 129.3 (2CH), 128.9 (2CH), 127.9 (CH), 127.5 (quat), 125.4 (CH) and 116.7 (CH); *m/z* 274 ($[M]^+$, 100%), 197 (24), 105 (33) and 77 (19).

2.31. 9*H*-imidazo[1,2-*a*]indol-9-one 215

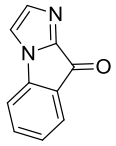

Mp 159-161°C; δ_H (400 MHz, $CDCl_3$): 7.66 (1H, d, *J* 7.4), 7.56 (1H, td, *J* 7.8, 1.2), 7.42 (1H, d, *J* 0.9), 7.32-7.24 (2H, m) and 7.19 (1H, d, *J* 7.7); δ_C (100 MHz, $CDCl_3$): 177.6 (quat), 145.9 (quat), 141.3 (quat), 137.3 (CH),

135.4 (CH), 128.2 (quat), 127.1 (CH), 125.3 (CH), 114.9 (CH) and 111.4 (CH); *m/z* 170 ($[M]^+$, 100%), 142 (17), 115 (34), 77 (8) and 51 (8); (Found: $[M]^+$ 170.0486 $C_{10}H_6ON_2$ requires *M* 170.0486).[66]

2.32. 2-(2-bromophenyl)-1,3-dioxolane 216

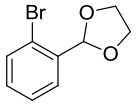

Ethane-1,2-diol (0.9 g, 16 mmol) was added to a solution of 2-bromobenzaldehyde (2.5 g, 13.5 mmol) and *p*-toluenesulfonic acid (0.04 g, 0.23 mmol) in toluene (15 ml). The mixture was then heated at reflux overnight using Dean-Stark apparatus to remove water evolved during the course of the reaction. The solution was allowed to cool to room temperature and solvent evaporated under reduced pressure. The crude residue was distilled resulting in a pale yellow oil (2.42 g, 78 %); bp 106-107 °C at 0.7 Torr; δ_H (400 MHz, $CDCl_3$): 7.60 (1H, dd, *J* 7.7, 1.6), 7.55 (1H, dd, *J* 8.0, 1.0), 7.33 (1H, t, *J* 7.5), 7.21 (1H, dt, *J* 7.7, 1.7), 5.55 (1H, s), 4.20-4.16 (2H, m) and 4.08-4.04 (2H, m); δ_C (400 MHz, CDCl3): 136.4 (quat), 132.8 (CH), 130.4 (CH), 127.6 (CH), 127.3 (CH), 122.8 (quat), 102.4 (CH) and 65.3 (2 CH_2). Spectra are in agreement with literature values.[107]

2.33. 1-[2-(1,3-dioxolan-2-yl)phenyl]-1H-imidazole 217

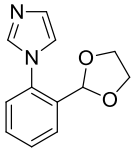

To a suspension of NaH (0.4 g 60% in mineral oil, 10 mmol) in DMF (3 cm^3), was added imidazole (0.61 g, 9 mmol) followed by a solution of **216** (2 g, 8.74 mmol) in DMF (3 cm^3). To the stirred solution Cu powder (0.06 g, 0.9 mmol) was added and the resulting mixture stirred at 140 °C for 4 h. After cooling, water (20 cm^3) was added. The mixture was extracted with DCM (2 × 20 cm^3) and, the organic fractions combined and concentrated under reduced pressure. The crude residue was purified by dry flash chromatography using [DCM : acetone (93 : 7)] as eluent to give a white solid (0.55 g, 29%); mp 94-96 °C.[108] (50% of starting material was recovered). δ_H (400 MHz, $CDCl_3$): 7.79-7.70 (2H, m), 7.53-7.42 (2H, m), 7.32-7.26 (1H, m), 7.21 (1H, t, *J* 1.2), 7.18 (1H, m), 5.51 (1H, s), 4.16-4.05 (2H, m), 4.01-3.90 (2H, m); δ_C (100 MHz, $CDCl_3$): 138.4 (CH), 136.4 (quat), 132.8 (quat), 130.1 (CH), 129.2 (CH), 128.8 (CH), 127.7 (CH), 126.4 (CH), 121.5 (CH), 99.5 (CH) and 65.5 (2 CH_2); *m/z* 217 ($[M]^+$, 38%), 188 (100), 171 (14), 144

(23), 133 (23), 117 (39), 90 (16) and 77 (12); (Found: $[M]^+$ 216.0893 $C_{12}H_{12}O_2N_2$ requires *M* 216.0893).

2.34. 2-(1*H*-imidazol-1-yl)benzaldehyde 213

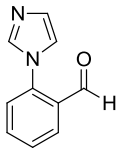

A solution of **217** (0.55 g, 2.53 mmol) in $HCl_{(aq)}$ 1N (8 cm^3) was stirred at room temperature for 2 h. Subsequently the acid was neutralised with saturated solution of $NaHCO_3$. The product was extracted with ethyl acetate (2 × 20 cm^3), the organic layers combined and dried over $MgSO_4$. After evaporation of the solvent under reduced pressure a yellow solid was obtained. The crude material was sufficiently pure to be used without further purification (0.36 g, 83%);. mp 45-47 °C;[67] δ_H (500 MHz, $CDCl_3$): 9.76 (1H, d, *J* 0.7), 8.01 (1H, dd, *J* 7.8, 1.5), 7.73 – 7.69 (1H, m), 7.68 (1H, m), 7.60 – 7.53 (1H, m), 7.39 (1H, dd, *J* 7.9, 1.0), 7.24 – 7.21 (1H, m) and 7.18 (1H, t, *J* 1.3); δ_C (100 MHz, $CDCl_3$): 188.3 (CH), 139.2 (quat), 138.2 (CH), 134.9 (CH), 130.7 (quat), 130.3 (CH), 129.1 (CH), 128.8 (CH), 126.8 (CH) and 121.8 (CH); *m/z* 172 ($[M]^+$, 86%), 144 (88), 117 (100), 90 (56), 77 (26) and 51 (21); (Found: $[M]^+$ 172.0644 $C_{14}H_{10}O_3N_2$ requires *M* 172.0642).

2.35. {[2-(1H-imidazol-1-yl)phenyl]methylidene}(methoxy)amine 198

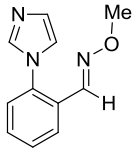

A solution of **213** (0.36 g, 2.11 mmol) and *O*-methylhydroxylamine hydrochloride (0.21 g, 2.5 mmol) in EtOH (15 cm^3) was reflux for 4 h. After allowing cooling to room temperature, the solvent was evaporated under reduced pressure and water (50 cm^3) was added and the pH was adjusted to 7. The solution was extracted twice with DCM (2 × 30 cm^3), the organic fractions combined and dried over $MgSO_4$. After filtration, solvent was evaporated to afford a pale orange oil. NMR analysis showed that the product did not need any further purification (0.33 g, 79%) bp 100-101 °C; δ_H (500 MHz, $CDCl_3$) 8.00 (1H, m), 7.78 (1H, s), 7.61 (1H, s), 7.47 (2H,m), 7.29 (1H, m), 7.22 (1H, m), 7.09 (1H, m) and 3.95 (3H, s); δ_C (125 MHz, $CDCl_3$): 142.1 (CH), 136.4 (CH), 134.4 (quat), 128.9 (CH), 128.3 (CH), 127.4 (CH), 126.7 (quat), 125.4 (CH), 125.2 (CH), 119.7 (CH) and 60.7 (CH_3); *m/z* 201 ($[M]^+$, 2%), 170 (100), 143 (25), 129 (11), 116 (20), 102 (9) and 89 (10); (Found: $[M]^+$ 201.0905 $C_{11}H_{11}ON_3$ requires *M* 201.0908).

FVP of {[2-(1H-imidazol-1-yl)phenyl]methylidene}(methoxy)amine 198

FVP of compound **198** (0.327 g, T_f 700 ˚C, T_i 52 °C, P 1.8→8 × 10^{-2} Torr, t 45 min) gave an orange solid that condensed on the first part of the U-trap. Dry flash chromatography was performed on the crude residue using [hexane : ethyl acetate (80 : 20)] as eluent to give imidazo[1,5-*a*]quinazoline **199** as a yellow solid (0.058 g, 21%) and imidazo[1,2-*a*]quinazoline **200** as an orange solid (0.166 g, 60%).

2.36. Imidazo[1,5-*a*]quinazoline 199

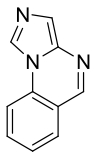

Mp 130-132 °C; δ_H (500 MHz, $CDCl_3$): 8.52 (1H, s), 8.49 (s, 1H), 7.92 (1H, d, J 8.3), 7.85 (1H, dd, J 7.8, 0.7), 7.81-7.77 (1H, m), 7.67 (1H, s) and 7.53 (1H, dd, J 14.3, 6.9); δ_C (125 MHz, $CDCl_3$): 191.5 (quat), 161.6 (quat), 148.6 (CH), 136.8 (quat), 133.2 (CH), 128.9 (CH), 126 (CH), 125.1 (CH), 122.3 (CH) and 113.9 (CH); *m/z* 169 (M^+, 100%), 142 (17), 115 (23), 84 (30) and 49 (36); (Found: $[M]^+$ 169.0635 $C_{10}H_7N_3$ requires M 169.0635).

2.37. Imidazo[1,2-*a*]quinazoline 200

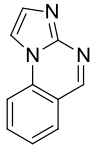

Mp 125-126 °C; δ_H (500 MHz, $CDCl_3$): 8.93 (1H, s), 7.94 (1H, dd, J 8.0, 0.6), 7.91 (1H, d, J 1.5), 7.86 (1H, d, J 8.1), 7.82 (1H, ddd, J 8.4, 7.0, 1.3), 7.73 (1H, d, J 1.4) and 7.53 (1H, ddd, J 8.1, 7.0, 1.3); δ_C (125 MHz, $CDCl_3$): 152.6 (CH), 146.9 (quat), 134.7 (quat), 133.3 (CH), 132.9 (CH), 129 (CH), 125.2 (CH), 118.2 (quat), 114.5 (CH) and 109.2 (CH); *m/z* 169 ($[M]^+$, 100%), 142 (8), 129 (18), 115 (23), 83 (48) and 49 (61); (Found: $[M]^+$ 169.0634 $C_{10}H_7N_3$ requires M 169.0635).

2.38. 2-(1*H*-pyrazol-1-yl)benzaldehyde 210

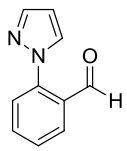

A solution of pyrazole (1.84 g, 27.1 mmol), 2-fluorobenzaldehyde (2.89 g, 23.3 mmol) and K_2CO_3 (4.15 g, 30 mmol) in DMSO (100 cm^3) was heated overnight at 100 °C. After cooling to room temperature, water (100 cm^3) was added and the solution was extracted with diethyl ether (3 × 70 cm^3). The ether extract was washed with water (2 × 100 cm^3) and dried over $MgSO_4$. After filtering and evaporating the solvent, the crude residue was purified by Kugelrohr

distillation to give a pale yellow solid (1.71g, 43%); bp 85-87 °C at 1 Torr; δ_H (500 MHz, $CDCl_3$): 10.05 (1H, d, *J* 0.5), 8.05 (1H, dd, *J* 7.7, 1.4), 7.84 (2H, dd, *J* 14.8, 2.0), 7.71 (1H, td, *J* 7.7, 1.6), 7.58-7.51 (2H, m), 6.60-6.49 (1H, m); δ_C (125 MHz, $CDCl_3$): 190.1 (CH), 142.3 (quat), 142.1 (CH), 134.3 (CH), 130.8 (CH), 130.3 (quat), 128.8 (CH), 128.1 (CH), 124.5 (CH), 108.1 (CH). ^{1}H Spectrum in agreement with literature values.[109]

2.39. 2-Pyrazol-1-yl-benzaldehyde *O*-methyl-oxime 186

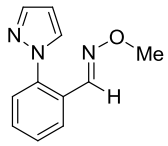

A solution of 2-(1*H*-pyrazol-1-yl)benzaldehyde (1.71 g, 9.9 mmol) and *O*-methylhydroxylamine hydrochloride (0.84 g, 10 mmol) in EtOH (25 cm^3) was heated at reflux for 4 h. After cooling to room temperature, the solvent was evaporated and water (30 cm^3) was added followed by an extraction with DCM (2 × 30 cm^3). The organic layers were combined and dried over $MgSO_4$. After filtration, volatiles were removed under reduced pressure and the resulting crude residue was purified by Kugelrohr distillation to give a yellow oil (1.59 g, 80%) bp 88-90 °C at 0.3 Torr; δ_H (500 MHz, $CDCl_3$): 8.04 (1H, s), 8.03 (1H, dd, *J* 6.7, 2.3), 7.78 (1H, d, *J* 1.7), 7.67 (1H, d, *J* 2.4), 7.49 (1H, dd, *J* 7.6, 1.6), 7.46-7.40 (2H, m), 6.49 (1H, t, *J* 2.1) and 3.99 (3H, s); δ_C (125 MHz, $CDCl_3$): 145.3 (CH), 141.3 (CH), 139.4 (quat), 131.2 (CH), 130.3 (CH), 128.7 (CH), 127.5 (quat), 127 (CH), 125.8 (CH), 107.1 (CH) and 62.2 (CH_3); *m/z* 201 ($[M]^+$, 55%), 170 (100), 156 (24), 143 (19), 129 (14), 116 (16) and 102 (16); (Found: $[M]^+$ 201.0894 $C_{11}H_{11}ON_3$ requires *M* 201.0897).

2.40. Pyrazolo[1,5-*a*]quinazoline 187

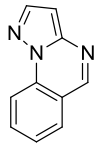

FVP of compound **186** (0.418 g, T_f 700 ˚C, T_i 54 °C, P 3.2 × 10^{-2} →9.5 × 10^{-2} Torr, t 50 min) gave an orange oil that was purified by dry flash chromatography using [hexane : ethyl acetate (90 : 10)] as eluent to give a white solid (0.18 g, 43%) mp 119-121 °C; δ_H (500 MHz, $CDCl_3$) 8.91 (1H, s), 8.50 (1H, d, J 8.4), 8.13 (1H, d, J 2.1), 7.97 (1H, d, J 7.9), 7.96-7.88 (1H, m), 7.66-7.52 (1H, m) and 6.85 (1H, d, J 2.1); δ_C 151.8 (CH), 145.8 (quat), 142.7 (CH), 136.3 (quat), 134.2 (CH), 128.4 (CH), 125.3 (CH), 118.5 (quat), 114.7 (CH) and 99.9 (CH); *m/z* 169 ($[M]^+$, 100%), 142 (12) and 115 (15); (Found: $[M]^+$ 169.0632 $C_{10}H_7N_3$ requires M 169.0635).

2.41. Quinazolin-2-yl-acetonitrile 211

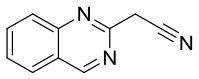

FVP of compound **187** (0.0745 g, T_f 950 ˚C, T_i 87 °C, P 4 × 10^{-2} Torr, t 35 min) gave an orange oil that was purified by dry flash chromatography using [hexane : ethyl acetate (80 : 20)] as eluent, yielding a colourless solid (0.35 g, 48%) mp 102-103 °C [lit.]; δ_H (500 MHz, $CDCl_3$): 9.44 (1H, s), 8.08 (1H, d, J 8.8), 8.03-7.96 (2H, m), 7.74 (1H, t, J 7.5) and 4.30 (2H, s); δ_C (125 MHz, $CDCl_3$): 161.4 (CH), 157.1 (quat), 150.4 (quat), 135 (CH), 128.4 (CH), 128.2 (CH), 127.3 (CH), 123.6 (quat), 116.3 (quat) and 28.8 (CH_2); *m/z* 169 ($[M]^+$, 100%), 142 (15), 129 (16), 102 (12) and 76 (13); (Found: $[M]^+$ 169.0636 $C_{10}H_7N_3$ requires M 169.0634).

Crystal data and structure refinement:

Empirical formula	**C10 H7 N3**
Formula weight	169.19
Wavelength	1.54178 A
Temperature	100 K
Crystal system	Monoclinic
Space group	P21/c
Unit cell dimensions	a = 9.9732(3) A alpha = 90 deg. b = 23.0821(7) A beta = 103.426(4) deg.

	c = 7.3106(3) A gamma = 90 deg.
Volume	1636.92(10) A^{-3}
Number of reflections for cell	4305 (2 < theta < 74 deg.)
Z	8
Density (calculated)	1.373 Mg/m^{-3}
Absorption coefficient	0.695 mm^{-1}
F(000)	704
Crystal description	colourless block
Crystal size	0.120 x 0.075 x 0.026 mm

Table 10: crystal data and structure refinement of compound 211.

Atomic coordinates (x 10^4) and equivalent isotropic displacement parameters (A^2 x 10^3). U(eq) is defined as one third of the trace of the orthogonalized U_{ij} tensor:

	x	y	z	U (eq)
N(11)	4602(2)	7571(1)	7166(3)	40
C(21)	5066(2)	7162(1)	7944(3)	31
C(31)	5691(2)	6656(1)	9014(3)	32
C(41)	5130(2)	6081(1)	8595(2)	27
N(51)	5959(2)	5636(1)	8166(3)	28
C(61)	5442(2)	5110(1)	7902(2)	27
C(71)	6272(2)	4609(1)	8286(3)	30
C(81)	5750(2)	4086(1)	7581(3)	33
C(91)	4392(2)	4039(1)	6458(3)	34
C(101)	3573(2)	4518(1)	6036(3)	32
C(111)	4084(2)	5064(1)	6777(2)	28
C(121)	3314(2)	5582(1)	6431(3)	30
N(131)	3814(2)	6086(1)	7117(2)	29
N(12)	10404(2)	10150(1)	7809(3)	46
C(22)	9842(2)	9736(1)	7240(3)	32

C(32)	9066(2)	9227(1)	6413(3)	35
C(42)	9689(2)	8652(1)	7166(3)	28
N(52)	8896(2)	8199(1)	6629(2)	29
C(62)	9467(2)	7670(1)	7152(3)	27
C(72)	8696(2)	7160(1)	6568(3)	32
C(82)	9294(2)	6630(1)	7031(3	33
C(92)	10669(2)	6581(1)	8090(3)	33
C(102)	11428(2)	7067(1)	8709(3)	30
C(112)	10833(2)	7621(1)	8239(2)	26
C(122)	11537(2)	8146(1)	8777(3)	29
N(132)	10999(2)	8658(1)	8245(2)	30

2.42. (4-Methyl-quinazolin-2-yl)-acetonitrile 212

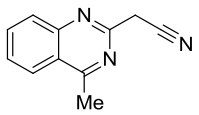

FVP of compound **190** (0.069 g, T_f 950 ˚C, T_i 88 °C, P 8.5 × 10^{-2} Torr, t 30 min) gave an orange oil that was purified by dry flash chromatography using [hexane : ethyl acetate (90 : 10)] as eluent to give a colourless solid (0.048 g, 50%); mp 104-106 °C; δ_H (400 MHz, $CDCl_3$): 8.12 (1H, dd, J 8.3, 0.7), 8.03 (1H, d, J 8.4), 7.92 (1H, ddd, J 8.4, 6.9, 1.4), 7.68 (1H, ddd, J 8.2, 6.9, 1.2), 4.20 (2H, s) and 2.97 (3H, s); δ_C (100 MHz, $CDCl_3$): 169.8 (quat), 156.3 (quat), 149.9 (quat), 134.3 (CH), 128.8 (CH), 128 (CH), 125.1 (CH), 123.0 (quat), 116.4 (quat), 28.8 (CH_2) and 21.7 (CH_3); *m/z* 183 ($[M]^+$, 100%), 168 (12), 143 (16) and 102 (10); (Found: $[M]^+$ 183.0792 $C_{11}H_9N_3$ requires M 183.0791).

2.43. 3-(2-formylphenyl)prop-2-enoate 250

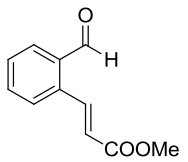

A mixture of methyl acrylate (3.10 cm^3, 34.8 mmol), $Pd(OAc)_2$ (0.15 g, 0.69 mmol), $n$$Bu_4NBr$ (0.56 g, 1.7 mmol) and K_2CO_3 (0.80 g, 5.8 mmol) was stirred for 5 min at room temperature under nitrogen. At the same time, a solution of 2-bromobenzaldehyde (1.28 g, 6.9 mmol) in DMF (4 cm^3) was degassed and then added to the stirring mixture. The

resulting mixture was then stirred for further 16 h at 70 °C. After cooling to room temperature, water was added (20 cm^3) and the solution extracted with ethyl acetate (2 × 15 cm^3). The combined organic fractions were dried over $MgSO_4$, filtered and solvent removed under reduced pressure. The resulting oil was purified by dry flash chromatography using [hexane : ethyl acetate (80 : 20)] as eluent to give a yellow solid (1.09 g, 83%); δ_H (360 MHz, $CDCl_3$): 10.27 (1H, s), 8.52 (1H, d, *J* 15.9), 7.91-7.81 (1H, m), 7.68-7.43 (3H, m), 6.37 (1H, d, *J* 15.9) and 3.82 (3H, s); δ_C (90 MHz, $CDCl_3$): 191.8 (CH), 166.6 (quat), 141.2 (CH), 136.3 (quat), 133.8 (CH), 133.6 (quat), 132.4 (CH), 129.8 (CH), 127.8 (CH), 122.5 (CH) and 51.8 (CH_3). Spectra are in agreement with the literature values.[110]

3-{2-[(methoxyimino)methyl]phenyl}prop-2-enoate 243 and {2-[(methoxyimino)-methyl]phenyl}but-3-enoate] 251

A solution of **250** (0.41 g, 2.16 mmol) and *O*-methylhydroxylamine hydrochloride (0.24 g, 2.5 mmol) in EtOH (30 cm^3) was heated at reflux for 5 h. The reaction mixture was allowed to cool to room temperature, the EtOH was removed under reduced pressure, water (30 cm^3) was added and the mixture was extracted with DCM (2 × 30 cm^3). After the organic fractions were combined and dried over $MgSO_4$, the solvent was removed under reduced pressure and the crude residue purified by dry flash chromatography using [hexane : ethyl acetate (80 : 20)] as eluent to give two products identified as 3-{2-[(methoxyimino)methyl]phenyl}prop-2-enoate **243** as a colourless oil (0.13 g, 27%) and {2-[(methoxyimino)-methyl]phenyl}but-3-enoate] **251** as a colourless oil (0.48 g, 30 %).

2.44. 3-{2-[(methoxyimino)methyl]phenyl}prop-2-enoate 243

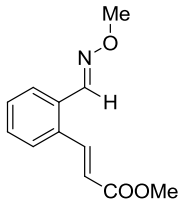

Bp 115-117 °C at 1 Torr. δ_H (360 MHz, $CDCl_3$): 8.30 (1H, s,), 8.01 (1H, d, *J* 15.8), 7.65-7.56 (1H, m), 7.47-7.39 (1H, m), 7.33-7.21 (2H, m), 6.23 (1H, d, *J* 15.8), 3.90 (3H, s) and 3.70 (3H, s); δ_C (90 MHz, $CDCl_3$): 166.7 (quat), 146.2 (CH), 141.6 (CH), 133.2 (quat), 130.7

(quat), 129.7 (CH), 129.5 (CH), 127.6 (CH), 127.1 (CH), 120.5 (CH), 62.0 (CH_3) and 51.6 (CH_3); *m/z* 219 ($[M]^+$, 1%), 188 (5), 160 (100) and 129 (34); (Found: $[M]^+$ 219.0889 $C_{14}H_{10}O_3N_2$ requires *M* 219.0890);

2.45. {2-[(methoxyimino)methyl]phenyl}but-3-enoate] 251

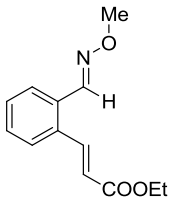

Bp 103-105 °C; δ_H (500 MHz, $CDCl_3$): 8.40 (1H, s), 8.11 (1H, d, *J* 15.8), 7.74-7.68 (1H, m), 7.58-7.51 (1H, m), 7.41-7.34 (2H, m), 6.32 (1H, d, *J* 15.8), 4.26 (2H, q, *J* 7.1), 4.00 (3H, s) and 1.33 (3H, t, *J* 7.1); δ_C (125 MHz, $CDCl_3$): 166.4 (quat), 146.45 (CH), 141.5 (CH), 133.5 (quat), 130.8 (quat), 129.7 (CH), 129.6 (CH), 127.8 (CH), 127.2 (CH), 121.2 (CH), 62.1 (CH_2), 60.5 (CH_3) , 14.2 (CH_3); *m/z* 233 ($[M]^+$, 2%), 188 (11), 160 (100), 129 (54) and 84 (4); . (Found: $[M]^+$ 233.1046 $C_{14}H_{10}O_3N_2$ requires *M* 233.1046).

2.46. Methyl 3-(5-Fluoro-2-formylphenyl)prop-2-enoate 254

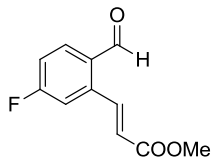

To a solution of 2-bromo-4-fluoro-benzaldehyde (0.5 g, 2.46 mmol) in toluene (5 cm^3) were added tri*o*-tolylphosphine (0.03 g, 0.1 mmol), methylacrylate (0.340 cm^3, 3.70 mmol), triethylamine (1 cm^3, 7.2 mmol) and $Pd(dba)_2$ (11 mg, 0.02 mmol). The mixture was heated at 120 °C for 5 days. After cooling to room temperature, the reaction mixture was diluted with water (100 cm^3) and extracted with DCM (2 × 70 cm^3). The combined organic layers were dried over $MgSO_4$ and filtered through a pad of celite. After evaporating the solvent, a brown solid was obtained that was then recrystalised from hexane to afford a pale yellow solid (0.17 g, 33%); mp 90-92 °C; δ_H (500 MHz, $CDCl_3$): 10.22 (1H, s), 8.49 (1H, d, *J* 15.9), 7.91 (1H, dd, *J* 8.6, 5.8), 7.30 (1H, dd, *J* 9.4, 2.4), 7.25-7.20 (1H, m), 6.37 (1H, d, *J* 15.9) and 3.83 (3H, s); δ_C (125 MHz, $CDCl_3$): 190 (CH), 166.2 (quat), 165.6 (quat, d, *J* 257.3), 139.8 (CH, d, *J* 1.9), 139.4 (quat, d, *J* 9.0), 135 (CH, d, *J* 10), 130.3 (quat, d, *J* 2.9), 123.8 (CH), 117.0 (CH, d, *J* 22.1), 114.8 (CH, d, *J* 23.0) and 52.0 (CH_3); *m/z* 208 ($[M]^+$, 9%), 149 (100), 136 (12) and 101 (11); (Found: $[M]^+$ 208.0530 $C_{11}H_9O_3F$ requires *M* 208.0530)

2.47. 3-{5-fluoro-2-[(methoxyimino)methyl]phenyl}prop-2-enoate 248

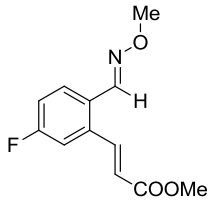

A solution of compound **254** (0.054 g, 0.26 mmol) and *O*-methylhydroxylamine hydrochloride (0.042 g, 0.5 mmol) in MeOH (7 cm^3) was heated to reflux for 5 h. After cooling to room temperature, solvent was evaporated and a colourless solid was obtained (0.047 g, 81%) mp 60-61 °C. NMR showed that the crude product was sufficiently pure to be taken on without any further purification; δ_H (400 MHz, $CDCl_3$): 8.34 (1H, s), 8.05 (1H, dd, *J* 15.8, 1.0), 7.72 (1H, dd, *J* 8.7, 5.8), 7.22 (1H, dd, *J* 9.6, 2.6), 7.08 (1H, td, *J* 8.3, 2.6), 6.32 (1H, d, *J* 15.8), 3.99 (3H, s) and 3.81 (3H, s); δ_C (100 MHz, $CDCl_3$): 166.5 (quat), 163.2 (quat, d, *J* 250.7), 145.4 (CH), 140.4 (CH, d, *J* 2.2), 135.5 (quat, d, *J* 7.9), 129.9 (CH, d, *J* 8.5), 127.2 (quat, d, *J* 3.2), 121.8 (CH), 117.1 (CH, d, *J* 22.0), 113.6 (CH, d, *J* 22.7), 62.2 (CH_3) and 51.8 (CH_3); *m/z* 237 ($[M]^+$, 3%), 206 (6), 178 (100) and 147 (20); (Found: $[M]^+$ 237.0795 $C_{12}H_{12}O_3NF$ requires *M* 237.0795)

2.48. 6-fluoroisoquinoline 245

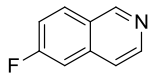

FVP of compound **248** (0.048 g, T_f 700 ˚C, T_i 57 °C, *P* 1.9→2.8 × 10^{-2} Torr, *t* 20 min) gave an orange oil that was purified by dry flash chromatography using [hexane : ethyl acetate (80 : 20)] as eluent, yielding a colourless solid (0.022 g, 75 %); mp 45-46 °C; δ_H (500 MHz, $CDCl_3$): 9.25 (1H, s), 8.55 (1H, d, *J* 5.8), 8.01 (1H, dd, *J* 9.0, 5.5), 7.64 (1H, d, *J* 5.8), 7.45 (1H, dd, *J* 9.3, 2.4), 7.39 (1H, td, *J* 8.8, 2.5); δ_C (125 MHz, $CDCl_3$): 163.08 (quat, d, *J* 252.6), 152.0 (CH, d, *J* 0.8 Hz), 143.7 (CH, s), 137.1 (quat, d, *J* 10.5), 130.6 (CH, d, *J* 9.8), 125.8 (quat, s), 119.9 (CH, d, *J* 5.3), 117.8 (CH, d, *J* 25.6) and 109.7 (CH, d, *J* 21.0); *m/z* 147 ($[M]^+$, 100%), 120 (31), 99 (6), 94 (6) and 74 (7); (Found: M^+ 147.0476 C_9H_6NF requires *M* 147.0479).

2.49. Methyl 3-(4-fluoro-2-formylphenyl)prop-2-enoate 250

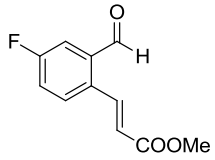

To a solution of 2-bromo-5-fluoro-benzaldehyde (0.5 g, 2.46 mmol) in toluene (5 cm^3) were added tri*o*-tolylphosphine (0.03 g,

0.1 mmol), methylacrylate (0.34 cm^3, 3.70 mmol), triethylamine (1 cm^3, 7.2 mmol) and $Pd(dba)_2$ (0.011 g, 0.02 mmol). The mixture was heated at 125 °C for 4 days. After cooling the reaction mixture was diluted with water (100 cm^3) and extracted with DCM (2 × 70 cm^3). The combined organic extracts were dried over $MgSO_4$ and filtered through a pad of celite. After evaporating the solvent, an orange solid was obtained that was then recrystalised from cyclohexane to afford a colourless solid (0.34 g, 71%) mp 139-141 °C. δ_H (500 MHz, $CDCl_3$) 10.29 (1H, d, *J* 1.5), 8.43 (1H, d, *J* 15.9), 7.65 (1H, dd, *J* 8.6, 5.1), 7.58 (1H, dd, *J* 8.5, 2.7), 7.33 (1H, td, *J* 8.2, 2.8), 6.35 (1H, d, *J* 15.9) and 3.83 (3H, s). Spectrum is in agreement with the literature.[111]

2.50. 3-{4-fluoro-2-[(methoxyimino)methyl]phenyl}prop-2-enoate 247

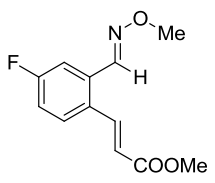

A solution of compound **250** (0.1 g, 5.2 mmol) and *O*-methylhydroxylamine hydrochloride (0.047 g, 5.6 mmol) in MeOH (20 cm^{-3}) was heated at reflux for 3 h. After cooling down, the solvent was removed under reduced pressure and the crude product was purified by dry flash chromatography using [hexane : ethyl acetate (90 : 10)] as eluent to give a colourless solid (0.86 g, 70%); mp 68-70 °C δ_H (500 MHz, $CDCl_3$); 8.40 (1H, s), 8.02 (1H, d, *J* 15.8), 7.56 (1H, dd, *J* 8.7, 5.6), 7.50 (1H, dd, *J* 9.6, 2.7), 7.10 (1H, td, *J* 8.3, 2.7), 6.30 (1H, d, *J* 15.8), 4.03 (3H, s) and 3.83 (3H, s); δ_C (125 MHz, $CDCl_3$): 166.7 (quat), 162.8 (quat, d, *J* 251.1), 142.8 (CH, d, *J* 1.6), 140.7 (CH), 132.1 (quat, d, *J* 8.7), 129.4 (quat, d, *J* 3.5), 128.8 (CH, d, *J* 8.6), 120.4 (CH, d, *J* 1.9), 116.9 (CH, d, *J* 11.3), 116.8 (CH, d, *J* 12.7), 62.5 (CH_3) and 51.7 (CH_3, *J* 19.5); *m/z* 237 ($[M]^+$, 1%), 178 (100), 147 (63) and 120 (7); (Found: $[M]^+$ 237.08065 $C_{12}H_{12}O_3NF$ requires *M* 237.08067).

2.51. 7-fluoroisoquinoline

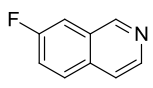

FVP of compound **247** (0.05 g, T_f 700 ˚C, T_i 68 °C, *P* 2.9→5.5 × 10^{-2} Torr, *t* 20 min) gave an orange oil that was purified by dry flash chromatography using [hexane : ethyl acetate (80 : 20)] as eluent to give a colourless solid (0.040 g, 79 %) mp 46-47 °C; δ_H (500 MHz, $CDCl_3$): 9.21 (1H, s), 8.51 (1H, d, *J* 5.7), 7.83 (1H, dd, *J* 9.0, 5.2), 7.64 (1H, d, *J* 5.7), 7.57 (1H, dd, *J* 8.8, 2.4) and 7.47

(1H, td, *J* 8.8, 2.5); δ_C ^{13}C NMR (126 MHz, $CDCl_3$) δ_C (125 MHz, $CDCl_3$): 160.9 (quat, d, *J* 249.5), 151.7 (CH, d, *J* 5.5), 142.5 (CH, d, *J* 2.8), 132.8 (quat), 129.28 (quat, d, *J* 8.1), 129.24 (CH, d, *J* 8.5), 121.1 (CH, d, *J* 25.6), 120.3 (CH) and 110.7 (CH, d, *J* 20.6); *m/z* 147 ($[M]^+$, 100%), 120 (26) and 69 (10); (Found: $[M]^+$ 147.0479 C_9H_6NF requires *M* 147.0479)

3. DFT calculations of energy surfaces

3.1

This section contains the Cartesian coordinates and energies for the energy surface shown in chapter 2 Figure 6. All the structures and energies were calculated at B3LYP/cc-pVDZ level, using Gaussian 03 and energies are quoted both in Hartrees (Ha) and kJ mol^{-1}. The values of calculated negative frequencies are reported (cm^{-1}) for transition state structures.

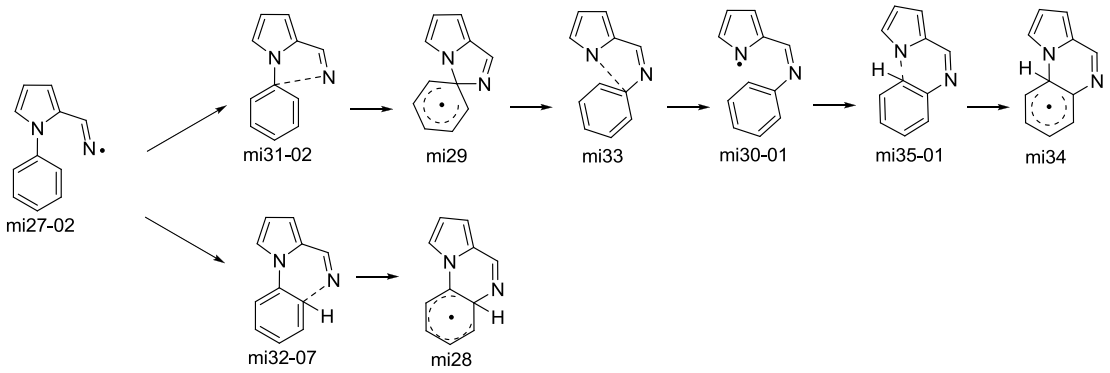

Scheme 154

Mi 27-02

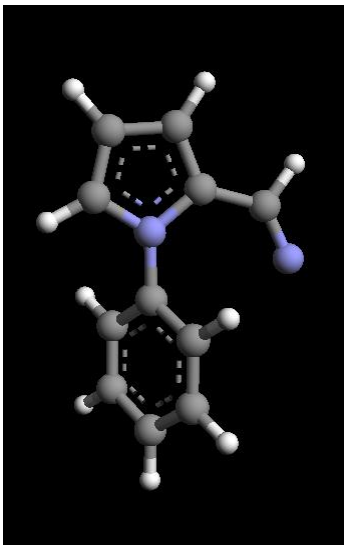

Energy = -534.049795 Ha = -1402155.748 kJ mol^{-1}

C	-3.041371	-0.098898	0.017981
C	-1.798626	0.516948	-0.101642
N	-0.824730	-0.456447	0.108077
C	-1.454297	-1.657409	0.351084
C	-2.823808	-1.468448	0.306345
C	-1.555645	1.912875	-0.449369
C	1.237008	0.605989	0.922772
C	2.628621	0.713203	0.895519
C	3.384003	-0.091995	0.037568
C	0.597369	-0.304639	0.073369
C	1.348210	-1.109017	-0.792774
C	2.741198	-1.004674	-0.803380
N	-0.467255	2.542078	-0.577728
H	-3.997836	0.405034	-0.103670
H	-0.865528	-2.544983	0.564929
H	-3.576884	-2.234936	0.470313
H	-2.494089	2.482683	-0.623993
H	0.645838	1.222527	1.599479
H	3.124433	1.427805	1.555599

H	4.472598	-0.006488	0.023278
H	0.835689	-1.802085	-1.462286
H	3.323703	-1.632576	-1.480926

mi31-02

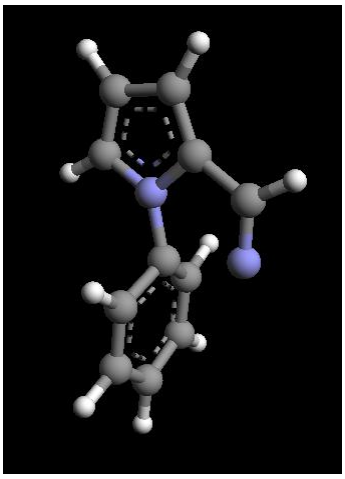

Energy = -534.0185255 Ha = -1402073.649 kJ mol^{-1}

Calculated Negative Frequency = -586.6398 cm^{-1}

C	-3.123748	0.108241	0.000721
C	-1.852220	0.665420	-0.001048
N	-0.926150	-0.354882	-0.001769
C	-1.573990	-1.561884	-0.000418
C	-2.940701	-1.303851	0.000855
C	-1.143705	1.930683	-0.000201
C	1.201830	-0.181473	1.234362
C	2.578529	-0.285502	1.220211
C	3.285336	-0.313530	0.001086
C	0.472952	0.016423	-0.000762
C	1.203402	-0.181790	-1.234886
C	2.580069	-0.285847	-1.218969
N	0.135402	1.911171	0.000128
H	-4.067437	0.647879	0.001437
H	-1.024939	-2.499258	-0.000733
H	-3.723364	-2.059262	0.001781
H	-1.677148	2.894766	0.000744

H	0.638916	-0.183402	2.169073
H	3.122484	-0.374880	2.163434
H	4.373316	-0.402248	0.001767
H	0.641586	-0.183850	-2.170263
H	3.125298	-0.375119	-2.161466

mi29

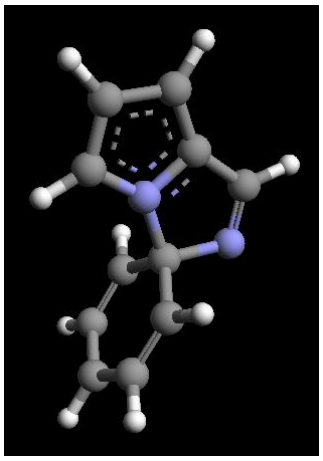

Energy = -534.0339942 Ha = -1402114.263 kJ mol^{-1}

C	-3.093562	-0.160440	0.000084
C	-1.912580	0.574629	-0.000265
N	-0.853460	-0.306091	-0.000984
C	-1.310808	-1.591039	-0.001181
C	-2.705023	-1.529678	-0.000581
C	-1.298663	1.886410	0.001112
C	1.219619	0.152598	1.258521
C	2.497840	-0.330833	1.228591
C	3.165334	-0.581955	0.000006
C	0.439742	0.442051	0.000207
C	1.220493	0.155141	-1.258327
C	2.498662	-0.328383	-1.228530
N	-0.003824	1.868341	0.001276
H	-4.106755	0.233508	-0.000021
H	-0.637061	-2.443267	-0.001801

H	-3.370015	-2.391059	-0.000258
H	-1.843777	2.834995	0.001857
H	0.703503	0.356114	2.198617
H	3.018221	-0.527247	2.169504
H	4.185790	-0.968163	-0.000013
H	0.705061	0.361162	-2.198247
H	3.019689	-0.522807	-2.169500

mi33

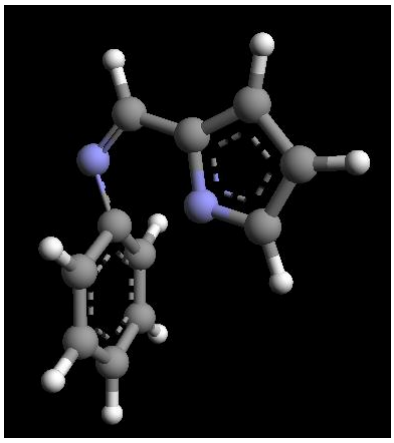

Energy = -534.0172811 Ha = -1402070.382 kJ mol^{-1}

Calculated Negative Frequency = -289.7431 cm^{-1}

C	3.095544	-0.149778	0.032477
C	1.851619	0.504613	-0.007693
N	0.859734	-0.433898	-0.114958
C	1.408297	-1.664957	-0.113207
C	2.810847	-1.529321	-0.030942
C	1.322842	1.833420	0.056510
C	-1.434649	0.463876	-1.222035
C	-2.522047	-0.379184	-1.188237
C	-2.998485	-0.892030	0.039860
C	-0.709648	0.790751	0.001045
C	-1.286253	0.317151	1.255461
C	-2.379235	-0.521580	1.253274
N	0.032166	1.973188	0.028281
H	4.074071	0.321186	0.105909

H	0.805170	-2.567335	-0.195924
H	3.528902	-2.348418	-0.038203
H	1.955760	2.724855	0.112874
H	-1.067369	0.897235	-2.152803
H	-3.035463	-0.638997	-2.116656
H	-3.867408	-1.552929	0.052181
H	-0.808468	0.641119	2.180554
H	-2.781488	-0.889516	2.199725

mi30-01

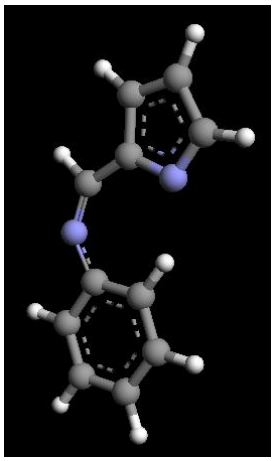

Energy = -534.0465458 Ha = -1402147.217 kJ mol^{-1}

C	3.390535	-0.766795	-0.000228
C	1.962627	-0.438826	-0.000178
N	1.788536	0.934910	0.000568
C	3.008870	1.444683	0.000863
C	4.054308	0.424395	0.000422
C	-1.332129	-0.607345	-0.000205
C	-2.640224	-1.168709	0.000715
C	-3.772804	-0.365143	0.000897
C	-1.209316	0.808512	-0.001019
C	-2.352770	1.602481	-0.000890
C	-3.632578	1.029703	0.000071
C	0.979562	-1.468742	-0.000671

N	-0.336112	-1.562987	-0.000395
H	3.808012	-1.772154	-0.000705
H	3.163460	2.526628	0.001413
H	5.128506	0.600659	0.000589
H	-2.711683	-2.257575	0.001259
H	-4.766454	-0.818317	0.001639
H	-0.214245	1.254468	-0.001552
H	-2.247310	2.690061	-0.001515
H	-4.518371	1.669439	0.000168
H	1.454629	-2.461952	-0.001167

mi35-01

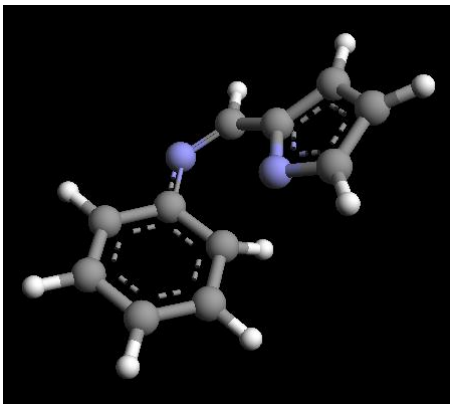

Energy = -534.0274203 Ha = -1402097.002 kJ mol^{-1}

Calculated Negative Frequency = -318.7850 cm^{-1}

C	-3.092837	0.325229	-0.171449
C	-1.712262	0.601515	-0.019988
N	-1.008065	-0.584377	-0.142644
C	-1.887028	-1.585495	-0.273030
C	-3.205557	-1.061192	-0.326070
C	1.101996	0.930347	0.199588
C	2.313239	1.027315	-0.514940
C	3.136343	-0.079205	-0.669526
C	0.745762	-0.338404	0.817131
C	1.644969	-1.442307	0.683706
C	2.794237	-1.318513	-0.068946

C	-1.037050	1.827416	0.243363
N	0.262764	2.012776	0.248377
H	-3.896317	1.059870	-0.168179
H	-1.561268	-2.620477	-0.374192
H	-4.113003	-1.634425	-0.508815
H	2.556794	1.988939	-0.969878
H	4.056055	0.002866	-1.252230
H	0.131932	-0.292222	1.718884
H	1.416584	-2.376066	1.201399
H	3.472876	-2.168878	-0.169235
H	-1.657430	2.721369	0.383089

mi34

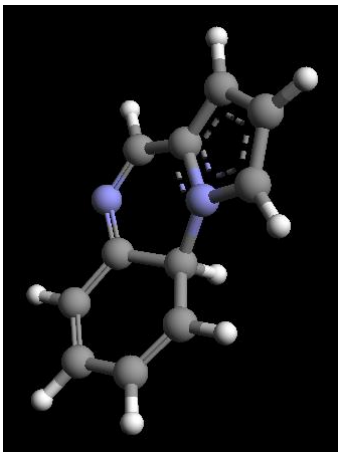

Energy = -534.0568049 Ha = -1402174.152 kJ mol^{-1}

C	-3.012740	0.308616	-0.234305
C	-1.683373	0.685839	-0.006164
N	-0.929725	-0.471882	0.103537
C	-1.750814	-1.557455	-0.017505
C	-3.048602	-1.103123	-0.245363
C	-1.011227	1.945320	0.070189
C	1.058935	0.947424	0.124832
C	2.423941	1.021641	-0.182699
C	3.209399	-0.119395	-0.308536

C	0.468052	-0.389608	0.566442
C	1.316028	-1.574749	0.191784
C	2.618470	-1.419160	-0.164084
N	0.299376	2.076976	0.076565
H	-3.842588	0.991767	-0.399937
H	-1.372167	-2.571918	0.057813
H	-3.915890	-1.736456	-0.415491
H	2.830025	2.015172	-0.383795
H	4.262748	-0.033605	-0.579945
H	0.888195	-2.571990	0.311315
H	3.230849	-2.303241	-0.359238
H	0.414560	-0.358350	1.683686
H	-1.611708	2.860859	0.057317

mi32-07

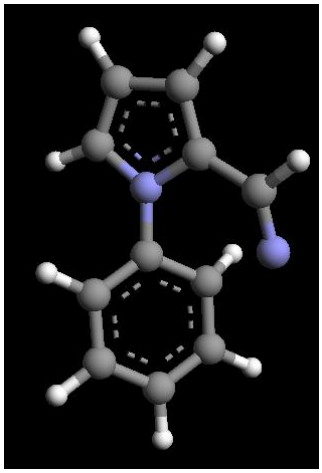

Energy = -534.0267681 Ha = -1402095.290 kJ mol^{-1}

Calculated Negative Frequency = -552.9239 cm^{-1}

C	3.010825	0.314594	-0.151556
C	1.665107	0.662901	-0.136472
N	0.937338	-0.476961	0.189577
C	1.804066	-1.529139	0.365073
C	3.096322	-1.065081	0.175089
C	0.968373	1.889474	-0.498931
C	-0.476313	-0.463210	0.165578

C	-1.219186	-1.455559	-0.464243
C	-2.612362	-1.329120	-0.549678
C	-1.086635	0.728305	0.684168
C	-2.517572	0.810063	0.594333
C	-3.249829	-0.184564	-0.026951
N	-0.264156	2.177273	-0.334730
H	3.834159	0.988376	-0.377957
H	1.433188	-2.512206	0.641286
H	4.001527	-1.659733	0.269723
H	1.594658	2.657410	-0.993015
H	-0.710705	-2.313844	-0.907738
H	-3.198156	-2.109394	-1.038696
H	-0.611415	1.189758	1.554919
H	-3.015888	1.680201	1.025339
H	-4.336421	-0.094730	-0.096253

mi28

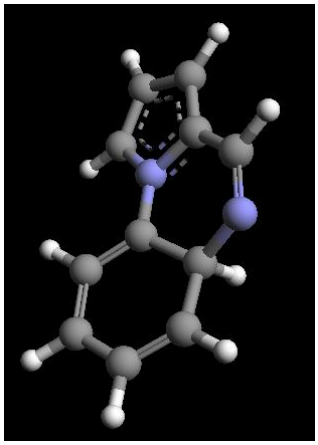

Energy = -534.0494495 Ha = -1402154.840 kJ mol^{-1}

C	3.020963	0.362746	-0.142791
C	1.672684	0.691471	-0.086292
N	0.954726	-0.486981	0.121935
C	1.837200	-1.542163	0.186362
C	3.121116	-1.043190	0.038725

C	0.931069	1.918256	-0.283726
C	-0.445266	-0.469230	0.111625
C	-1.035956	0.880460	0.458853
C	-2.506874	0.945942	0.158304
C	-1.226247	-1.570765	-0.160910
C	-2.630057	-1.450749	-0.234761
C	-3.243292	-0.170297	-0.115863
N	-0.330831	2.062405	-0.085748
H	3.836868	1.065713	-0.293471
H	1.489274	-2.555673	0.359619
H	4.033291	-1.634051	0.069674
H	1.494710	2.791567	-0.640190
H	-0.922010	0.997640	1.569331
H	-2.958869	1.938150	0.211346
H	-0.757214	-2.535102	-0.367519
H	-3.235091	-2.330023	-0.459799
H	-4.320263	-0.081062	-0.279463

3.2

This section contains the Cartesian coordinates and energies for the energy surface shown in chapter 2 Figure 7. All the structures and energies were calculated at B3LYP/cc-pVDZ level, using Gaussian 03 and energies are quoted both in Hartrees (Ha) and kJ mol^{-1}. The values of calculated negative frequencies are reported (cm^{-1}) for transition state structures.

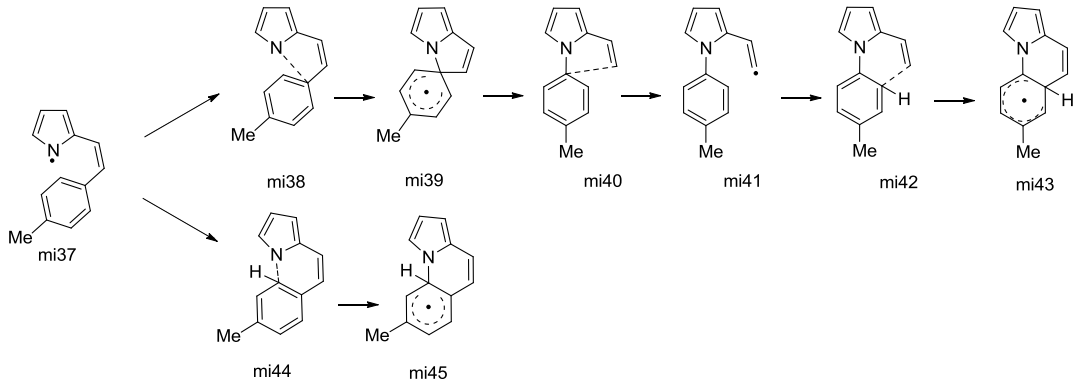

Scheme 155

mi37

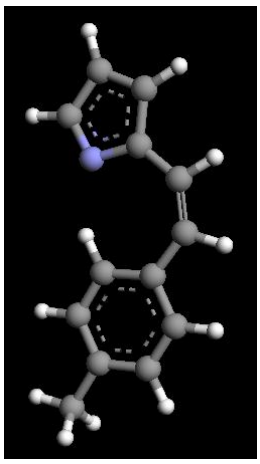

Energy = -557.3385771 Ha = -1463300.794 kJ mol^{-1}

C	3.971925	0.453164	0.000349
C	2.513530	0.363405	-0.000010
N	2.119050	-0.967791	0.000268
C	3.240614	-1.668171	0.000006
C	4.434319	-0.832510	0.000170
C	-0.874761	0.895467	-0.000093
C	-2.127978	1.565715	-0.000115
C	-3.326192	0.866772	-0.000122
C	-0.893752	-0.520237	-0.000082
C	-2.104251	-1.208481	-0.000099
C	-3.340306	-0.541193	-0.000113
C	1.684203	1.503833	-0.000062
C	0.308740	1.728285	-0.000088
C	-4.644952	-1.295808	-0.000064
H	4.548418	1.377060	0.000541
H	3.218393	-2.760870	0.000027
H	5.466363	-1.179431	0.000227
H	-2.143885	2.659030	-0.000129
H	-4.271764	1.416031	-0.000144
H	0.056050	-1.057638	-0.000108

H	-2.090528	-2.301890	-0.000115
H	2.264816	2.432748	-0.000029
H	0.059853	2.795568	-0.000103
H	-4.484037	-2.383592	-0.000701
H	-5.252256	-1.041471	-0.885503
H	-5.251600	-1.042445	0.886112

mi38

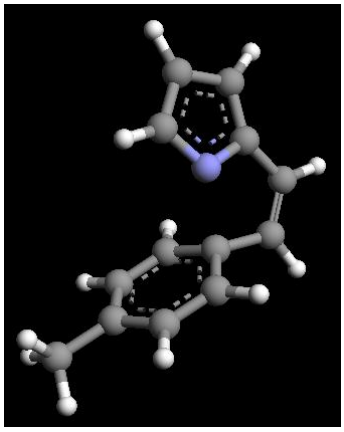

Energy = -557.2825262 Ha = -1463153.632 kJ mol^{-1}

Calculated Negative Frequency = -448.8027 cm^{-1}

C	3.355660	-0.691058	0.167686
C	2.358208	0.269286	-0.010235
N	1.211791	-0.355979	-0.485523
C	1.412671	-1.691288	-0.484250
C	2.750135	-1.941006	-0.123497
C	2.148341	1.665632	0.261209
C	-1.107408	1.044235	-1.109915
C	-2.323955	0.403611	-1.062679
C	-2.755075	-0.296052	0.095921
C	-0.170018	0.964277	-0.004819
C	-0.674159	0.331494	1.198996
C	-1.906681	-0.294323	1.223361
C	0.851069	2.045510	0.173105
C	-4.083030	-1.002329	0.110907
H	4.376083	-0.515469	0.502615

H	0.660142	-2.387545	-0.850423
H	3.244734	-2.911485	-0.161698
H	2.968534	2.354963	0.468754
H	-0.804076	1.596708	-2.001281
H	-2.990244	0.452555	-1.928843
H	-0.035682	0.342043	2.083756
H	-2.239695	-0.785482	2.141583
H	0.511490	3.082106	0.213335
H	-4.880886	-0.368658	-0.311123
H	-4.377085	-1.294678	1.129677
H	-4.050402	-1.921136	-0.502419

mi39

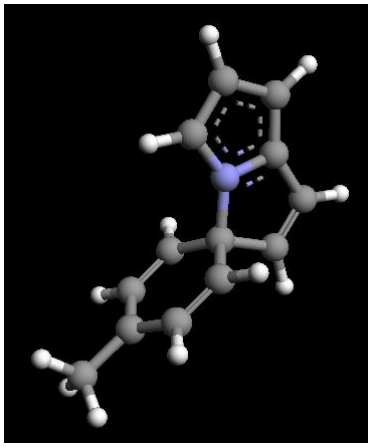

Energy =-557.3066668 Ha = -1467973.280 kJ mol^{-1}

C	3.483010	-0.416578	-0.000064
C	2.395625	0.445722	0.000009
N	1.242886	-0.316255	0.000128
C	1.559039	-1.649554	0.000144
C	2.946163	-1.740386	0.000033
C	1.988872	1.839889	-0.000104
C	-0.806854	0.274047	-1.252264
C	-2.137314	-0.036665	-1.220485

C	-2.858721	-0.193746	0.000007
C	0.004730	0.505734	0.000020
C	-0.806928	0.274282	1.252296
C	-2.137401	-0.036437	1.220495
C	0.639858	1.912277	-0.000100
C	-4.311177	-0.577248	-0.000058
H	4.533608	-0.136768	-0.000160
H	0.794025	-2.420687	0.000254
H	3.514229	-2.668352	0.000037
H	2.676267	2.685474	-0.000181
H	-0.273605	0.382753	-2.199038
H	-2.670036	-0.179117	-2.165726
H	-0.273741	0.383166	2.199085
H	-2.670179	-0.178709	2.165731
H	0.018371	2.805689	-0.000154
H	-4.438479	-1.677074	-0.001102
H	-4.832213	-0.194465	-0.891901
H	-4.831863	-0.196137	0.892689

mi40

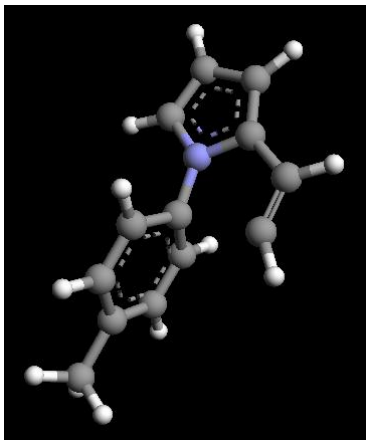

Energy = -557.2704077 Ha = -1463121.814 kJ mol^{-1}

Calculated Negative Frequency = -449.1627 cm^{-1}

C	3.540535	-0.013799	-0.000046
C	2.302708	0.611522	-0.000001
N	1.326172	-0.369652	-0.000002
C	1.926297	-1.610655	-0.000046
C	3.297719	-1.419267	-0.000076
C	1.776755	1.964779	0.000064
C	-0.809122	-0.173533	-1.221496
C	-2.195501	-0.200168	-1.208144
C	-2.922829	-0.190729	0.000035
C	-0.079694	-0.051055	0.000035
C	-0.809100	-0.173739	1.221527
C	-2.195513	-0.200347	1.208175
C	0.451746	2.074149	0.000107
C	-4.430211	-0.185936	-0.000065
H	4.506687	0.485178	-0.000053
H	1.329790	-2.518523	-0.000057
H	4.045057	-2.209515	-0.000113
H	2.468663	2.817303	0.000080
H	-0.253467	-0.208585	-2.159892
H	-2.736890	-0.255451	-2.156607
H	-0.253452	-0.208955	2.159920
H	-2.736901	-0.255761	2.156627
H	-0.275884	2.883495	0.000161
H	-4.825606	0.846151	-0.003296
H	-4.837018	-0.684849	0.893306
H	-4.836915	-0.690257	-0.890475

mi41

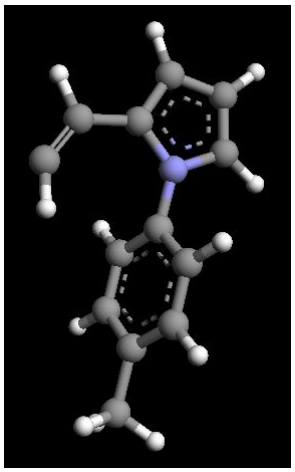

Energy = -557.2819893 Ha = -1463152.222 kJ mol^{-1}

C	-3.472610	-0.042161	0.081226
C	-2.221364	0.554226	-0.048936
N	-1.272326	-0.461539	0.039960
C	-1.922221	-1.667958	0.218778
C	-3.283784	-1.438908	0.248350
C	-1.956456	1.967316	-0.311244
C	0.804900	0.293012	1.108942
C	2.197355	0.393744	1.109104
C	2.967157	-0.131833	0.059530
C	0.151016	-0.330426	0.040382
C	0.901810	-0.863914	-1.013534
C	2.294243	-0.767650	-0.996064
C	-0.832841	2.604301	-0.607465
C	4.471632	-0.003972	0.052149
H	-4.419250	0.491982	0.033834
H	-1.346724	-2.581427	0.339862
H	-4.053041	-2.196182	0.378533
H	-2.876916	2.569267	-0.267289
H	0.217403	0.695933	1.935322
H	2.696712	0.882728	1.949543

H	0.386576	-1.348098	-1.845151
H	2.869046	-1.191215	-1.823992
H	4.953310	-0.931937	-0.294476
H	4.862272	0.229935	1.053678
H	4.797782	0.803333	-0.626737
H	0.226087	2.411788	-0.760151

mi42

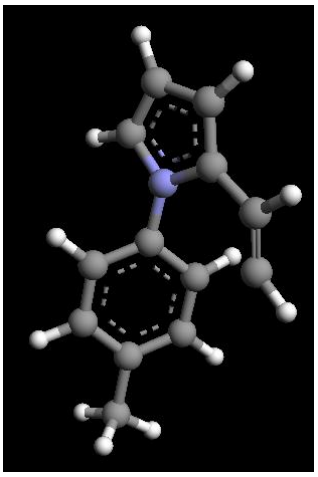

Energy = -557.2758494 Ha = -1463136.102 kJ mol^{-1}

Calculated Negative Frequency = -407.7119 cm^{-1}

C	3.456492	0.183482	-0.136936
C	2.140397	0.628418	-0.144210
N	1.333663	-0.461343	0.181544
C	2.130669	-1.571944	0.377365
C	3.449002	-1.199271	0.198914
C	1.582895	1.923136	-0.506648
C	-0.082666	-0.419296	0.159195
C	-0.827951	-1.347663	-0.564683
C	-2.221023	-1.232934	-0.626383
C	-0.728421	0.670226	0.802180
C	-2.142895	0.745989	0.744198
C	-2.896314	-0.176658	0.019110
C	0.308818	2.280455	-0.360538

C	-4.399994	-0.069353	-0.067155
H	4.325207	0.800585	-0.356056
H	1.687764	-2.522529	0.660719
H	4.312132	-1.851060	0.309843
H	2.305950	2.625815	-0.949606
H	-0.315588	-2.150724	-1.097819
H	-2.792645	-1.970915	-1.194771
H	-0.200951	1.196712	1.597951
H	-2.648462	1.546346	1.290278
H	-4.787209	0.722888	0.590339
H	-4.887731	-1.016387	0.216964
H	-4.722375	0.162787	-1.096803
H	-0.225786	3.198368	-0.608299

mi43

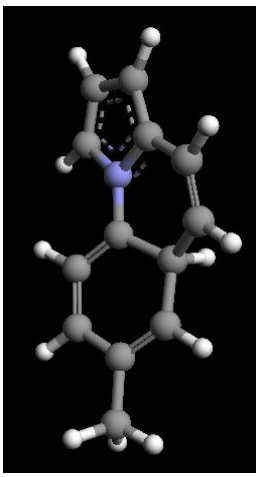

Energy = -557.3249804 Ha = -1463265.096 kJ mol^{-1}

C	3.456488	0.288210	-0.211272
C	2.129001	0.678301	-0.123412
N	1.366191	-0.468599	0.126386
C	2.211766	-1.563014	0.184318
C	3.505137	-1.122055	-0.010868
C	1.455872	1.946690	-0.291624
C	-0.034777	-0.438422	0.151138

C	-0.645275	0.894448	0.525738
C	-2.123543	0.947853	0.241160
C	-0.821451	-1.539663	-0.109481
C	-2.225361	-1.433124	-0.156583
C	-2.873801	-0.161747	-0.029655
C	0.142532	2.070641	-0.025862
C	-4.368312	-0.079399	-0.230180
H	4.296255	0.954526	-0.394005
H	1.827300	-2.556007	0.393165
H	4.393809	-1.748499	0.004916
H	2.049652	2.793345	-0.642791
H	-0.532562	0.975084	1.642236
H	-2.602265	1.927698	0.327194
H	-0.353807	-2.501055	-0.330672
H	-2.821543	-2.322091	-0.371939
H	-4.735464	0.952034	-0.125527
H	-4.900223	-0.705837	0.506283
H	-4.656857	-0.445515	-1.230114
H	-0.377288	3.024194	-0.143952

mi44

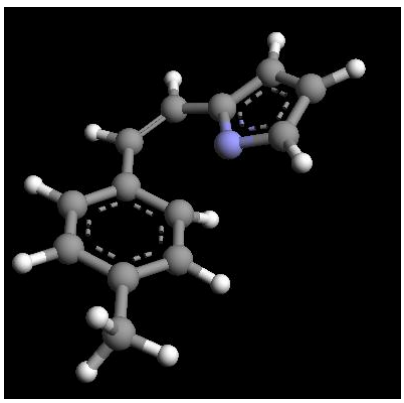

Energy = -557.303685 Ha = -1463209.185 kJ mol^{-1}

Calculated Negative Frequency = -384.7188 cm^{-1}

C	-3.498161	-0.232776	-0.156683
C	-2.219679	0.369463	-0.028958
N	-1.252793	-0.626373	-0.127706
C	-1.874679	-1.804745	-0.229914
C	-3.283345	-1.608371	-0.274915
C	0.573833	1.312919	0.198113
C	1.811709	1.653685	-0.392742
C	2.834278	0.729022	-0.508478
C	0.420114	-0.020700	0.758976
C	1.511745	-0.941574	0.644003
C	2.685253	-0.596070	0.002694
C	-1.859159	1.733535	0.138646
C	-0.553692	2.190860	0.163780
C	3.830401	-1.568781	-0.121677
H	-4.451790	0.292549	-0.160498
H	-1.316231	-2.736185	-0.324600
H	-4.030850	-2.383514	-0.436435
H	1.935200	2.659100	-0.804298
H	3.769375	1.008897	-0.999615
H	-0.189524	-0.092522	1.662677
H	1.415082	-1.925899	1.108694
H	-2.674938	2.461277	0.138920
H	4.750153	-1.163310	0.332883
H	4.060246	-1.767488	-1.182724
H	3.603562	-2.529958	0.361917
H	-0.372437	3.262865	0.039937

mi45

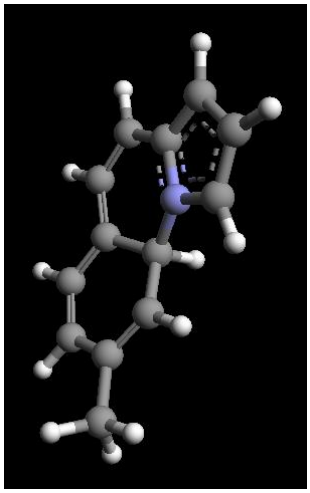

Energy = -557.3344448 Ha = -1463289.945 kJ mol^{-1}

C	-3.362922	-0.350878	-0.235863
C	-2.187768	0.388804	-0.055270
N	-1.144286	-0.515476	0.110554
C	-1.646981	-1.790231	0.068966
C	-3.016848	-1.719138	-0.159878
C	-1.911849	1.788598	-0.074258
C	0.477450	1.350033	0.120914
C	1.819982	1.729655	-0.056894
C	2.847318	0.801608	-0.096197
C	0.193635	-0.080748	0.557186
C	1.299731	-1.042138	0.206538
C	2.568013	-0.616295	-0.035693
C	-0.608853	2.243798	-0.027709
C	3.700975	-1.583805	-0.271476
H	-4.346612	0.072576	-0.425462
H	-1.010530	-2.659071	0.200054
H	-3.681100	-2.572361	-0.274728
H	2.038289	2.787650	-0.228959
H	3.875253	1.131818	-0.261607

H	1.087084	-2.111163	0.262866
H	0.135762	-0.049164	1.674731
H	-2.747176	2.478853	-0.199796
H	4.496827	-1.447290	0.481014
H	4.164319	-1.417628	-1.258987
H	3.362414	-2.629024	-0.223144
H	-0.395823	3.307557	-0.162051

3.3

This section contains the Cartesian coordinates and energies for the energy surface shown in chapter 3 Figure 14. All the structures and energies were calculated at B3LYP/6-31G level, using Gaussian 03 and energies are quoted both in Hartrees (Ha) and kJ mol^{-1}. The values of calculated negative frequencies are reported (cm^{-1}) for transition state structures.

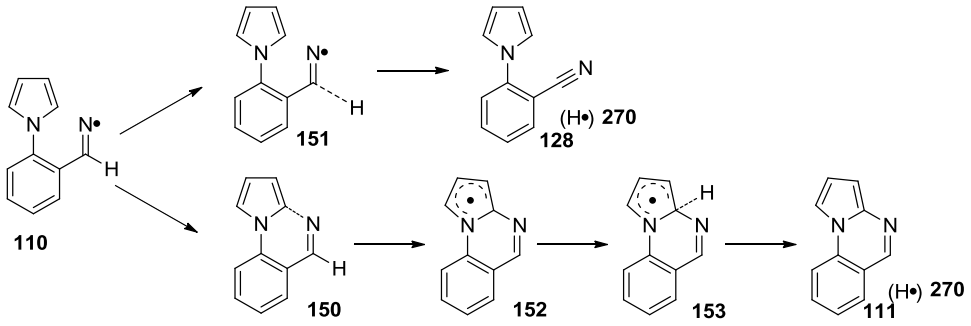

Scheme 156

110

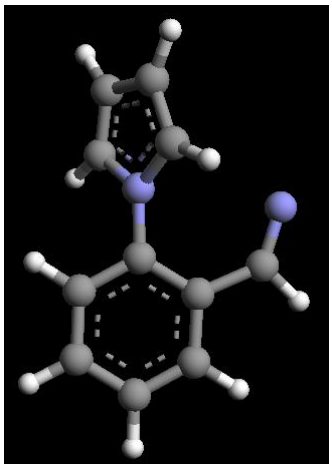

Energy = -533.8707962 Ha = -1401685.783 kJ mol^{-1}

C	-1.038101	2.226828	0.480849
C	-0.030090	1.316419	0.712869
N	-0.293306	0.1759036	-0.053199
C	-1.482552	0.380423	-0.761223
C	-1.950868	1.639690	-0.453752
H	1.116347	3.206075	0.927706
H	0.827207	1.364676	1.361327
H	-1.853419	-0.370183	-1.439887
H	-2.839004	2.099501	-0.860121
C	0.429000	-1.049666	-0.031652
C	1.822384	-1.119958	-0.281831
C	2.448335	-2.381378	-0.228941
C	-0.287326	-2.228820	0.228255
C	0.352166	-3.469410	0.256335
C	1.731669	-3.547207	0.036378
C	2.676466	0.028641	-0.662848
H	3.515976	-2.437697	-0.419459
H	-1.349819	-2.152630	0.429505
H	-0.222059	-4.366292	0.463008
H	2.241011	-4.504259	0.065193

N	2.403892	1.271099	-0.736861
H	3.704479	-0.261400	-0.934809

151

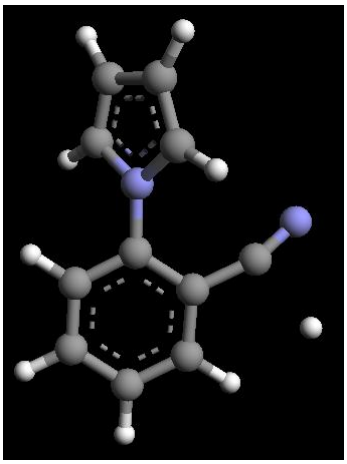

Energy = -533.8097455 Ha = -1401544.177 kJ mol^{-1}

Calculated Negative Frequency = -822.0900 cm^{-1}

C	-3.298289	-0.046473	0.574533
C	-1.994799	0.336480	0.793229
N	-1.164928	-0.500936	0.037562
C	-1.970199	-1.417775	-0.652926
C	-3.283723	-1.148535	-0.343089
C	0.252573	-0.513273	0.029042
C	1.020917	0.673276	-0.102644
C	2.426827	0.586290	-0.085320
C	0.916545	-1.744978	0.145798
C	2. 30969	-1.814109	0.132964
C	3.070874	-0.644185	0.024204
C	0.385969	1.949499	-0.335713
N	-0.374434	2.776730	-0.720225
H	-4.170318	0.407354	1.019815
H	-1.583713	1.105630	1.424135
H	-1.532327	-2.134685	-1.327751
H	-4.144297	-1.668126	-0.736135
H	3.002380	1.500431	-0.175687

H	0.322721	-2.642391	0.273234
H	2. 798868	-2.777617	0.228101
H	4.153985	-0.690008	0.026314
H	1.596319	3.066742	0.571525

128

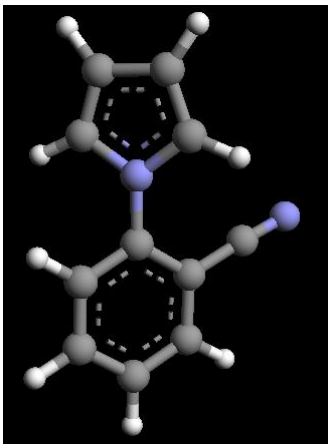

Energy = -533.318395 Ha = -1400235.446 kJ mol^{-1}

C	-3.151392	0.132919	0.521168
C	-1.847916	0.490927	0.779806
N	-1.011954	-0.350039	0.034026
C	-1.813978	-1.241979	-0.691828
C	-3.130592	-0.955807	-0.411914
C	0.404426	-0.372727	0.047649
C	1.175693	0.816995	0.017983
C	2.584119	0.730230	0.041491
C	1.065856	-1.610955	0.077269
C	2.459168	-1.679275	0.077763
C	3.224589	-0.506476	0.066932
C	0.582630	2.11544	-0.072588
N	0.151428	3.204799	-0.154891
H	-4.027090	0.593708	0.951833
H	-1.442668	1.242126	1.435549
H	-1.372231	-1.954073	-1.369032
H	-3.988688	-1.455540	-0.834967

H	3.160479	1.648200	0.023273
H	0.473126	-2.516543	0.126989
H	2.946320	-2.648153	0.104539
H	4.3074513	-0.555849	0.078292

150

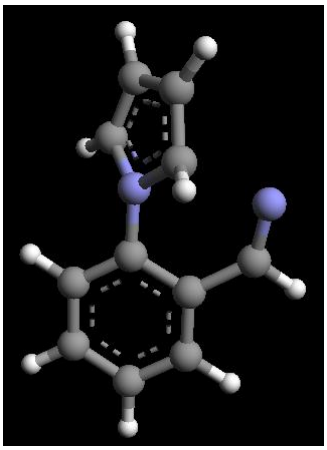

Energy = -533.8567451 Ha = -1401648.892 kJ mol^{-1}

Calculated Negative Frequency = -469.0721 cm^{-1}

C	-3.048037	0.347249	0.400153
C	-1.686174	0.550213	0.764181
N	-0.959351	-0.492842	0.134679
C	-1.820109	-1.234095	-0.673572
C	-3.107201	-0.729671	-0.508905
C	0.453979	-0.512468	0.114772
C	1.168903	-1.715430	0.161048
C	2.565812	-1.693890	0.125725
C	1.128977	0.725100	0.007496
C	2.532986	0.721709	-0.021735
C	3.251499	-0.474010	0.045675
C	0.378953	1.987107	-0.187623
N	-0.869030	2.232390	-0.000997
H	-3.874073	0.939708	0.761303
H	- 1.439882	-1.992694	-1.338519
H	-3.990436	-1.103282	-1.005093

H	0.628969	-2.652303	0.246513
H	3.118008	-2.626715	0.171301
H	3.057327	1.66869	-0.115132
H	4.335947	-0.458536	0.027311
H	0.990502	2.816745	-0.572793
H	-1.353442	0.881469	1.739614

152

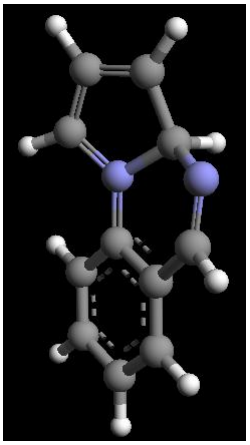

Energy = 533.8814739 Ha = -1401713.7262 kJ mol^{-1}

C	-3.089556	1.721033	-0.020022
C	-2.561911	3.124062	0.125260
N	-1.099288	2.877400	0.363884
C	-0.823673	1.519513	0.234208
C	-2.029844	0.830027	0.005751
H	-4.138252	1.505164	-0.154021
H	-2.662929	3.683850	-0.826947
H	0.165182	1.126750	0.410885
H	-2.100320	-0.243494	-0.098262
C	-0.306291	3.906346	0.855332
C	1.097622	3.916913	0.768136
C	1.812168	4.991925	1.296849
C	-0.985337	4.969314	1.517194
C	-0.238942	6.035902	2.041577

C	1.151274	6.060762	1.926523
C	-2.425860	4.838341	1.732870
H	1.615153	3.106765	0.266188
H	2.894171	5.003398	1.211003
H	-0.760607	6.839756	2.554016
H	1.719613	6.892262	2.328261
N	-3.198576	3.969324	1.157767
H	-2.888265	5.502431	2.462884

153

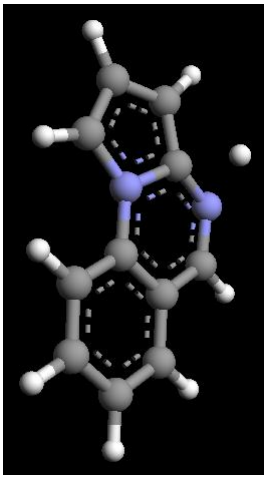

Energy = -533.8363114 Ha = -1401595.243 kJ mol^{-1}

Calculated Negative Frequency = -904.1153 cm^{-1}

C	3.052107	0.233853	-0.055911
C	1.713471	0.659992	-0.213923
N	0.893890	-0.514832	-0.053312
C	1.720985	-1.614516	0.059258
C	3.042312	-1.169391	0.062847
C	-0.498509	-0.408800	-0.070237
C	-1.352981	-1.523665	-0.105179
C	-2.732124	-1.331909	-0.102987
C	-1.035631	0.908091	-0.029556
C	-2.436050	1.068149	-0.026171
C	-3.280036	-0.035783	-0.063728

C	-0.127105	2.034274	0.039812
N	1.175340	1.9 26779	-0.032029
H	3.903577	0.894228	-0.074689
H	1.332503	-2.615651	0.143145
H	3.907250	-1.808863	0.153603
H	-0.942960	-2.525899	-0.145671
H	-3.389447	-2.194465	-0.136458
H	-2.845557	2.073438	0.006707
H	-4.356128	0.098117	-0.063285
H	-0.538958	3.031997	0.166327
H	1.694744	0.683440	-1.994041

111

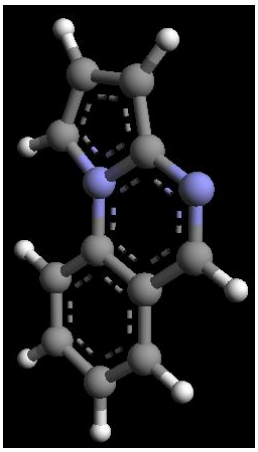

Energy = -533.3441094 Ha = -1400302.959 kJ mol^{-1}

C	3.028855	0.233435	-0.099259
C	1.705287	0.654749	-0.097544
N	0.883090	-0.517602	-0.066433
C	1.708731	-1.628184	- 0.049392
C	3.024784	-1.184699	-0.068978
C	-0.511715	-0.410404	-0.057802
C	-1.364684	-1.526985	-0.027613
C	-2.743792	-1.338433	-0.020870
C	-1.051185	0.906234	-0.081336

C	-2.453545	1.062910	-0.073727
C	-3.294385	-0.042418	-0.043900
C	-0.146041	2.032338	-0.112036
N	1.162561	1.910388	-0.119765
H	3.882565	0.890939	-0.119988
H	1.317762	-2.631195	-0.025157
H	3.893648	-1.825324	-0.062206
H	-0.953180	-2.529109	-0.009692
H	-3.399393	-2.202619	0.002437
H	-2.864686	2.067913	-0.091686
H	-4.370836	0.089161	-0.038298
H	- 0.555269	3.038426	-0.130255

270

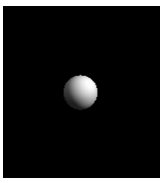

Energy = -0.5002728 Ha = -1313.474 kJ mol^{-1}

H	-0.648046	0.447152	0

3.4

This section contains the Cartesian coordinates and energies for the energy surface shown in chapter 4 Figure 43. All the structures and energies were calculated at B3LYP/cc-pVDZ level, using Gaussian 03 and energies are quoted both in Hartrees (Ha) and kJ mol^{-1}. The values of calculated negative frequencies are reported (cm^{-1}) for transition state structures.

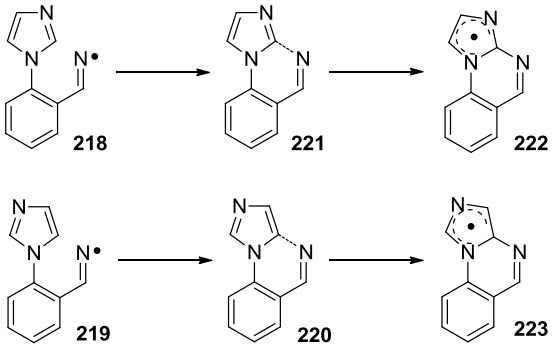

Scheme 157

219

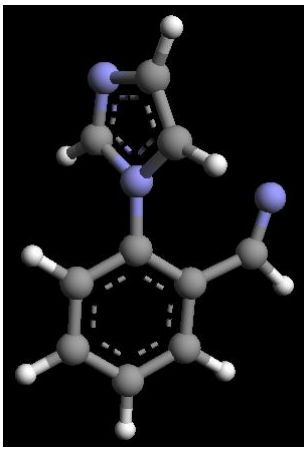

Energy = -550.0902722 Ha = -1444270.261 kJ mol^{-1}

C	-3.12 5827	-0.036858	0.567918
C	-1.858169	0.341099	0.935211
N	-1.006121	-0.309818	0.051559
C	-1.816748	-1.04 3732	-0.791924
N	-3.090574	-0.894071	-0.513476
C	0.415001	-0.340441	0.063493
C	1.200520	0.826960	-0.085189
C	2.600213	0.697804	-0.066279
C	1.042539	-1.584628	0.205651
C	2.434702	-1.690831	0.204781
C	3.219325	-0.542839	0.077057
C	0.650220	2.188552	-0.312983
N	-0.544694	2.581743	-0.317254
H	-4.066271	0.263281	1.024920
H	-1.483340	0.984146	1.723520
H	-1.398808	-1.640360	-1.600409
H	3.209168	1.597695	-0.181664
H	0.419036	-2.470928	0.333296
H	2.902193	-2.670103	0.317646
H	4.308675	-0.612461	0.083762
H	1.428430	2.957092	-0.514856

223

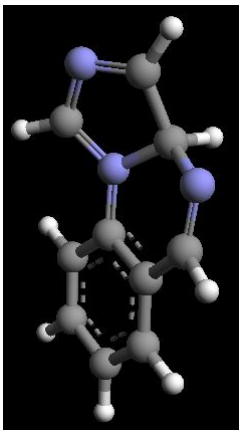

Energy = -550.1039089 Ha = -1444306.064 kJ mol^{-1}

C	3.008557	0.186826	0.082876
C	1.655173	0.662479	0.557114
N	0.854742	-0.536277	0.221776
C	1.712110	-1.485476	-0.304945
N	2.976768	-1.065427	-0.378989
C	-0.528743	-0.438338	0.135000
C	-1.392968	-1.543160	0.184030
C	-2.769529	-1.339633	0.084617
C	-1.050134	0.867557	-0.046151
C	-2.437983	1.043141	-0.142972
C	-3.300264	-0.050055	-0.067590
C	-0.094536	1.963890	-0. 240571
N	1.168934	1.913881	-0.015662
H	3.921022	0.779554	0.125974
H	1.653327	0.807511	1.664024
H	1.355587	-2.443021	-0.678450
H	-0.989421	-2.547788	0.321 938
H	-3.440415	-2.200080	0.136821
H	-2.835488	2.050686	-0.292424
H	-4.379825	0.094182	-0.136304
H	-0.493264	2.908703	-0.638478

218

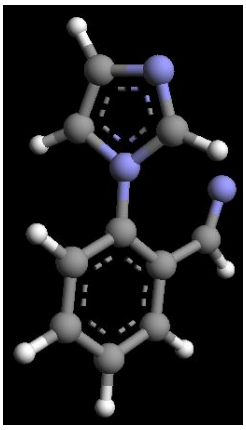

Energy = -550.090306 Ha = -1444270.350 kJ mol^{-1}

N	-3.113875	-0.034708	0.657034
C	-1.857505	0.262090	0.891161
N	-1.001237	-0.343133	-0.008159
C	-1.804373	-1.086499	-0.864610
C	-3.092569	-0.867978	0.443025
C	0.420277	-0.363530	0.029783
C	1.191789	0.814408	-0.099194
C	2.592466	0.707333	-0.042410
C	1.060935	-1.599252	0.185636
C	2.453595	-1.684172	0.224718
C	3.224763	-0.524154	0.118722
C	0.619546	2.164481	-0.344063
N	-0.583519	2.531104	-0.352805
H	-1.486995	0.891306	1.695974
H	-1.380759	- 1.652672	-1.688390
H	-4.010431	-1.260333	-0.875971
H	3.190863	1.616043	-0.142846
H	0.446591	-2.495006	0.290508
H	2.932861	-2.657265	0.349282
H	4.314444	-0.578441	0.154678
H	1.383721	2.944914	-0.552950

222

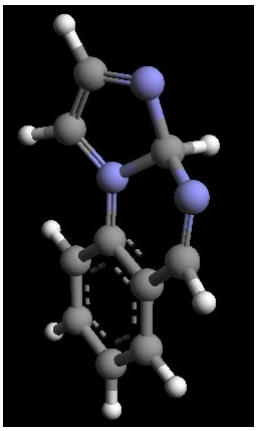

Energy = -550.1065872 Ha = -1444313.096 kJ mol^{-1}

N	3.046430	0.2710091	0.096905
C	1.695873	0.626527	0.476884
N	0.854044	-0.560646	0.127616
C	1.705853	-1.559922	-0.261353
C	3.003387	-0.996315	-0.265973
C	-0.522143	-0.449752	0.081704
C	-1.403666	-1.544536	0.110594
C	-2.777967	-1.316075	0.062824
C	-1.029628	0.871234	-0.038773
C	-2.416241	1.068874	-0.090886
C	-3.293321	-0.013610	-0.027546
C	-0.062470	1.955339	-0.236260
N	1.208727	1.876735	-0.069439
H	1.681670	0.735765	1.587930
H	1.359220	-2.533088	-0.598464
H	3.907644	-1.530021	-0.567113
H	-1.013812	-2.560234	0.195656
H	-3.460802	-2.167713	0.104198
H	-2.801770	2.086516	-0.196103
H	-4.371982	0.148333	-0.060043
H	-0.458214	2.916517	-0.596030

3.5

This section contains the Cartesian coordinates and energies for the energy surface shown in the paper **'Structural studies of some push–pull *N*-arylbenzazoles'** included at the end of this thesis in the Appendix. All the structure and energies were calculated at B3LYP/6-31G level, using Gaussian 03 and energies are quoted both in Hartrees (Ha) and kJ mol^{-1}.

9-(2-Carbomethoxyphenyl)-9*H*-carbazole

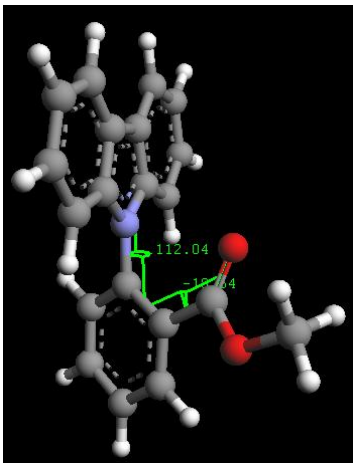

Energy = -976.1352403 Ha = -2562857.715 kJ mol^{-1}

Torsion angle 1 = 112.04°

Torsion angle 2 = –18.64°

C	2.145547	1.035336	-0.356927
C	0.787091	0.909528	-0.758973
N	0.344218	-0.389037	-0.450256
C	1.400483	-1.090959	0.158951
C	2.535094	-0.235459	0.229092
C	-0.963319	-0.903732	-0.682196
C	-2.104746	-0.414722	-0.001060
C	-3.370438	-0.929713	-0.339943
C	-1.112768	-1.912356	-1.645670
C	-2.372326	-2.435409	-1.946317
C	-3.506800	-1.934069	-1.298427
C	-1.994642	0.571760	1.105885

O	-0.983257	0.830109	1.767217
C	2.820741	2.242024	-0.583203
C	0.104945	1.955632	-1.386545
C	3.722809	-0.714067	0.797628
C	3.763985	-2.021466	1.287321
C	2.627807	-2.851133	1.216276
C	1.431320	-2.398026	0.653521
C	2.143416	3.294941	-1.202019
C	0.799962	3.149180	-1.599812
O	-3.205960	1.186001	1.365106
C	-3.218698	2.145863	2.477144
H	-4.239229	-0.538920	0.173330
H	-0.228044	-2.263652	-2.164494
H	-2.467782	-3.215879	-2.693969
H	-4.490666	-2.323762	-1.536423
H	3.857624	2.357139	-0.282694
H	-0.927600	1.848882	-1.700537
H	4.598831	-0.075936	0.861055
H	4.677899	-2.402900	1.730875
H	2.67920	-3.861774	1.609050
H	0.557495	-3.038250	0.609417
H	2.655378	4.234791	-1.381107
H	0.293227	3.978274	-2.083766
H	-4.238914	2.523624	2.505041
H	-2.503571	2.948850	2.287395
H	-2.956427	1.644964	3.411668

9-(2-Nitrophenyl)-9*H*-carbazole

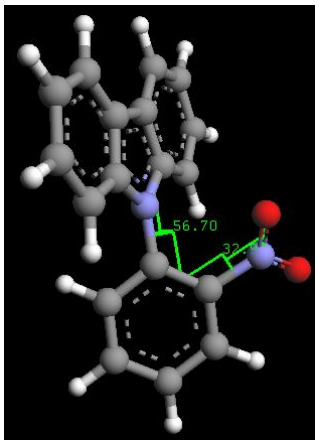

Energy = -952.7506593 Ha = -2501461.147 kJ mol^{-1}

Torsion angle 1 = 56.60°

Trosion angle 2 = 32.94°

C	-3.556712	-1.127118	0.314228
C	-2.365712	-0.446807	0.029964
C	-2.055770	0.941171	-0.269208
C	-0.649573	1.027815	-0.452374
N	-0.094972	-0.260807	-0.288009
C	-1.138833	-1.163887	0.011780
C	-1.081652	-2.532203	0.290078
C	-2.283703	-3.188787	0.571035
C	-3.510107	-2.497527	0.580089
C	-2.841234	2.092498	-0.409820
C	-2.221792	3.302097	-0.730588
C	-0.827754	3.367222	-0.916598
C	-0.023221	2.232027	-0.783920
C	2.295677	0.001159	0.347332
C	3.644097	-0.297535	0.121421
C	3.994588	-1.254898	-0.828387
C	1.271134	-0.604581	-0.410301
C	1.650184	-1.561216	-1.368742
C	2.990662	-1.896671	-1.565463

N	2.011296	0.937508	1.441487
O	2.865614	1.848515	1.657943
O	0.968648	0.767868	2.128100
H	-4.502612	-0.595130	0.334351
H	-0.140584	-3.069897	0.300910
H	-2.267136	-4.251233	0.791759
H	-4.425743	-3.035248	0.802559
H	- 3.916940	2.044711	-0.273057
H	-2.818189	4.201897	-0.838318
H	-0.364970	4.316361	-1.166195
H	1.049112	2.297080	-0.931226
H	4.392517	0.217914	0.709366
H	5.038299	-1.497659	-0.990930
H	0.873522	-2.014305	-1.973466
H	3.252679	-2.639015	-2.311600

1-(2-Carbomethoxyphenyl)-1*H*-indole

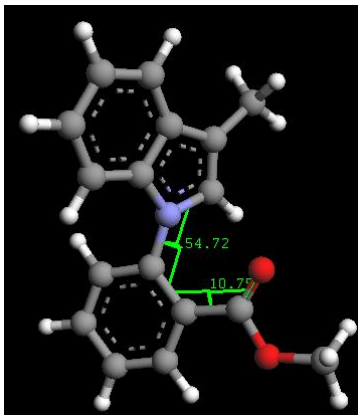

Energy = -861.8254304 = -2262735.595 kJ mol^{-1}

Torsion angle 1 = 54.72°

Torsion angle 2 = 10.75°

C	-3.929749	-0.435083	-0.320405
C	-2.618638	-0.529511	0.175884
C	-1.670250	0.475805	-0.169912
C	-1.999705	1.546718	-1.009094
C	-3.309454	1.615541	-1.488348

C	-4.267114	0.637802	-1.145268
C	-1.944355	-1.497081	1.019078
C	-0.649000	-1.070705	1.146281
N	-0.452668	0.128701	0.440089
C	-2.555132	-2.723038	1.627682
C	0.736577	0.903355	0.427209
C	2.008648	0.378579	0.077122
C	3.137406	1.219254	0.175968
C	0.635905	2.251093	0.817810
C	1.760823	3.071993	0.877195
C	3.022464	2.551127	0.565619
C	2.191063	-0.990027	-0.469603
O	1.307949	-1.763373	-0.861371
O	3.529153	-1.341070	-0.541684
C	3.822408	-2.654327	-1.127353
H	-4.667895	-1.191224	-0.071036
H	- 3.593058	2.434782	-2.141511
H	-5.276522	0.721361	-1.535536
H	-1.825591	-3.270051	2.234029
H	-2.926868	-3.412486	0.857846
H	-3.406644	-2.474983	2.275598
H	4.103625	0.806084	-0.080080
H	1.655198	4.106693	1.186697
H	3.906032	3.177273	0.624051
H	3.457350	-2.700529	-2.155731
H	4.906927	-2.737918	-1.090218
H	3.345258	-3.443799	-0.542724
H	-1.265923	2.294010	-1.289226
H	-0.337701	2.633413	1.100727
H	0.166281	-1.516972	1.691736

1-(2-Nitrophenyl)-1*H*-indole

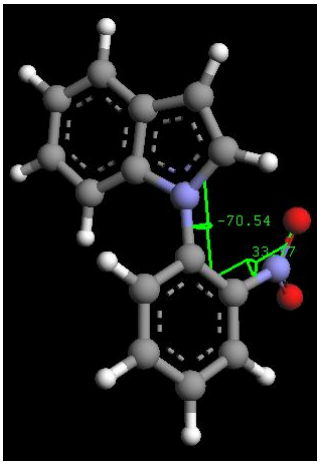

Energy = -799.1314919 Ha = -2098131.719 kJ mol^{-1}

Torsion angle 1 = -70.54°

Torsion angle 2 = -33.77°

C	-3.908934	-0.385242	-0.033737
C	-2.594574	-0.645964	-0.458848
C	-1.537523	0.181884	0.016685
C	-1.761963	1.243205	0.901137
C	-3.077446	1.480816	1.303267
C	-4.140496	0.676340	0.839860
C	-2.002537	-1.635513	-1.327991
C	-0.654360	-1.414502	-1.356044
N	-0.337029	-0.310753	-0.535498
C	0.910914	0.363419	-0.458607
C	2.089578	-0.170478	0.112545
C	3.261940	0.591481	0.202836
C	0.965821	1.691661	-0.922642
C	2.134474	2.448202	-0.843120
C	3.292665	1.895717	-0.281631
N	2.162718	-1.515891	0.680873
O	2.939532	-1.686965	1.666888
O	1.475068	-2.438212	0.160925
H	-4.729969	-1.005652	-0.379040

H	-0.947933	1.857035	1.270591
H	-3.284093	2.295481	1.989785
H	-5.151068	0.887179	1.174643
H	-2.523055	-2.419250	-1.856422
H	0.127983	-1.945080	-1.868309
H	4.130079	0.141345	0.666402
H	0.066249	2.113551	-1.354802
H	2.142633	3.463158	-1.225378
H	4.207191	2.474018	-0.219857

1-(2-Carbomethoxyphenyl)-1*H*-benzimidazole

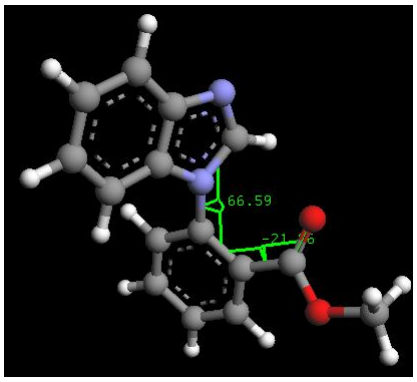

Energy = -838.546089 Ha = -2201615.335kJ mol^{-1}

Torsion angle 1 = 66.59°

Torsion angle 2 = -21.86°

C	3.982134	-0.961381	-0.094155
C	2.677567	-0.789503	-0.567916
C	1.802335	0.128943	0.065802
C	2.194081	0.883601	1.175574
C	3.501001	0.699654	1.635301
C	4.383799	-0.208162	1.009909
N	2.021933	-1.416197	-1.644658
C	0.804981	-0.915502	-1.654510
N	0.589929	0.032871	-0.642915
C	-0.551513	0.867740	-0.450945
C	-1.835928	0.376963	-0.105572
C	-2.880874	1.300712	0.095910

C	-0.354450	2.253390	-0.571980
C	-1.402464	3.151249	-0.368268
C	-2.674587	2.672364	-0.036100
C	-2.122997	-1.069043	0.066608
O	-1.476709	-2.014882	-0.402860
O	-3.250594	-1.278974	0.833175
C	-3.642084	-2.680238	1.043582
H	4.646876	-1.666223	-0.580096
H	3.843634	1.265957	2.495453
H	5.390148	-0.320945	1.399789
H	-3.855821	0.917502	0.366382
H	-1.227046	4.216388	-0.476339
H	-3.497517	3.361132	0.120101
H	-2.843335	-3.218538	1.557476
H	-4.539579	-2.626309	1.656369
H	-3.843864	-3.163807	0.085387
H	1.519874	1.577832	1.664667
H	0.633471	2.611789	-0.837272
H	0.022551	-1.185375	-2.340861

2-Methyl-1-(2-nitrophenyl)-1*H*-benzimidazole

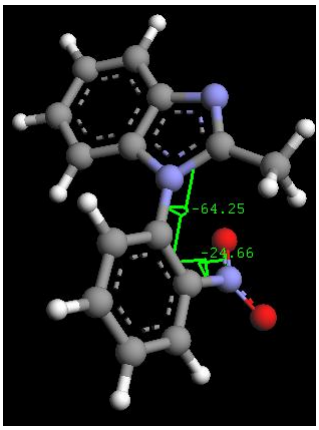

Energy = -854.4740188 Ha = -2140166.946 kJ mol^{-1}

Torsion angle 1 = -64.25°

Torsion angle 2 = -24.66°

C	3.871013	-0.403616	0.010357
C	2.526617	-0.591056	0.346457
C	1.559004	0.376879	-0.018715
C	1.892542	1.534623	-0.725341
C	3.240651	1.706642	-1.053348
C	4.216417	0.753238	-0.690241
N	1.912398	-1.648405	1.037697
C	0.624642	-1.362060	1.087176
N	0.337925	-0.125043	0.465005
C	-0.917040	0.529938	0.361938
C	-2.022970	0.015985	-0.348052
C	-3.252253	0.685480	-0.356417
C	-1.079923	1.756876	1.026951
C	-2.294489	2.444654	0.992549
C	-3.388836	1.903438	0.306556
N	-1.950027	-1.219830	-1.139099
O	-3.037541	-1.832738	-1.356475
O	-0.831365	-1.595430	-1.584540
C	-0.414654	-2.208183	1.737601
H	4.609084	-1.146918	0.288501
H	1.147068	2.266399	-1.016438
H	3.542115	2.591910	-1.603877
H	5.251593	0.924483	-0.966441
H	-4.077018	0.238938	-0.895818
H	-0.237541	2.148500	1.585092
H	-2.390041	3.390748	1.513998
H	-4.338932	2.424508	0.286047
H	0.090478	-2.948024	2.360576
H	-1.019549	-2.749663	1.000207
H	-1.092402	-1.619627	2.366226

1-(2-Nitrophenyl)-1*H*-indazole

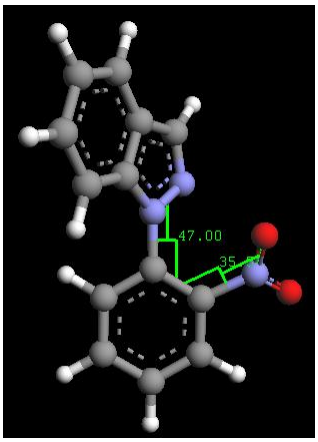

Energy = -818.1417705 Ha = -2140166.946 kJ mol^{-1}

Torsion angle 1 = 47.00°

Torsion angle 2 = 35.55°

C	-3.838213	-0.606629	0.221609
C	-2.466528	-0.712025	0.512645
C	-1.566284	0.285038	0.046868
C	-2.000801	1.374999	-0.723753
C	-3.363347	1.454093	-0.999587
C	-4.275774	0.478827	-0.529775
C	-1.648971	-1.657771	1.215306
N	-0.367528	-1.307131	1.201562
N	-0.307152	-0.103558	0.486678
C	0.939675	0.525828	0.294187
C	2.078807	-0.181021	-0.135469
C	3.330309	0.437346	-0.201172
C	1.082092	1.886944	0.605431
C	2.321745	2.520223	0.492585
C	3.453069	1.793113	0.103168
N	2.007510	-1.570546	-0.603229
O	3.012741	-2.306105	-0.382763
O	0.990064	-1.932547	-1.251815
H	-4.536867	-1.360167	0.569727

H	-1.308339	2.118472	-1.100495
H	-3.735152	2.282118	-1.594417
H	-5.328867	0.581178	-0.768882
H	-1.949567	-2.560525	1.723001
H	4.183513	-0.154268	-0.507265
H	0.218692	2.428721	0.972814
H	2.408339	3.573023	0.738291
H	4.421313	2.275531	0.036529

9-(2-Carbomethoxyphenyl)-9*H*-carbazole at different torsion angles

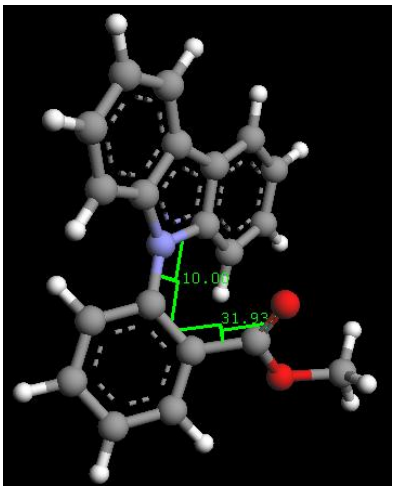

Energy = -976.1204047 Ha = -2562818.764 kJ mol^{-1}

Torsion angle 1 (fixed) = 10°

Torsion angle 2 (free rotation) = 31.93°

C	-2.582418	0.273798	0.076841
C	-1.757267	-0.876140	-0.029801
N	-0.460815	-0.481539	-0.514047
C	-0.481358	0.940664	-0.604366
C	-1.776863	1.419755	-0.294733
C	0.686915	-1.309764	-0.314402
C	1.975300	-0.819449	0.028301
C	3.105624	-1.646164	-0.127213
C	0.607915	-2.620582	-0.834410
C	1.728812	-3.442989	-0.933963
C	2.994462	-2.952590	-0.595380
C	2.158093	0.412979	0.837687

O	1.392239	0.812740	1.721702
C	-3.908593	0.158169	0.509884
C	-2.236366	-2.129517	0.370676
C	-2.072866	2.783629	-0.419233
C	-1.084718	3.653486	-0.879592
C	0.182866	3.159142	-1.240977
C	0.492749	1.801818	-1.126050
C	-4.399075	-1.098028	0.868044
C	-3.560867	-2.224604	0.811080
O	3.347508	1.053716	0.552066
C	3.653744	2.239903	1.366034
H	4.070415	-1.243475	0.155850
H	-0.334353	-2.965358	-1.237870
H	1.617865	-4.448465	-1.327057
H	3.876721	-3.574108	-0.700230
H	-4.539706	1.038282	0.582957
H	-1.611461	-3.011256	0.374338
H	-3.063232	3.154112	-0.174117
H	-1.297708	4.712737	-0.978857
H	0.932043	3.840490	-1.631815
H	1.463562	1.439067	-1.440321
H	-5.423941	-1.204787	1.207622
H	-3.941770	-3.192451	1.121111
H	4.610238	2.595823	0.988200
H	3.721575	1.967555	2.421518
H	2.870929	2.989859	1.236298

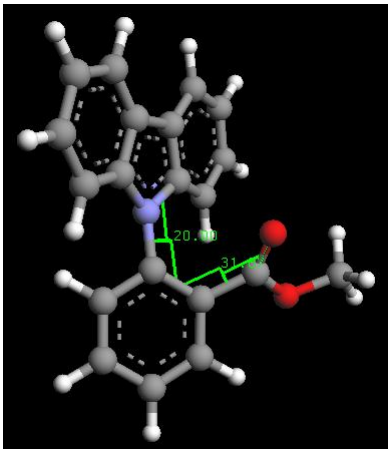

Energy = -976.1259923 Ha = -2562833.435 kJ mol^{-1}

Torsion angle 1 = 20°

Torsion angle 2 = 31.87°

C	-2.579287	0.224526	0.085319
C	-1.720286	-0.903155	0.006865
N	-0.445306	-0.482520	-0.485171
C	-0.499757	0.929448	-0.630820
C	-1.808210	1.381831	-0.326291
C	0.725314	-1.285423	-0.358256
C	1.988202	-0.780613	0.044902
C	3.141576	-1.570318	-0.129405
C	0.678694	-2.573395	-0.930644
C	1.822710	-3.361401	-1.049003
C	3.068952	-2.854639	-0.663667
C	2.117608	0.436235	0.886984
O	1.312536	0.806025	1.748708
C	-3.898917	0.074118	0.528520
C	-2.154550	-2.164899	0.428806
C	-2.137830	2.734248	-0.485453
C	-1.170992	3.616962	-0.967225
C	0.111257	3.148142	-1.310937
C	0.457319	1.802671	-1.162225
C	-4.345266	-1.190152	0.916381
C	-3.473366	-2.292781	0.876734
O	3.303565	1.104051	0.655233
C	3.556085	2.283487	1.496852

H	4.091871	-1.160428	0.189895
H	-0.257612	-2.925280	-1.344208
H	1.745509	-4.351970	-1.485472
H	3.968026	-3.449405	-0.780729
H	-4.560171	0.933128	0.584615
H	-1.497026	-3.023915	0.436591
H	-3.136445	3.087053	-0.247607
H	-1.410865	4.667620	-1.093060
H	0.844745	3.840573	-1.711946
H	1.441231	1.458016	-1.456360
H	-5.364515	-1.322358	1.263920
H	-3.824738	-3.265513	1.205825
H	4.521697	2.659434	1.164372
H	3.583614	1.997820	2.550607
H	2.767497	3.022917	1.343601

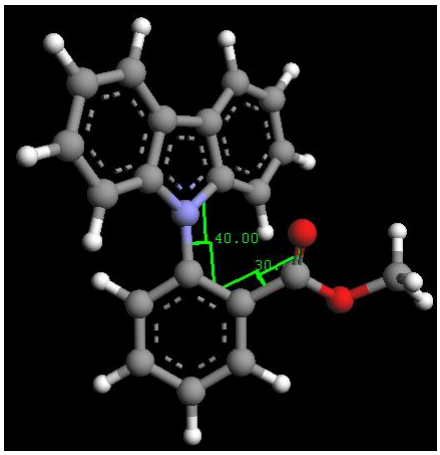

Energy = -976.1329583 Ha = -2562851.724 kJ mol^{-1}

Torsion angle 1 = 40°

Torsion angle 2 = 30.40°

C	-2.577040	0.101610	0.116396
C	-1.632283	-0.959491	0.087700
N	-0.407486	-0.465277	-0.423536
C	-0.563904	0.916202	-0.676440
C	-1.900715	1.289006	-0.373893
C	0.808483	-1.199767	-0.450268

C	2.025904	-0.688503	0.062264
C	3.219742	-1.399626	-0.163617
C	0.822795	-2.423549	-1.143312
C	2.007856	-3.139655	-1.314732
C	3.217089	-2.619483	-0.838647
C	2.063573	0.481018	0.977411
O	1.185837	0.799940	1.786556
C	-3.876256	-0.137929	0.581622
C	-1.958766	-2.238392	0.549988
C	-2.321682	2.606721	-0.595680
C	-1.417610	3.529672	-1.123764
C	-0.102874	3.139046	-1.442835
C	0.338161	1.829854	-1.232214
C	-4.214414	-1.418305	1.024265
C	-3.260119	-2.453043	1.013692
O	3.250671	1.178602	0.871150
C	3.411055	2.323029	1.780328
H	4.143338	-0.987224	0.223051
H	-0.101099	-2.783490	-1.580387
H	1.990888	-4.084007	-1.848932
H	4.145760	-3.158316	-0.991255
H	-4.607470	0.663992	0.607353
H	-1.229665	-3.039349	0.565131
H	-3.339972	2.904085	-0.365191
H	-1.730130	4.554030	-1.298006
H	0.582710	3.865451	-1.867785
H	1.349323	1.541844	-1.495447
H	-5.216998	-1.617265	1.388252
H	-3.535288	-3.438026	1.377237
H	4.387277	2.736739	1.535199
H	3.371893	1.989387	2.819566

H	2.615810	3.050249	1.604751

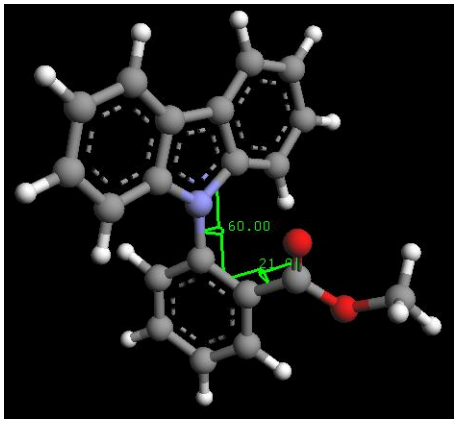

Energy = -976.1351626 Ha = -2562857.511 kJ mol^{-1}

Torsion angle 1 = 60°

Torsion angle 2 = 21.99°

C	-2.558064	-0.130931	0.199057
C	-1.474465	-1.051377	0.158389
N	-0.361199	-0.412469	-0.421859
C	-0.719825	0.911575	-0.737997
C	-2.079179	1.114957	-0.373897
C	0.920381	-1.001589	-0.607250
C	2.086305	-0.499861	0.020983
C	3.330163	-1.083136	-0.286875
C	1.025155	-2.091844	-1.485049
C	2.262125	-2.682866	-1.749479
C	3.421678	-2.168252	-1.158344
C	2.023274	0.558442	1.062804
O	1.046101	0.845612	1.762537
C	-3.786484	-0.536732	0.736720
C	-1.594915	-2.351719	0.657356
C	-2.679955	2.356909	-0.618350
C	-1.929297	3.368768	-1.220490
C	-0.586913	3.145834	-1.584342
C	0.034315	1.915819	-1.351755
C	-3.917652	-1.837609	1.227664
C	-2.830232	-2.731939	1.189507

O	3.237983	1.201032	1.212762
C	3.300006	2.228582	2.261254
H	4.217420	-0.681079	0.184798
H	0.125326	-2.450829	-1.971495
H	2.321665	-3.525691	-2.430204
H	4.388783	-2.609994	-1.372708
H	-4.624203	0.152604	0.776673
H	-0.759340	-3.042137	0.641364
H	-3.716414	2.529822	-0.345444
H	-2.382659	4.335543	-1.413473
H	-0.022240	3.943088	-2.057520
H	1.066270	1.751255	-1.641466
H	-4.863799	-2.163205	1.647439
H	-2.950168	-3.735914	1.584339
H	4.313209	2.621589	2.204132
H	3.102825	1.783160	3.238901
H	2.560536	3.007747	2.065869

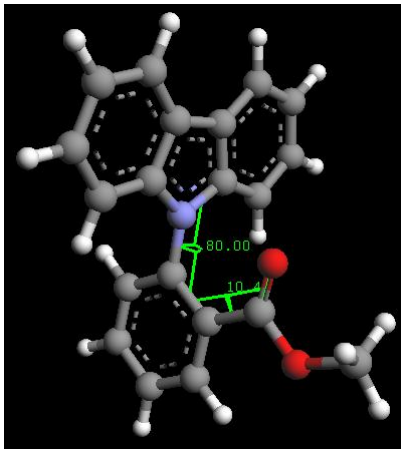

Energy = -976.13498 Ha = -2562857.032 kJ mol^{-1}

Torsion 1 = 80°

Torsion 2 = 10.45°

C	-2.443301	-0.522492	0.235976
C	-1.202488	-1.178547	0.001478
N	-0.312132	-0.261203	-0.580671
C	-0.960326	0.978120	-0.707734
C	-2.289385	0.849496	-0.215802
C	1.047163	-0.528854	-0.925104
C	2.128902	-0.188093	-0.076185

C	3.440216	-0.466164	-0.505878
C	1.301046	-1.147106	-2.157021
C	2.608150	-1.430530	-2.561851
C	3.680724	-1.083884	-1.733690
C	1.912450	0.428193	1.260408
O	0.836935	0.547198	1.857356
C	-3.502067	-1.241292	0.806645
C	-1.004449	-2.522877	0.327909
C	-3.144717	1.958666	-0.252791
C	-2.671233	3.166376	-0.770852
C	-1.352108	3.273439	-1.253710
C	-0.479474	2.181911	-1.230189
C	-3.313262	-2.585936	1.134077
C	-2.076043	-3.216724	0.896769
O	3.098414	0.870613	1.817250
C	2.999449	1.476217	3.151462
H	4.262939	-0.195746	0.142401
H	0.456437	-1.393196	-2.790562
H	2.785808	-1.910787	-3.518359
H	4.699639	-1.293586	-2.041148
H	-4.456366	-0.759058	0.995096
H	-0.052878	-3.011644	0.150294
H	-4.162382	1.881542	0.117624
H	-3.324219	4.032496	-0.802827
H	-1.005006	4.221394	-1.652947
H	0.534618	2.269290	-1.604817
H	-4.125587	-3.152164	1.578009
H	-1.950132	-4.261823	1.162009
H	4.020235	1.755704	3.404886
H	2.597746	0.753651	3.865130
H	2.345779	2.350345	3.119565

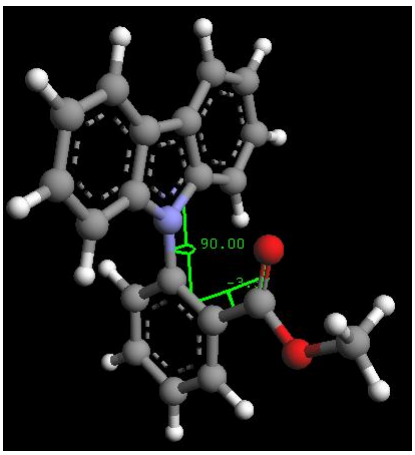

Energy = -976.1349413 Ha = -2562856.93 kJ mol^{-1}

Torsion 1 = 90°

Torsion 2 = -3.37°

C	2.345557	0.772012	-0.043657
C	1.041917	1.091950	-0.516010
N	0.307771	-0.097714	-0.649665
C	1.114818	-1.173683	-0.245548
C	2.391921	-0.669641	0.128604
C	-1.063791	-0.188072	-1.038091
C	-2.131034	-0.060539	-0.114570
C	-3.452348	-0.155427	-0.591040
C	-1.343100	-0.410104	-2.393272
C	-2.660581	-0.506818	-2.849092
C	-3.717835	-0.377195	-1.942804
C	-1.889998	0.161323	1.336588
O	-0.795753	0.201399	1.909906
C	3.275461	1.801528	0.152733
C	0.657223	2.407392	-0.788990
C	3.383084	-1.562908	0.556271
C	3.092404	-2.928134	0.608236
C	1.820647	-3.407065	0.236486
C	0.815247	-2.537673	-0.195632
C	2.899130	3.119350	-0.117338
C	1.602680	3.415789	-0.582310

O	-3.073327	0.324128	2.033595
C	-2.946230	0.541830	3.480192
H	-4.263343	-0.054263	0.117591
H	-0.508563	-0.502976	-3.078945
H	-2.857461	-0.679466	-3.901957
H	-4.744558	-0.448382	-2.285576
H	4.275370	1.578854	0.512442
H	-0.339443	2.640461	-1.147630
H	4.363912	-1.198963	0.846602
H	3.851748	-3.628993	0.939562
H	1.615612	-4.471918	0.286593
H	-0.162682	-2.910756	-0.479580
H	3.610414	3.925004	0.032916
H	1.330976	4.447134	-0.784821
H	-3.969656	0.645997	3.835311
H	-2.365397	1.445801	3.675031
H	-2.449724	-0.311233	3.947566

1-(2-Carbomethoxyphenyl)-1*H*-indole at different torsion angles

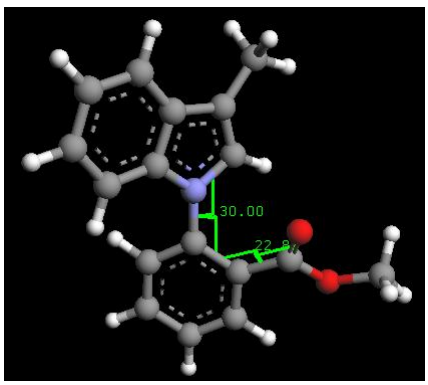

Energy = -861.8228581 Ha = -2262728.841 kJ mol^{-1}

Torsion angle 1 = 30°

Torsion angle 2 = 22.85°

C	3.938734	-0.602771	0.180251
C	2.585616	-0.641127	-0.192328
C	1.753246	0.486412	0.062367
C	2.241156	1.616040	0.731310

C	3.589276	1.626495	1.098181
C	4.434817	0.534655	0.816715
C	1.764759	-1.665274	-0.807712
C	0.499809	-1.153555	-0.894721
N	0.459835	0.168214	-0.412141
C	2.224889	-3.017344	-1.260513
C	-0.696948	0.976668	-0.293088
C	-1.997512	0.456622	-0.049405
C	-3.109580	1.319161	-0.153378
C	-0.568748	2.344467	-0.609968
C	-1.677548	3.185871	-0.662684
C	-2.961615	2.671387	-0.447292
C	-2.237619	-0.904952	0.490047
O	-1.444970	-1.592034	1.147315
O	-3.525856	-1.342421	0.232760
C	-3.901808	-2.633043	0.824176
H	4.585250	-1.453387	-0.012141
H	3.988604	2.492241	1.616892
H	5.478303	0.577183	1.112147
H	1.399724	-3.593107	-1.692253
H	2.634689	-3.602189	-0.426300
H	3.014012	-2.945076	-2.021054
H	-4.091690	0.902905	0.028937
H	-1.540857	4.234102	-0.908205
H	-3.832397	3.314573	-0.508900
H	-3.825847	-2.587620	1.912897
H	-4.930524	-2.793498	0.507270
H	-3.246478	-3.423707	0.452797
H	1.601757	2.453270	0.981955
H	0.408980	2.727385	-0.871760
H	-0.381317	-1.603200	-1.319661

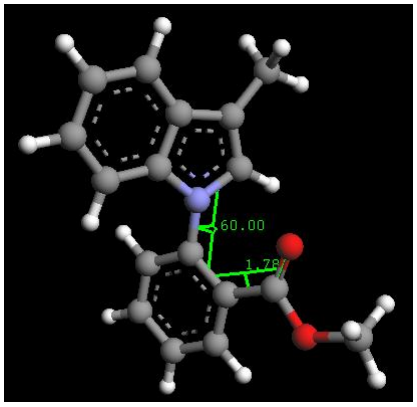

Energy = -861.8253447 Ha = -2262735.37 kJ mol^{-1}

Torsion 1 = 60°

Torsion 2 = 1.78°

C	3.932441	-0.388045	0.373826
C	2.636202	-0.500988	-0.156707
C	1.651662	0.463496	0.204221
C	1.931931	1.514344	1.085462
C	3.228295	1.602900	1.596872
C	4.220428	0.663894	1.243351
C	2.009105	-1.453268	-1.052106
C	0.705209	-1.058488	-1.194204
N	0.457262	0.103689	-0.442727
C	2.667177	-2.639738	-1.689387
C	-0.738276	0.871635	-0.460906
C	-2.013463	0.355016	-0.107774
C	-3.136579	1.203456	-0.208450
C	-0.631284	2.216432	-0.859828
C	-1.751679	3.042677	-0.928426
C	-3.015209	2.530990	-0.610088
C	-2.208470	-1.019053	0.420544
O	-1.335809	-1.865940	0.651365
O	-3.543453	-1.289231	0.673276
C	-3.839912	-2.613232	1.231817
H	4.697573	-1.113596	0.115050
H	3.474373	2.407048	2.283194

H	5.218085	0.761429	1.659780
H	1.968522	-3.179863	-2.336887
H	3.034477	-3.349951	-0.936406
H	3.529924	-2.346375	-2.302612
H	-4.104629	0.798503	0.052905
H	-1.640705	4.074174	-1.246591
H	-3.895823	3.160911	-0.672850
H	-3.338771	-2.738485	2.194080
H	-4.922116	-2.629001	1.346503
H	-3.503366	-3.395974	0.548527
H	1.171263	2.232177	1.371386
H	0.346380	2.593140	-1.136541
H	-0.087388	-1.510763	-1.766882

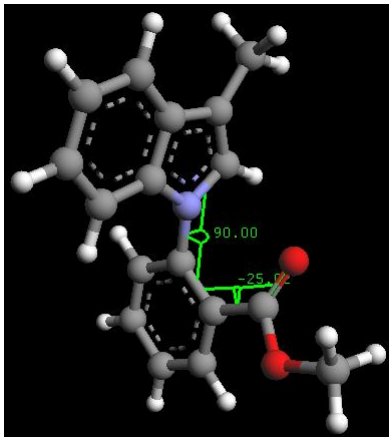

Energy = -861.8241314 Ha = 2262732.184 kJ mol^{-1}

Torsion 1 = 90°

Torsion 2 = -25.02°

C	-3.735765	0.241487	0.669964
C	-2.600304	0.093737	-0.146791
C	-1.400078	-0.418410	0.427966
C	-1.313909	-0.785117	1.776267
C	-2.456959	-0.627468	2.561156
C	-3.656009	-0.118691	2.014604
C	-2.336652	0.356673	-1.546263
C	-1.027204	0.009904	-1.770365

N	-0.439071	-0.461410	-0.586908
C	-3.306811	0.912797	-2.545223
C	0.883481	-0.987110	-0.453246
C	1.997281	-0.168903	-0.150570
C	3.254201	-0.772618	0.039278
C	1.053979	-2.374078	-0.561807
C	2.311282	-2.958207	-0.386391
C	3.414351	-2.153424	-0.082594
C	1.881669	1.310037	-0.060265
O	1.036848	2.020520	-0.616031
O	2.881951	1.849727	0.725918
C	2.884993	3.313156	0.856157
H	-4.662089	0.631615	0.258995
H	-2.423205	-0.900257	3.611366
H	-4.526103	-0.008085	2.654267
H	-2.847049	1.005388	-3.534901
H	-3.661261	1.910181	-2.252241
H	-4.194618	0.274412	-2.650314
H	4.099090	-0.141352	0.282400
H	2.425746	-4.032977	-0.480861
H	4.393504	-2.597822	0.060460
H	1.948798	3.650912	1.305284
H	3.733242	3.531681	1.501848
H	3.002344	3.780091	-0.124291
H	-0.393846	-1.175836	2.198037
H	0.183780	-2.982985	-0.779602
H	-0.440496	0.080343	-2.672446

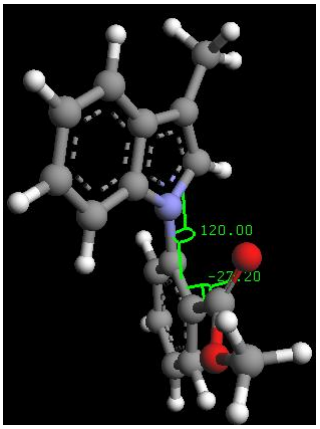

Energy = -861.8249564 Ha = -2262734.35 kJ mol^{-1}

Torsion 1 = 120°

Torsion 2 = -27.20°

C	3.570527	0.706039	-0.467856
C	2.543650	-0.140072	-0.013345
C	1.228448	0.024289	-0.535577
C	0.927846	0.991541	-1.501708
C	1.966159	1.817257	-1.934103
C	3.274670	1.678852	-1.421349
C	2.507580	-1.240142	0.929029
C	1.215404	-1.701263	0.941866
N	0.418904	-0.949397	0.060527
C	3.659388	-1.756124	1.737996
C	-0.967984	-1.165303	-0.164818
C	-1.940659	-0.169661	0.091140
C	-3.284880	-0.430631	-0.233970
C	-1.370279	-2.406291	-0.681491
C	-2.714420	-2.664584	-0.957543
C	-3.674360	-1.667983	-0.747353
C	-1.600264	1.101232	0.782956
O	-0.683651	1.274332	1.592851
O	-2.482334	2.112951	0.452462
C	-2.269700	3.401052	1.127294
H	4.580526	0.600858	-0.083501
H	1.763688	2.578870	-2.680672
H	4.058444	2.339107	-1.779191

H	3.354973	-2.595645	2.371994
H	4.071661	-0.978592	2.394779
H	4.481552	-2.105099	1.098533
H	-4.018110	0.345481	-0.055331
H	-3.006291	-3.630840	-1.355700
H	-4.717606	-1.854116	-0.978388
H	-1.268064	3.776348	0.908362
H	-3.036002	4.057280	0.719321
H	-2.382159	3.285181	2.207628
H	-0.074114	1.099930	-1.903285
H	-0.609544	-3.151172	-0.886804
H	0.769840	-2.489318	1.529057

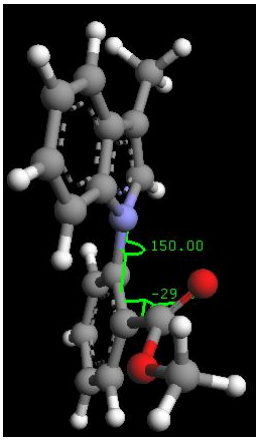

Energy = -861.8229432 Ha = -2262729.065 kJ mol^{-1}

Torsion 1 = 150°

Torsion 2 = -29.07°

C	3.518688	0.973525	-0.447258
C	2.576531	0.018595	-0.030288
C	1.193627	0.227525	-0.301969
C	0.755615	1.338098	-1.034019
C	1.712938	2.266521	-1.446755
C	3.080513	2.095703	-1.147735
C	2.709296	-1.261824	0.635378
C	1.447294	-1.782756	0.732081
N	0.493225	-0.884818	0.208764

C	3.983374	-1.878187	1.127889
C	-0.857844	-1.237060	-0.034419
C	-1.917990	-0.299605	0.046030
C	-3.206795	-0.681966	-0.373510
C	-1.138778	-2.542486	-0.479182
C	-2.432131	-2.916087	-0.842396
C	-3.471117	-1.978321	-0.811315
C	-1.766413	1.006533	0.735988
O	-1.014833	1.250132	1.685710
O	-2.629881	1.959770	0.225248
C	-2.618149	3.267559	0.896726
H	4.574397	0.830570	-0.238073
H	1.394822	3.136643	-2.012353
H	3.796592	2.841568	-1.477687
H	3.802486	-2.859628	1.578499
H	4.468726	-1.249708	1.886351
H	4.707357	-2.014650	0.313395
H	-4.000566	0.052481	-0.319578
H	-2.620100	-3.929937	-1.180690
H	-4.473369	-2.256019	-1.118294
H	-1.613818	3.694512	0.865356
H	-3.324458	3.874389	0.333503
H	-2.931395	3.160889	1.937759
H	-0.287054	1.484184	-1.288254
H	-0.322201	-3.247421	-0.581472
H	1.121757	-2.697974	1.201055

References

[1] J. I. G. Cadogan, C. L. Hickson and H. McNab, *Tetrahedron*, 1986, **42**, 2135.
[2] F. M. McMillan, University of Edinburgh, PhD Thesis, 2007.
[3] A. R. Forrester, M. Gill, C. J. Meyer, J. S. Sadd and R. H. Thomson, *J. Chem. Soc., Perkin Trans. 1*, 1979, 606.
[4] (i) P. S. Dewar, A. R. Forrester and R. H. Thomson, *J. Chem. Soc. (C)*, 1971, 3950; (ii) A. R. Forrester, M. Gill, C. J. Meyer, J. S. Sadd and R. H. Thomson *J. Chem. Commun*., 1975, 291.
[5] (i) J. Bovin, E. Fouquet and S. Z. Zard, *Tetrahedron Lett.*, 1990, **31**, 85, 3545; (ii) J. Bovin, E. Fouquet and S. Z. Zard, *J. Am. Chem. Soc*., 1991, **113**, 1054; (iii) J. Bovin, E. Fouquet and S. Z. Zard, *Tetrahedron Lett*., 1991, **32**, 4299; (iv) J. Boivin, A.-M. Schiano and S. Z. Zard, *Tetrahedron Lett*., 1992, **33**, 7849; (v) J. Bovin, E. Fouquet and S. Z. Zard, *Tetrahedron* , 1994, **50**, 1745, 1757, 1769; (vi) J. Boivin, A.-M. Schiano and S. Z. Zard, *Tetrahedron Lett*., 1994, **35**, 249; A.-C. Callier-Dublanchet, B. Quiclet-Sire and S. Z. Zard, *Tetrahedron Lett*., 1995, **36**, 8791; (vii) J. Bovin, A.-C. Callier-Dublachet, B. Quiclet-Sire, A.-M. Schiato and S. Z. Zard, *Tetrahedron*, 1995, **51**, 6517; (viii) S. Z. Zard, *Synlett*., 1996, 1148; (ix) M.-H. Le Tadic-Biadatti, A.-C. Callier-Dublanchet, J. H. Horer, B. Quiclet-Sire, S. Z. Zard and M. Newcomb, *J. Org. Chem*., 1997, **62**, 559; (x) A.-C. Callier-Dublachet, B. Quiclet-Sire and S. Z. Zard *Tetrahedron Lett*., 1997, **38**, 2463.
[6] J. Bovin, A.-M. Schiano, S. Z. Zard and H. Zhang, *Tetrahedron Lett*., 1999, **40,** 4531.
[7] W. R. Browman, C. F. Bridge, P. Brookes, M. O. Cloonan and D. C. Leach, *J. Chem. Soc., Perkin Trans. 1*, 2002, 58.
[8] D. Griller, G. D. Mendenhall, W. Van Hoof and K. U. Ingold, *J. Am. Chem. Soc*., 1974, **96**, 6068.
[9] J. Boivin, E. Fouquet, A.-M. Schiano and S. Z. Zard, *Tetrahedron*, 1994, **50**, 1769.
[10] (a) D. H. R. Barton, *Aldrichimica Acta*, 1990, **23**, 3; (b) D. H. R. Barton and S. Z. Zard, *Janssen Chim. Acta*, 1986**, 4**, 3; (c) D. H. R. Barton and N. Ozbalik, *Phosphorus, Sulfur and Silicon*, 1989, **43**, 349; (d) D. Crich and L. Quintero, *Chem. Rev*., 1989, **89**, 1413.
[11] J. Lalevée, X. Allonas, J. P. Fouassier, H. Tachi, A. Izumitami, M. Shirai and M. Tsunooka, *J. Photochem. and Photobiol.*, 2002, **151**, 27.
[12] F. Potela-Cubillo, J. S. Scott and J. C. Walton, *Chem. Comm*., 2007, 4041.
[13]T. Sato and H. Obase, *Tetrahedron Lett.*, 1967, **8**, 1633.
[14] L. J. Winters, J. F. Fisher and E. R. Ryan, *Tetrahedron Lett.*, 1971, **12**, 129.
[15] K. J. Bird, A. W. K. Chan and W. D. Crown, *Aust. J. Chem.*, 1976, **29**, 2281.
[16] (a) H. McNab, *J. Chem. Soc., Perkin Trans. 1*, 1980, 2200. (b) H. McNab, *J. Chem. Soc., Chem. Comm.*, 1980, 422.
[17] C.L Hickson and H. McNab, *J. Chem. Soc, Perkin Trans. 1*, 1984, 1569.
[18] W. D. Crown and A. N. Khan, *Aust. J. Chem.*, 1976, **29**, 2289.
[19] R Leardini, H. McNab, D. Nanni, S. Parsons, D. Reed and A. G. Tenan, *J. Chem. Soc., Perkin Trans. 1*, 1998, 1833.
[20] J. Turner, University of Edinburgh, Final Year Project Report, 1984.
[21] M. BLack, J. I. G. Cadogan, R. Leardini, H. McNab, G. McDougald, D. Nanni, D. Reed and A. Zampatori, *J. Chem. Soc., Perkin Trans. 1*, 1998, 1825.
[22] R. Leardini, H. McNab, M. Minozzi, D. Nanni, D. Reed and G. Wright, *J. Chem. Soc., Perkin Trans. 1*, 2001, 2704.
[23] A. Milligan, University of Edinburgh, PhD Thesis, 2003.
[24] J. I. G. Cadogan, C. L. Hickson and H McNab, *Tetrahedron***,** 1986, **42**, 2135.
[25] T. Creed, R. Leardini, H. McNab, D. Nanni, I. S. Nicolson and D. Reed, *J. Chem. Soc., Perkin Trans. 1*, 2001, 1079.
[26] Review, J. I. G. Cadogan, C. L. Hickson and H. McNab, *Tetrahedron* 1986, **42**, 2135.
[27] H. McNab, *J. Chem. Soc., Perkin Trans. 1*, 1984, 371.
[28] H. McNab and G. S. Smith, *J. Chem. Soc., Perkin Trans. 1*, 1984, 381.
[29] C. L. Hickson and H. McNab, *J. Chem. Soc., Perkin Trans. 1*, 1984, 1569.
[30] R. J. Gritter and R. J. Chriss, *J. Org. Chem*., 1964, **29**, 1163.

[31] (a) S. M. Blinder, M. L. Peller, N. W. Lord, L. C. Aamodt and N. S. Ivanchukov, *J. Chem. Phys*., 1962, **36**, 540-544; (b) D. A. Blank, S. W. North and Y. T. Lee, *Chem. Phys*., 1994, **187**, 35-47; (c) A. J. Gianola, T. Ichino, R. L. Hoenigman, S. Kato, V. M. Bierbaum and W. C. Lineberger, *J. Phys. Chem. A*, 2004, **108**, 10326.
[32] (a) G. B. Bacskay, M. Martoprawiro and J. C. Mackie, *Chem. Phys. Lett*., 1998, **290**, 391-398; (b) M. J. Fadden and C. M. Hadad, *J. Phys. Chem A*, 2000, **104**, 6324-6331; (c) H. Luo and M. C. Lin, *Chem. Phys. Lett*., 2001, **343**, 219-224; (d) G. da Silva, E. E. Moore and J. W. Bozzelli, *J. Phys. Chem A*, 2006, **110**, 13979-13988; (e)Y.-Q. Qiu, H.-L. Fan, S.-L. Sun, C.-G. Liu and Z.-M. Su, *J. Phys. Chem. A*, 2008, **112**, 83.
[33] P. R. Bovy, J. D. B. Reitz, J. T. Collins, T. S. Chamberlain, G. M. Olins, V. M. Corpus, E. G. McMahon; M. A. Palomo, J. P. Koepke, G. J. Smits, D. E. McGraw and J. F. Gawt, *J. Med. Chem.*, 1993, **36**, 101.
[34] J. M. Patterson, *Synthesis*, 1976, 281.
[35] W. Hinz, R. A. Jones and T. Anderson, *Synthesis* 1986, 620.
[36] C. L. Hickson and H. McNab, *J. Chem.Res. (S),* 1989, 176.
[37] K. Ogawa, Eur. Pat. Appl. EP 575923, 1993.
[38] M. J. Frisch, G. W. Trucks, H. B. Schlegel, G. E. Scuseria, M. A. Robb, J. R. Cheeseman, J. A. Montgomery, Jr., T. Vreven, K. N. Kudin, J. C. Burant, J. M. Millam, S. S. Iyengar, J. Tomasi, V. Barone, B. Mennucci, M. Cossi, G. Scalmani, N. Rega, G. A. Petersson, H. Nakatsuji, M. Hada, M Ehara, K. Toyota, R. Fukuda, J. Hasegawa, M. Ishida, T. Nakajima, Y. Honda, O. Kitao, H. Nakai, M. Klene, X. Li, J. E. Knox, H. P. Hratchian, J. B. Cross, V. Bakken, C. Adamo, J. Jaramillo, R. Gomperts, R. E. Stratmann, O. Yazyev, A. J. Austin, R. Cammi, C. Pomelli, J. W. Ochterski, P. Y. Ayala, K. Morokuma, G. A. Voth, P. Salvador, J. J. Dannenberg, V. G. Zakrzewski, S. Dapprich, A. D. Daniels, M. C. Strain, O. Farkas, D. K. Malick, A. D. Rabuck, K. Raghavachari, J. B. Foresman, J. V. Ortiz, Q. Cui, A. G. Baboul, S. Clifford, J. Cioslowski, B. B. Stefanov, G. Liu, A. Liashenko, P. Piskorz, I. Komaromi, R. L. Martin, D. J. Fox, T. Keith, M. A. Al-Laham, C. Y. Peng, A. Nanayakkara, M. Challacombe, P. M. W. Gill, B. Johnson, W. Chen, M. W. Wong, C. Gonzalez and J. A. Pople, Gaussian03; Gaussian, Inc., Wallingford CT, 2004.
[39] *C.f.* J. de Mendoza, C. Millan and P. Rull, *J. Chem. Soc., Perkin Trans. 1*, 1981, 403.
[40] A. D. MacPherson, University of Edinburgh, PhD Thesis, 1994
[41] A. D. Josey and E. L. Jenner, *J. Org. Chem.*, 1966, **27**, 2466.
[42] A. Garofalo, G. Ragno, G. Campiani, A. Brizzi and V. Nacci, *Tetrahedron*, 2000, **56**, 9351.
[43] H. Goda, H. Ihara, C. Hirayama and M. Sato, *Tetrahedrom Lett.*, 1994, **35**, 1565.
[44] R. Tyas, University of Edinburgh, PhD Thesis, 2005.
[45] R. Glaser, J. Blount, K. Mislow, *J.Am.Chem.Soc*, 1980, **102**, 2777.
[46] M. Artico, G. De Marino and V. Nacci, *Annali di Chimica*, 1967, **57**, 1431.
[47] E. E. Garcia, J. G. Riley and R. I. Fryer, *J. Org. Chem*, 1968, **4**, 1358.
[48] J. Fraser, *The University of Edinburgh*, Final Year Project, 2007-2008.
[49] M. Alajarin, B. Bonillo, M.-M. Ortin, R.-A. Orenes and A. Vidal, *Org. Biomol. Chem.*, 2011, **9**, 6741.
[50] T. Klingstedt, A. Alberg, P. Dunbar and A. Martin, *J. Het. Chem.*, **1985**, *22*, 1545.
[51] H. Xu, W.-Q. Liu, L.-L. Fan, Y. Chen, L.-M. Yang, L. Lv and Y.-T. Zheng, *Chem. Pharm. Bull*, 2008, **56,** 720.
[52] Alder R. W. Alder, S. P. East, J. N., Harvey and M. T. Oakley, *J. Am. Chem. Soc*, 2002, **125**, 5375.
[53] S. I. Wharton, J. B. Henry, H. McNab and A. R. Mount, *Chem. Eur. J.*, 2009, **15**, 5482 .
[54] K. Johnston, *The University of Edinburgh*, 2007-2009
[55] P. H. Hansen, *Carbon-Carbon Spin-Spin Coupling Constants*, 1981, **4**, pg 273.
[56] L. A. Crawford, H. McNab, A. R. Mount and S. I. Wharton, *J. Org. Chem*, 2008, **73**, 6642.
[57] J.-F. Brière, G. Dupas, G. Quéguiener and J. Bourguignon, *Heterocycles*, 2000, **52**, 1371.
[58] G. Van Baelen, G. L. F. Lemière, R. A. D. and B. U. W. Maes, *ARKIVOC*, 2009, **vi**, 174.
[59] G. Van Baelen, S. Hostyn, L. Dhooghe, P. Tapolcsányi, P. Mátyus, G. Lemière, R. Dommisse, M. Kaiser, R. Brun, P. Cos, L. Maes, G. Hajós, Z. Riedl, I. Nagy, B. U. W. Maes and L. Pieters, *Biorg. Med. Chem.*, 2009, **17**, 7209.

[60] G. Van Baelen, C. Meyers, G. L.F. Lemière, S. Hostyn, R. Dommisse, L. Maes, K. Augustyns, A. Haemers, L. Pieters, B. U.W. Maes, *Tetrahedron*, 2008, **64**, 11802.
[61] A. Kubillus, *The University of Edinburgh*, Final Year Project, 2007-2008.
[62] B. A. Blight, A. Camara-Campos, S. Djurdjevic, M. Kaller, D. A. Leigh, F. M. McMillan, H. McNab and A. M. Z. Slawin, *J. Am. Chem. Soc.*, 2009, **131**, 14116.
[63] L. Steven, T. Ryouji and T. Kouichirou, *Bridgestone Corporation*, 2009, **WO 2009051700 A1** 20090423**.**
[64] I. Masahiko, O. Seiji, *Japanese Kokai Tokkyo Koho*, 1994, **JP19920278781** 19921016.
[65] J. Rosevear and J. F. K. Wilshire, *Aust. J. Chem.*, 1991, **44**, 109.
[66] X.-D. Yang, L Li and H.-B. Zhang, *Helvetica Chimica Acta*, 2008, **91**, 1435.
[67] M. V. Peters, R. S. Stoll, R. Goddard, G. Buth, and S. Hecht, *J. Org. Chem.*, 2006, **71**, 7840.
[68] Rodway et al., patent, *Aspro-Nicholas Ltd*, 1971, **DE19722206012 19720209**.
[69] J. A. Joule and K. Mills J. A. Joule and K. Mills, *Heterocyclic Chemistry*, fourth edition 2000, pg 12.
[70] T. Körtvélyesi and L, *Reac.Kinet.Catal.Lett*, 1995, **56**, 371.
[71] K. W. Bentley, *Isoquinoline Alkaloids*, 1998, CRC Press.
[72] A. Bischler and B. Napierlaski, *Ber.*, 1893, **26**, 1903.
[73] A. Pictet and T. Spengler, *Ber. Dtsch. Chem. Ges.*, 1911, **44**, 2030.
[74] A. Pictet and A. Gams, *Ber.*,1910, **43**, 2384.
[75] E. D. Cox and J. M. Cook, *Chem. Rev.*, 1995, **95** (6), 1797.
[76] E. D. Cox and J. M. Cook, *Chem. Rev.*, 1995, **95**, 1797.
[77] M. Wu and S. Wang, *Synthesis*, 2010, 587.
[78] C. Pomeranz, *Monatsh.*, 1893, **14,** 116; P. Fritsch, *Ber.*, 1893, **26,** 419.
[79] M. J. Bevis, E. J. Forbes, N. N. Naik, B. C. Uff ; *Tetrahedron*, 1971, **27**, 1253.
[80] E. Schlittler, J. Müller, *Helv. Chim. Acta*, 1948, **31,** 914, 1119.
[81] E. W. Gill and A. W. Bracher; *Heterocycl. Chem.*, 1983, **20**, 1107.
[82] E. Awuah and A. Capretta, *J.Org. Chem.*, 2010, **75**, 5627.
[83] N. Guimond, S. I. Gorelsky, and K. Fagnou, *J. Am. Chem. Soc.*, 2011, **133**, 6449.
[84] K. R. Roesch and R. C. Larock, *J.Org. Chem.*, 1998, **63**, 5306.
[85] K. R. Roesch and R. C. Larock, *J.Org. Chem.*, 2001, **67**, 86.
[86] N. Guimond and K. Fagnou, *J. Am. Chem. Soc.*, 2009, **131**, 12050.
[87] P. C. Too, Y.-F. Wang and S. Chiba, *Org. Lett.*, 2010, **12**, 5688.
[88] R. Alfonso, P. J. Campos, B. Garcia and M. A. Rodriguez, *Org. Lett.*, 2006, **8**, 3521.
[89] M. Black, J. Cadogan, H. McNab, A. MacPherson, P. Roddam, C. Smith and H. Swenson, *J. Chem. Soc. Perkin Trans. 1*, 1997, 2483.
[90] J. I. G. Cadogan, C. L. Hickson and H. McNab, *Tetrahedron*, 1986, **42**, 2135.
[91] A. D. MacPherson , The University of Edinburgh, PhD Thesis 1994, pg 97-98, unpublished work.
[92] M. Freira et all, *Tetrahedron*, 2004, **60**, 2673
[93] J. Tsuji, *Palladium Reagents and Catalysts: New Perspectives for the 21st Century*, second edition, 2004.
[94] A. F. Littke and G. C. Fu, *J. Am. Chem. Soc.*, 2001, **123**, 6989.
[95] J. A. Joule and K. Mills, *Heterocyclic Chemistry*, fourth edition, 2000, pg 12.
[96] M. Bellas and H. Suschitzky, *J. Chem. Soc.*, 1964, 4561.
[97] G. Smith, The University of Edinburgh, final year project report 2010-2011unpublished work.
[98] M. Artico, F. Corelli, S. Massa, G. Stefancich, L. Avigliano, et al; *J. Med. Chem.*, 1988, **31**, 4, 802.
[99] Mazzola et al., *J. Org. Chem.*, 1967, **32**, 486.
[100] S. Boyer, E. Blazier, M. Barabi, G. Long, G. Zaunius et al., *J. Het. Chem.*, 1988, **25**, 1003.
[101] S. Raines et al., *J. Org. Chem.*, 1971, **36**, 3992.
[102] S. Raines, S. Y. Chai, F. P. Palopoli, *J. Het. Chem.*, 1976, **13**, 711.
[103] L. A. Crawford, N. C. Clemence, H. McNab and R. G. Tyas, *Org. Biomol. Chem.*, 2008, **69**, 2334.
[104] D. I. Chai and M. Lautens, *J. Org. Chem.*, 2009, **74**, 3054. |
[105] R. Glaser, J. F. Blount, and K. Mislow, *J. Am. Chem. Soc*. 1980, **102**, 2777.

[106] G. Van Baelen, C. Meyers, G. L.F. Lemie`re, S. Hostyn, R. Dommisse,L. Maes, K. Augustyns, A. Haemers, L. Pieters and B. U.W. Maes, *Tetrahedron*, 2008, **64,** 11802.
[107]M. V. Peters, R. S. Stoll, R. Goddard, G. Buth, and S. Hecht, *J. Org. Chem.*, 2006, **71**, 7840.
[108] P. Cozzi, G. Carganico, D. Fusar, M. Grossoni, M. Menichincheri,V. Pinciroli, R. Tonani, F. Vaghi and P. Salvati, *J. Med. Chem.*, 1993, **36**, 2964.
[109] J. Rosevear and J. E. K. Wilshire, *Aust. J. Chem.*, 1991, **44**, 1097.
[110] M. Freira et all, *Tetrahedron*, 2004, **60**, 2673.
[111] D. Enders, A. A. Narine, F. Toulgoat, T. Bisschops, *Angew. Chem. Int. Ed.*, 2008, **47**, 5661.

Appendix

Structural studies of some push–pull *N*-arylbenzazoles†‡

Lynne A. Crawford, Maria Ieva, Hamish McNab* and Simon Parsons*

Received 25th February 2010, Accepted 11th June 2010
First published as an Advance Article on the web 2nd July 2010
DOI: 10.1039/c0dt00029a

X-Ray crystal structures, and calculated structures (at B3LYP/6-31G level) are reported for seven *N*-arylbenzazoles (two carbazoles, indoles and benzimidazoles, and one indazole) bearing electron withdrawing groups in the 2-position of the *N*-aryl ring. The structures are markedly non-planar by rotation around the *N*-aryl bond, with the substituent in most cases lying s-*E* in relation to the *N*-aryl bond; intermolecular electrostatic interactions in the crystal rationalise the two examples in which an s-*Z* conformation is observed. A large interplanar angle between the benzazole and the *N*-aryl planes is associated with a small interplanar angle between the planes of the *N*-aryl group and the substituent and *vice versa*.

Introduction

We report an analysis of the X-ray crystal structures of a range of push–pull benzazole derivatives **1–7**. These compounds all have a benzazole core [either carbazole (**1** and **2**), indole (**3** and **4**), benzimidazole (**5** and **6**) or indazole (**7**)] with an *N*-aryl group bearing a strong electron withdrawing group [either carbomethoxy (**1**, **3** and **5**) or nitro (**2**, **4**, **6** and **7**)] in the 2-position of the *N*-aryl ring.

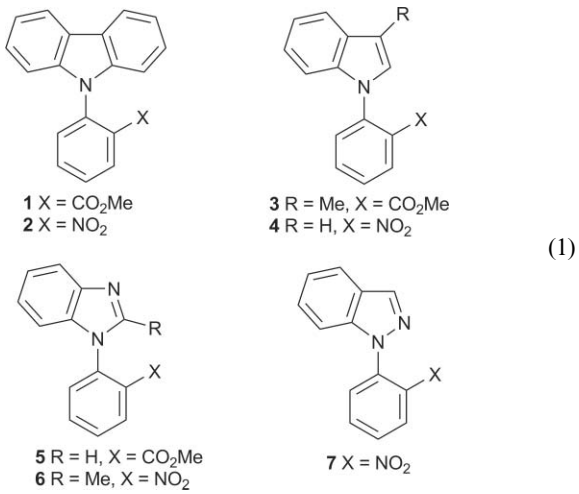

(1)

For maximum delocalisation of the azole nitrogen atom lone pair, through to the electron withdrawing group, the systems would ideally be planar. In compounds **1–7**, this ideal state is impossible owing to the *peri*-interactions of the *N*-aryl group and the fused benzene ring of the benzazole, exacerbated by the presence of a bulky *ortho*-substituent. It was therefore of interest to correlate the way in which the systems cope with these competing influences. In the solid-state, crystal packing forces can provide a further complication, and so the X-ray crystallographic studies have been complemented by calculations of the gas-phase structures, made at B3LYP/6-31G level.[1]

Results and discussion

General

Compounds **1–4** and **6–7** were made from the corresponding azole by standard S_NAr procedures.[2–6] Compound **5** required a three-step procedure in which the final step was cyclisation of *N*-(2-carbomethoxyphenyl)-*o*-phenylenediamine[7] with formic acid.[8] This compound shows unusual ^{1}H NMR behaviour (ESI‡) in which broadened areas of the spectrum are sharpened both at higher and lower temperatures. This may be due to exchange between two identical sites.

Plots of the X-ray crystal structures of **1–7** are given in Fig. 1–7, respectively, and diagrams of corresponding calculated structures are reported in the ESI.‡ All are significantly non-planar, suggesting that push–pull conjugation is not a significant feature in their structures. The solid-state structure of **1** shows eight molecules in the unit cell at atmospheric pressure and its pressure dependent polymorphism has been previously reported.[2] The structure of **3** is disordered with *ca.* 10% showing an s-*E* configuration around the *N*-aryl bond (ESI‡).

Bond lengths and angles

Bond lengths and angles of **1–7** are generally unexceptional. The bond lengths between the azole nitrogen atoms and the *N*-aryl rings might have been expected to be short due to delocalisation. Those of the eight molecules of **1** fall in the range 1.410(5)–1.445(5) Å (average 1.432 Å); the average is close to the value for *N*-phenylcarbazole itself[9] (1.427 and 1.420 Å, for the two molecules in the unit cell). There is no obvious correlation between the C–N bond lengths and the interplanar angle between the carbazole and the *N*-aryl group. For compounds **2–7**, the C–N bond length is in the range 1.409(5)–1.4282(18) Å.

For compounds **2**, **4** and **6**, the lengths of the two N–O bonds in the nitro group differ by around 1σ or less in the

School of Chemistry, The University of Edinburgh, West Mains Road, Edinburgh, UK EH9 3JJ UK. E-mail: H.McNab@ed.ac.uk, S.Parsons@ed.ac.uk; Fax: +44 131 650 4743; Tel: +44 131 650 4718; +44 131 650 5804

† This paper is dedicated to Professor David Rankin, in recognition of his seminal contributions to structural science.

‡ Electronic supplementary information (ESI) available: NMR data for **5**, crystallographic data, Cartesian coordinates, calculated energies. See DOI: 10.1039/c0dt00029a

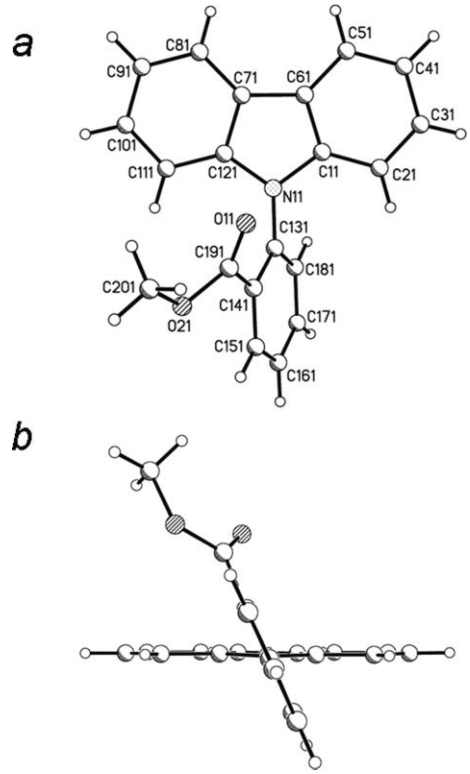

Fig. 1 Plots of one of the eight molecules of **1** showing (a) the crystallographic numbering scheme and (b) a side view in which the heterocyclic ring is approximately orthogonal to the plane of the paper.

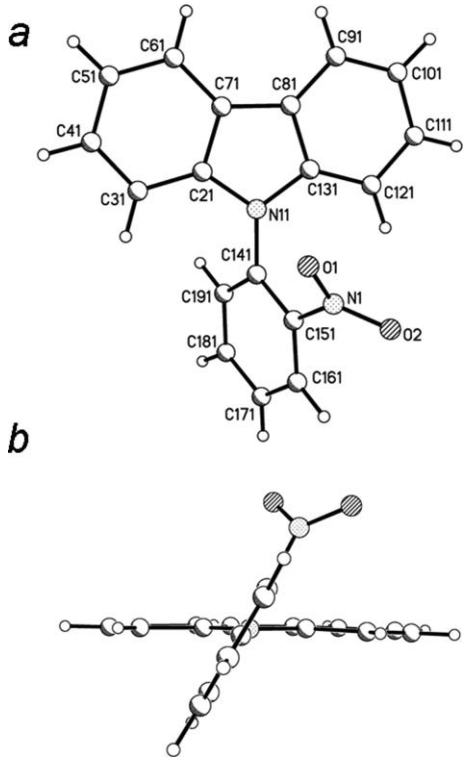

Fig. 2 Plots of **2** showing (a) the crystallographic numbering scheme and (b) a side view in which the heterocyclic ring is approximately orthogonal to the plane of the paper.

X-ray structure; however the situation is very different for the indazole derivative **7**, in which these parameters differ by some 5σ [1.196(5) Å and 1.231(5) Å]. This difference is not reflected in the calculated structure (N111–O112 1.260 Å; N111–O111 1.265 Å. There are no obvious inter- or intra-molecular interactions to account for this difference in the crystal; indeed, if the two N–O distances are strongly restrained to be equal, R_1 increases by only 0.004. It is possible that the high mosacity in the crystal used for data collection compromised the peak shapes, degrading the accuracy of the integrated intensities. A search of the Cambridge Crystallographic database (ESI‡) reveals that the N–O bonds of nitro groups differ by ≥0.035 Å in less than 1% of hits; although unusual, this situation is therefore not unprecedented.

Interplanar angles

Compounds **1–7** are composed of three, essentially planar, sub-units, *viz* the benzazole (or dibenzazole) ring, the *N*-aryl group and the nitro (or carbomethoxy) substituent. It is clear from the side views shown in Fig. 1–7, that there are substantial angles between the planes of the benzazole and the *N*-aryl group, and between those of the *N*-aryl group and the substituent (Table 1). These results are broadly supported by the calculations (ESI‡).

Table 1 Interplanar angles (°) for **1–8**

	Benzazole-*N*-aryl (X-ray)	Benzazole-*N*-aryl (calc.)[a]	*N*-aryl-substituent (X-ray)	*N*-aryl-substituent (calc.)[a]
1[b]	65.78(13)	63.96	33.6(2)	18.64
	78.09(14)		21.8(2)	
	59.81(14)		39.3(2)	
	60.04(13)		38.9(2)	
	62.42(13)		38.4(2)	
	80.77(13)		21.7(2)	
	81.12(13)		21.7(2)	
	74.05(14)		20.7(2)	
2	61.11(5)	56.70	40.48(9)	32.94
3[c]	115.13(8)	54.72	37.21(6)	10.75
4	47.17(4)	70.54	41.11(6)	33.77
5[d]	116.40(3)	66.59	34.49(3)	21.86
6	68.64(5)	64.25	47.31(17)	24.66
7	40.29(11)	47.00	47.35(27)	35.55

[a] Dihedral angles reported; calculated at B3LYP/6-31G level. [b] Eight independent molecules in the unit cell. [c] Major conformer; substituent is s-*Z*. [d] Substituent is s-*Z*.

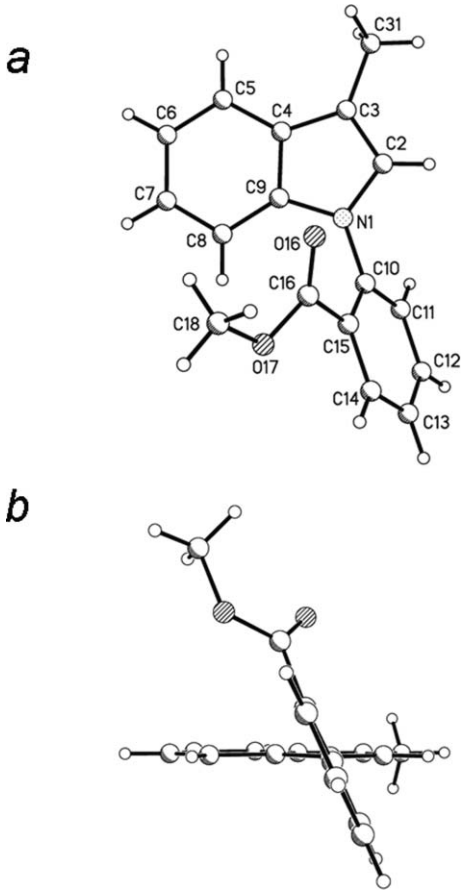

Fig. 3 Plots of the major rotamer of **3** showing (a) the crystallographic numbering scheme and (b) a side view in which the heterocyclic ring is approximately orthogonal to the plane of the paper. The coordinates plotted in this figure have been inverted relative to the asymmetric unit for consistency with other figures in this paper. This operation is consistent with the space group.

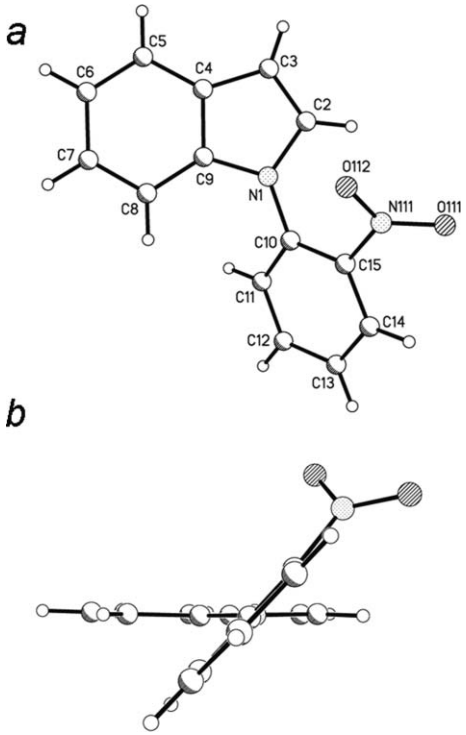

Fig. 4 Plots of **4** showing (a) the crystallographic numbering scheme and (b) a side view in which the heterocyclic ring is approximately orthogonal to the plane of the paper.

In all cases except **7** (which has only a lone pair on the site adjacent to the *N*-aryl group) the angle between the benzazole and the *N*-aryl ring is greater than that between the *N*-aryl group and the substituent. The carbazole **1** and the 2-methylbenzimidazole **6**, with non-hydrogen substituents on the site adjacent to the *N*-aryl group, correspondingly have the largest benzazole-*N*-aryl angle.

Although the same trends are evident, there is little quantitative correspondence between the calculated and X-ray interplanar angles.

In all of the calculated structures, and in most of the solid-state structures, the position of the substituent is s-*E* with respect to the *N*-C(aryl) bond. However, in the two carbomethoxy compounds, **3** (major conformer) and **5**, an s-*Z* configuration is adopted so that the substituent lies in the direction of the fused benzene ring (Fig. 3 and 5). Calculations on **3** suggest that the energy surface created by *N*-aryl bond rotation is very flat (ESI‡) (difference of less than 7 kJ mol^{-1} between energy maximum and minimum in the dihedral angle range 30–150°) and so crystal packing could readily account for these differences. Indeed, it is likely that electrostatic interactions are responsible for the conformation of these molecules in the crystal. Thus the Hirshfield surfaces shown in Fig. 8 and 9 demonstrate that **3** and **5** show very similar electrostatic potentials, with an electron rich region close to the s-*Z* carbonyl group creating a pocket for the electron deficient region of the *N*-aryl group, thus controlling the packing forces.

Data for the X-ray structures shown in Table 1 suggest that structures with a large benzazole-*N*-aryl angle tend to show a small *N*-aryl-substituent angle. These parameters are plotted in Fig. 10 and show modest correlation with a straight line fit ($R^2 = 0.64$). The point furthest from the line is for the 2-methylbenzimidazole **6**, where increased steric factors may introduce further complications. If this point is ignored, R^2 improves to 0.85. The correlation is also somewhat better if the eight conformers of **1** are treated separately from **2–7** (R^2 0.91) (ESI‡). Calculations on **1**, in which the benzazole–*N*-aryl angle is fixed, also show a relation between the two interplanar angles though in this case the correlation shows a very good exponential fit (R^2 0.99). Unfortunately, the experimental data do not cover a wide enough range (restricted to benzazole–*N*-aryl interplanar angles of *ca.* 40–80°) for any exponential correlation to become evident. Overall, these results suggest that in the cases where conjugation from the benzazole nitrogen atom is reduced by a large interplanar angle, the systems can compensate by increasing the interaction between the *N*-aryl group and the substituent, by reducing these interplanar angles.

Conclusions

We have shown, by consideration of a range of related *N*-arylbenzazole structures with electron withdrawing substituents in the 2-position of the aryl ring, that the non-planarity

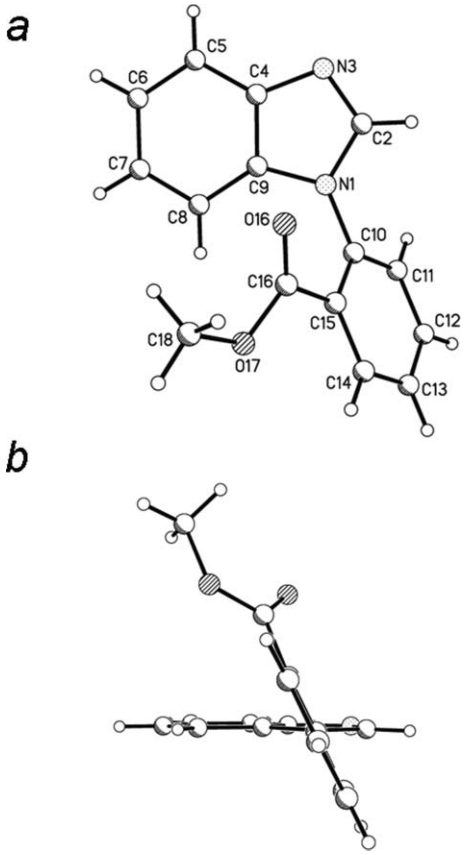

Fig. 5 Plots of **5** showing (a) the crystallographic numbering scheme and (b) a side view in which the heterocyclic ring is approximately orthogonal to the plane of the paper.

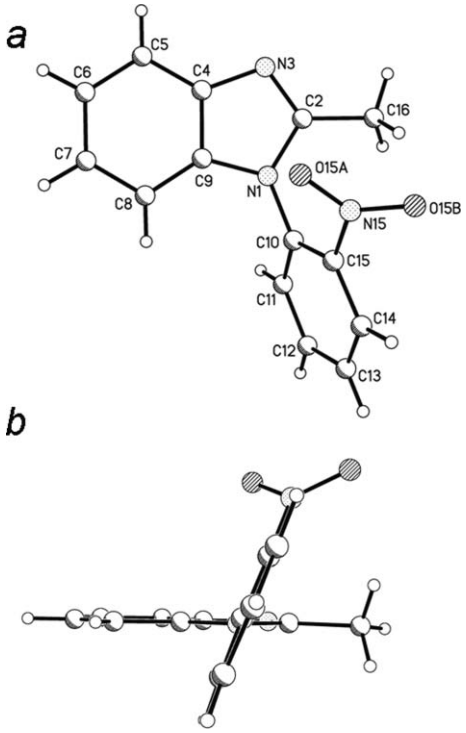

Fig. 6 Plots of **6** showing (a) the crystallographic numbering scheme and (b) a side view in which the heterocyclic ring is approximately orthogonal to the plane of the paper.

of the systems severely limits push–pull conjugation between the nitrogen atom of the azole and the electron withdrawing substituent. The unexpected s-*Z* configurations of the carbomethoxy compounds **3** and **5** in the solid-state (not reproduced as global minima in the calculated structures) may be explained by intermolecular electrostatic interactions. Interplanar angles between the benzazole and the *N*-aryl group, and between the *N*-aryl group and the substituent are linearly related in the solid-state.

Experimental

NMR spectra were recorded for solutions in $CDCl_3$. Chemical shifts are quoted relative to TMS and coupling constants are given in Hertz. ^{13}C NMR signals refer to one CH resonance unless otherwise stated. Mass spectra were recorded under electron impact conditions.

Compounds **1**,[2] **2**,[3] **3**,[4,5] **4**[4] and **7**[6] were prepared according to literature procedures.

1-(2-Carbomethoxyphenyl)-1*H*-benzimidazole 5

Methyl 2-(2-aminophenylamino)benzoate[7] (1 mmol) and formic acid (10 cm^3) were heated for 2 h at 130 °C. The solution was cooled and ether was added. The solution was extracted with HCl (2 M, 3 × 50 cm^3). The aqueous layer was made alkaline with aqueous potassium carbonate solution and then extracted with ether (3 × 50 cm^3), dried ($MgSO_4$) and the solvent removed under reduced pressure to give **5** (60%) mp 88–89 °C (from toluene) [lit.,[8] 88 °C] δ_H (250 MHz) 8.08 (1H, ddd, ^3J 7.7, ^4J 1.7, ^5J 0.3), 8.00 (1H, br s), 7.85 (1H, br d, ^3J 6.9), 7.70 (1H, td, ^3J 7.5, ^4J 1.6), 7.58 (1H, td, ^3J 7.7, ^{4}J 1.4), 7.14–7.48 (4H, m) and 3.46 (3H, s); δ_C (63 MHz) 165.63 (quat), 143.32, 135.08 (quat), 133.19, 131.82, 128.95, 128.28, 123.46, 122.35, 120.22, 109.68 and 52.29 (CH_3) (3 quaternaries missing – see ESI‡); *m*/*z* 252 (M^+, 100%), 220 (55), 192 (39), 166 (15), 140 (13), 92 (32), 83 (15) and 76 (22). This compound has been reported in a patent.[8]

2-Methyl-1-(2-nitrophenyl)-1*H*-benzimidazole 6

2-Methylbenzimidazole (0.01 mol) and 2-fluoronitrobenzene (0.01 mol) were heated at 125 °C for 8 h in DMF (15 cm^3) with stirring, in the presence of anhydrous potassium carbonate (0.01 mol). The reaction mixture was poured into water (100 cm^3) and extracted with dichloromethane (6 × 30 cm^3). The combined organic layers were washed with water (3 × 15 cm^3), dried ($MgSO_4$) and concentrated *in vacuo* to provide **6** (78%), mp 110–111 °C; (Found: C, 66.05; H, 4.25; N, 16.75. $C_{14}H_{11}N_3O_2$ requires C, 66.4; H, 4.35; N, 16.6%); δ_H (360 MHz) 8.21 (1H, dd, ^3J 8.1, ^4J 1.5), 7.87 (1H, td, ^3J 7.8, ^4J 1.6), 7.75–7.80 (2H, m), 7.54 (1H, dd, ^3J 7.8, ^4J 1.5), 7.18–7.32 (2H, m), 6.92 (1H, dd, ^3J 8.1, ^4J 1.1) and 2.47 (3H, s); δ_C (90 MHz) 152.04 (quat), 147.31 (quat), 143.23 (quat), 136.83 (quat), 134.87, 131.53, 131.05, 130.03 (quat), 126.35, 123.54, 123.23, 119.79, 109.43 and 14.47 (CH_3); *m*/*z* 253 (M^+, 57%), 236 (8), 206 (23), 181 (42), 132 (100), 104 (28), 91 (39) and 77 (40).

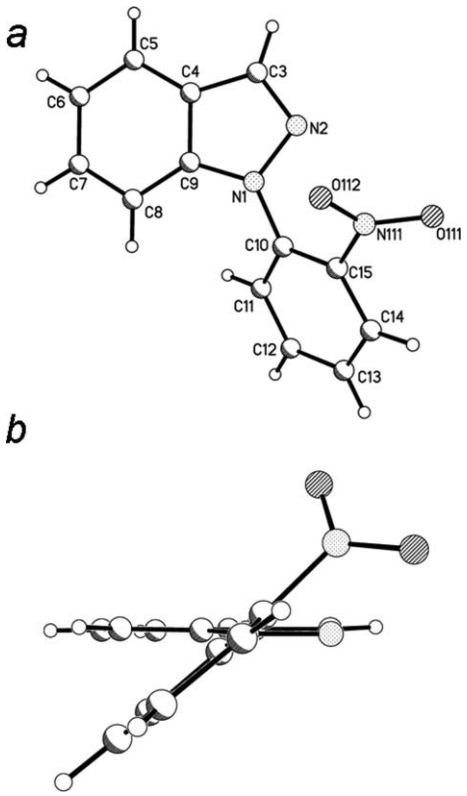

Fig. 7 Plots of **7** showing (a) the crystallographic numbering scheme and (b) a side view in which the heterocyclic ring is approximately orthogonal to the plane of the paper. The coordinates plotted in this figure have been inverted relative to the asymmetric unit for consistency with other figures in this paper. This corresponds to an inversion twinning operation.

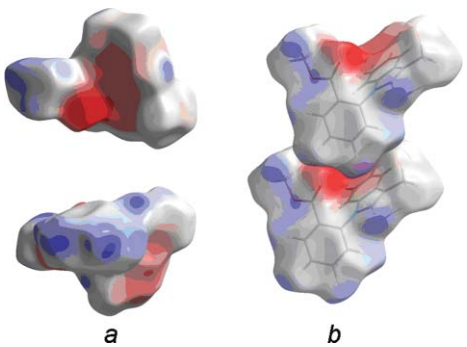

Fig. 8 (a) Views of Hirshfeld surfaces mapped with the individual electrostatic potentials of the main conformer of **3** and (b) a view showing how the electron rich region close to the carbonyl oxygen atom of the ester group creates a pocket suitable for the more electron-deficient area of the *N*-aryl group of an adjacent molecule. Positive regions are shown in blue, and negative in red. The range mapped was ±0.05 au.

Calculations

Calculations were carried out at B3LYP/6-31G level using the Gaussian set of programs.[1] Tables of coordinates and energies are given in the ESI.‡

Hirshfeld surface plots[10] were calculated using the program CrystalExplorer.[10c] Electrostatic potentials were mapped over the range ±0.05 au with red corresponding to net negative charge and blue corresponding to net positive charge. Wavefunctions were calculated using STO-3G basis sets.

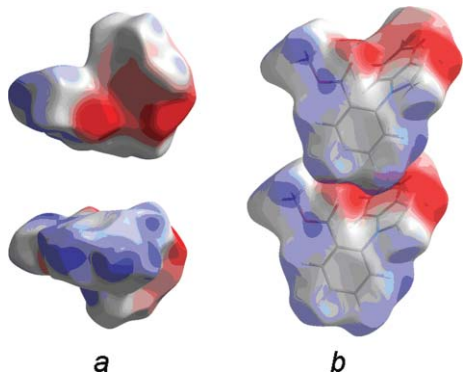

Fig. 9 (a) Views of Hirshfeld surfaces mapped with the individual electrostatic potentials of **5** and (b) a view showing how the electron rich region close to the carbonyl oxygen atom of the ester group creates a pocket suitable for the more electron-deficient area of the *N*-aryl group of an adjacent molecule. Colours and ranges were the same as Fig. 8.

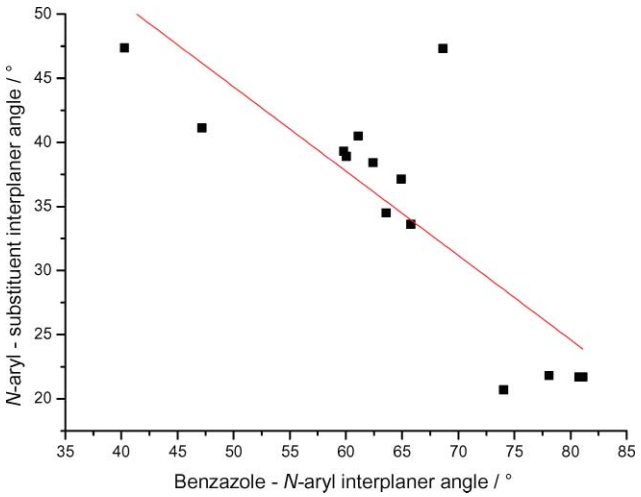

Fig. 10 Plot of benzazole–*N*-aryl interplanar angle *versus* *N*-aryl-substituent interplanar angle for **1** (8 molecules) and **2–7** (X-ray data).

Crystal structures

Crystallographic data for compounds **1–7** are available on the Cambridge Database, having been previously deposited by us. REFCODES are **1** (CARZIF), **2** (SEMTAG), **3** (CARZOL), **4** (PELDUG), **5** (CARZUR), **6** (PELFES) and **7** (PELDOA). Data for **1** have been previously published.[2] Crystal and refinement statistics are recorded as Table 1 in the ESI.‡ Searches of the Cambridge Database[11] used version 5.31 with updates to November 2009. Structures were solved and refined using SHELXTL,[12] and visualised with XP[12] and MERCURY.[13] Structure analyses were accomplished with PLATON.[14]

Acknowledgements

We are grateful to EPSRC and to EaStChem for the award of Research Studentships (to L. A. C. and M. I., respectively). We also acknowledge Dr Alice Dawson and the late

Dr Andrew Parkin, for their assistance in the determination of some of the crystal structures. This work has made use of the resources provided by the EaStCHEM Research Computing Facility (http://www.eastchem.ac.uk/rcf). This facility is partially supported by the eDIKT initiative (http://www.edikt.org).

Notes and references

1 M. J. Frisch, G. W. Trucks, H. B. Schlegel, G. E. Scuseria, M. A. Robb, J. R. Cheeseman, J. A. Montgomery, Jr., T. Vreven, K. N. Kudin, J. C. Burant, J. M. Millam, S. S. Iyengar, J. Tomasi, V. Barone, B. Mennucci, M. Cossi, G. Scalmani, N. Rega, G. A. Petersson, H. Nakatsuji, M. Hada, M. Ehara, K. Toyota, R. Fukuda, J. Hasegawa, M. Ishida, T. Nakajima, Y. Honda, O. Kitao, H. Nakai, M. Klene, X. Li, J. E. Knox, H. P. Hratchian, J. B. Cross, V. Bakken, C. Adamo, J. Jaramillo, R. Gomperts, R. E. Stratmann, O. Yazyev, A. J. Austin, R. Cammi, C. Pomelli, J. W. Ochterski, P. Y. Ayala, K. Morokuma, G. A. Voth, P. Salvador, J. J. Dannenberg, V. G. Zakrzewski, S. Dapprich, A. D. Daniels, M. C. Strain, O. Farkas, D. K. Malick, A. D. Rabuck, K. Raghavachari, J. B. Foresman, J. V. Ortiz, Q. Cui, A. G. Baboul, S. Clifford, J. Cioslowski, B. B. Stefanov, G. Liu, A. Liashenko, P. Piskorz, I. Komaromi, R. L. Martin, D. J. Fox, T. Keith, M. A. Al-Laham, C. Y. Peng, A. Nanayakkara, M. Challacombe, P. M. W. Gill, B. Johnson, W. Chen, M. W. Wong, C. Gonzalez, and J. A. Pople, *Gaussian03*, Gaussian, Inc., Wallingford CT, 2004.
2 R. D. L. Johnstone, M. Ieva, A. R. Lennie, H. McNab, S. Parsons, E. Pidcock, and J. E. Warren, *CrystEngComm*, 2010, 10.1039/b917290d.
3 S. I. Wharton, J. B. Henry, H. McNab and A. R. Mount, *Chem.–Eur. J.*, 2009, **15**, 5482–5490.
4 L. A. Crawford, H. McNab, A. R. Mount and S. I. Wharton, *J. Org. Chem.*, 2008, **73**, 6642–6646.
5 L. A. Crawford, N. C. Clemence, H. McNab and R. G. Tyas, *Org. Biomol. Chem.*, 2008, **6**, 2334–2339.
6 O. Tsuge and H. Samura, *J. Heterocycl. Chem.*, 1971, **8**, 707–710.
7 R. A. Bunce and J. E. Schammerhorn, *J. Heterocycl. Chem.*, 2006, **43**, 1031–1035.
8 F. Clemence and O. Le Martret, *Ger. Offen.*, 1970, 1914005.
9 C. Avendaño, M. Espada, B. Ocaña, S. García-Granda, M. del Rosario Díaz, B. Tejerina, F. Gómez-Beltrán, A. Martínez and J. Elguero, *J. Chem. Soc., Perkin Trans. 2*, 1993, 1547–1555.
10 (*a*) J. J. McKinnon, M. A. Spackman and A. S. Mitchell, *Acta Crystallogr., Sect. B: Struct. Sci.*, 2004, **60**, 627–668; (*b*) M. A. Spackman and D. Jayatilaka, *CrystEngComm*, 2009, **11**, 19–32; (*c*) S. K. Wolff, D. J. Grimwood, J. J. McKinnon, D. Jayatilaka and M. A. Spackman, *CrystalExplorer*, University of Western Australia, Perth, Australia, 2005.
11 F. H. Allen, *Acta Crystallogr., Sect. B: Struct. Sci.*, 2002, **B58**, 380–388.
12 G. M. Sheldrick, *SHELXTL-XP*. University, of Göttingen, Germany, 2001.
13 C. F. Macrae, I. J. Bruno, J. A. Chisholm, P. R. Edgington, P. McCabe, E. Pidcock, L. Rodriguez-Monge, R. Taylor, J. van de Streek and P. A. Wood, *J. Appl. Crystallogr.*, 2008, **41**, 466–470.
14 A. L. Spek, *PLATON – A Multipurpose Crystallographic Tool*, Utrecht University, Utrecht, The Netherlands, 2004.

